GEOLOGIC CONTROLS ON SHALLOW GROUNDWATER QUALITY IN THE SOCORRO BASIN, NEW MEXICO

By

Brad Talon Newton

Thesis

Submitted in partial fulfillment of the requirements for the degree of

Master of Science in Hydrology

New Mexico Institute of Mining and Technology
Department of Earth and Environmental Science

January, 2004

ABSTRACT

Proper water resource management along the Middle Rio Grande entails satisfying many different needs with a limited water supply and requires an understanding of the regional hydrologic system. This study focuses on a reach of the Rio Grande that flows through the Socorro Basin, located in central New Mexico. The water quality of the Rio Grande deteriorates as it flows downstream due to many factors such as evapotranspiration, irrigation return flow, wastewater disposal, and the introduction of deep sedimentary brines. High-chloride waters were observed in the shallow groundwater system in the Socorro basin. These high-chloride waters are geochemically similar to typical sedimentary brines. Previous hypotheses for the upwelling of the high-chloride waters include structural controls such as cross-basin faults and the leakage of geothermal waters along Rio Grande rift faults. This thesis develops a hypothesis that relates the flow paths of the high-chloride waters to a synrift structure, the Socorro accommodation zone (SAZ). The SAZ is a 2-km –wide, topographically high zone that separates tilted half grabens of opposite polarity.

Stable- isotope and groundwater-chemistry data were used to identify different water types in the shallow aquifer system. The observed spatial relationship among the different water types suggested that some regional flow paths might be controlled by cross-basin structures related to the Rio Grande rift. Some known faults strike across the basin, but have no surficial expression in the Rio Grande valley. The geometry of SAZ

can give clues about whether or not one would expect cross-basin structures in the area where these high-chloride waters are observed. Cross-basin structures associated with the SAZ might act as conduits for certain water types including the high-chloride waters. The mechanism by which these high-chloride waters are forced up to the shallow system may be related to differences in permeabilities in a highly fractured fault zone and the leakage of geothermal waters along these structures. The actual source of these high-chloride waters cannot be conclusively identified.

ACKNOWLEDGEMENTS

The completion of this thesis required the contributions of many different people. First of all, I would like to thank my advisor, Rob Bowman (New Mexico Tech) and committee members, Fred Phillips (New Mexico Tech) and Peggy Johnson (NMBGMR) for their expertise and guidance. Thank you to the New Mexico interstate Stream Commission and the U.S. Army Corps of Engineers for the funding of this project. S.S. Papadopulos & Associates played a large role in initiating fieldwork for this project and in providing several publications about the study area. I would also like to thank Richard Chamberlain and Steve Cather (NMBGMR) for sharing their vast knowledge about the geology of the Socorro Basin with me. Other people who helped me interpret the data include Alan Sanford (New Mexico Tech) and Sean Connell (NMBGMR). I would like to acknowledge many friends and colleagues including Laura Wilcox, Bayani Cardenas, Tim Miller, Michelle Pate, Ezra Noble, and Greg Pargas for fieldwork assistance. And last but not least, I would like to thank my lovely wife, Cynthia Connolly for her patience and support.

TABLE OF CONTENTS

Page

LIST OF FIGURES

Page

LIST OF TABLES

Page

INTRODUCTION

Overview

The Middle Rio Grande is a reach of the Rio Grande that runs through central New Mexico from Cochiti Reservoir to Elephant Butte Reservoir (Figure 1). Along this reach, the Rio Grande supplies water for riparian vegetation, agriculture, municipal uses, and endangered species habitat. The amount of water that New Mexico communities north of Elephant Butte Reservoir are allowed to use from the Middle Rio Grande is mandated by the Rio Grande Compact based on flows at the Otowi gage, located north of Santa Fe. Water that is not allotted for central New Mexico is stored at Elephant Butte Reservoir to be delivered to southern New Mexico and Texas. Therefore, it is important to convey water adequate for compact obligations along the Middle Rio Grande to Elephant Butte Reservoir. This study focuses on a critical reach of the river between San Acacia and Elephant Butte Reservoir. Along this reach, losses from the river to the shallow alluvial aquifer and diversions for agriculture often cause the river to dry up during the summer, making it difficult to deliver water to Elephant Butte. Proper water resource management entails satisfying many different needs with a limited water supply and requires an understanding of the regional hydrologic system.

The amount and quality of water in the Rio Grande at any given time is very important for water resource management. As the amount of water in the river decreases, it becomes more difficult to allocate water for the many uses. Water quality of the Rio

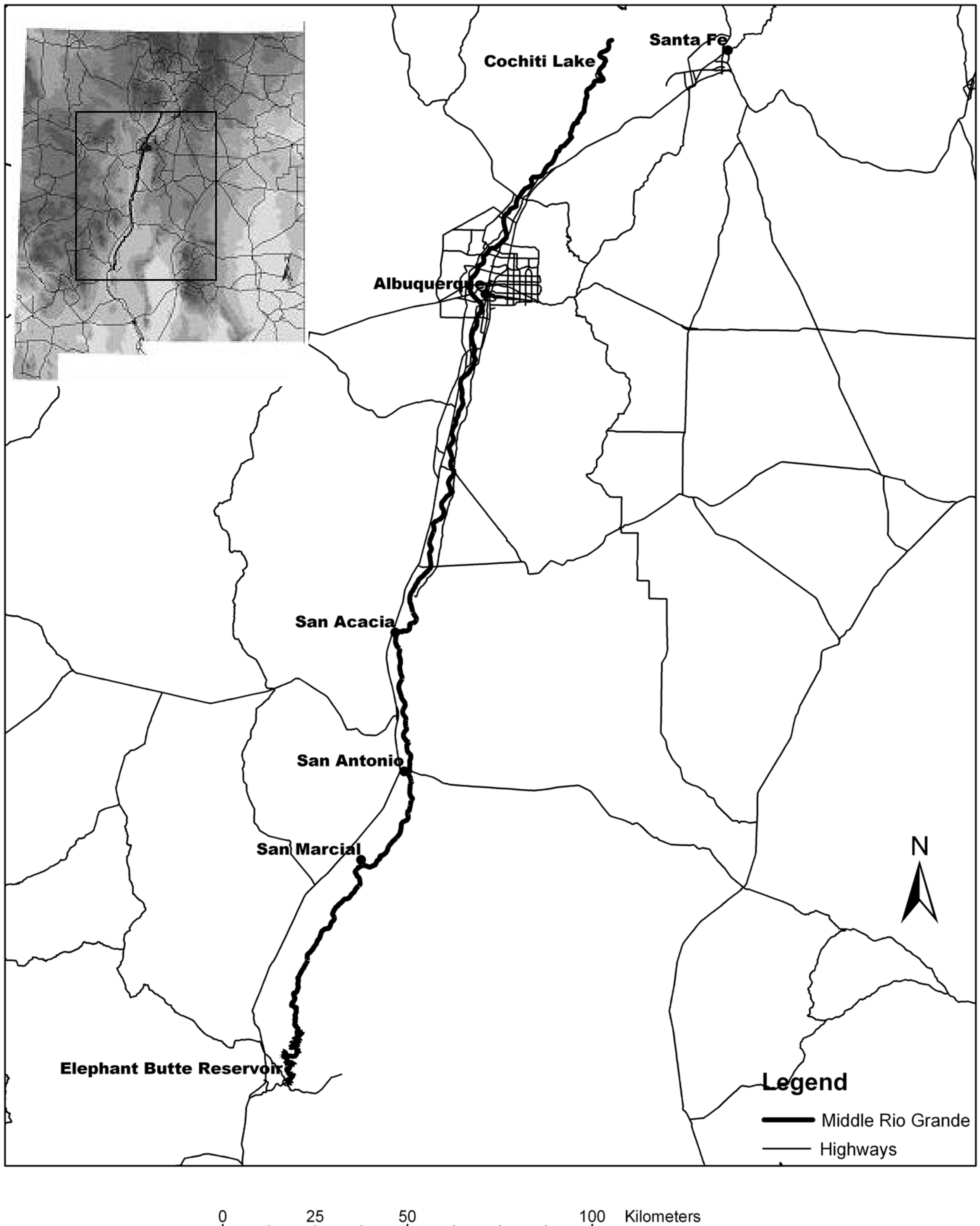

Figure 1 Location of Middle Rio Grande

Grande also has a direct impact on how that water can be used, making it necessary to understand what controls the water quality of the Rio Grande. Possible factors that affect water quality include evapotranspiration, irrigation return flow, wastewater disposal, mineral weathering, and the upwelling of deep groundwaters. As the Rio Grande flows south, the water quality decreases due to increasing TDS. Mills (2003) demonstrated that while evapotranspiration, irrigation return flow, and wastewater disposal does indeed affect the water quality of the Rio Grande, the introduction of deep sedimentary brines may also play a large role in the degradation of quality of water in the Rio Grande. Therefore it is necessary to learn more about where these saline waters are coming from and what mechanisms are forcing them up to the shallow hydrologic system.

This study is part of a larger project funded by the New Mexico Interstate Stream Commission and the Army Corps of Engineers. The primary objective of this project is to create a hydrologic model of the reach of the Rio Grande between San Acacia and Elephant Butte Reservoir that includes groundwater/surface-water interactions (Wilcox, 2003). Groundwater levels were monitored in wells that are located along transects that go across the river (Wilcox, 2003). The New Mexico Interstate Stream Commission has constructed a preliminary regional model and Wilcox (2003) constructed a telescopic model of a reach where the largest river seepage rates were observed (Papodopulos, 2002; Newton et al, 2002). Groundwater and surface-water samples were collected along the well transects for chemical and isotopic analyses. These analyses will be discussed in this thesis.

This study focuses on the regional hydrologic system in the Socorro Basin (figure 2) located between San Acacia and San Marcial. Isotopic and chemical analyses of

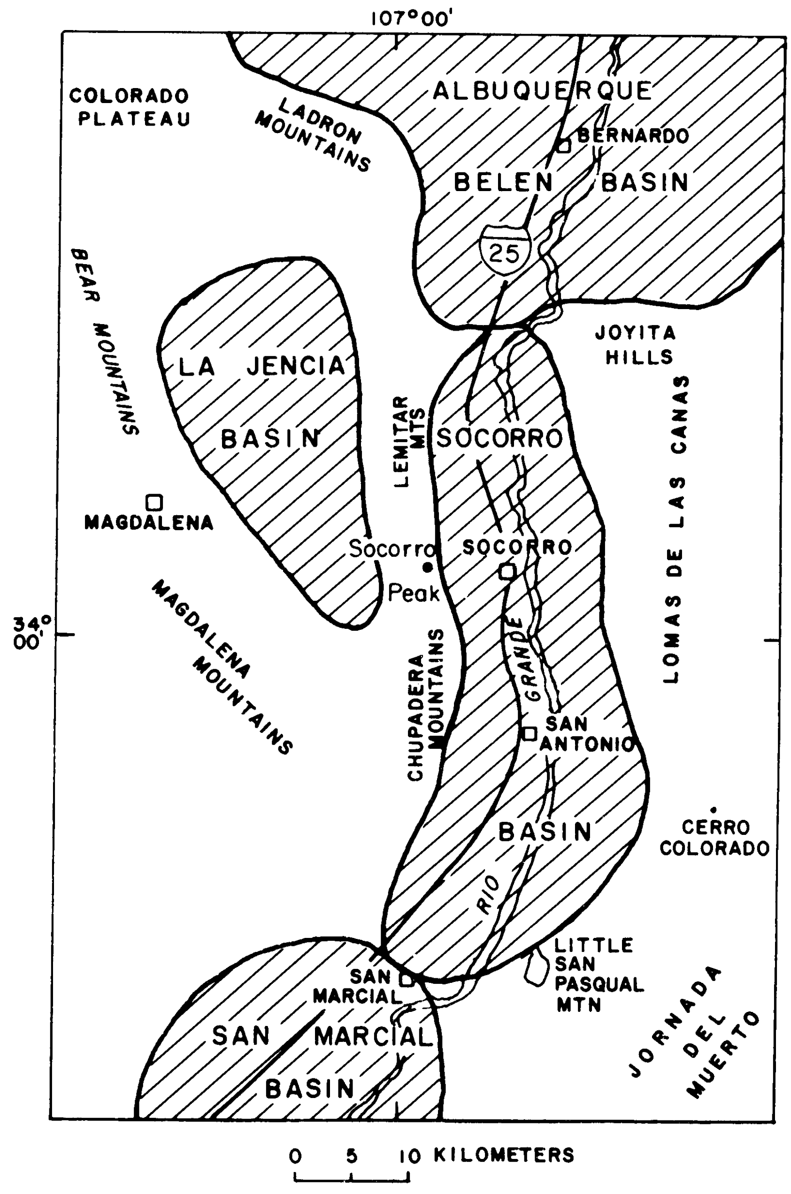

Figure 2 General location of basin boundaries in the study area (Anderholm, 1983)

groundwater and surface water in the Socorro Basin indicate that there are several distinct water types that come from different sources. Among these water types in the shallow aquifer system, a high-chloride water was identified that is believed to be a deep sedimentary brine similar to those that Mills (2003) attributed to much of the degradation of the water quality of the Rio Grande. This thesis develops a hypothesis that relates the flow paths of these different water types that produce the observed spatial variability of groundwater chemistry in the Socorro Basin, as well as the presence of these high-chloride waters to the structural framework of the Socorro Basin

Purpose and Objectives

In addition to gaining a better understanding of the regional hydrologic system in the Socorro basin, the main purpose of this study is to formulate a hypothesis to explain the observed spatial variability of groundwater chemistry in the Socorro Basin. The objectives of this study are:

1) to use the stable isotopes of hydrogen and oxygen to identify primary water types in the shallow aquifer in the San Acacia reach.
2) to characterize the general water chemistry of both groundwater and surface water in the study area
3) to use water chemistry to evaluate regional flow paths in the Socorro Basin
4) to use water chemistry to identify different mixing processes in the Socorro Basin
5) to assess the role of the structural framework of the Socorro Basin on the spatial variability of groundwater chemistry and the upwelling of deep sedimentary brines into the shallow aquifer system.

DESCRIPTION OF STUDY AREA

Location

Figure 3 shows the study area, which is in central New Mexico within the Rio Grande rift between San Acacia and Elephant Butte Reservoir. The Rio Grande rift is a structure dominated by extensional tectonics. It is made up of several basins that are connected by the Rio Grande. The San Acacia reach of the river flows through two basins, the Socorro Basin in the north and the San Marcial Basin to the south (figure 2). The northern boundary of the study area is very close to the boundary between the Albuquerque Basin and the Socorro Basin at San Acacia. The study area is bounded by the Lemitar Mountains, Socorro Peak, and the Chupadera Mountains to the west and the Joyita Hills, the Lomas de las Canas uplift, Cerro Colorado, and Little San Pascual Mountain to the east (figure 4). The La Jencia Basin (figure 2), located just to the west of the Socorro Basin, is also an important feature, whose relevance will be discussed later.

Climate and Vegetation

The study area is located within the northern limits of the Chihuahuan Desert and has an arid to semiarid climate. Annual precipitation in Socorro averages approximately 9.5 inches (WRCC, 2004), much of which is a result of afternoon thunderstorms during the summer (July through September). Higher altitudes receive significantly more

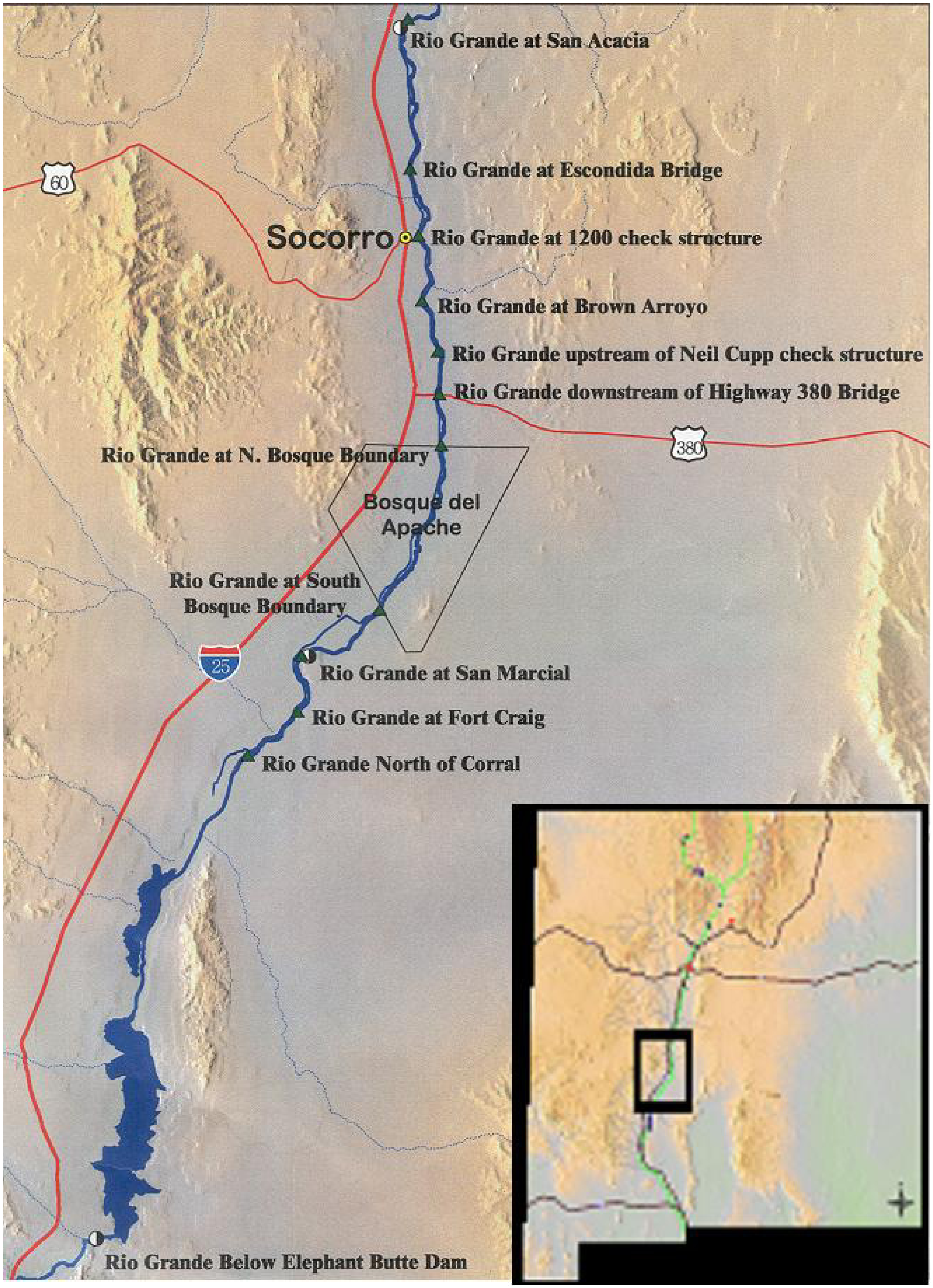

Figure 3 Location of study area with landmarks indicated, modified from Papadopulos (2000)

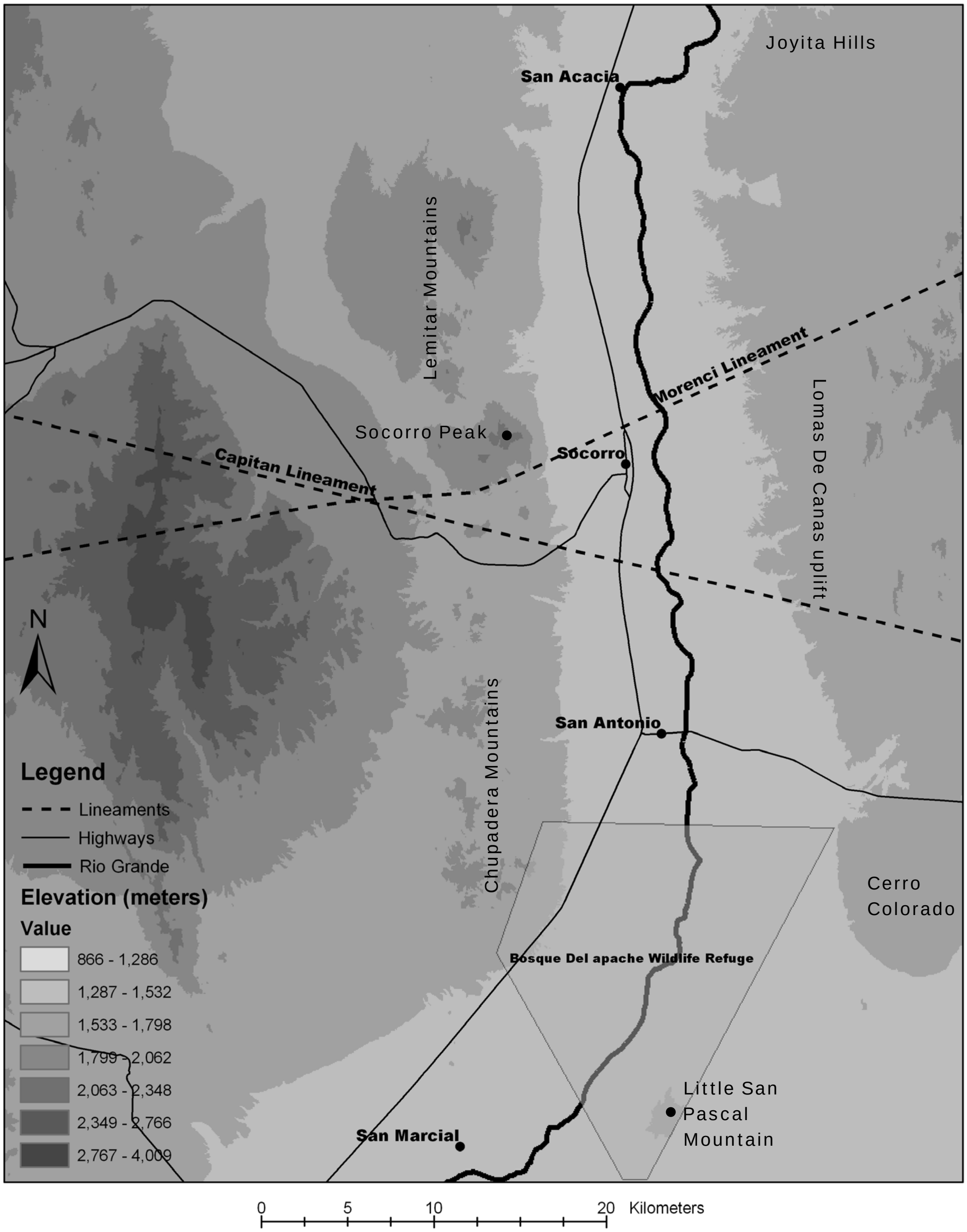

Figure 4 Location of study area, boundaries of the Socorro Basin, and structural features

precipitation. In Magdalena just west of the study area, the annual average precipitation is 11.75 inches (WRCC, 2004).

Vegetation in the study area is primarily dominated by grass and shrubs, such as mesquite and creosote, except along the Rio Grande. Areas adjacent to the Rio Grande are characterized by riparian vegetation and farmland. Riparian vegetation includes cottonwoods, willows, tamarisk, and Russian olive. Most agriculture takes place on the flood plain west of the Rio Grande.

Geologic Setting

The Rio Grande Rift

The Rio Grande rift is an extensional structure, characterized by a chain of half grabens, with the Colorado Plateau to the west and the interior of the continental crayton on the east. To the north, linked basins terminate in Central Colorado, but this might not represent the northern extent of the rift (Chapin and Cather, 1994). The northern and central Rio Grande rift, between central Colorado and just north of Soccorro, New Mexico, is made up of four axial basins, the most southern of which is the Albuquerque Basin. To the south of the Albuquerque Basin, the rift widens into a series of parallel basins and intrarift tilted block uplifts, such as the Socorro Basin and the La Jencia Basin, which are separated by the Lemitar Mountains and Socorro Peak. Throughout the Rio Grande rift, the axial basins are asymmetric half grabens, hinged down on one side with major fault boundaries on the opposing sides. The sense of asymmetry changes from basin to basin with transfer faults or accommodation zones dividing east-tilted and west-tilted basins or basin segments (Chapin and Cather, 1994).

The Socorro Area

This section will provide a general description of lithologic units and then concentrate on the structural history from the beginning of rifting. Detailed geologic maps of the 7.5 minute quadrangles of the area were constructed by Cather and Chamberlain, but because some of them are still in preliminary stages of completion and the difficulty of capturing the amount of detail that they contain, these maps are not presented in this thesis. Instead, a simplified geologic map of the Socorro area modified from Cather et al. (1994) (figure 5), a geologic cross-section modified from Chapin et al. (1978) (figure 6), and a stratigraphic column from Cather et al. (1994) (figure 7) are provided. It should be noted that although the approximate location of the geologic cross-section is shown on the geologic map shown in figure 5, the cross-section was constructed from an older geologic map. Therefore the geologic units shown on the cross-section may not perfectly correlate to those shown on the geologic map, but the cross-section suitably depicts the structural geometry and spatial relationships among the different geologic units for the purpose of this thesis. Also, the Quaternerary alluvium shown on the geologic map is included in the Sierra Ladrones Formation on the cross-section.

Stratigraphy and Lithology

For some of the older geology, the geologic map (figure 5) lumps many different rocks into a single category. This paragraph will give a brief description of the rocks in each category. Proterozoic rocks consist of low grade metasedimentary and metavolcanic rocks intruded by granitic and gabbroic plutons and diabase dikes (Chapin

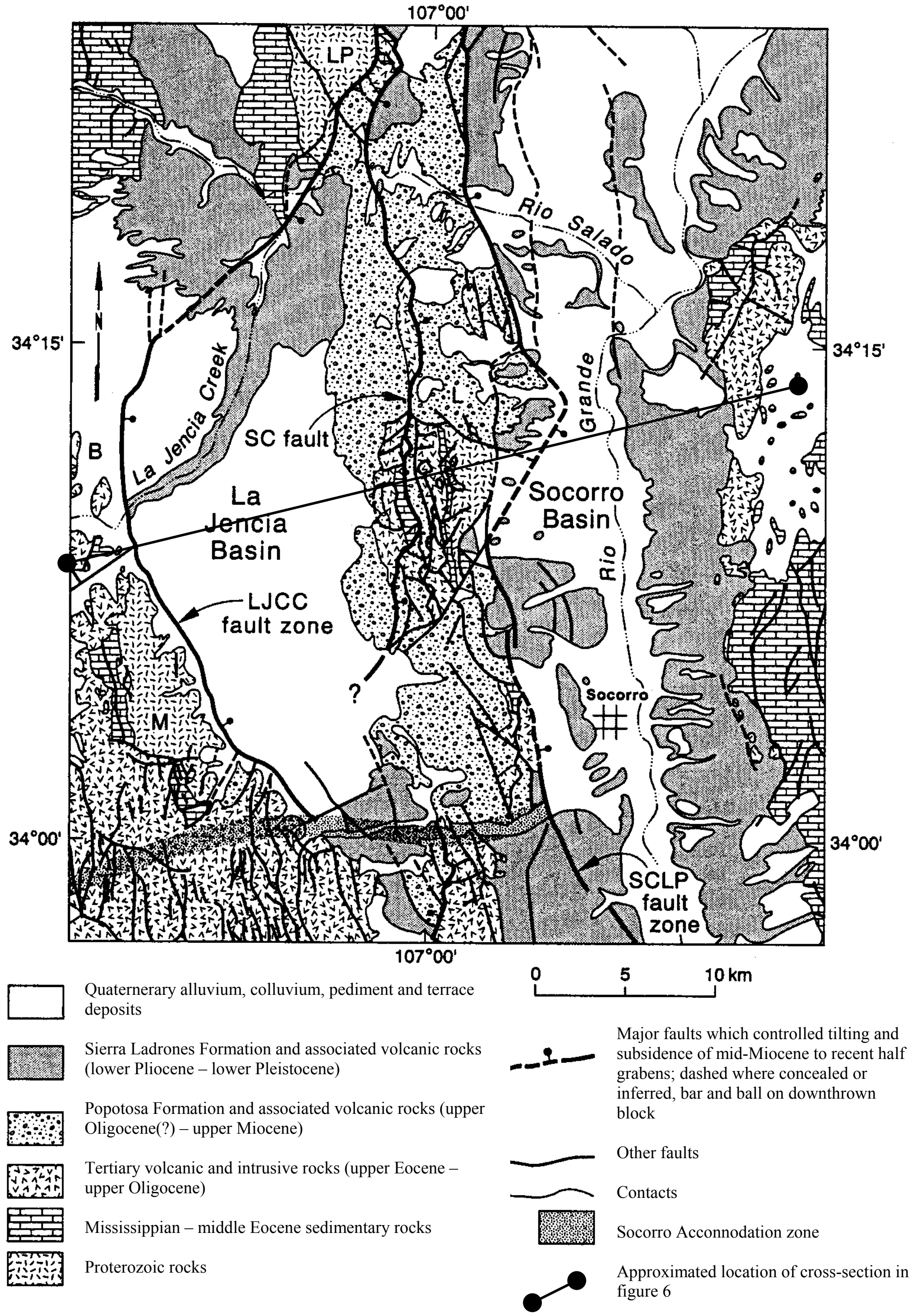

Figure 5 Simplified Geological map of the Socorro and La Jencia Basins modified from Cather et al. (1994)

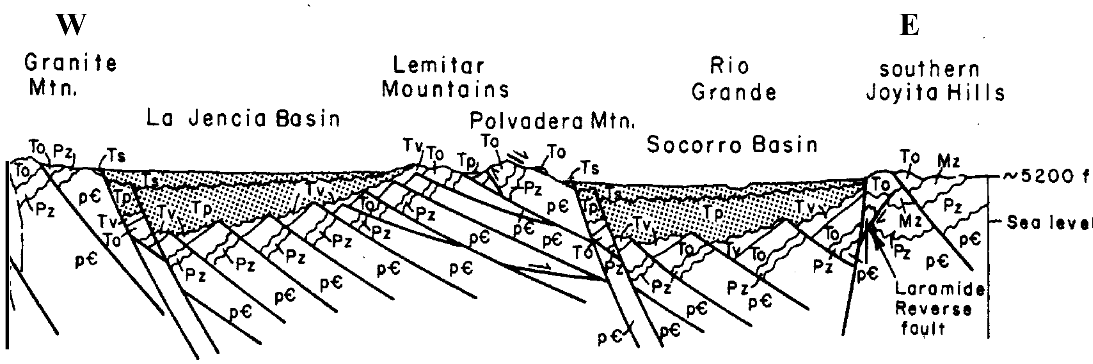

Santa Fe Group
- Ts – Sierra Ladrones Formation, includes minor post Santa Fe alluvium
- Tp – Popotosa Formation

Tv – Syn-rift volcanic rocks

To – Pre-rift volcanic rocks

Mz – Mesozoic rocks

Pz – Paleozoic rocks

Pε - Precambrian rocks

Figure 6 Geologic cross-section of La Jencia and Socorro Basins modified from Chapin et al. (1978). The location of the cross-section is shown on figure 5

et al., 1978). Mississippian – middle Eocene sedimentary rocks include Paleozoic limestones such as the Sandia Formation and Madera limestone near Socorro. The Sandia Formation is made up of shales, quartzites and limestones. To the East of the Rio Grande, Permian rocks include the Bursum Formation, the Abo Formation, the Yeso Formation, Glorieta Sandstone and the San Andres Formation, which are characterized by mudstones, sandstones, conglomerates, and limestones (Cather, 1982). Mesozoic mudstones, sandstones, and shales are observed to the east of the Rio Grande. These Mesozoic rocks include Triassic rocks, such as the Santa Rosa Sandstone, and the Chinle Formation and Cretaceous rocks such as Dakota Sandstone and the Mancos Shale. Middle Eocene rocks include the Baca formation, which is characterized by conglomerate and sandstone consisting of detritus from Paleozoic, Precambrian, and Mesozoic sources (Cather, 1982). Tertiary volcanic rocks include volcaniclastic rocks, ash-flow tuffs, and

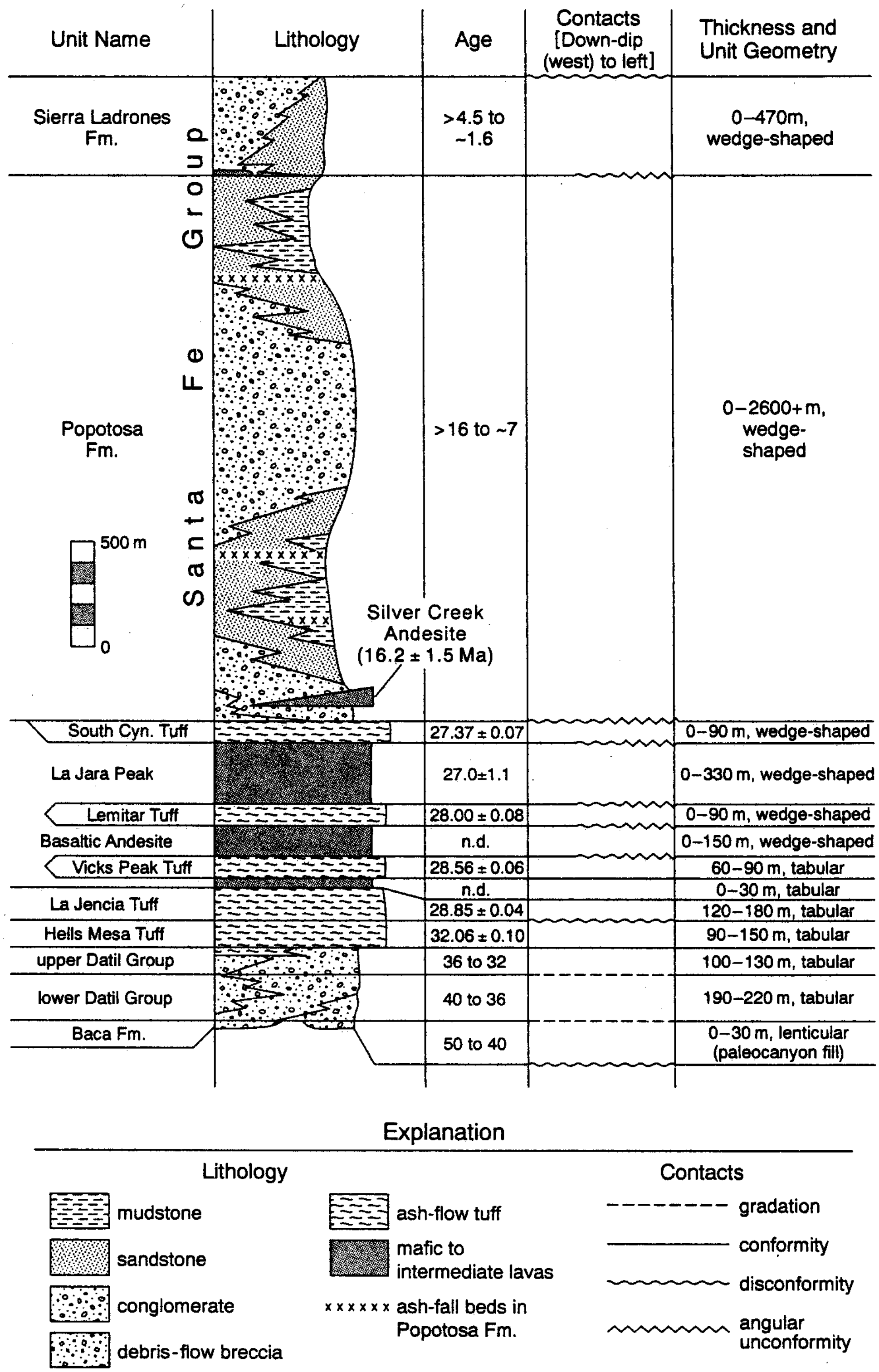

Figure 7 Stratigraphic column for Socorro area from Cather et al. (1994)

basaltic and rhyolitic lavas. The following geologic description of the Santa Fe Group is based on Cather (1996). The Popotosa Formation or lower Santa Fe Group (lower Miocene - upper Miocene) is made up of many different facies. The lower Popotosa Formation includes volcanic flows, domes and coarse tephra, and an axial stream facies that is characterized by interbedded fluvial conglomerate, sandstone, siltstone, and claystone. Cather (1994) describes this facies as being "characterized primarily as relatively fine-grained fluvial sequences that are stratigraphically juxtaposed between the relatively coarser deposits of laterally opposed piedmont systems." This stratigraphic relationship may have some important hydrological implications that will be discussed later. The upper Popotosa formation is mainly composed of a playa facies that is characterized by a dominance of red-brown mudstone. Piedmont facies at the margins of the basin include sandstone, conglomerate and debris flow. The Sierra Ladrones formation (upper Santa Fe Group) generally consists of piedmont deposits and sediments related to the development of the ancestral Rio Grande. Piedmont facies range from conglomerate dominated to sandstone dominated facies. The axial-river facies includes channel and floodplain deposits of ancestral Rio Grande consisting of sandstone, mudstone, and conglomerate. The axial river facies intertoungue with the piedmont facies laterally from the center of the basin to the basin margins.

Structural History

The major structural features in the study area are the Socorro Basin, La Jencia Basin, the Chupadera Mountains, the Socorro Peak-Lemitar Mountains, and the Morenci and Capitan Lineaments (figure 4). Three events that influenced the structural geology of this area are ancestral Rocky Mountain tectonism, Laramide tectonism, and Rio Grande rifting. Evidence of all three of these events is observed in the Joyita Hills and the resulting structural trends appear to be due to the reactivation of Proterozoic structures (Beck and Chapin, 1994). Based on the age of synrift volcanic rocks, rifting in the Socorro area began between 28.8 and 27.4 Ma (Chapin and Cather, 1994), causing the collapse of a Laramide uplift that encompassed much of the study area (Cather et. al, 1994; Chamberlain et al., 1986). Rifting in the Socorro area ultimately formed the Popotosa basin as a result of domino style normal faulting (Chamberlain, 1983; Beck and Chapin, 1994). There were two main episodes of rapid extension (Chapin and Cather, 1994; Cather et al., 1994) during the formation of the Popotosa Basin. The first period of rapid extension (late Oligocene, 28.6 – 27.4 Ma) resulted in the formation of multiple half grabens defined by narrowly spaced (2 – 5 km) planar rotational normal faults. In the northern section of the Popotosa Basin, which was approximately 45 km long (Chapin and Cather, 1994), the normal faults dipped to the east with hanging wall fault blocks tilting to the west. In the southern part of the Popotosa Basin, normal faults dipped to the west with fault blocks tilting to the east. The area separating the tilt domains is called the Socorro Accommodation Zone, which will be discussed in detail below. This episode of faulting and rotation of fault blocks, lasting about 1.2 m.y., resulted in approximately 25% extension (Chapin and Cather, 1994). Ash-flow tuffs and mafic lavas (Tertiary volcanics described above), resulting from volcanism associated with rifting, buried the fault block topography. Debris flow, alluvial fan, and fluvial deposits of the Popotosa formation began to fill in the closed Popotosa Basin. During the deposition of the Popotosa Formation, the second episode of extension occurring between 16 and 10 Ma

(Chapin and Cather, 1994), resulted in the uplift of the Lemitar mountain block, which divided the Popotosa Basin into two separate basins: the Socorro Basin and the La Jencia Basin. During the early Pliocene, the ancestral Rio Grande breached the Socorro Basin, interconnecting the Socorro Basin to the Albuquerque Basin in the north and to the San Marcial Basin in the South. The Sierra Ladrones Formation in the Socorro Basin was deposited as axial river deposits interfingering with bordering piedmont deposits. The Sierra Ladrones Formation represents aggradation of the ancestral Rio Grande. Post Santa Fe incision began in early or middle Pleistocene time.

The Socorro Accommodation Zone (SAZ)

An important feature of the structural geology of the Socorro Basin is the Socorro Accommodation Zone (SAZ). The SAZ is a two-kilometer-wide boundary between two domains in which domino-style fault blocks are tilted in opposite directions (Chapin, 1989). Figure 8 shows the location of the SAZ as defined by Chapin. To the north of the SAZ, fault blocks are rotated and tilted to the west, while fault blocks to the south of the SAZ are tilted to the east. The following description of the SAZ is from Chapin (1989). The SAZ is relatively linear feature that is oriented along the Morenci lineament at a high angle to the trend of the Rio Grande rift. Within the SAZ, stratal tilts are sub-horizontal to gently tilted. The SAZ is approximately perpendicular to synrift faults with very few faults parallel to the SAZ. There is no noticeable evidence of strike-slip offset, and the SAZ is not marked as a noticeable shear zone at the surface. The location of springs and K- metasomatism indicates groundwater movement along the SAZ, and there is evidence

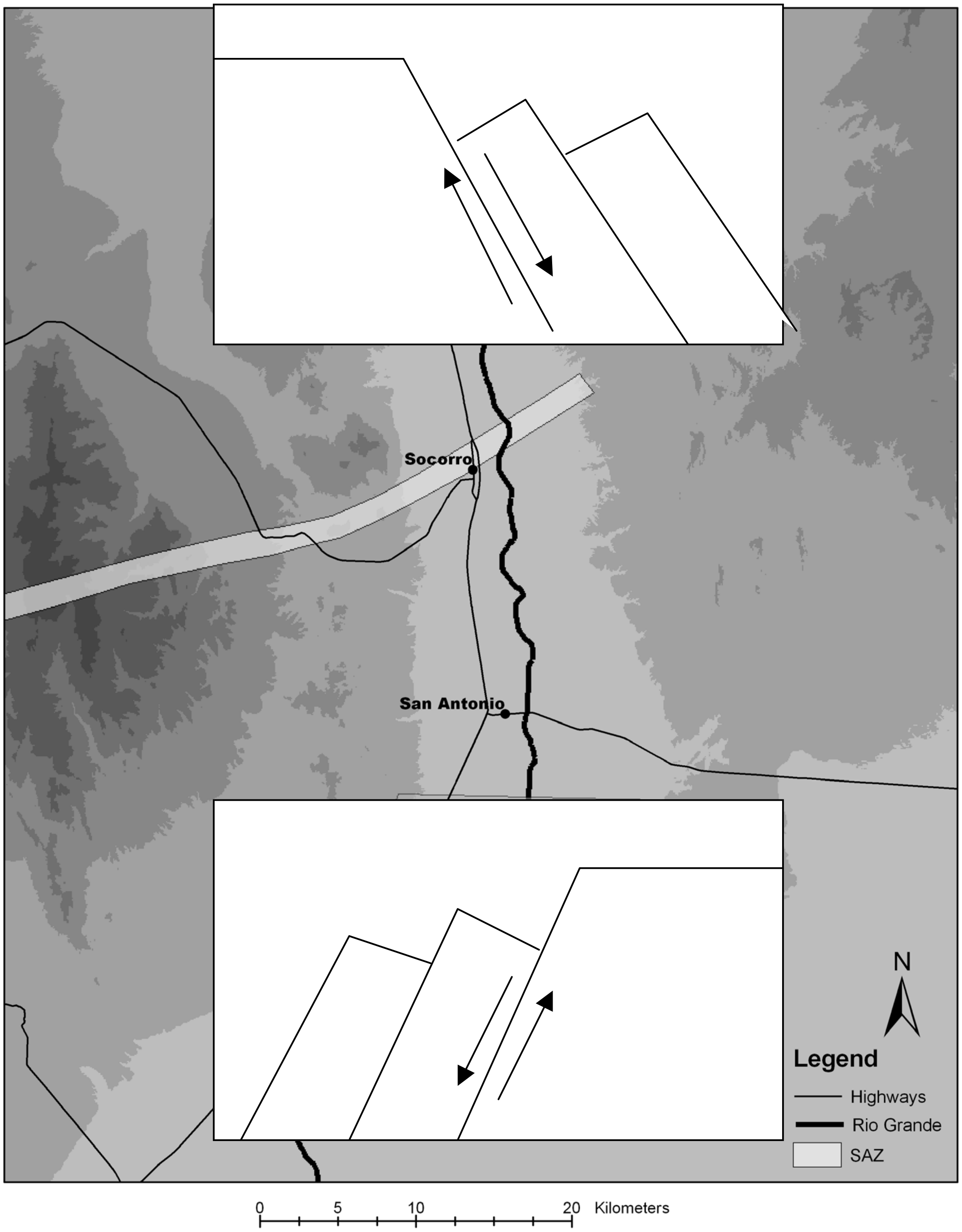

Figure 8 Location of the Socorro Accommodation Zone as defined by Chapin (1989) and fault block tilt directions in the Socorro Basin

that the SAZ has leaked magmas since before 27.9 Ma. The SAZ is also the southern boundary of a mid-crustal magma body.

Gravity Data and Their Implications About the Structural Framework of the Socorro Basin

Some geophysical data are available that are quite helpful in studying the structural geology in the Socorro Basin. Gravity due to the mass between an observation point and a given datum is called a Bouger anomaly. This type of data can be helpful in geologic studies because it is dependent on the density of the material below the point where the gravity measurement is taken. The highest resolution gravity survey in the area was done by Sanford (1968). Figure 9 shows the residual Bouger gravity map for the Socorro and San Antonio 7.5-minute quadrangles. The residual Bouger anomalies represent the part of the total Bouger anomaly attributable to near surface geologic features. According to the residual anomaly map, the Socorro Basin is characterized by a series of gravity lows that represent the Rio Grande graben . Areas bounding the Rio Grande depression with a narrow contour spacing represent faults with large displacement, while relatively wide contour spacing probably indicates step faulting with or without rotation.

Hydrologic Setting

Surface Water Hydrology

The surface water system includes the Rio Grande and a complex system of drains and canals that parallel the river. Irrigation takes place between March 1st and

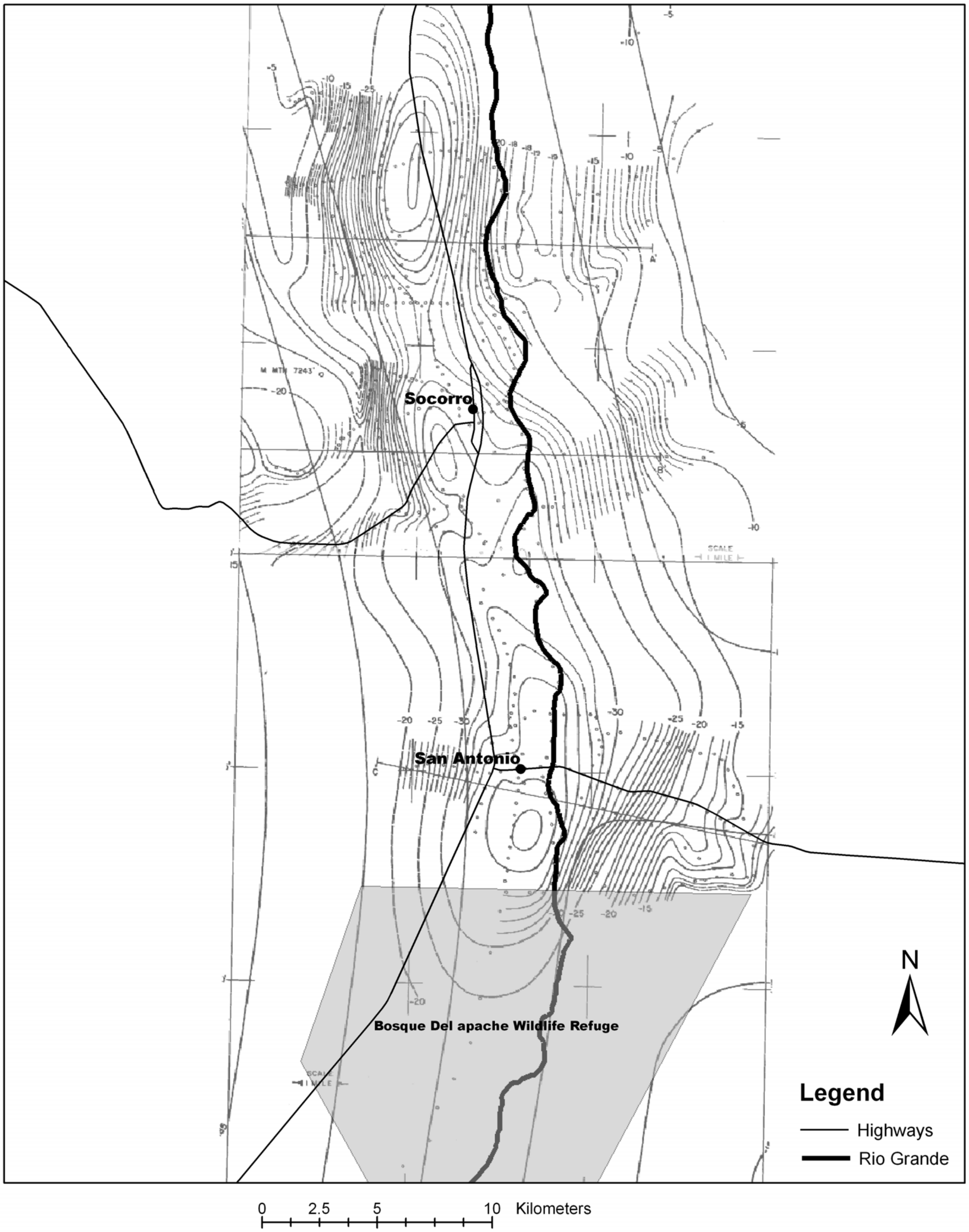

Figure 9 Residual Bouger anomaly map of the Socorro and San Antonio quadrangles (Sanford, 1968)

October 31st, when water is diverted from the river at a diversion structure at San Acacia to the Socorro Main Canal, which supplies water to irrigated fields. Water in irrigation drains is primarily derived from shallow groundwater seepage. During the non-irrigation season, the Socorro Main Canal and other canals that carry water to irrigated fields are dry, but drains continue to capture irrigation return flow.

The San Acacia reach of the Rio Grande loses water to the shallow aquifer. Estimated seepage rates from the Rio Grande range between 0 and 21 cfs/mile, with the highest losses observed between Brown Arroyo and HWY 380 (Papadopulos, 2002; Newton et al, 2002).

Another important feature in the surface water system is the Low Flow Conveyance Channel (LFCC). The LFCC is a canal just west of the river that runs from San Acacia almost all the way to Elephant Butte Reservoir. The LFCC was built in the 1950's to convey water to Elephant Butte Reservoir in a more efficient manner. Initially, water was diverted from the river into the LFCC. However, in the 1980's, the diversion of water from the river into the LFCC was discontinued due to problems with maintaining the connection between the LFCC and the reservoir as a result of sedimentation. The LFCC is the low point in the hydrologic system and therefore gains water from both the east and west (Figure 10). Presently, most of the water in the LFCC is derived from groundwater seepage. During the summer months, water from the LFCC is often pumped into the river in order to keep water in the Rio Grande.

Groundwater Hydrology

Figure 11 is a generalized geological cross-section (Anderholm, 1984) from west to east across the Socorro Basin and the Jencia Basin that shows the principal and minor

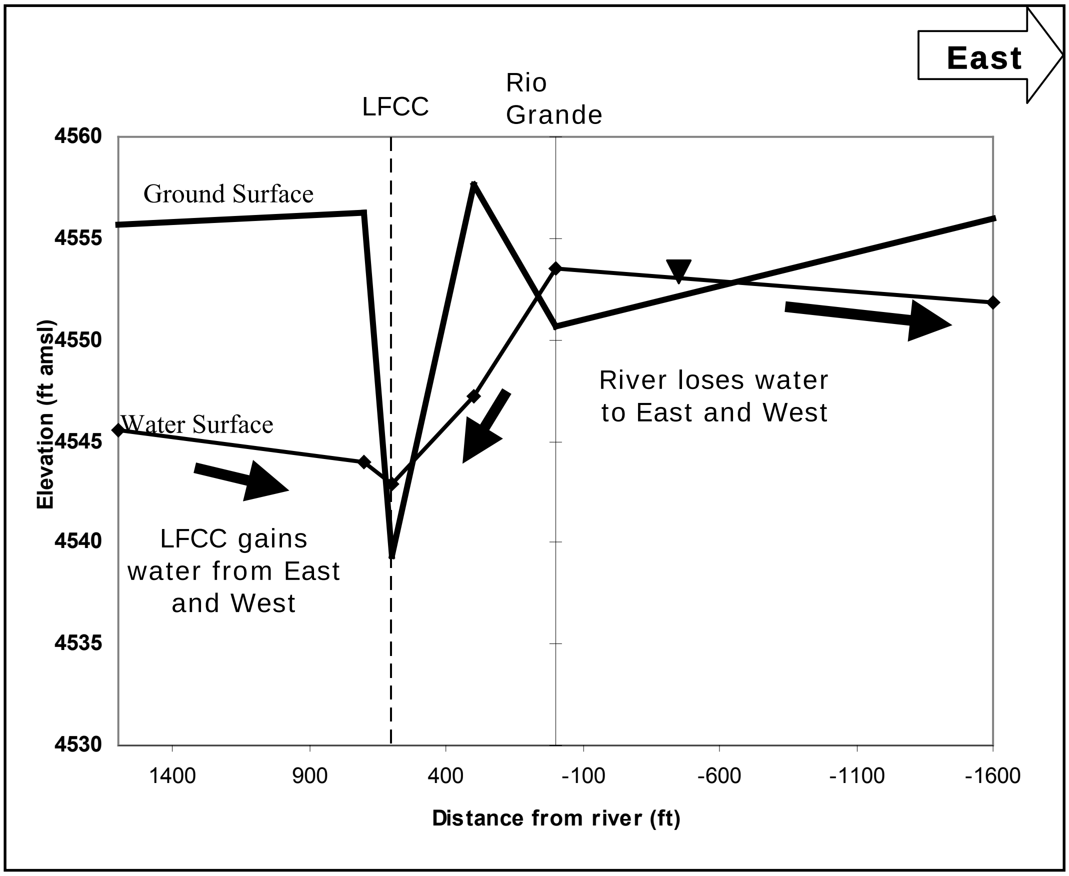

Figure 10 Water level data showing relationship between groundwater and surface water on transect located just south of Neil Cupp.

aquifer systems. The primary aquifer system includes the Sierra Ladrones Formation (upper Santa Fe Group) and the Popotosa aquifer (lower Popotosa Formation), separated by the Popotosa confining bed (Upper Popotosa Formation). The thicknesses of these units are not well known but have been estimated to be 0 to 470 meters (1500 feet) for the Sierra Ladrones Formation , and 0 to 2600 meters (8500 feet) for the Lower Santa Fe Group (Mailloux et al, 1999), which includes the Popotosa aquifer and the Popotosa confining unit. The Sierra Ladrones Formation, which consists of ancestral Rio Grande Deposits, has an estimated mean permeability of $10^{-13.7}$ m^2 (Mailloux et al., 1999). The Popotosa confining bed is dominantly comprised of Playa deposits and has an estimated

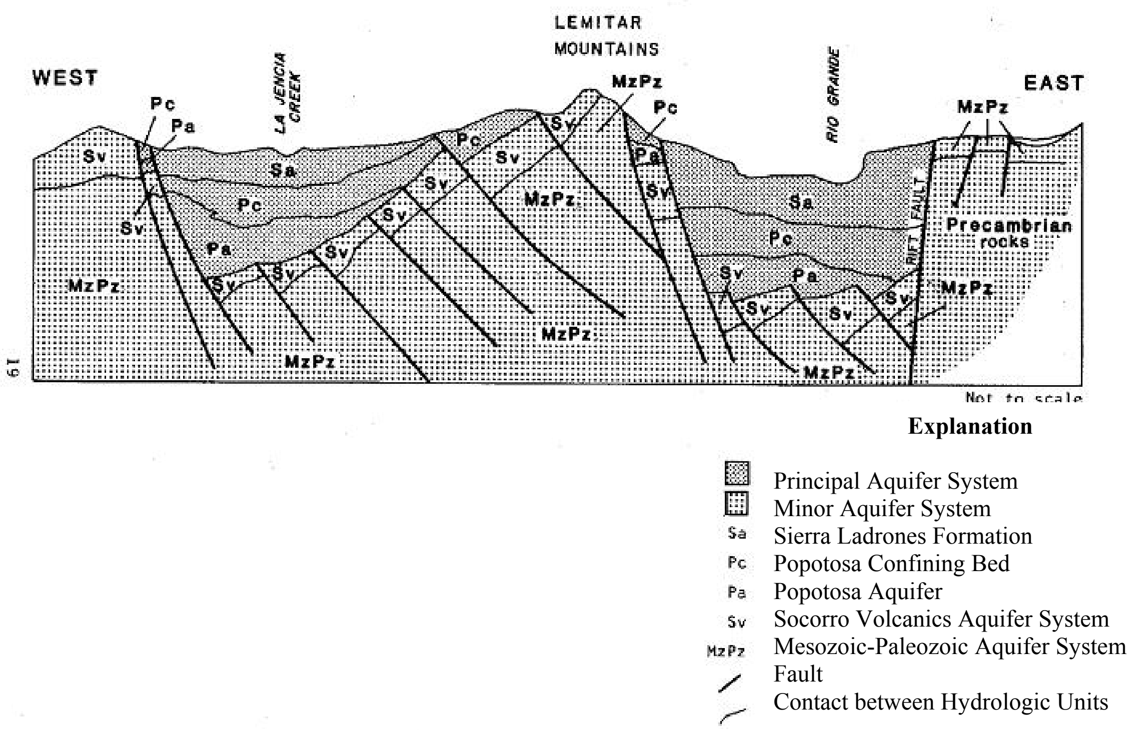

Figure 11 Generalized cross-section through La Jencia Basin and the Socorro Basin (Anderholm, 1984)

mean permeability of 10^{-16}m^2 (Mailloux et al., 1999). The Popotosa aquifer is composed of sandy silt stone, coarse sandstones, and conglomerates, with estimated mean permeabilities ranging from $10^{-15.3}$ m^2 to $10^{-13.5}$ m^2 (Mailloux et al, 1999). The minor aquifer systems are composed of Tertiary volcanics, and Mesozoic and Paleozoic sedimentary rocks (Anderholm, 1984). These units that make up the minor aquifer systems are characterized by low permeability, and therefore produce significantly less water than the primary aquifer system. Secondary permeability, such as fractures, is believed to be an important factor in the minor aquifer systems (Anderholm, 1984).

The shallow alluvial aquifer, present within the Rio Grande flood plain consists mainly of Quaternary Rio Grande deposits. This aquifer overlies the Sierra Ladrones

Formation and ranges in thickness from 0 to 100 feet (Papodopulos, 2002). The estimated mean permeability based on an aquifer test (Mailloux et al, 1999) ranges from $10^{10.6}$ m^2 to $10^{10.8}$ m^2. Anderholm (1983) constructed a water table map for the Socorro Basin (figure 12), showing that groundwater in the shallow aquifer mainly flows from north to south within the basin, with water coming into the shallow system from the east and west. The indicated hydrologic discontinuities are mainly due to structures related to the Rio Grande rift. At the regional scale that this water table map is shown, the Rio Grande appears to be a gaining stream along the entire reach. In fact, on a smaller scale, the Rio Grande is a losing stream along this entire reach as can be seen in figure 10.

High-Chloride Waters in the Socorro Basin

Location of High-Chloride waters

Figure 13 shows a topographic map of the study area along with chloride concentrations in groundwater. Sample locations shown include samples collected for this study, as well samples collected by Brandvold (2001). The high-chloride waters of interest are orange and red points within the ovals in figure 13. The most northern location where these high-chloride waters are observed is in the Luis Lopez Drain. Most of these high-chloride waters are located around San Antonio on both sides of the river, with the most southern location of these high-chloride waters in the Bosque Del Apache.

Origin of High-Chloride Waters

The high-chloride waters that are of interest for this study are believed to be sedimentary brines that originate deep within the Socorro Basin. The water chemistry

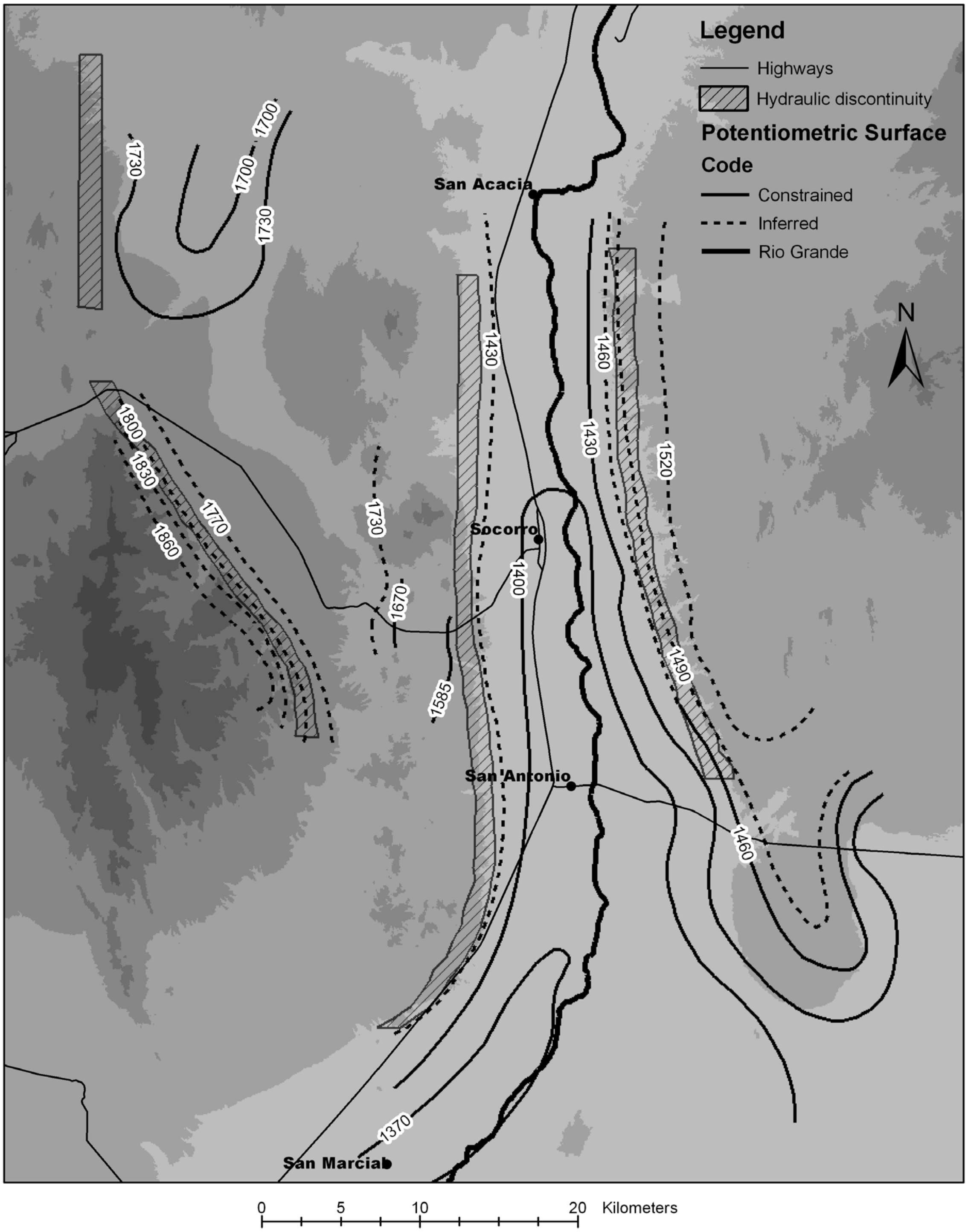

Figure 12 Pontentiometric surface contour map of study area (Anderholm, 1983). Water table elevations are in meters.

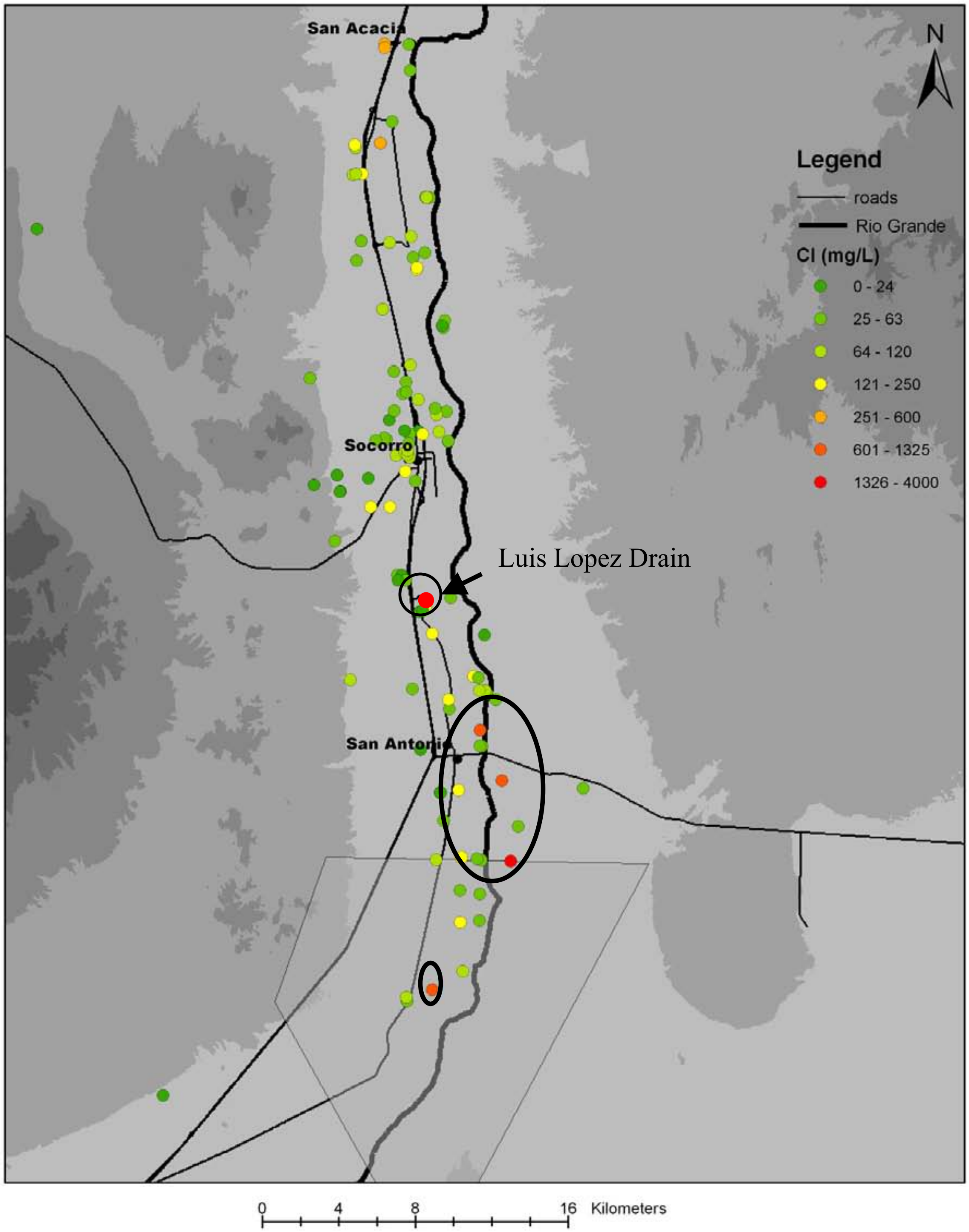

Figure 13 Chloride concentrations (mg/L) in groundwater in study area. Orange and red points within ovals indicate high-chloride waters of interest.

that supports this origin will be discussed later. Mills (2003) demonstrated that high-chloride waters similar to those observed in the shallow groundwater system in the Socorro Basin might be contributing significantly to the deterioration of the water quality in the Rio Grande. Figure 14 shows the TDS values of the Rio Grande as a function of distance from the headwaters in Colorado. Interestingly, south of Albuquerque, the TDS values are observed to increase in a stepwise fashion. Mills (2003) hypothesized that in these areas along the Rio Grande, sedimentary brines are being introduced into the river. Figure 15 shows a conceptual model developed by Mills (2003) that suggests that these high-chloride waters are forced up to the shallow hydrologic system at the terminal ends of the basins through faults and fractures. As can be seen in figure 13, most of the high-chloride waters in the Socorro Basin are north of the terminal end of the basin near San Marcial, and therefore, imply a more complex scenario of brine discharge than the simple conceptual model presented in figure 15. Anderholm (1984) observed these same high-chloride waters in the shallow groundwater system near San Antonio and offered two hypotheses to explain their presence. Figure 16 is a conceptual model of one of Anderholm's hypotheses that involves faults that cut across the basin and cause the juxtaposition of permeable rocks with rocks of lower permeability, resulting in the upwelling of deep groundwaters. Anderholm's other hypothesis suggests that these brines are related to geothermal water leaking upward along rift faults that do not necessarily cross the basin, and mixing with water traveling along deep flow paths from the La Jencia Basin (Figure 17). Anderholm also suggests that the Capitan lineament (Figure 4) may be involved in the upwelling of these high-chloride waters because it coincides with the most northern occurrence on these high-chloride waters. Both of

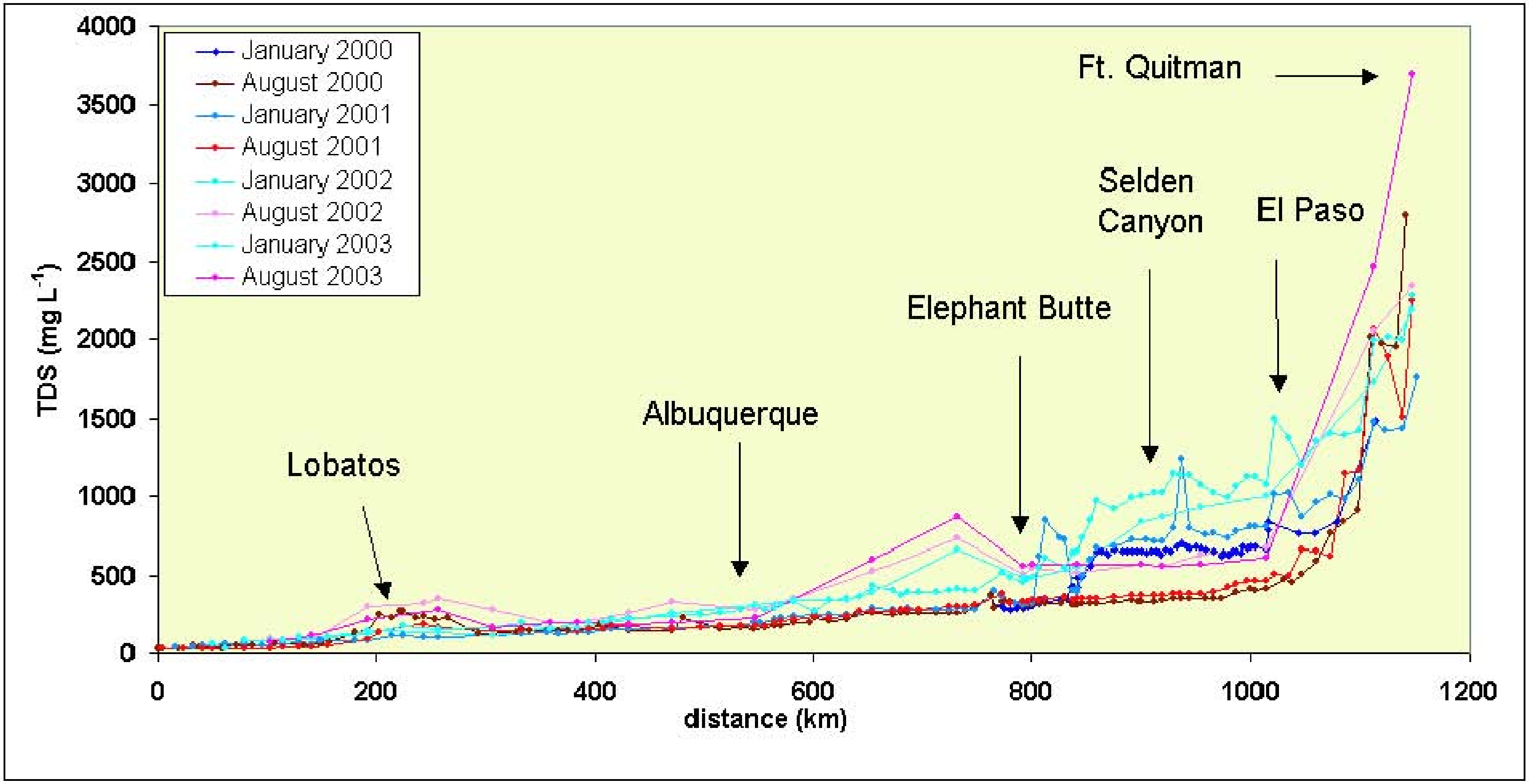

Figure 14 TDS in the Rio Grande as a function of distance from the headwaters in Colorado (Mills, 2003)

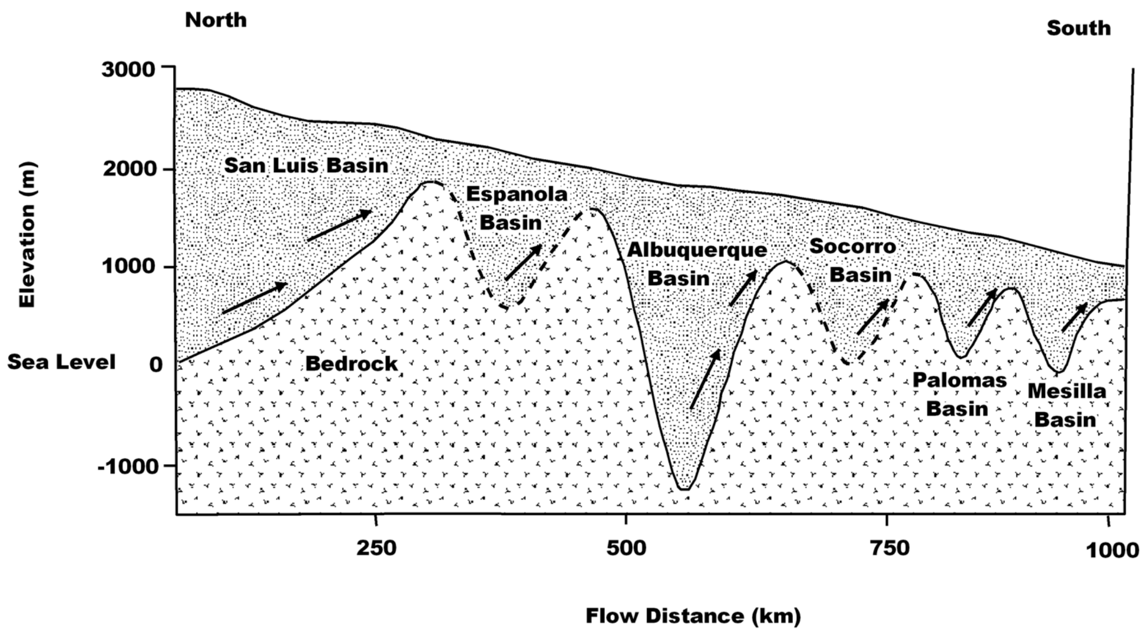

Figure 15 Schematic hydrogeologic cross-section parallel to river path (Mills, 2003)

Anderholm's hypotheses and Mill's hypothesis relate the upwelling of deep water with structures, such as faults in the Rio Grande rift.

These high-chloride waters are believed to be sedimentary brines based on water chemistry. The main indicator of sedimentary brines was a high Cl concentration and a high Cl/Br ratio. Waters of different sources have easily distinguishable chemical signatures in terms of chloride and bromide: meteoric waters tend to have a low Cl concentration and a Cl/Br ratio less than 150; wastewater tends to have a much higher Cl concentration and a Cl/Br ratio of 300 to 600; deep groundwaters and geothermal waters commonly have high chloride concentrations and Cl/Br ratios of 1000 or greater (Davis et al., 1998). High-chloride waters chemically similar to those observed in the shallow

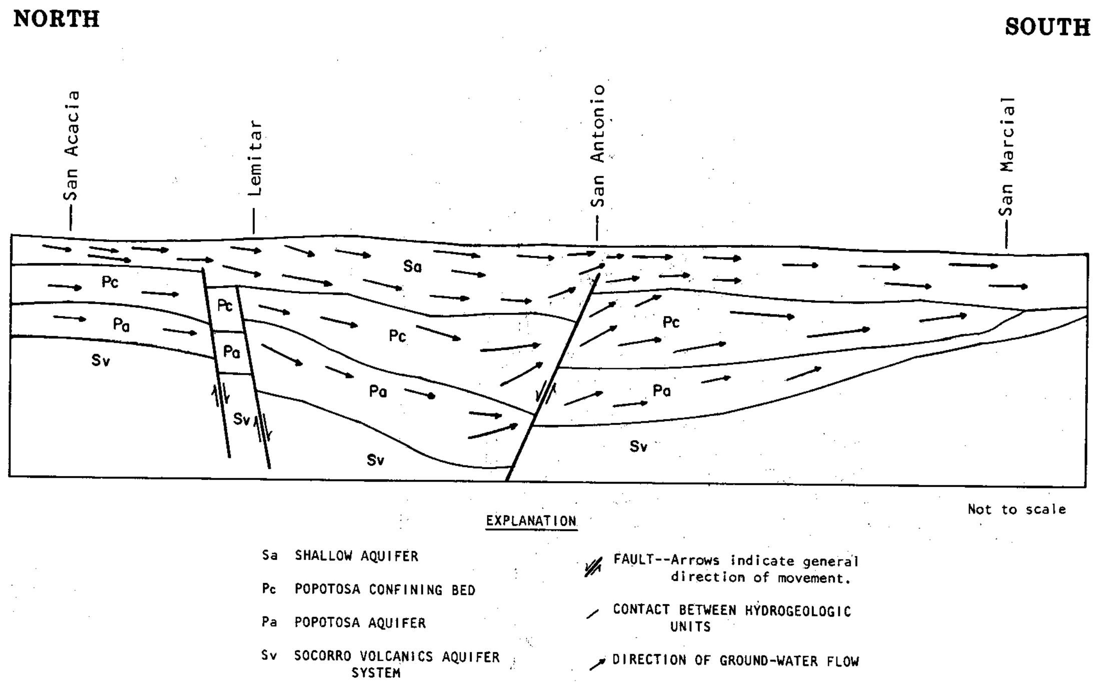

Figure 16 Anderholm's (1984) conceptual model for the transporting of deep waters to shallow system involving a cross-basin fault

groundwater system in the Socorro Basin have been observed in other areas of the Rio Grande rift. Goff et al (1983) observed similar high-chloride waters near the Lucero Uplift, which forms the western topographic and structural boundary of the Albuquerque Basin portion of the Rio Grande rift, located approximately 75 miles north of the study area. Bothern (2003) also observed similar high-chloride waters in the Mesilla Basin, the southern-most basin in the Rio Grande rift, located about 120 miles south of the Socorro Basin. The presence of these high-chloride waters appears to be associated with Rio Grande rift faults.

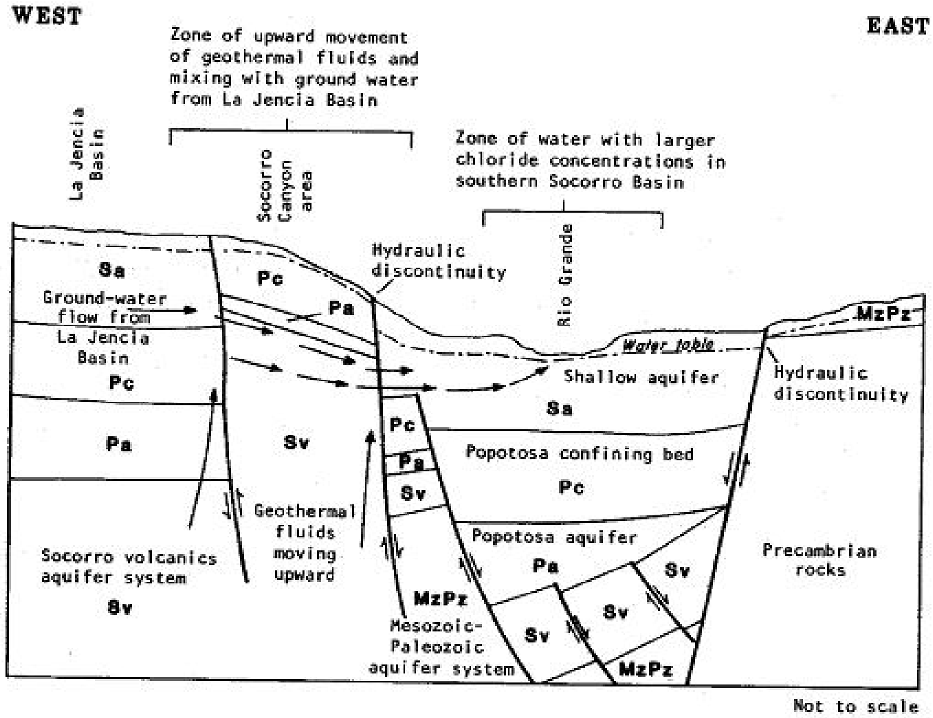

Figure 17 Anderholm's (1984) conceptual model of upwelling of deep geothermal waters along rift faults

METHODS

Water Chemistry Sampling

Groundwater and surface water samples were collected three times a year from selected wells, the Rio Grande, the LFCC and selected canals and drains in the study area. The water samples were analyzed for water chemistry and most samples were also analyzed for the stable isotopes of oxygen and hydrogen. Table 1 shows the dates of each sampling event as well as the analytes for which the samples were tested.

Table 1 Dates of sampling events and analytes for which the samples were tested

Sampling Event	Dates of Event	Analytes
1	2/15/02 – 2/18/02	$CaCO_3$, HCO_3^-, Cl^-, SO_4^{2-}, NO_3^-, PO_4^{3-}, F^-, Br^-, Na^+, K^+, Mg^+, Ca^{2+}, B, SiO_2, Sr^{2+}, Al, Li, $\delta^{18}O$, δD
2	6/11/02 – 6/13/02	$CaCO_3$, HCO_3^-, Cl^-, SO_4^{2-}, NO_3^-, PO_4^{3-}, F^-, Br^-, Na^+, K^+, Mg^+, Ca^{2+}, B, Sr^{2+}, $\delta^{18}O$, δD
3	10/12/02 – 10/14/02	$CaCO_3$, HCO_3^-, Cl^-, SO_4^{2-}, NO_3^-, PO_4^{3-}, F^-, Na^+, K^+, Mg^+, Ca^{2+}, B, SiO_2, Sr^{2+}, $\delta^{18}O$, δD
4	3/01/03	$CaCO_3$, HCO_3^-, Cl^-, SO_4^{2-}, NO_3^-, PO_4^{3-}, F^-, Br^-, Na^+, K^+, Mg^+, Ca^{2+}, B, SiO_2, Sr^{2+}
5	6/16/03	$CaCO_3$, HCO_3^-, Cl^-, SO_4^{2-}, NO_3^-, PO_4^{3-}, F^-, Br^-, Na^+, K^+, Mg^+, Ca^{2+}, B, SiO_2, Sr^{2+}

Sample Locations

Sample locations were selected in order to meet two primary objectives: to obtain a sufficient distribution and diversity of samples to provide good baseline water quality characterization of surface and groundwater in the study area and to obtain information that can be used to determine different water sources and mixing ratios of water in the hydrologic system. Most groundwater samples were collected from observation wells installed by the Bureau of Reclamation (BOR) in 1993 and 1994. The BOR wells were installed in transects that go across the LFCC. These transects are named according to a river mile, where river mile zero is at Caballo Dam, 27 miles south of Elephant Butte Dam. Table 2 lists the BOR wells that were sampled along with their locations and total depths. Geographical coordinates for each sample location are provided in appendix I. Figure 18 shows the location of each of the BOR well transects and figure 19 shows the location of each BOR well on each transect. Additional wells used for water quality sampling include domestic wells and observation wells that were installed in 2003 by the Interstate Stream Commission (ISC) and the Army Corps of Engineers (ACE). The domestic wells include Thomas well, Perinni Well, and Cather Well. The ISC/ ACE wells that were sampled include HWY-W07 A, B, C, ESC-W03A, BRN-E01A, B, C, and BRN-E06A. Figure 18 shows the location of the domestic wells described above. The locations of all of the ISC/ACE wells except HWY-W07 A, B, and C are also shown on figure 18. The HWY-W07 wells are located near the BOR transect at river mile 87.62 and can be seen in figure 19. The A, B, and C designations for the ISC/ACE wells indicate total well depth where A indicates ~20 ft, B indicates~50 ft and C indicates ~100 ft.

Water Sample Collection

The procedure for sample collection of groundwater was similar to the low-flow groundwater-sampling procedures described by Puls and Barcelona (1996). A peristaltic

Table 2 List of groundwater sample locations, well depth, and sample events. For position: E-east of river, B-between river and LFCC, W-west of LFCC

Well ID	River Mile	Location	Position	Well depth (ft)	Sample Events
W-109.49-2	109.49	Near Lemitar	B	19.06	1,2,3
W-109.49-3	109.49	Near Lemitar	W	20.27	1,2,3
W-109.49-4	109.49	Near Lemitar	W	26.6	1,2,3
W-114.60-2	114.60	South of San Acacia	B	24.15	1,2,3,4,5
W-114.60-3	114.60	South of San Acacia	W	24.35	1,2,3,4,5
W-68.72-1	68.72	San Marcial	B	12.54	1,2,3,4,5
W-68.72-3	68.72	San Marcial	W	18.66	1,2,3,4,5
W-68.72-4	68.72	San Marcial	W	19.8	4
W-68.72-5	68.72	San Marcial	W	122.58	1,2,3
W-68.72-6	68.72	San Marcial	W	35.02	1,2,3
W-83.98-1	83.98	North Bosque Boundary	E	26.41	1,2,3
W-83.98-3	83.98	North Bosque Boundary	W	18.3	1,2,3
W-83.98-4	83.98	North Bosque Boundary	W	19.41	1
W-87.62-1	87.62	North of HWY 380	B	19.5	4,5
W-87.62-2	87.62	North of HWY 380	B	13.85	1,2,3,4,5
W-87.62-3	87.62	North of HWY 380	W	18.41	1,2,3,4,5
W-87.62-4	87.62	North of HWY 380	W	14.2	1,2,3,4,5
W-91.28-1	91.28	South of Neil Cupp	E	74.45	1,2,3
W-91.28-3	91.28	South of Neil Cupp	B	13.78	1,2,3,5
W-91.28-3.5	91.28	South of Neil Cupp	W	17.71	1,2,3,5
W-91.28-4	91.28	South of Neil Cupp	W	21.37	1,2,3
W-99.59-1	99.59	Near Socorro	B	10.84	1
W-99.59-4	99.59	Near Socorro	B	54.79	1,2,3
W-EB-11-20	66.36	South of San Marcial	B	14.39	1,2,3,4
W-Thomas	102.93	Near Escondida	E	5.62	1,2,3
W-PERINI1	88.5	North of HWY 380	W	80	2,3
W-Cather	86.19	South of San Antonio	W	100	3

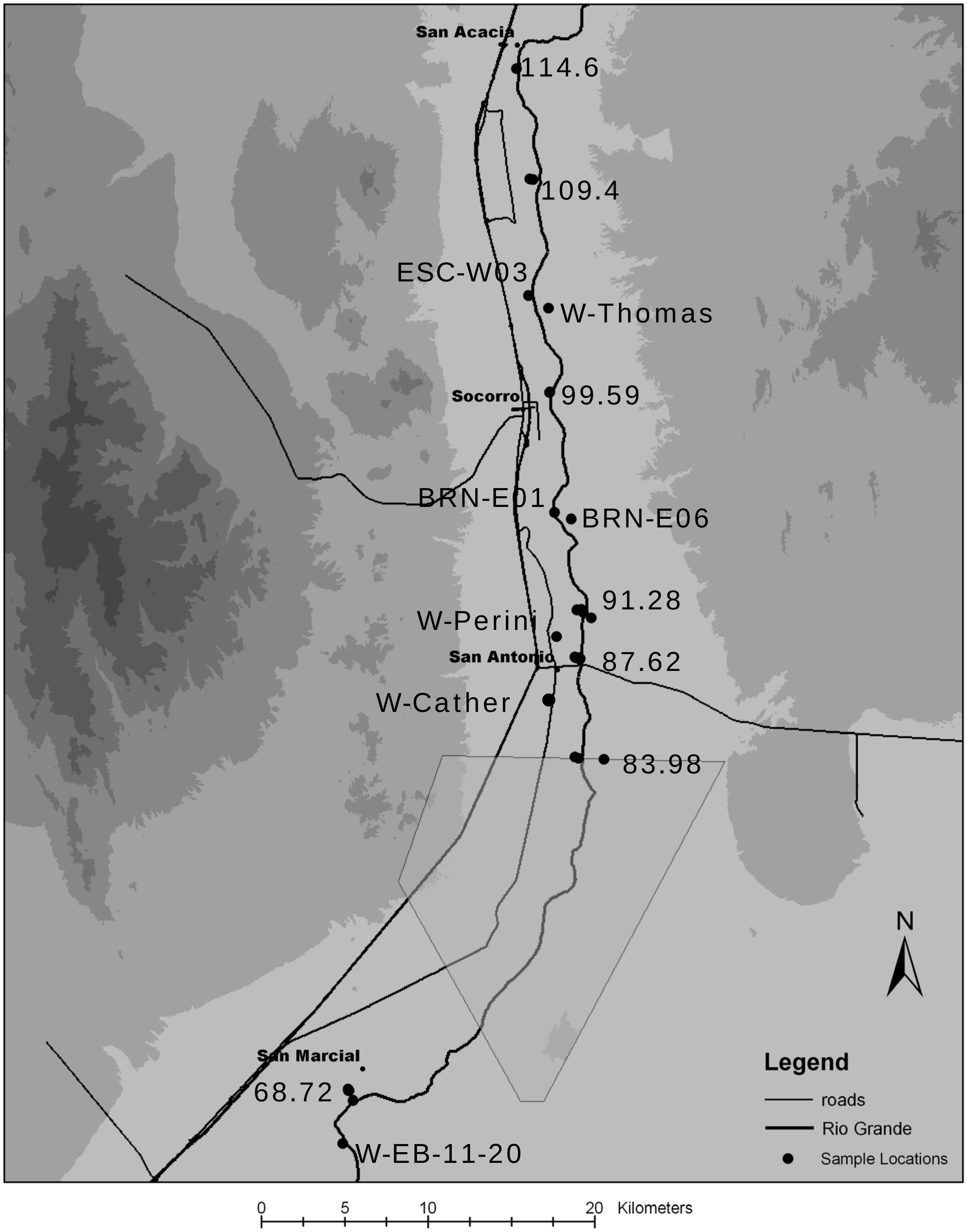

Figure 18 Well transect locations and some individual sampling locations

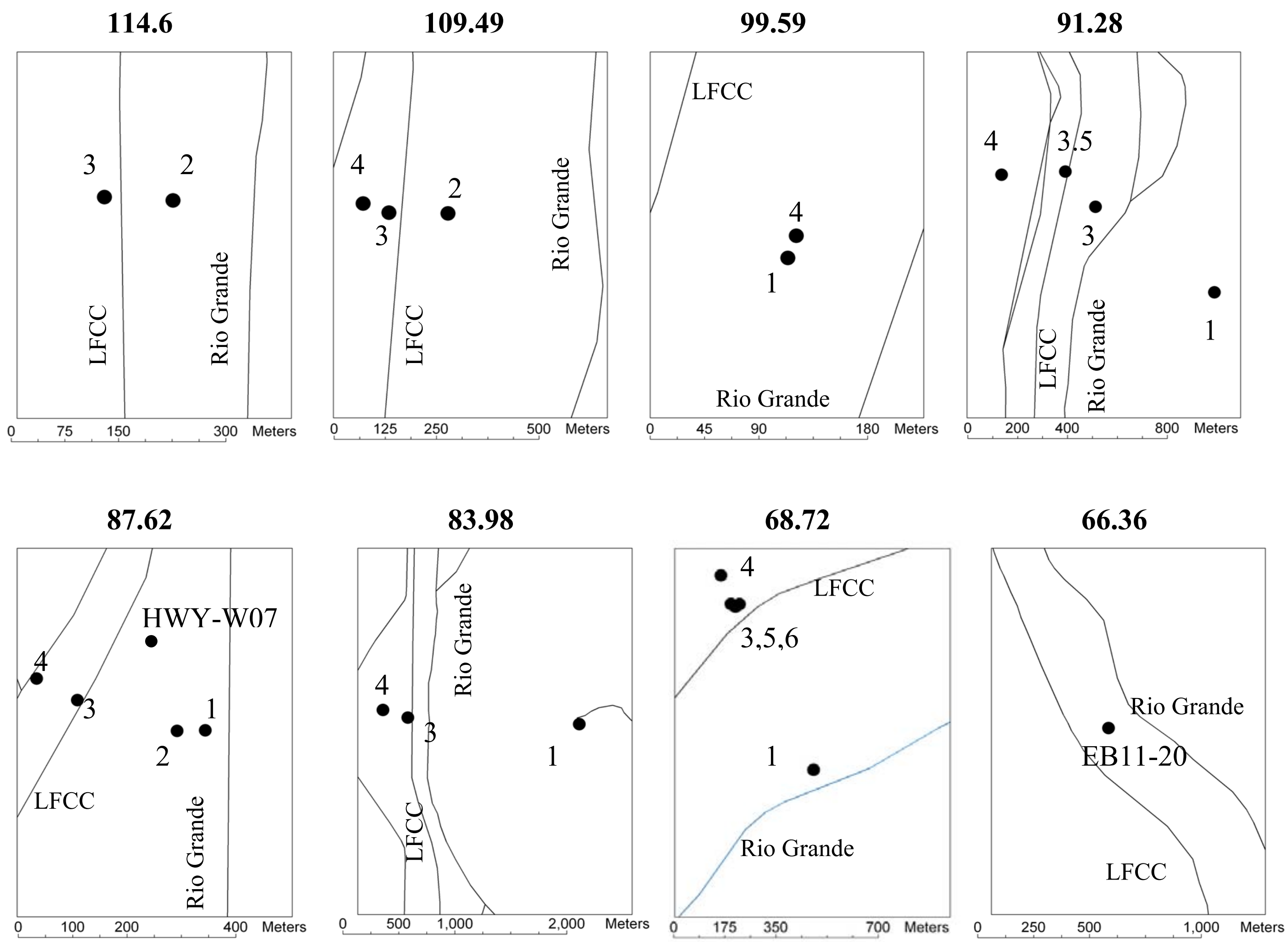

Figure 19 Location of individual wells on transects labeled by river mile. Numbers indicate individual wells on transects.

pump was used to purge water from the well at a low flow rate (usually less than 1 L/min). Water was purged until at least 10 equipment volumes had been pumped and water levels and field parameters of pH, electrical conductivity, temperature, and dissolved oxygen stabilized. These parameters were monitored with an Aqua-Check Water Analyzer (manufactured by AquaMetrix in Markham, Ontario) in the field. After parameter stabilization, the water was pumped through a 0.45 μm filter and sampled. The sampling equipment was flushed with deionized water between the collection of different samples.

Surface water samples were collected by placing a bucket under the water surface while pointing the opening of the bucket upstream. This was done after field parameters of pH, electrical conductivity, temperature, and dissolved oxygen were measured. The water was then filtered through a 0.45 μm filter using the pumping system and sampled.

Chemical and Isotopic Analyses

Water samples were analyzed for the stable isotopes of oxygen and hydrogen in the Stable Isotope Mass Spectrometry Laboratory of the New Mexico Institute of Mining and Technology. The hydrogen isotope ratios were determined by reacting the water with zinc at 550 deg C to form H_2 gas (IAEA, 1998b). The hydrogen gas was then analyzed on a Finnigan Delta model gas-source magnetic-sector isotope-ratio mass spectrometer. The oxygen isotope ratios were determined by equilibrating CO_2 gas with the water sample in a water-dominated system (IAEA, 1998a). The CO_2 was then analyzed on the same mass spectrometer. The $\delta^{18}O$ value of the water was then calculated based on equilibrium relationship between CO_2 gas and liquid water. All stable isotope values are reported in delta notation as a per mille deviation from a standard,Vienna Standard Mean Ocean Water (VSMOW):

$$\delta = \left(\frac{R_{sample} - R_{std}}{R_{std}} \right) * 1000$$

where R is the ratio of the number of the less common isotope to that of the more common isotope (eg. $^{18}O/^{16}O$) in the sample of interest. The reproducibility of the δD and $\delta^{18}O$ values was ± 2 ‰ and ± 0.3 ‰ respectively.

Chemical analyses were performed by the New Mexico Bureau of Geology and Mineral Resources Analytical Chemistry laboratory in Socorro, New Mexico. Cations were analyzed with an Agilent 7500 inductively coupled plasma mass spectrometer using the EPA 200.8 method. Anions were analyzed with a Dionex DX 600 ion chromatograph with an AS 50 auto sampler using an AS 14 column set. The EPA 200.8 method was used for anion analyses.

RESULTS AND DISCUSSION

Introduction

In this section, I will present data and discuss its implications on structural controls on groundwater quality in the Socorro Basin. Ultimately, I will develop a hypothesis to relate the observed spatial variability of groundwater chemistry, including the presence of high-chloride waters in the shallow aquifer in the Socorro Basin, to regional flow paths that are controlled by cross-basin structures related to the SAZ.

Stable Isotope results

Introduction

Stable isotopes of hydrogen and oxygen are useful for tracing different sources of groundwater because most groundwater originates as precipitation. Meteoric waters generally plot on the global meteoric water line (GMWL) in $\delta D/ \delta^{18}O$ space with the linear equation: $\delta D = 8\delta^{18}O + 10$ (Craig, 1961). The stable-isotope composition of individual meteoric waters is controlled by isotopic fractionation related to the processes of condensation and evaporation. During condensation, the isotopically heavier water molecules condense at a slightly higher rate than the lighter molecules. Therefore the resulting condensate will have a heavier isotopic signature than that of the water vapor. As condensation of a finite reservoir of water vapor continues, the isotopic composition of the water vapor progressively becomes lighter as does the condensate (Dansgaard, 1964). This process can be modeled based on Rayleigh condensation with immediate removal of precipitation or with a part of the condensate being kept in the cloud during the rain-out process. There are many factors that influence the spatial distribution of the isotopic composition of precipitation, but in general the isotopic composition of meteoric waters depends on the measure of the average degree of rain-out of moisture from a given air mass, on the way from the source region to the site of precipitation (Rozanski et al., 1993). As water condensates and rains out of an air mass, the isotopic signature of precipitation tends to evolve roughly along the GMWL from a heavy to light isotopic composition. Because approximately 60% of precipitation originates as evaporation from the ocean between 30ºS and 30ºN (Rozanski et al., 1993), precipitation in these areas tends to have relatively heavy isotopic compositions on average. Movement of water vapor away from the equator results in a rough trend of decreasing isotopic composition with increasing latitude. For example, precipitation in Colorado will generally have, on average, a lighter isotopic signature (depleted of the heavy isotopes) than precipitation in Socorro, NM. It should be noted that trends in the isotopic composition of precipitation are observed on many different scales, both spatially and temporally. There can be a large amount of variability in the isotopic composition of precipitation from one storm event to the next, but the trends described above can be observed in mean annual values. Seasonal trends in the isotopic composition of precipitation are also observed, with a heavier values in the summer and lighter values in the winter.

Stable isotopes of hydrogen and oxygen are also useful for evaluating different processes that affect precipitation after it is rained out. These processes include evaporation, water-mineral interactions, mixing with other water types, etc. Figure 20

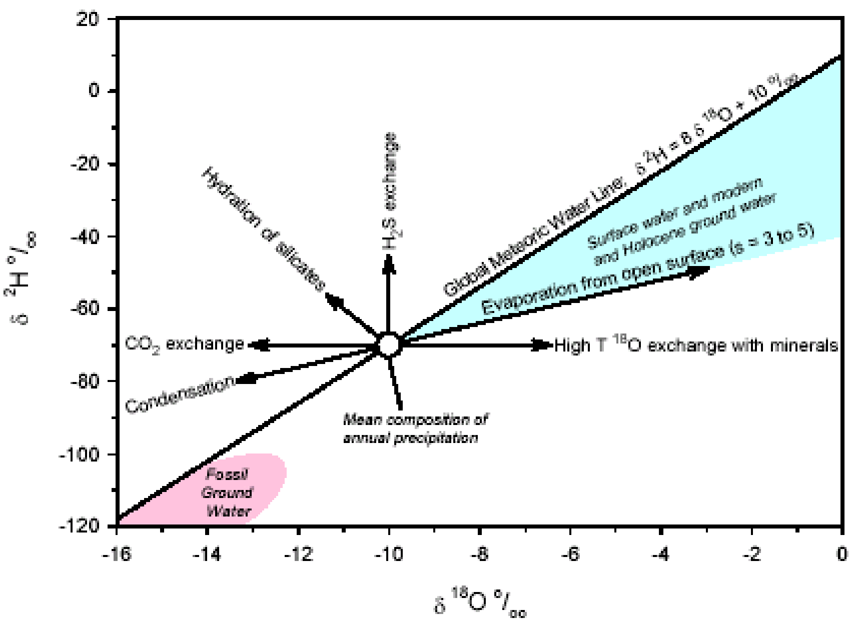

Figure 20 Deviations in isotopic composition from the meteoric water line. The mean composition of annual precipitation is just an example and not representative of any water analyzed for this study (Johnson et al.,2002).

shows how the isotopic composition of water undergoing different processes will deviate from the global meteoric water line.

Stable isotopes of oxygen and hydrogen were used to determine the major sources of water that contribute to the hydrological system in the study area under the assumption that the isotopic composition of groundwater is representative of that of the source of recharge. In most low-temperature systems, the isotopic composition of groundwater is usually not altered due to rock/water interactions, making these stable isotopes a good tool for the identification of different water sources.

Stable-Isotope Composition of the Rio Grande

Because the San Acacia reach of the Rio Grande is a losing stream (Newton et al., 2002; Papadopulos, 2000) and the river is one of the primary sources of groundwater, it is important to understand what controls the isotopic composition of the Rio Grande. Figure 21 shows how the stable-isotope composition of the Rio Grande water evolved as the water flows downstream from the headwaters in Colorado to Fort Quitman, Texas during the summer of 2001 (Mills, 2003). At the headwaters in Colorado, the isotopic composition of the Rio Grande plotted close to the global meteoric water line and most likely represented local snowmelt. As this water flows down stream, the isotopic composition evolves along the observed evaporation line. Therefore, the isotopic composition of Rio Grande water appears to be controlled mainly by evaporation. Figure 22 shows the isotopic composition of the Rio Grande in the study area during February,

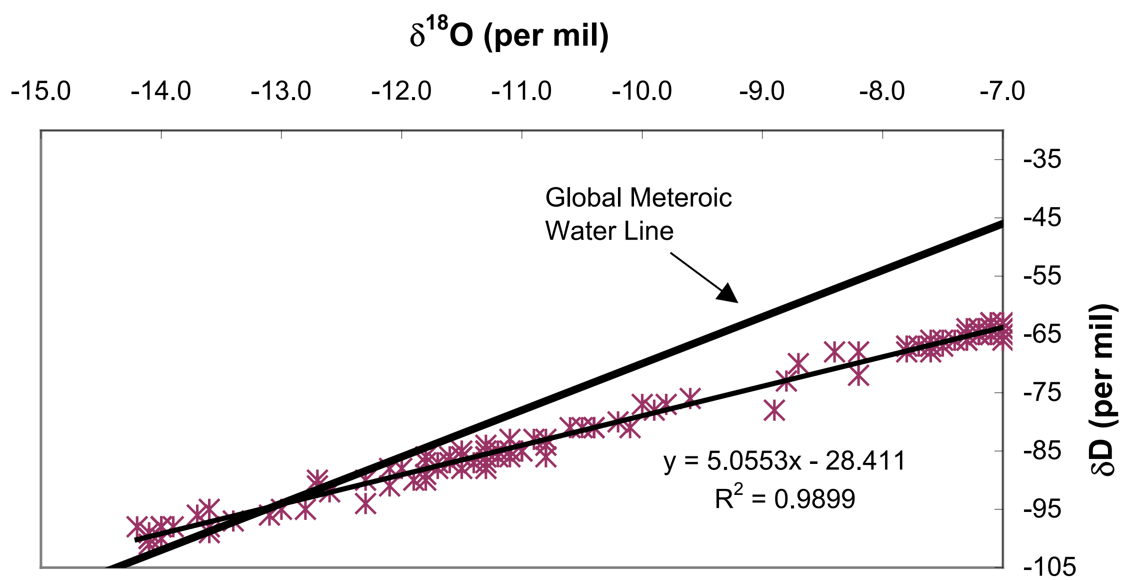

Figure 21 Stable-isotope composition of Rio Grande from the headwaters to Fort Quitman, TX during the summer of 2001 (Mills, 2003)

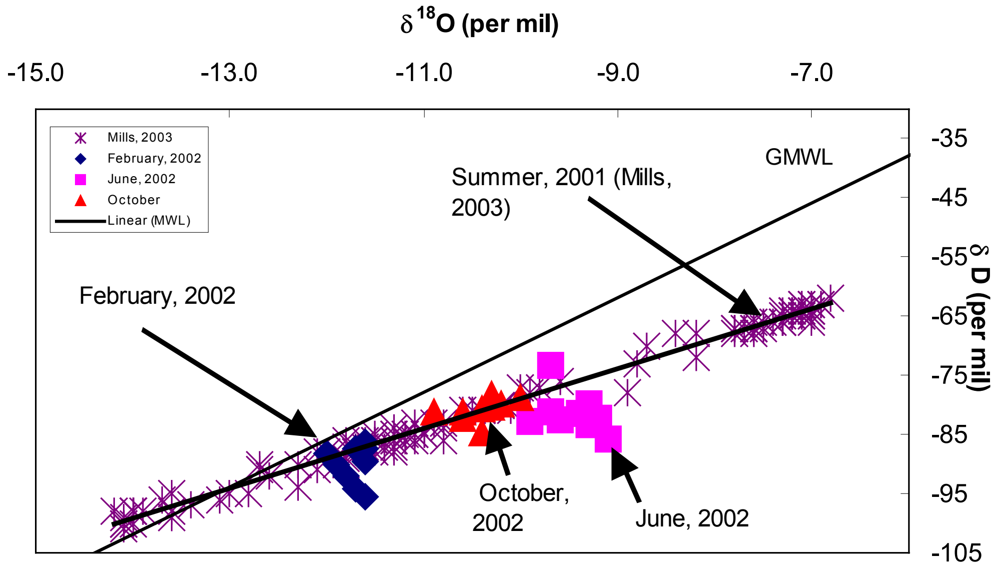

Figure 22 Stable-isotope composition of the Rio Grande in the study area at different times of the year along with stable-isotope composition of river water along the Rio Grande during the summer of 2001 (Mills, 2003)

2002, June, 2002 and October, 2002. River water was observed to have lighter isotopic values in February, heavier isotopic values in June and intermediate isotopic values in October. This shows that the river experiences more evaporation in the summer during high temperatures and less evaporation during times of lower temperatures, as expected. The isotopic composition of river water within the study area during February and June 2002, plots close but not directly on the evaporation line observed during the summer of 2001 (Mills, 2003). This suggests that the evaporation line may have a slightly different slope from year to year and from season to season depending on evaporation conditions such as relative humidity and average temperature. The isotopic composition of river water during October 2002 plots directly on the evaporation line observed by Mills (2003).

Stable-isotope Composition of Shallow Groundwater and the LFCC

Figure 23 shows stable-isotope data for all groundwater, river water and LFCC water samples collected in February and June 2002. All of these data generally fall on a line similar to the observed evaporation line in figure 21. Notice that June river water plots on the heavy end of this line and February river water plots on the light end of this

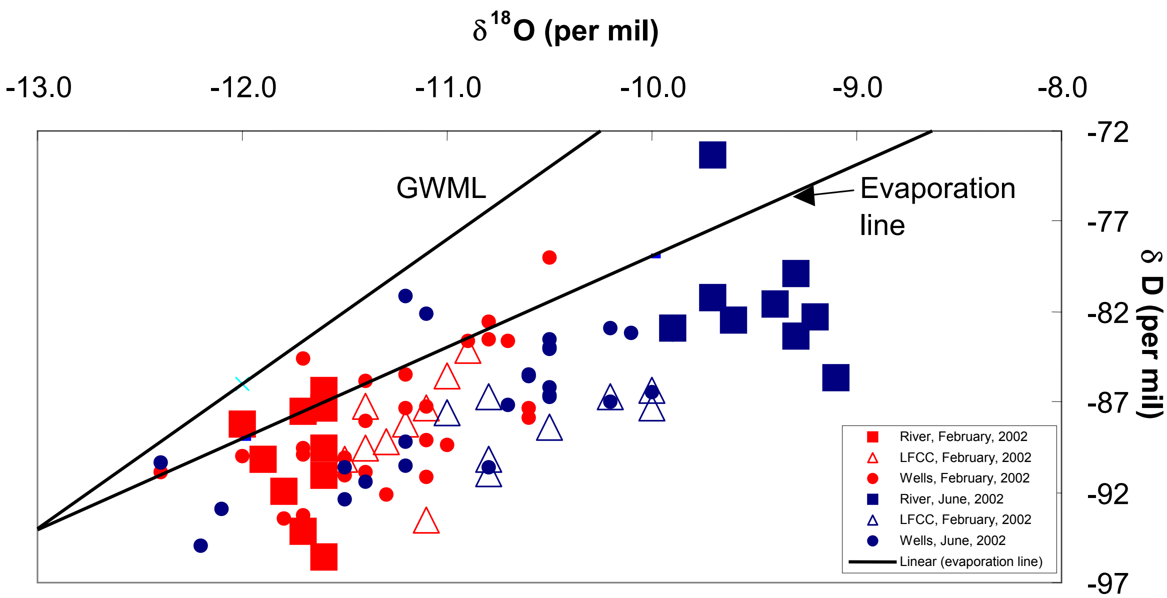

Figure 23 Stable-isotope composition of shallow groundwater, and surface water in the study area

line. Most of the groundwater and LFCC samples plot in between these two river-water end members. Also, the seasonal fluctuations of the isotopic composition of groundwater and LFCC water are much less than those observed for river water, suggesting that this line is a mixing line and that all of the LFCC and groundwater samples are predominantly river water. The significant scatter observed in this mixing line may be due to the seasonal fluctuation of the slope of the evaporation line along which the isotopic composition of river water evolves, or mixing with some other water source.

Groundwater samples that are isotopically lighter than winter river samples may represent river water from a time when it was characterized by a lighter isotopic composition than observed in the surface water samples collected.

Figure 24 shows stable isotope data for water samples collected during October 2002. Stable-isotope values for most groundwater, LFCC, and river samples plot close to the Rio Grande evaporation line; however, many data points have been shifted towards

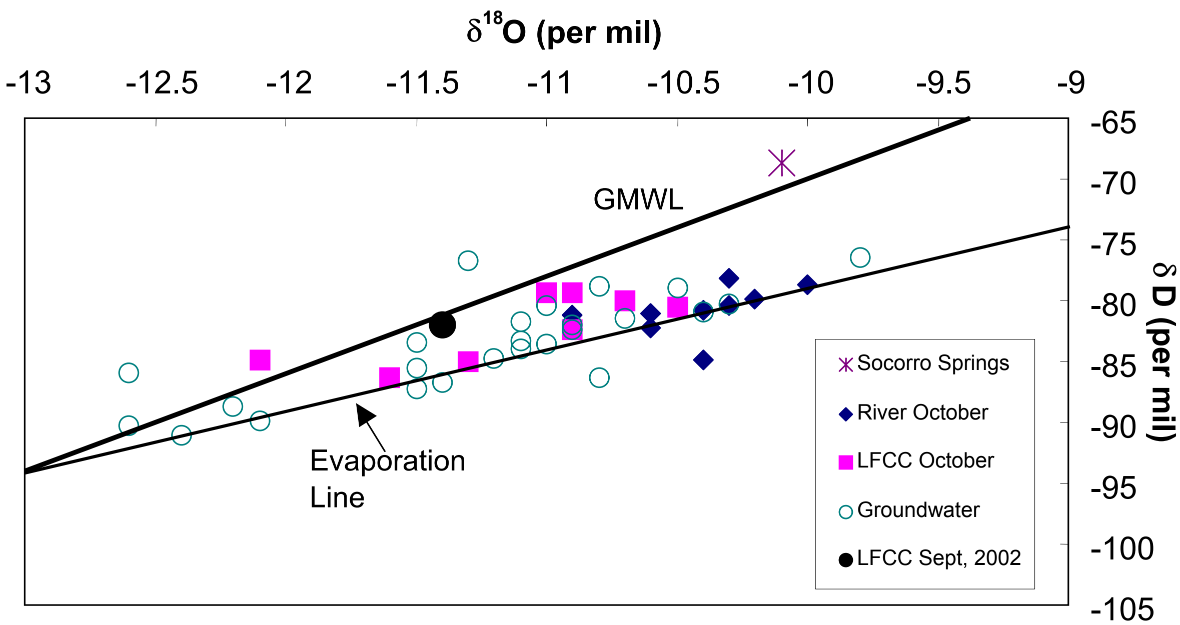

Figure 24 Stable-isotope composition of water samples collected October, 2002

the meteoric water line relative to the isotopic values for samples collected earlier in 2002. Also the observed variability of the isotopic composition of these waters, especially for the LFCC and groundwaters, is much higher than that observed in February or June. This isotopic shift may be a result of a small input of local precipitation into the system. During 2002 much of the year's precipitation occurred during the months of July, August, and September (figure 25). Figure 24 also shows the isotopic composition

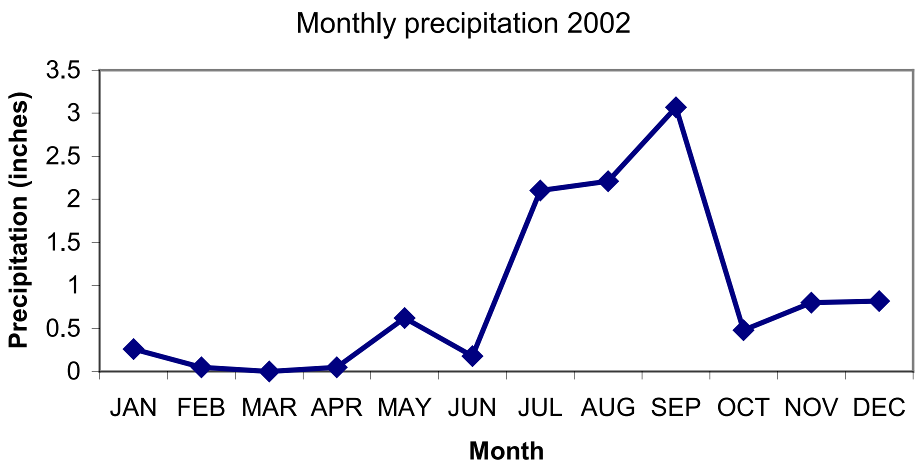

Figure 25 Monthly precipitation in Socorro, NM in 2002

of the LFCC during one of the storm events in September 2002 (labeled LFCC Sept, 2002). This data point plots on the meteoric water line and probably does represent a local precipitation component because during the time of the storm events in September, water from local drains was diverted to the LFCC to accommodate the unusually large amount of water in the drainage system. However, there is not enough evidence to conclude that these differences in isotopic composition of groundwaters are a result of the addition of a local precipitation component.

Another source that should be noted and will be discussed in more detail below is Socorro Springs. The stable-isotope composition of the Socorro Springs water in October 2002 is also shown in figure 24. Socorro Springs is a warm spring is believed to be recharge from La Jencia Basin to the west. Figure 26 shows Barroll and Reiter's (1990) conceptual model describing how groundwater recharge in the La Jencia Basin

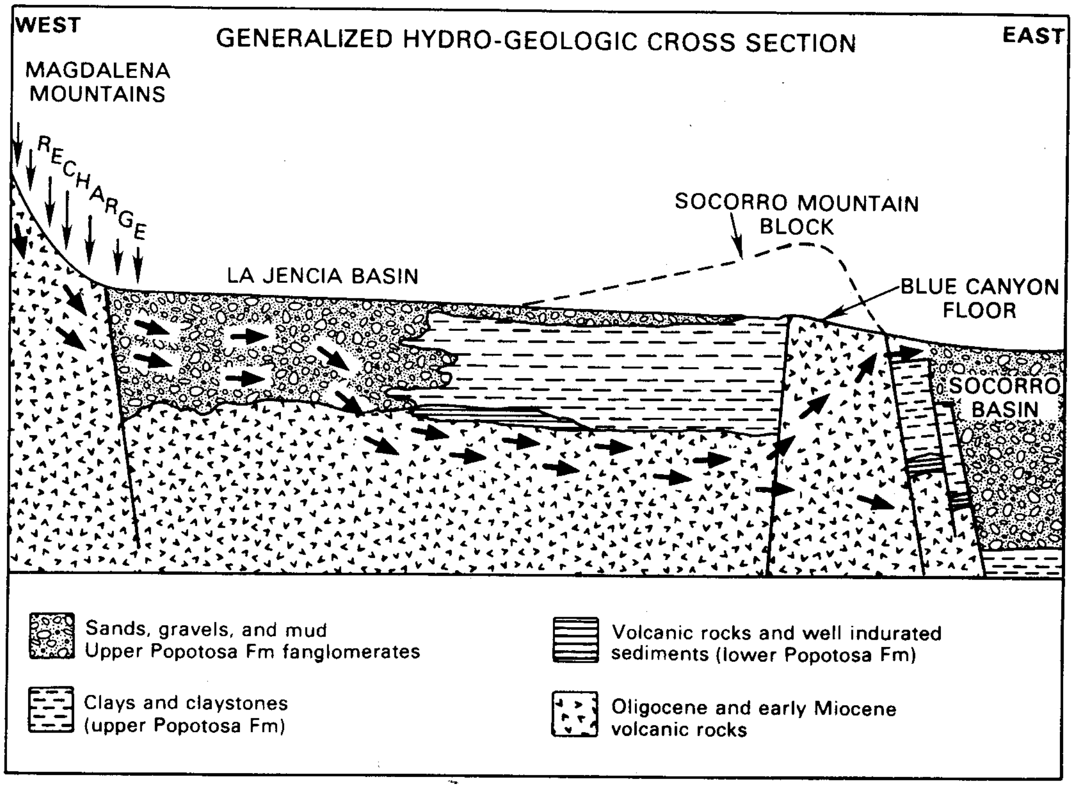

Figure 26 Conceptual model of Socorro Springs (Barroll and Reiter, 1990)

travels along a relatively deep flow path towards the Socorro Basin and is forced up into the shallow groundwater system by playa deposits of the Popotosa confining bed. The stable-isotope composition of Socorro Springs as seen in Figure 24, is quite different than that of the river and probably represents precipitation near the Magdelena Mountains.

Water -Chemistry Results

Introduction

Water-chemistry data were also used to identify different water sources, but unlike the stable isotopes of oxygen and hydrogen, the chemistry of natural waters is usually controlled by rock/water interactions. Therefore, the chemistry of a water sample reflects the type of minerals that the water has come in contact with, which depends on the flow path. Water chemistry was also used to determine mixing ratios among different water types.

Water Chemistry of the Rio Grande

According to the stable isotope data, the Rio Grande is the dominant water source in the shallow groundwater system. Therefore, in order to quantify mixing with other sources in the hydrologic system, it is important to know how the water chemistry of the Rio Grande varies spatially and temporally. Figure 27 shows Stiff diagrams representing the chemical signature of river water along the river from north (top) to south (bottom) for February, June, and October 2002. The general water chemistry for the river was observed to be dominated by HCO_3, Ca, and Na. TDS values were around 400 mg/L. During February 2002, the chemical composition of river water was very constant all along the reach. During June and October, the chemical composition of the river again was fairly constant spatially north of the Bosque Del Apache (river mile 83.98). The most southern samples collected in June and October 2002, had very different chemical compositions than the samples collected north of the Bosque Del Apache (river mile 83.98). This was due to pumping water from the LFCC into the river in the southern part of the study area. There were slight differences in the chemical signature of river water at different times, but in general, the chemical composition of the river appeared to be constant during the year of 2002.

In order to look at the temporal variability of the water chemistry of the river on a longer time scale, historic water chemistry data collected by the USGS at San Marcial

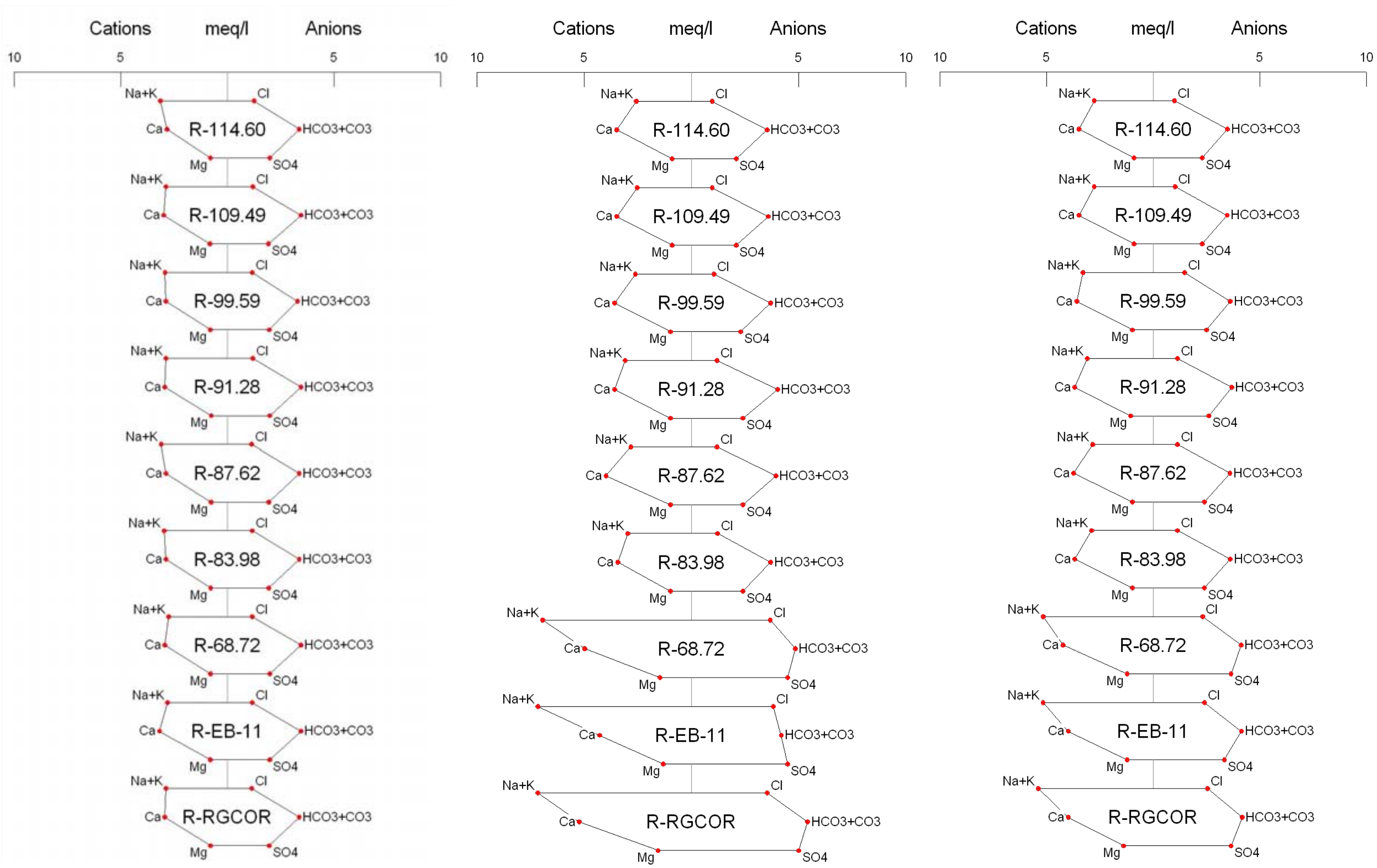

February 2002 **June 2002** **October 2002**

Figure 27 Stiff diagrams representing water chemistry of the Rio Grande at different locations and for different times. The sample Ids are indicated in the centers of the diagrams. The Stiff diagrams are arranged spatially from north (top) to south (bottom).

(river mile 68.72) was analyzed. Figure 28 shows Stiff diagrams representing the chemical composition of the Rio Grande for different times of the year between 1987 and 2000. In general, concentrations of major ions relative to each other were observed to be constant and very similar to those observed for the river samples collected for this study. The general shape of Stiff diagrams is fairly constant but the size varies. This variability is most likely due to changes in the amount of evaporation that river water experienced by the time it arrived at this reach. A different chemical signature was observed in the historic data in figure 28 usually around July or August, during the monsoon season. During this time, river water was observed to have elevated concentrations of calcium, sodium, and sulfate, probably due to a more local source such as the Rio Salado or the Rio Puerco, which are both tributaries that feed into the Rio Grande, north of the study area.

From the above discussion, it appears that the concentrations of the major ions relative to each other in the Rio Grande are rather constant both in space and time within the study area. Variable concentrations were observed due to pumping of LFCC water into the river, different amounts of evaporation, depending on specific conditions, and contributions from local precipitation.

Water Chemistry of the LFCC and Shallow Groundwater

Stable-isotope data indicated that all of the LFCC and shallow groundwater samples collected in the flood plain were primarily derived from the Rio Grande. This makes sense because this reach of the river loses water to the shallow aquifer and water used for irrigation is ultimately river water. Therefore, if the chemical composition of

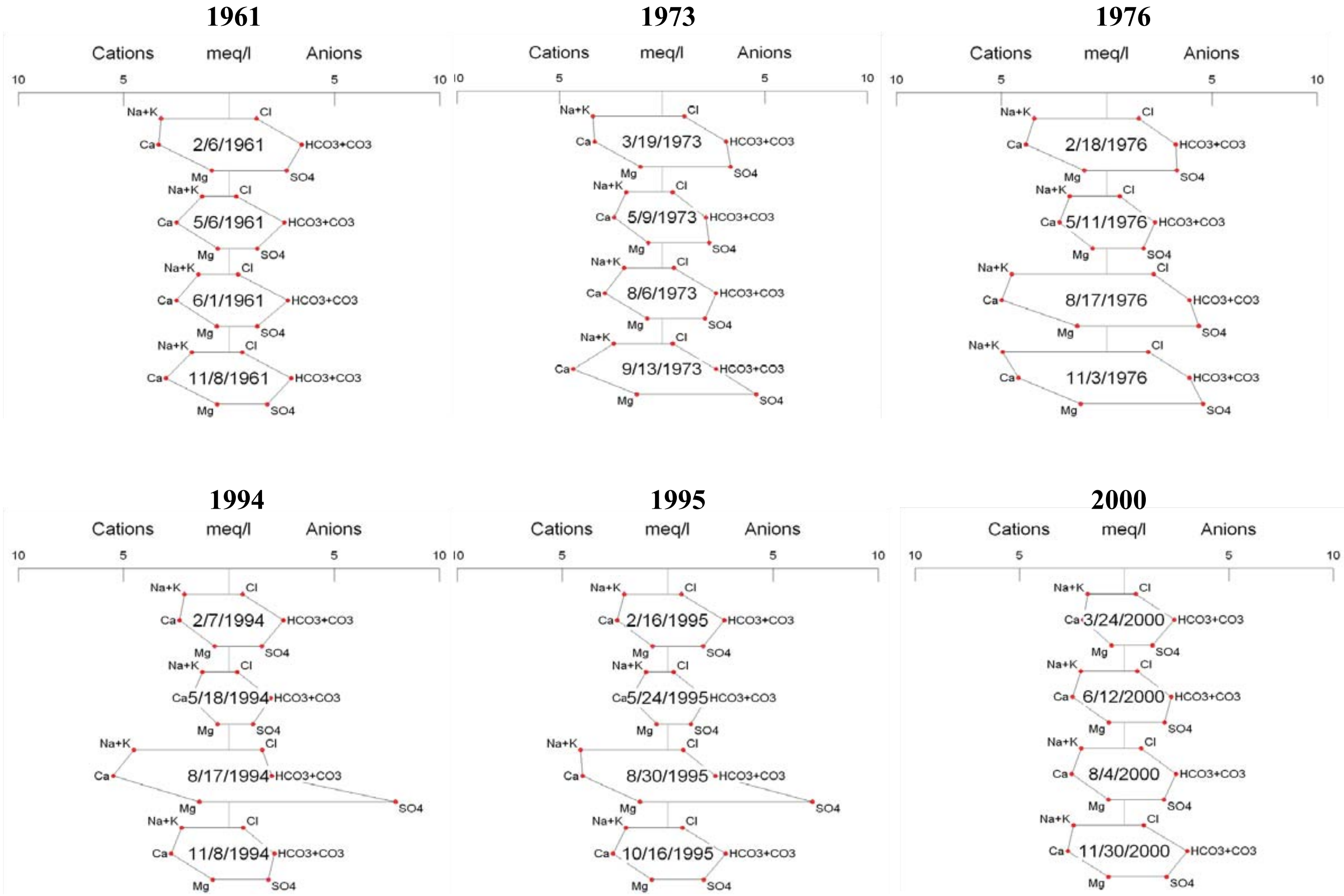

Figure 28 Stiff diagrams representing historic water chemistry data for the Rio Grande at San Marcial (river mile 68.72)

groundwater differs from that of the river, it is probably due to processes such as mixing with water of a different chemical composition, or water/mineral interactions. Observing the spatial and temporal variability of the water chemistry of the LFCC and shallow groundwater can help to better understand the hydrologic system. In this section, the water chemistry for shallow groundwater and LFCC samples will be characterized both spatially and temporally. Water samples are divided into groups depending on location. The four groups of water samples that will be discussed are groundwater between the river and LFCC, groundwater west of the LFCC, LFCC water, and groundwater east of the river.

Groundwater between the River and the LFCC

Because this reach of the Rio Grande loses water to the shallow aquifer, one would expect that shallow groundwater between the river and LFCC to be primarily river water and to have a similar chemical signature. In general, this is what was observed. Most of the groundwater between the river and the LFCC was found to be chemically similar to that of the river but with slightly higher TDS values than the river. Figure 29, 30, and 31 compare the chemical signature of water between the river and the LFCC to that of river water and LFCC water for different points on the river and for different times of year. In areas north of the Bosque Del Apache (top five Stiff diagrams for each sampling date), groundwater between the river and the LFCC has a chemical signature very similar to that of the river, with slight differences in the relative amounts of sodium and calcium. These slight differences in the relative concentrations of sodium and calcium may be a result of a small amount of mixing with other water types in the shallow groundwater system or water/mineral interactions. Temporal variability of

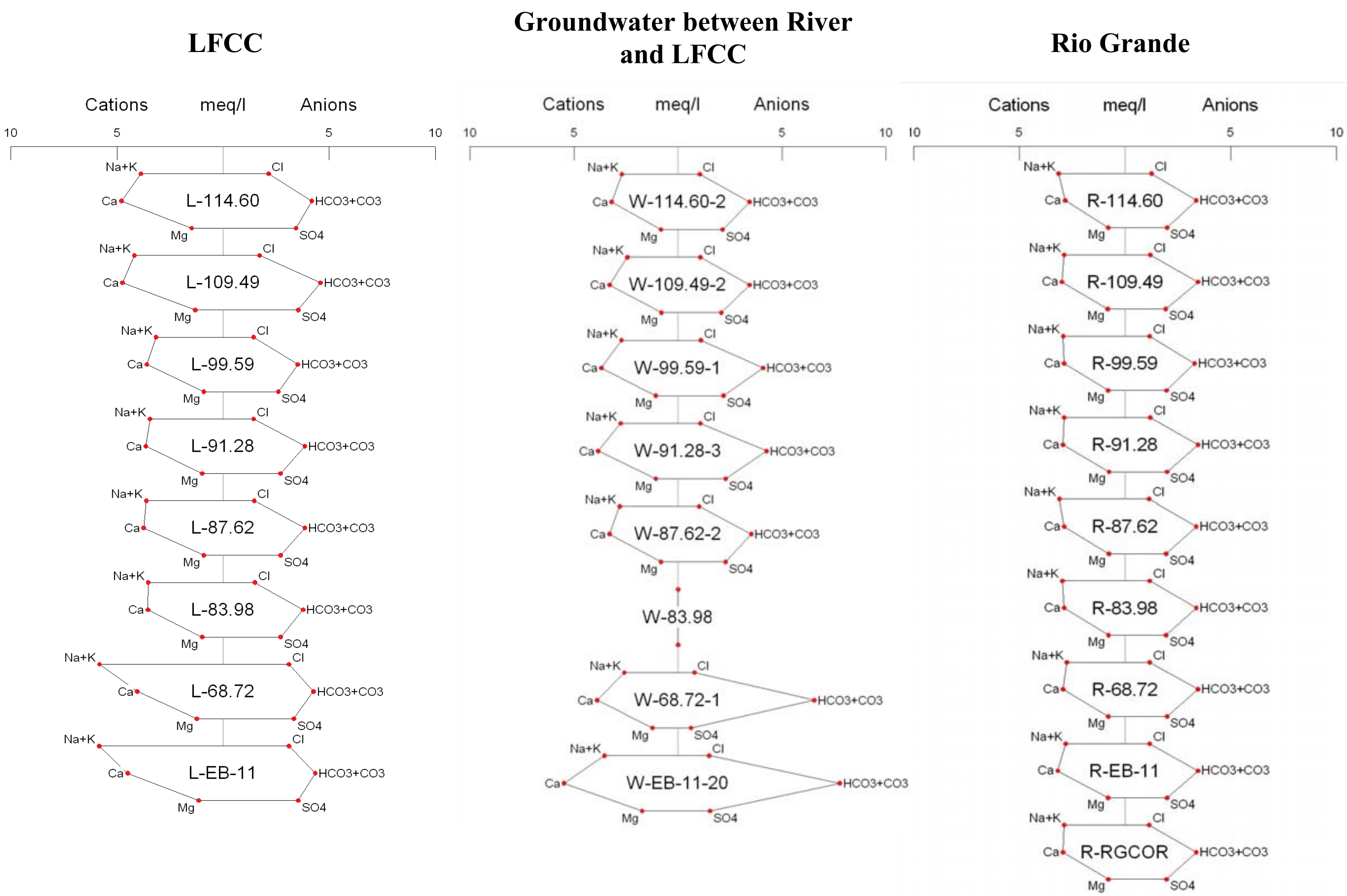

Figure 29 Stiff diagrams representing water chemistry of the river, groundwater between the river and the LFCC and the LFCC for February 2002. The locations indicated in center of diagrams are shown in figure 19. The Stiff diagrams are arranged spatially from north (top) to south (bottom and from west (left) to east (right). Samples were not collected for spaces with a river-mile label but no Stiff diagram.

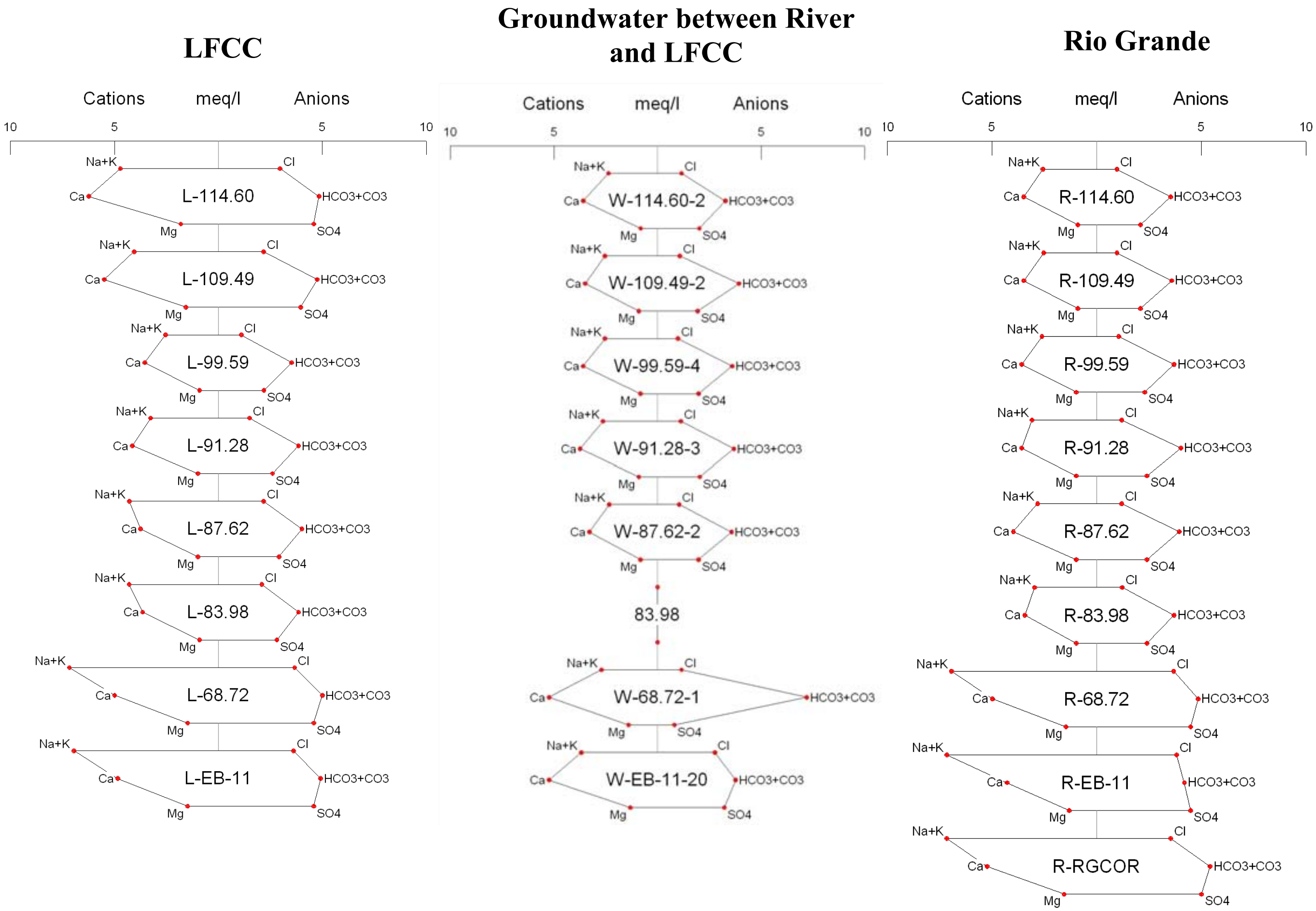

Figure 30 Stiff diagrams representing water chemistry of the river, groundwater between the river and the LFCC and the LFCC for June 2002. The locations indicated in center of diagrams are shown in figure 19. The Stiff diagrams are arranged spatially from north (top) to south (bottom) and from west (left) to east (right). Samples were not collected for spaces with a river-mile label but no Stiff diagram.

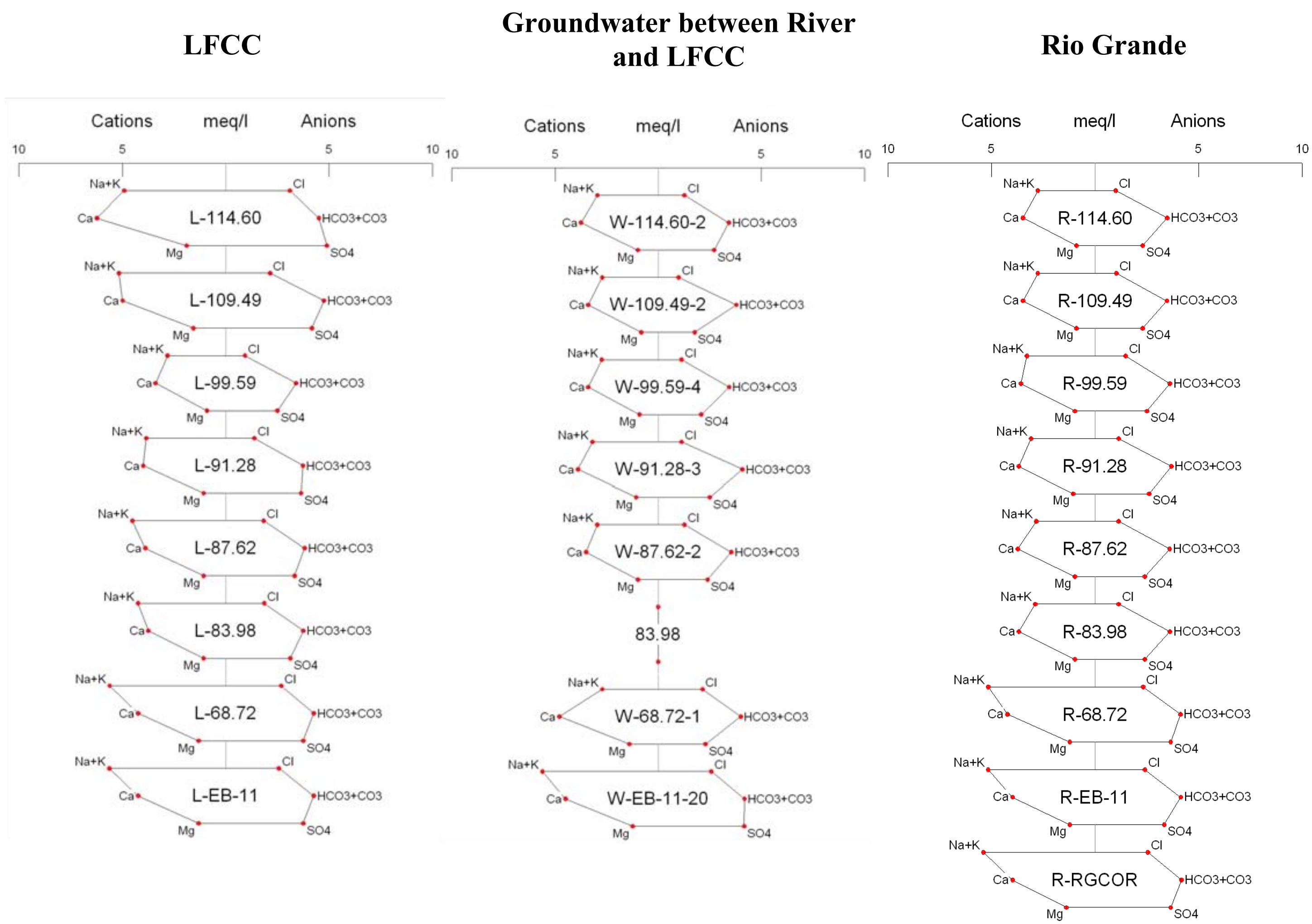

Figure 31 Stiff diagrams representing water chemistry of the river, groundwater between the river and the LFCC and the LFCC for October 2002. The locations indicated in center of diagrams are shown in figure 19. The Stiff diagrams are arranged spatially from north (top) to south (bottom) and from west (left) to east (right). Samples were not collected for spaces with a river-mile label but no Stiff diagram.

groundwater north of the Bosque Del Apache (river mile 83.98) is rather small. To the south of the Bosque Del Apache, the effects of pumping LFCC water into the river can be seen in the water chemistry of the river. The groundwater in this area during February, 2002 displays a very different chemical signature than that of the river. As time goes on, the chemical signature of these southern groundwaters evolve until they are rather similar to that of the river in this area. This can be seen especially in the well farthest to the south, indicating that groundwater in this area is recharged by river seepage. However, it is unclear why there was such a large difference in chemical signatures of the river and groundwater during February.

Groundwater West of the LFCC

Stable isotope data showed that shallow groundwater within the flood plain to the west of the LFCC is primarily river water. All irrigation in this area takes place to the west of the LFCC. The use of river water for irrigation and regional gradients, as shown in figure 32, can explain the isotopic signature of shallow groundwater to the west of the LFCC. Unlike the stable-isotope data, the water chemistry for much of the shallow groundwater to the west of the LFCC was observed to be different from that of the river. Figures 33, 34, and 35 show the high spatial variability of water chemistry for shallow groundwater west of the LFCC. This variability is probably due to a combination of evapotranspiration, water/mineral interactions, and mixing with other water types, and indicates a complex hydrologic system. TDS values ranged between 370 and 1840 mg/L. Among the water chemistry data presented in figures 33, 34, and 35, a few recognizable chemical signatures were observed. Chemical signatures similar to that of the river were

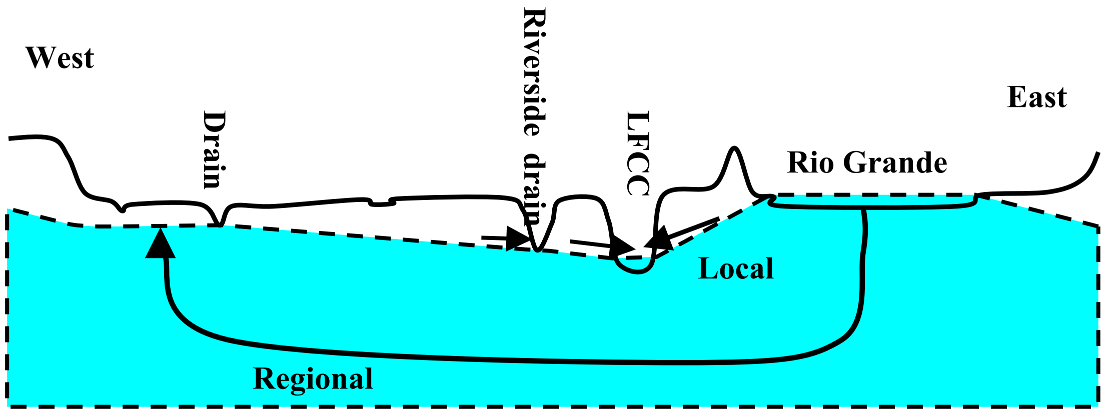

Figure 32 Conceptual model of regional and local hydraulic gradients in the hydrologic system.

observed for the samples W-109.49-4, W-83.98-4, and W-83.98-3. During February 2002, W-87.62-4 was characterized by a chemical signature that is probably a result of mixing with high-chloride waters. Other chemical signatures, such as those with a relatively high Na concentration may represent mixing of river water and other water types or cation exchange due to water/mineral interactions.

Differences between figures 33, 34 and 35 represent how the water chemistry of shallow groundwater west of the LFCC changes with time. In general, the chemical signature of shallow groundwater did not change significantly; however, a few water samples show significant changes in the water chemistry throughout the year. Temporal variability in water chemistry can be seen for sample W-87.62-4, located just north of HWY 380 and around twenty feet east of the Socorro Riverside Drain. During non-irrigation season (February, 2002), shallow groundwater in this area has a much higher TDS value than the river and is relatively enriched in sodium and sulfate. During irrigation season (June, 2002), this groundwater sample displays a chemical signature

W **E**

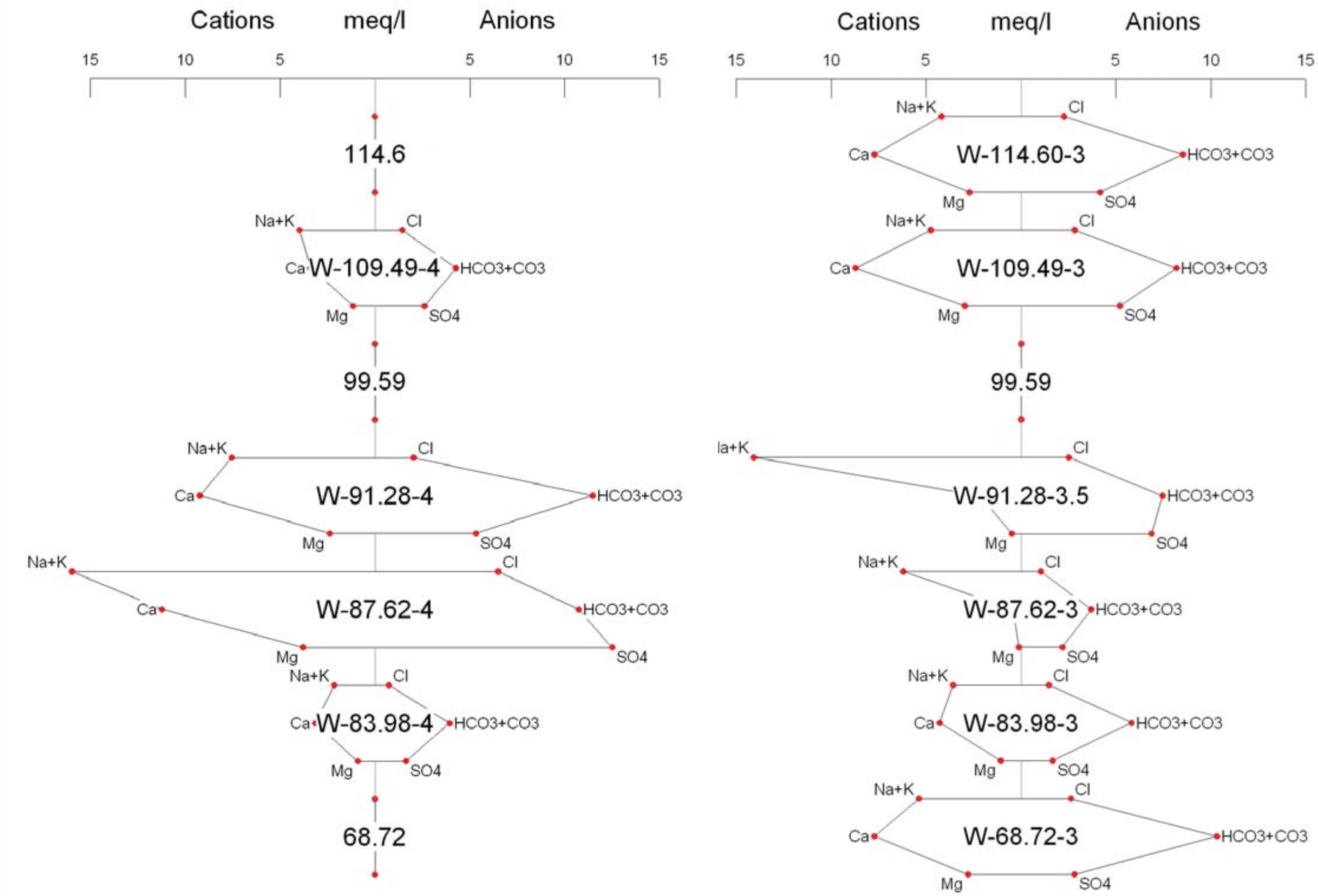

Figure 33 Stiff Diagrams representing shallow groundwater west of the LFCC for February 2002. The Stiff diagrams are arranged spatially from north (top) to south (bottom) and from west (left) to east (right). Samples were not collected for spaces with a river-mile label but no Stiff diagram.

W

E

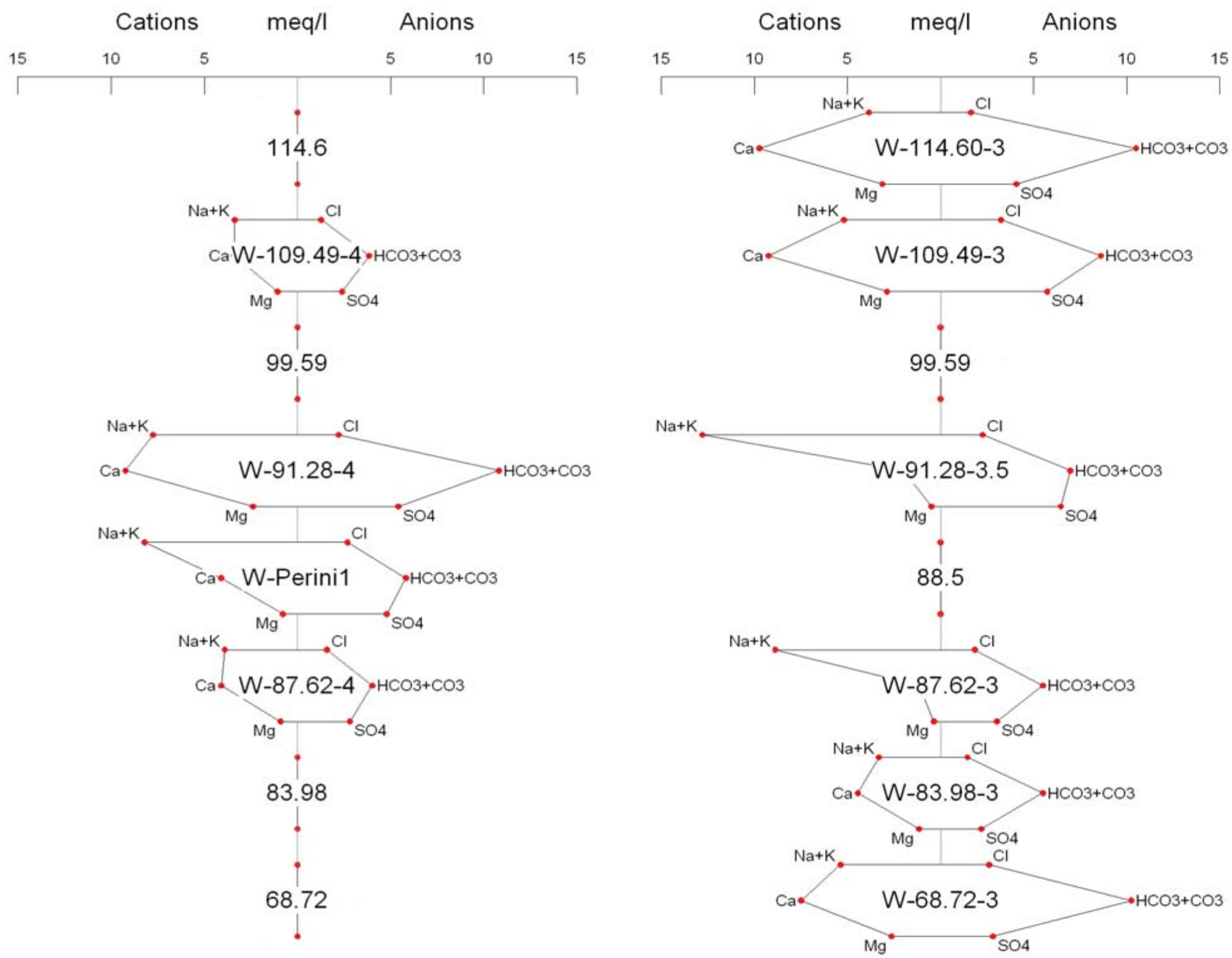

Figure 34 Stiff Diagrams representing shallow groundwater west of the LFCC for June 2002. The Stiff diagrams are arranged spatially from north (top) to south (bottom) and from west (left) to east (right). Samples were not collected for spaces with a river-mile label but no Stiff diagram.

W **E**

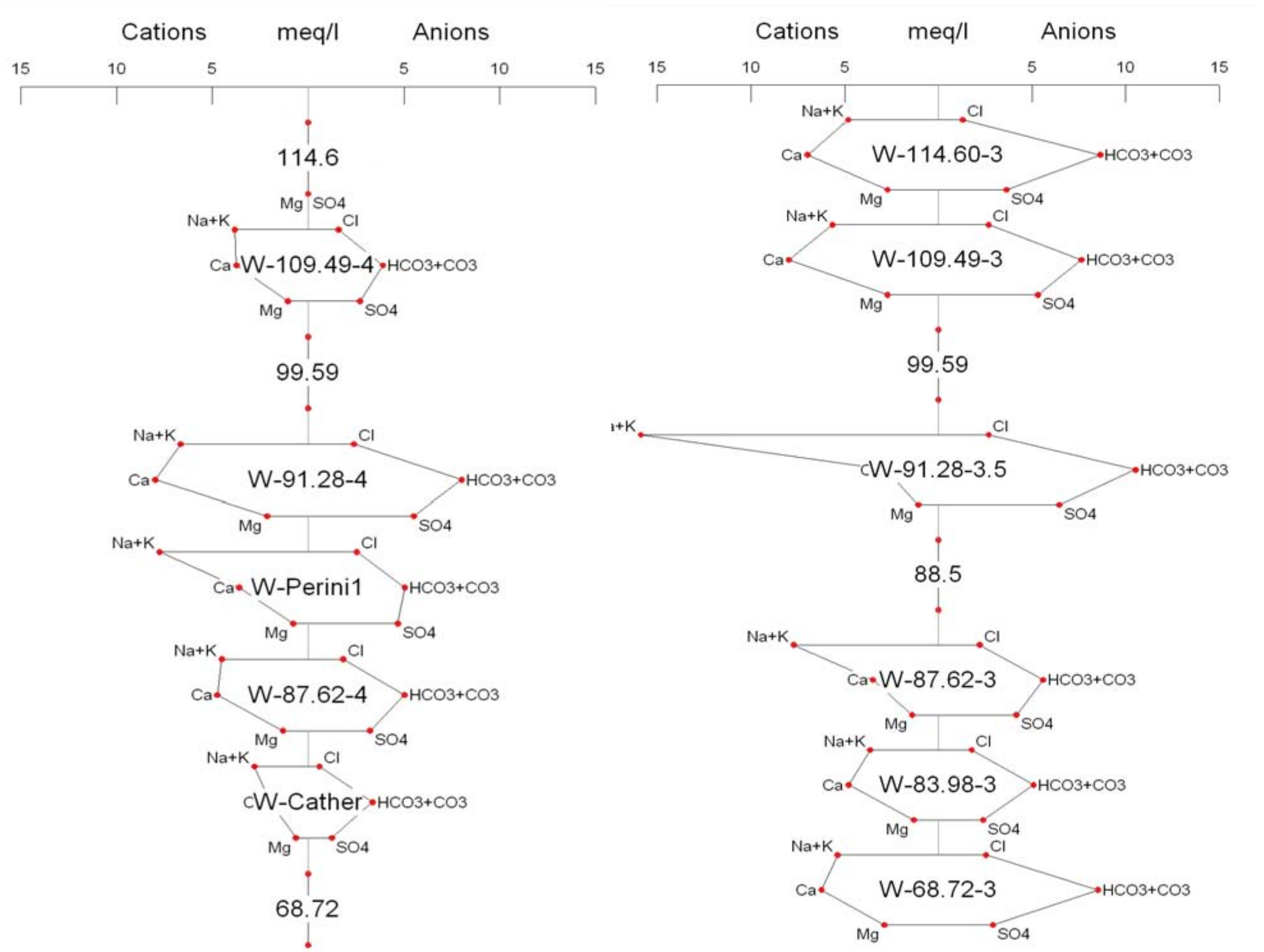

Figure 35 Stiff Diagrams representing shallow groundwater west of the LFCC for October 2002. The Stiff diagrams are arranged spatially from north (top) to south (bottom) and from west (left) to east (right). Samples were not collected for spaces with a river-mile label but no Stiff diagram.

more similar to that of the river. In October, the water chemistry still looked similar to that of the river, but with a slightly higher TDS value than observed in June. The temporal changes in the water chemistry in this area appear to be related to irrigation. During non-irrigation season, water chemistry in this area reflects different water types, specifically water with a high-chloride component, probably coming from the west. During irrigation season, irrigation return flow originating as river water probably dominates the shallow groundwater system in this area, explaining why the water chemistry more resembles that of the river. The water chemistry of groundwater in this area will be discussed in greater detail below when mixing processes are considered.

Another groundwater sample that should be mentioned can be seen in figure 35, labeled W- Cather. This well is located just south of HWY 380, approximately 3 km west of river and slightly above the floodplain. This sample had a TDS value of 330 mg/L, which is lower than most other samples that were collected. This water sample was enriched in sodium and had relatively high arsenic concentrations. The water chemistry of this sample probably represents mixing with another source that is coming from the west. This will be discussed further below.

Water Chemistry of the LFCC

Most of the water in the LFCC is derived from groundwater seepage from the east and the west (Newton et al., 2002). Figures 29, 30, and 31 show Stiff diagrams representing the major ion chemistry of the LFCC at different points along the LFCC for three different sampling events. The same general spatial pattern was observed for all three sampling events. TDS values ranged between 400 and 800 mg/L, with higher values in the north and south. The chemical signature of the two LFCC samples farthest to the north may represent a mixture of river water and what Anderholm (1984) called regional groundwater, which may come from the Albuquerque Basin to the north. The chemical signatures of the four central LFCC samples were similar to that of the river and may suggest that most of the water in the LFCC in this area is derived from river seepage to the east. However, because groundwater seepage from the west is probably primarily irrigation return flow (which may have a very similar chemical signature to that of the river), it is not possible to tell the relative amount of groundwater seepage that comes from either side of the LFCC. LFCC water south of the Bosque Del Apache was characterized by a very different chemical signature that is relatively enriched in sodium concentrations. This chemical signature is believed to represent mixing with deep sedimentary brines. This will be discussed further below.

Water Chemistry of Groundwater East of River

For this study there were very few wells on the east side of the river to sample, making spatial and temporal characterization of groundwater chemistry in the flood plain to the east of the river difficult. Stable-isotope data from these samples again showed that the dominant water source in the shallow aquifer is river water. However, there is evidence of mixing with other water types that probably originate from the highlands to the east. Figure 36 shows Stiff diagrams that represent the water chemistry for shallow groundwater samples collected east of the river. For the samples shown, TDS values range between 390 and 730 mg/L. Relative concentrations of calcium, bicarbonate and sulfate were observed to be higher than that of the river. The elevated TDS values and the different relative ion concentrations may be due to a small amount of mixing with

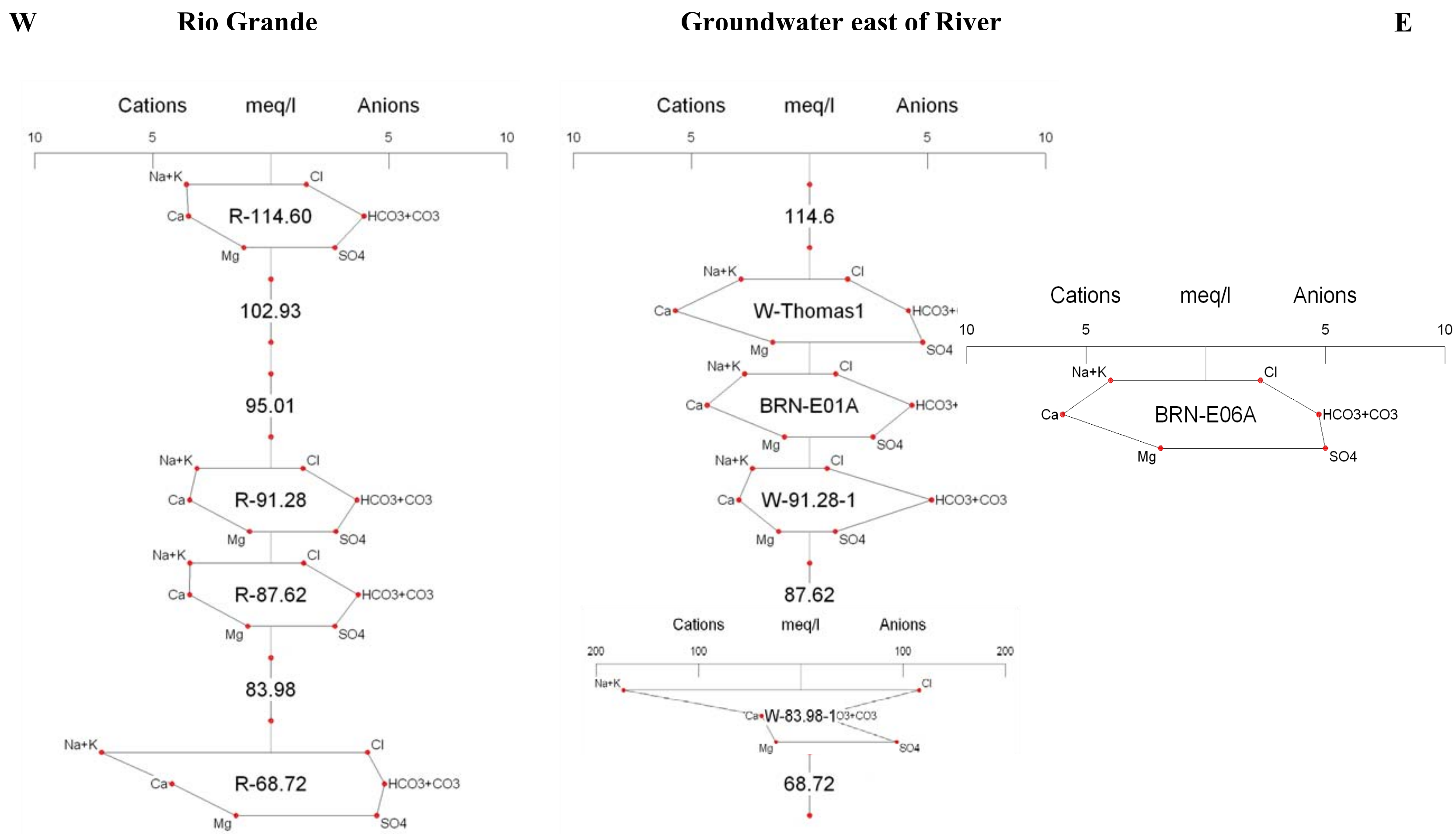

Figure 36 Stiff diagrams representing the water chemistry of the Rio Grande and of shallow groundwater east of river. The Stiff diagrams are arranged spatially from north (top) to south (bottom) and from west (left) to east (right). All samples were collected during June 2003 except for W-91.28, W-83.98, and W-Thomas1, which were collected during June 2002. Samples were not collected for spaces with a river-mile label but no Stiff diagram.

other water types. A representative Stiff diagram from a shallow well-named W-83.98, located approximately one mile east of the river at the North boundary of the Bosque Del Apache is shown in figure 36. This water sample has the highest TDS value of all water samples collected (~13000 mg/L). The representative Stiff diagram is shown with a different scale because it is too large with respect to the other Stiff diagrams. Relative ion concentrations of chloride, sodium, and sulfate are extremely high. The high Cl/Br ratio (~1100) associated with this sample and the chemical similarity to other high-chloride waters associated with the Rio Grande Rift suggests that this water is a sedimentary brine originating from deep in the basin. This sample will be discussed in more detail later.

Water Chemistry of Drains and Springs

Water samples from certain springs and drains were collected for chemical analyses. Figure 37 shows locations where most of these samples were collected along with Stiff diagrams representing the general chemistry data for most of the samples. It should be noted that all sample locations are located west of the river.

Drains and canals sampled include Drain Unit 7 (D-Unit7), two locations on the Luis Lopez drain (D-LLDR3,4), Socorro Main (D-SMC-91.28), the Elmendorf drain, (D-ELMDR), and the Socorro Riverside Drain (D-SRD-91.28, D-SRD87.62) (figure 38). Drain Unit 7 carries irrigation return flow from the north into the Socorro Main Canal at San Acacia. Water from this drain ultimately comes from the river north of San Acacia, which explains the observed river-like chemical signature. Water samples collected from the Luis Lopez drain were observed to have much higher TDS values than other samples

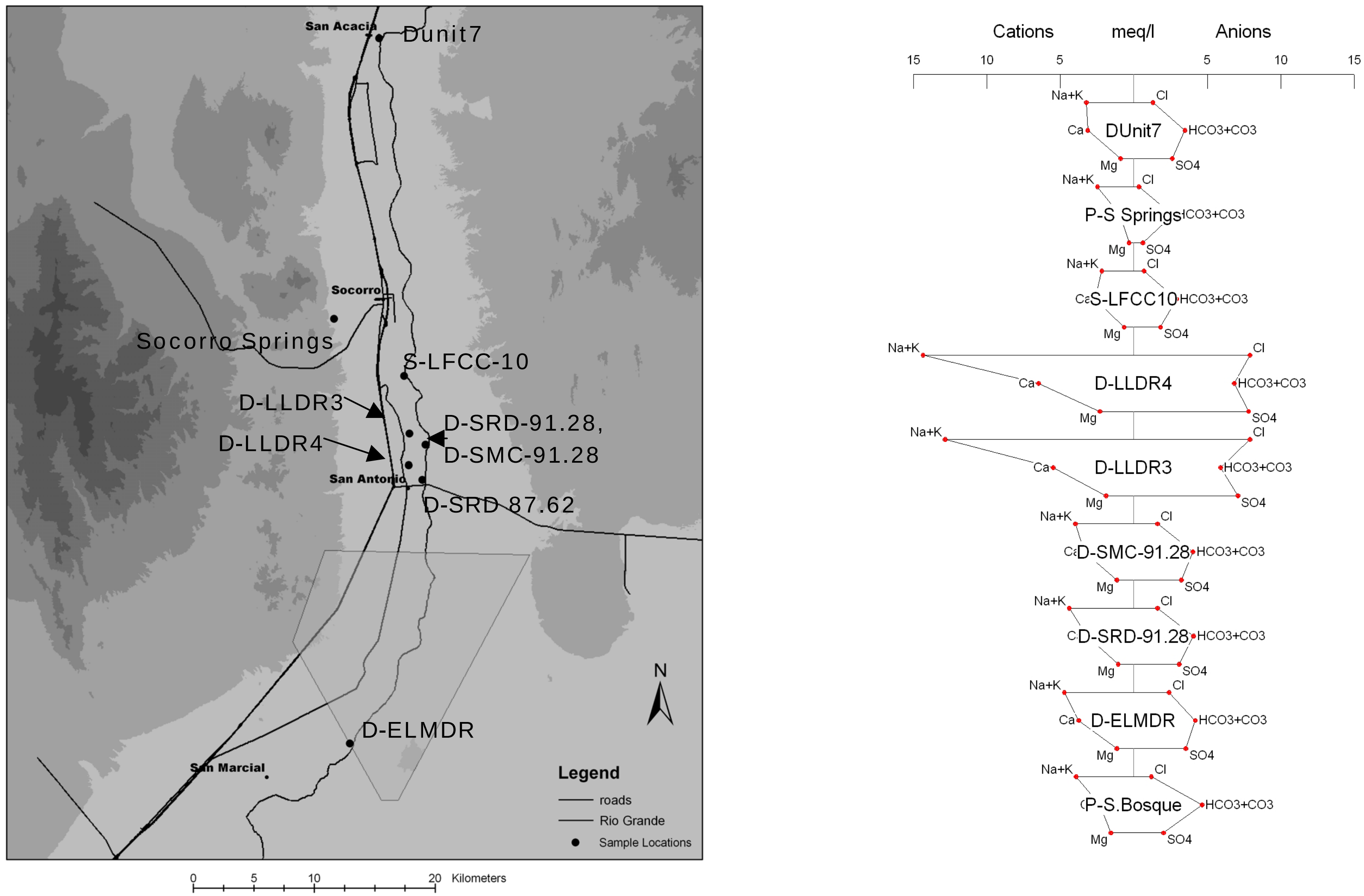

Figure 37 Sample locations for springs and drains and Stiff diagrams representing the water chemistry of water samples.

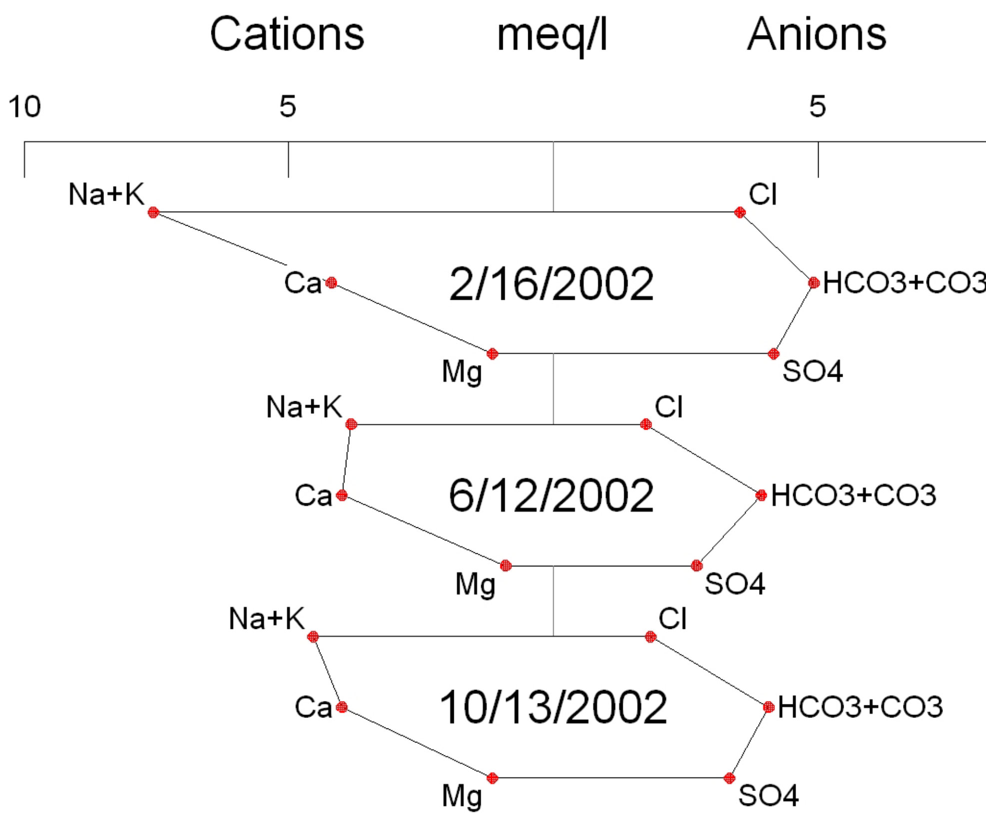

Figure 38 Stiff diagrams representing water chemistry for River-side Drain at river mile 87.62 for different times.

(1270-1390 mg/L), and appeared chemically similar to the high-chloride waters believed to be sedimentary brines, both with respect to the general chemical signature (W-83.98-1), and the high Cl/Br ratio (1000). Mills (2003) also observed these high-chloride waters where the Luis Lopez Drain begins (figure13). Water samples from the Socorro Main Canal, the Socorro Riverside Drain at river mile 91.28, and the Elmendorf Drain were observed to have very similar chemical signatures to each other with TDS values of 540-610 mg/L. These water samples appeared chemically similar to water in the southern part of the LFCC, which is primarily a mixture of river water and high-chloride waters. Interestingly, the Elmendorf drain routes all irrigation return flow for the irrigation district to the LFCC, just south of Bosque del Apache. However, the LFCC seems to acquire this chemical signature somewhere within Bosque del Apache before water from the Elmendorf Drain is introduced.

The two springs sampled were Socorro Springs (P-S Springs) and a spring located on the west bank of the LFCC at Brown Arroyo (S-LFCC10). Socorro Springs had a chemical signature different from that of the river and a low TDS value of ~200 mg/L. A high relative concentration of sodium is probably a result of ion exchange reactions between the water and rhyolitic volcanic material rich in sodium plagioclase (Hem, 1985).

S-LFCC10 was characterized by a TDS value of 340 mg/L, lower than that of the LFCC and the river, and a chemical signature almost identical to that of the river with no sign of mixing or mineral/water interactions. The concentration of dissolved solids (figure 37), which is controlled by the amount of evaporation that takes place in the river, was lower than samples representing river water chemistry in the study area since 1997, indicating that water from this spring originated as river water at least seven years ago. Water that discharges at this spring may either originate from river seepage east of the LFCC or irrigation return flow west of the LFCC. Either way, this spring might be evidence of compartmentalization by faults that limits river/groundwater interaction or shallow groundwater mixing. However, further analysis of this spring is necessary to determine its source. These findings are interesting because this is close to the northern extent of where high-chloride waters are observed in the shallow groundwater system.

The implications of how different structures such as fractures and faults in this area affect the regional hydrology will be discussed later in this thesis.

The sample P-S.Bosque came from a pond west of the LFCC and south of San Marcial. The chemical signature looks similar to that of drains and the LFCC, but according to stable isotope data, this sample plots farthest out on the evaporation line defined by Mills (2003), indicating that it has undergone the highest level of evaporation with an original isotopic composition similar to that of the river. However, this sample had a TDS value of 440 mg/L, which is similar to that of the river; this value would be much higher if this water was evaporated river water. This water may be a mixture of evaporated river water and Socorro Springs type water.

Figure 38 shows how the water chemistry of the Socorro Riverside Drain at river mile 87.62 (D-SRD-87.62) changes with time. The observed temporal variations are similar to those observed for W-87.62-4 discussed above. A high-chloride component was observed during non-irrigation season, while during irrigation season, water in this drain was more chemically similar to river water.

Identification of End Members and Mixing Relationships

As indicated above, river water appeared to be the primary water type in the shallow alluvial aquifer. However, differences in water chemistry indicate mixing with other water types. In order to calculate mixing ratios, end members must be identified. With river water as an obvious end member, two other end members were identified based on water chemistry that displayed the largest deviations from that of the river. It should be noted that the end members used in the following mixing analysis, with the exception of Socorro Springs, may not represent the pure end members and probably have a river water component to them. Also, the end members that will be discussed are most likely not the only end members in this complex system, but this study focuses on them to help explain the relationship between regional flow paths and the structural framework of the Socorro Basin. Figure 39 shows the water chemistry for the three end

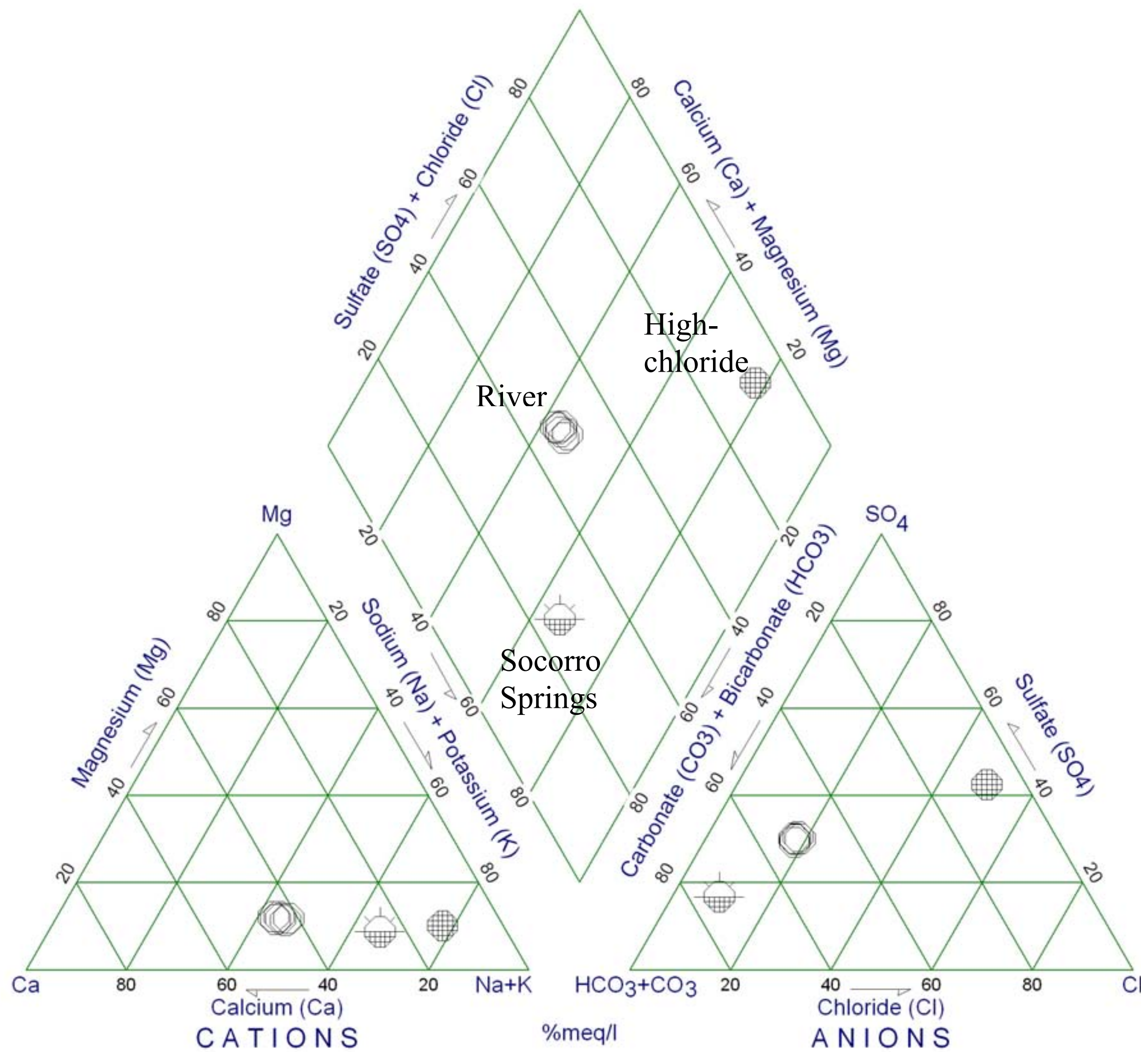

Figure 39 Three end members plotted on a Piper Diagram.

members plotted on a Piper diagram. The three end members that will be discussed are river water, high-chloride water, and Socorro Springs-type water. The origins of these end members were discussed above. The high-chloride end member was observed in the shallow aquifer east of the river at the north Bosque Del Apache boundary (W-83.98-1). It can be seen in figure 39 that the end members plot in different areas in the diamond part of the Piper diagram. A triangle formed by connecting the three points defines the area on the Piper diagram for waters resulting from the mixing of the three end members. Figure 40 shows a piper diagram with most of the groundwater and surface water samples collected in the study area plotted.

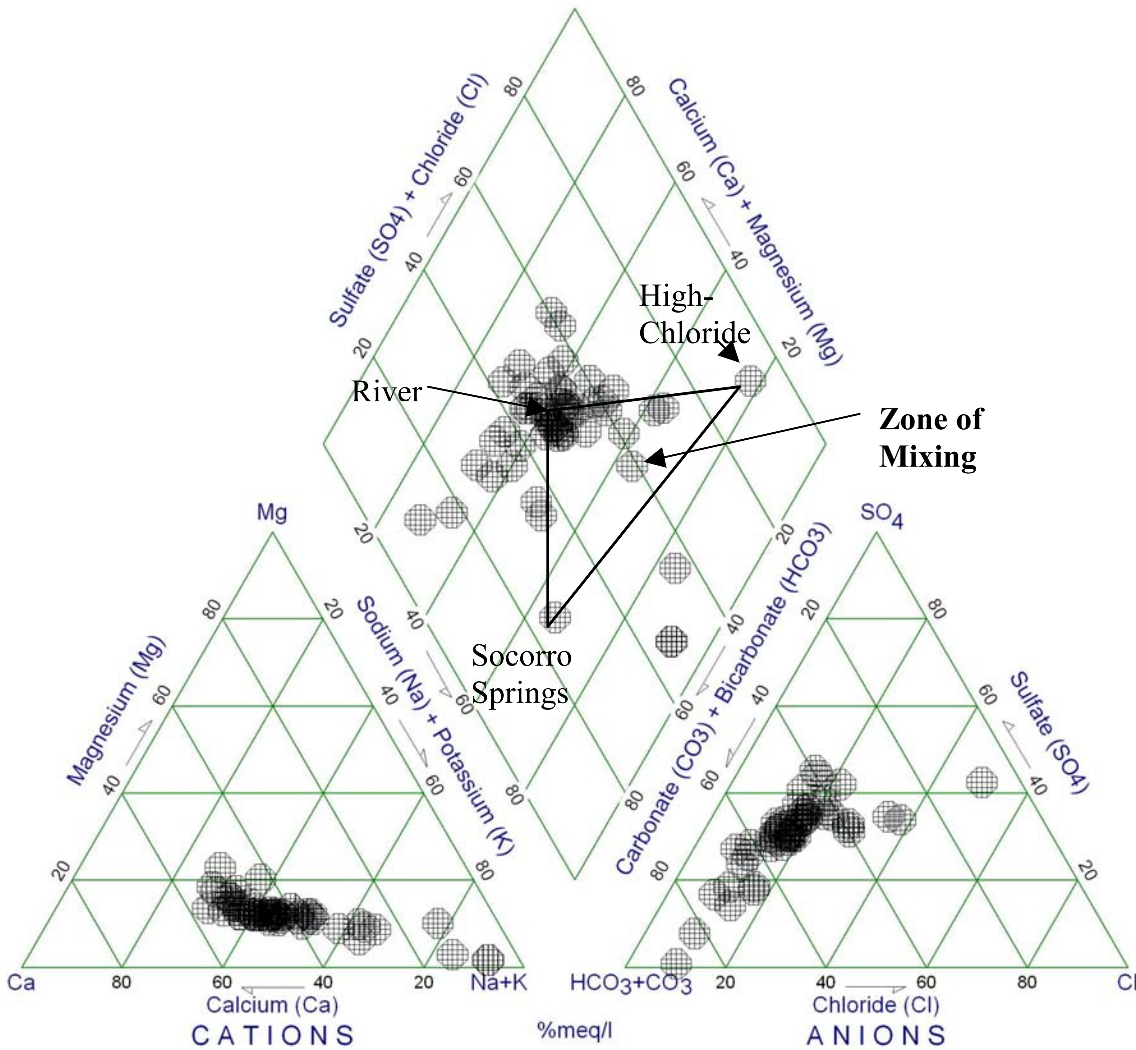

Figure 40 Groundwater and surface water samples. Shaded area denotes area of mixing between the three defined end members.

Notice that most of the water samples plot near river water. Again, this shows that the dominant water type in the system is river water. Mixing of the three defined end members can explain the chemical composition of some of the water samples, but it is obvious that other water types are present in the system. Other water types may include regional groundwater coming from the Albuquerque basin, mountain-front recharge from the east, and local precipitation. Calculated mixing ratios and the spatial relationship among these mixed waters are discussed below.

Spatial Relationships Among Mixed Waters

An example of the mixing processes mentioned above can be seen in figure 41.

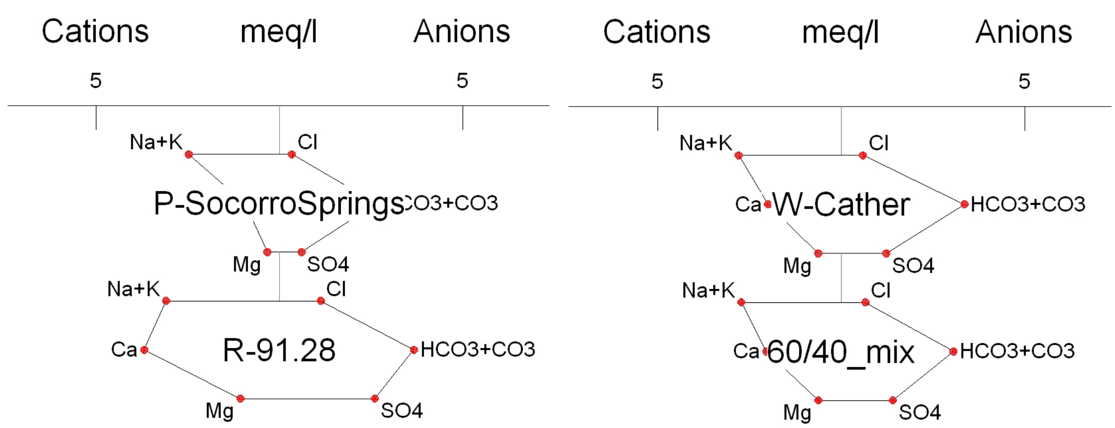

Figure 41 Stiff diagrams representing end members on left, observed Stiff diagram for water sample (top, right) and mixing model (bottom, right), 60% Socorro Springs and 40 % River water.

The two end members are Socorro Springs and river water and the presumed mixture of these two water types is the Cather well sample. A mixing model representing 60% Socorro Springs-type water and 40% river water produces a Stiff diagram almost identical to that representing the water chemistry of the Cather well.   Assuming that these mixing processes control the water chemistry observed for some groundwater samples, the spatial occurrence of these mixed waters may give insight to regional hydrologic processes in the Socorro Basin.

Figure 42 shows the location of Socorro Springs- mixed waters that were identified from water chemistry data obtained from this study and from Brandvold (2002). These samples were identified based on the shape and size of the representative Stiff diagrams. Samples are mostly a mixture of river water and Socorro Springs type water; however, some of them appear to have a high-chloride component (figure 43). Socorro Springs –mixed waters were observed near Socorro where the springs are located. Other Socorro Springs-mixed waters were observed south of Socorro and appear to be spatially associated with high-chloride water. Interestingly, these mixed waters were observed to the west of the high-chloride waters. The spatial and chemical relationship between Socorro Spring mixed waters and high-chloride waters may have important implications for the origin and mechanism of upwelling of high-chloride waters. Both of these water types appear to be associated with synrift faults, suggesting that a structure or structures related to the Rio Grande rift may control regional flow paths of Socorro Springs type waters and high-chloride waters.

Figure 43 shows water chemistry for the three end members, Socorro Spring-river -mixed waters, and water samples from the Luis Lopez drain and the southern end of the LFCC plotted on a Piper diagram. As mentioned above, the Socorro Springs- river-mixed waters appear to be mainly a mixture of river water and Socorro Springs type waters, but some samples appear to have a high-chloride component. Also, the drains and LFCC samples appear to be mostly a mixture of river water and high-chloride water

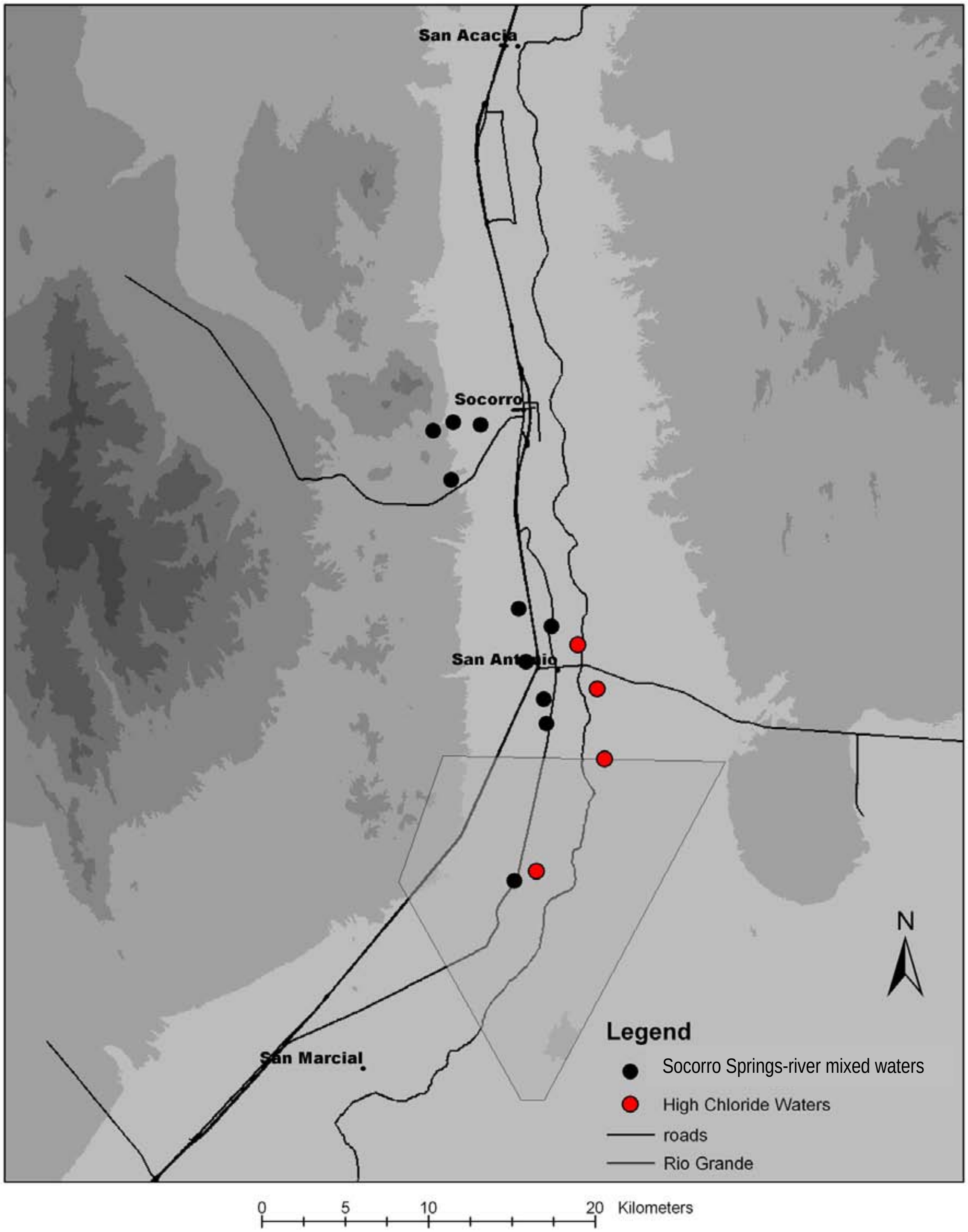

Figure 42 Location of Rio Grande-Socorro Springs mixed waters and high-chloride waters.

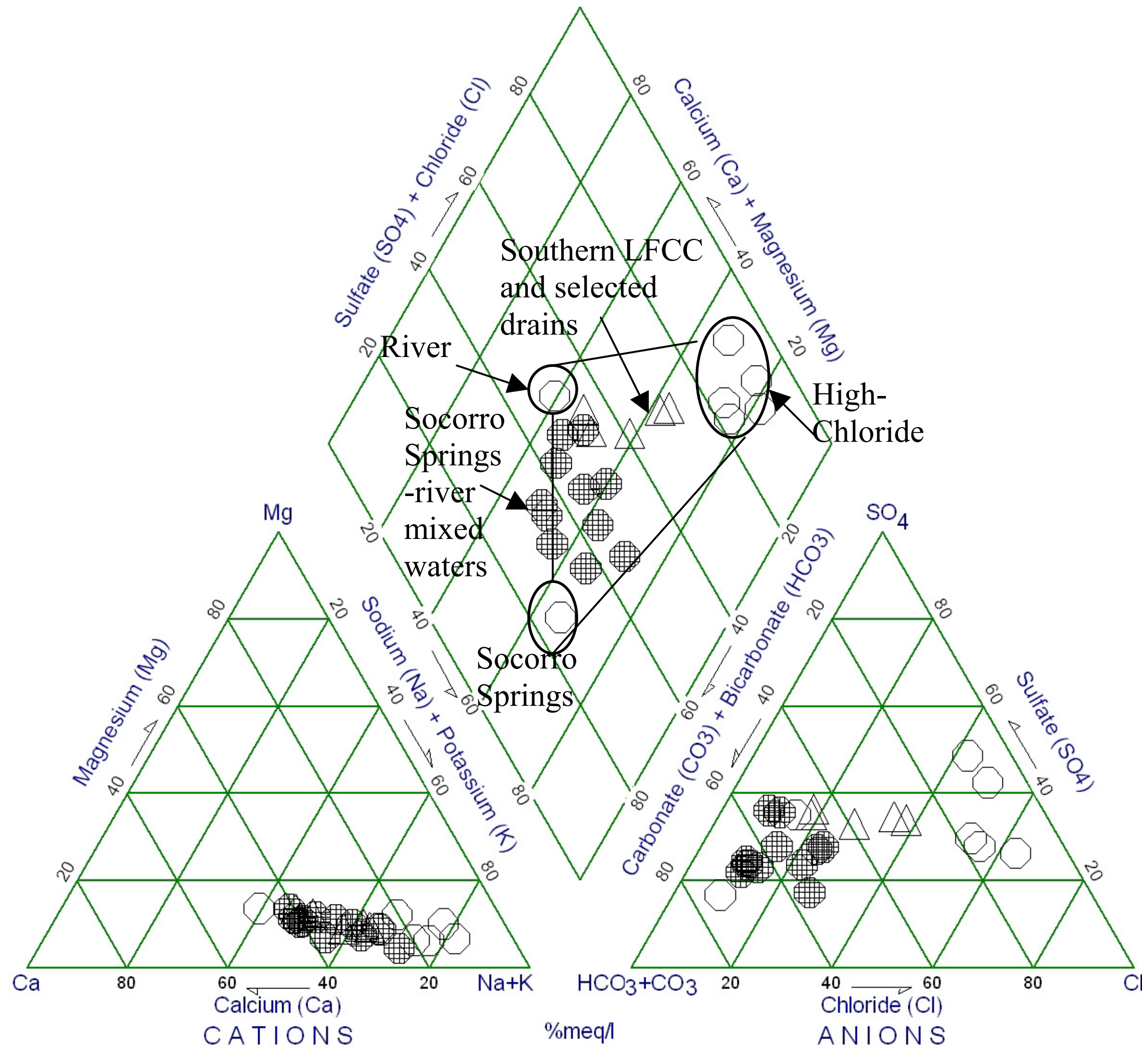

Figure 43 Socorro Springs mixed waters, selected drains and LFCC samples plotted on Piper diagram along with end members.

with a small component of Socorro Springs water. The spatial relationship among these different types of waters indicates that the suggested mixing relationships are valid. Water chemistry data from this study and from Brandvold (2001) that appeared to be a mixture of all three end members were identified and the location of these sampling sites were plotted on a map (figure 44). Again, most of these mixed waters appear near Socorro Springs and close to high-chloride waters; however, some of these mixed waters

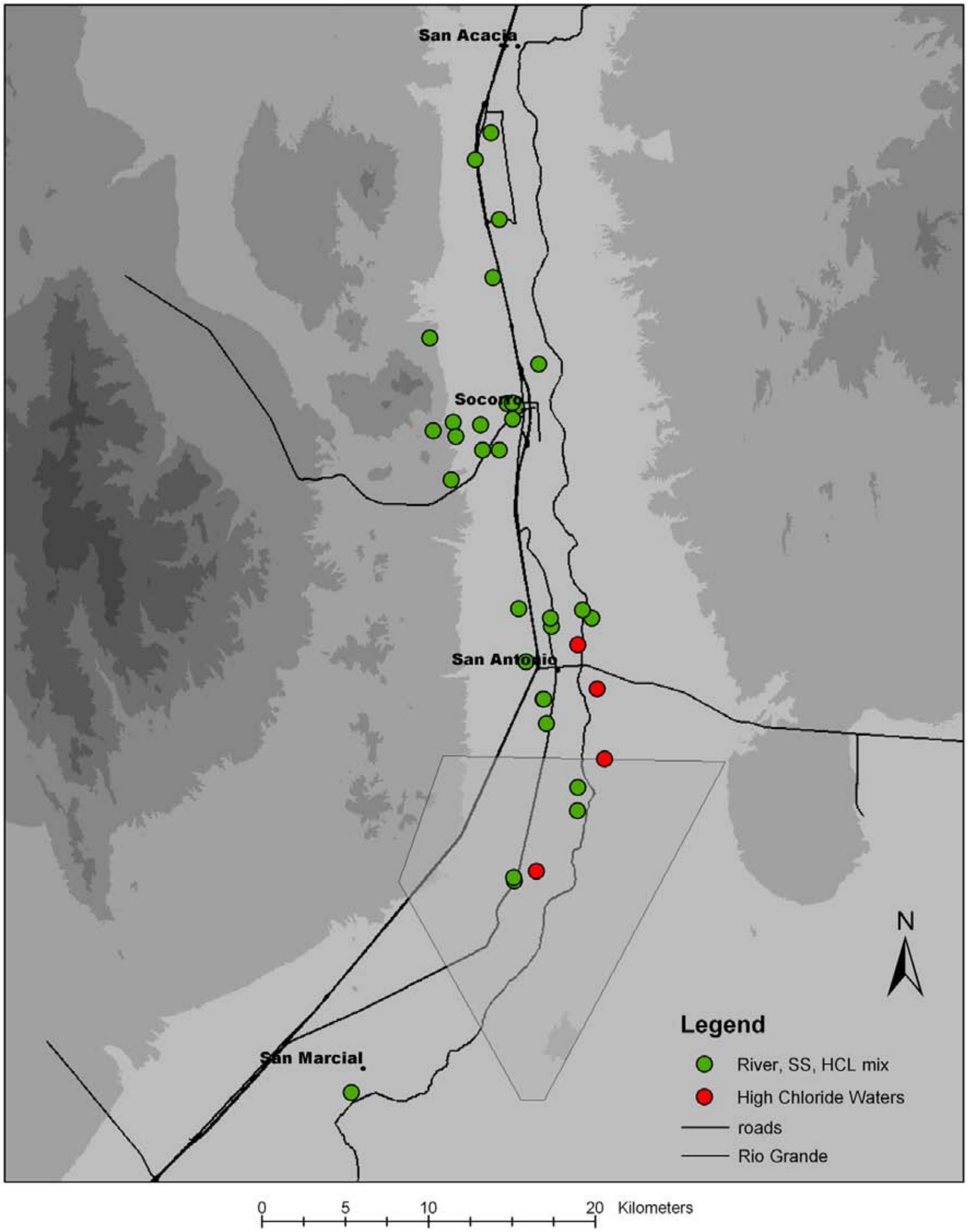

Figure 44 Location of river-high- chloride-Socorro Springs mixed waters.

were observed north of Socorro, possibly representing mountain front recharge from the west.

Evidence for Structures that may Control Regional Flow Paths and the Upwelling of High-Chloride waters

Understanding the structural framework of the Socorro Basin is difficult, as recent basin fill buries any structures that might cross the basin. Direct physical evidence of structures that might be controlling regional groundwater flow paths is scarce because no surficial expression is present in the center of the basin. One line of evidence was to project the continuation of mapped Quaternary faults. The presence of known geologic structures such as the SAZ might also suggest the presence of cross-basin structures. Other methods, including geophysical techniques, are also useful to study the subsurface geology. Techniques used to study the structural framework of the Socorro Basin include the use of GIS, geophysical data, and geomorphology. Geophysical and geomorphological evidence is discussed in appendices V and VI.

Projected Quaternary Faults

Figure 45 shows the location of mapped Quaternary faults provided by the New Mexico Bureau of Geology and Mineral Resources, along with the locations of high-chloride waters and waters that are a mixture of Socorro Springs type waters, high-chloride waters and river water. It is important to note that if the upwelling of high-chloride waters is structurally controlled, then the structures of interest are probably older structures that are related to rifting. However, Quaternary faults can help to identify

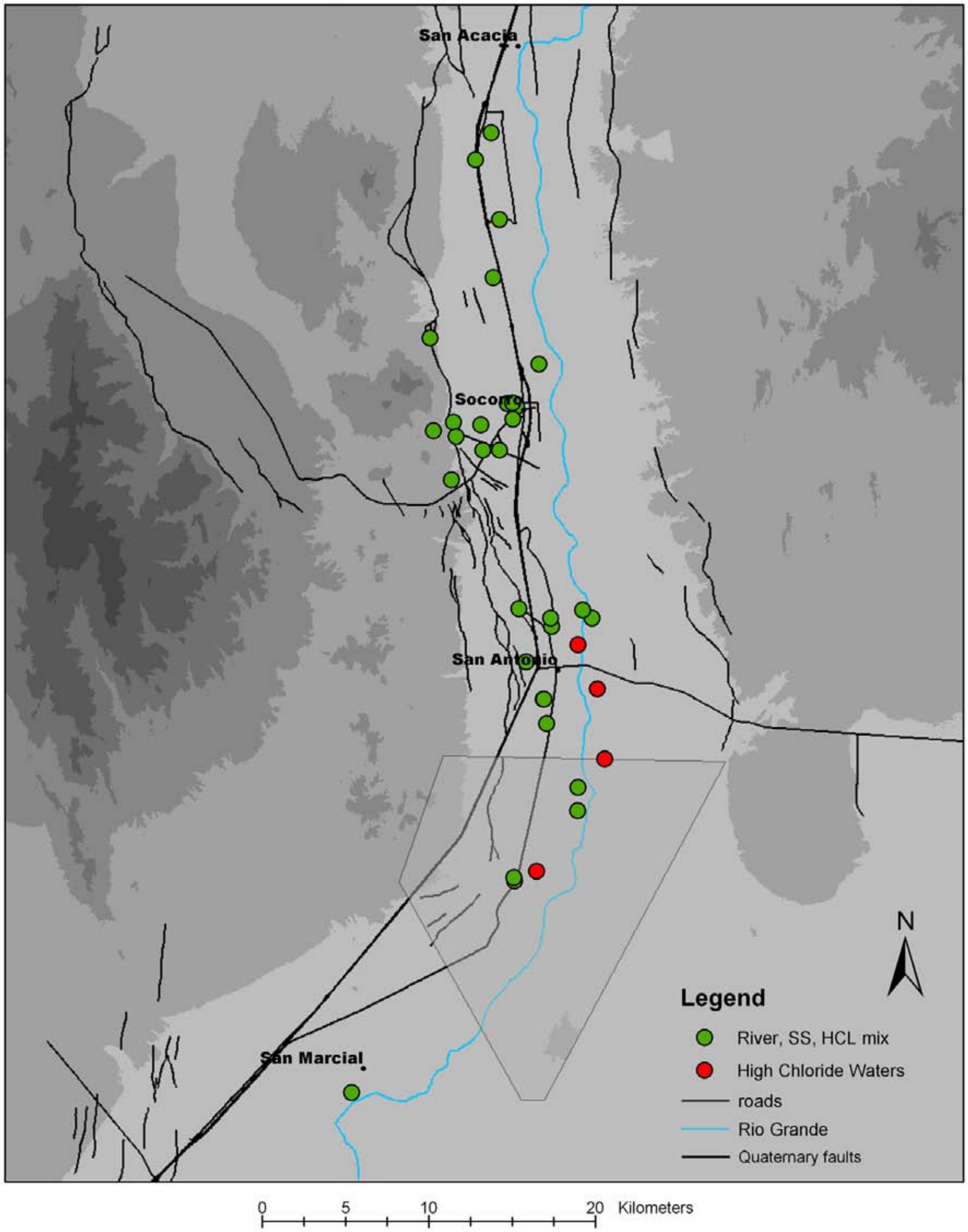

Figure 45 Location of Mapped Quaternary faults and water samples

older structures along which these young faults may propagate. Many of the Quaternary faults on the west side of the Socorro Basin begin striking to the southeast just south of Socorro. Although surficial expressions of these faults are absent in the Rio Grande Valley, projections of the faults along strike to the southeast are coincident with the area where the river- Socorro springs- high-chloride mixed waters are located. Also, some of the mapped Quaternary faults on the east side of the basin strike to the northwest towards the faults on the west side. So, the question is: do these Quaternary faults represent structures that go across the basin? Experts on the geology of the Socorro basin do not entirely agree on whether or not these faults continue across the basin (Richard Chamberlain and Steve Cather, personal communications, NMBGMR, 2003). In order to begin to answer this question, it is necessary to look at existing structural data and assess whether or not we might expect structures to cross the basin.

The SAZ and Its Implications About Cross-Basin Structures

All extensional terrains such as the Rio Grande Rift are divided into regionally extensive domains of uniformly dipping normal fault systems. This regional segmentation of rifts is accommodated by groups of structures called transfer zones and accommodation zones (Faulds and Varga,1998). An accommodation zone is defined as a group of structures that accommodate the transfer of strain between overlapping zones or systems of normal faults (Faulds and Varga, 1998). Figure 46 shows classifications for different observed geometries of accommodation zones presented by Faulds and Varga (1998). These different types of accommodation zones were examined in order to determine what geometry was most similar to that observed for the SAZ. The anticlinal

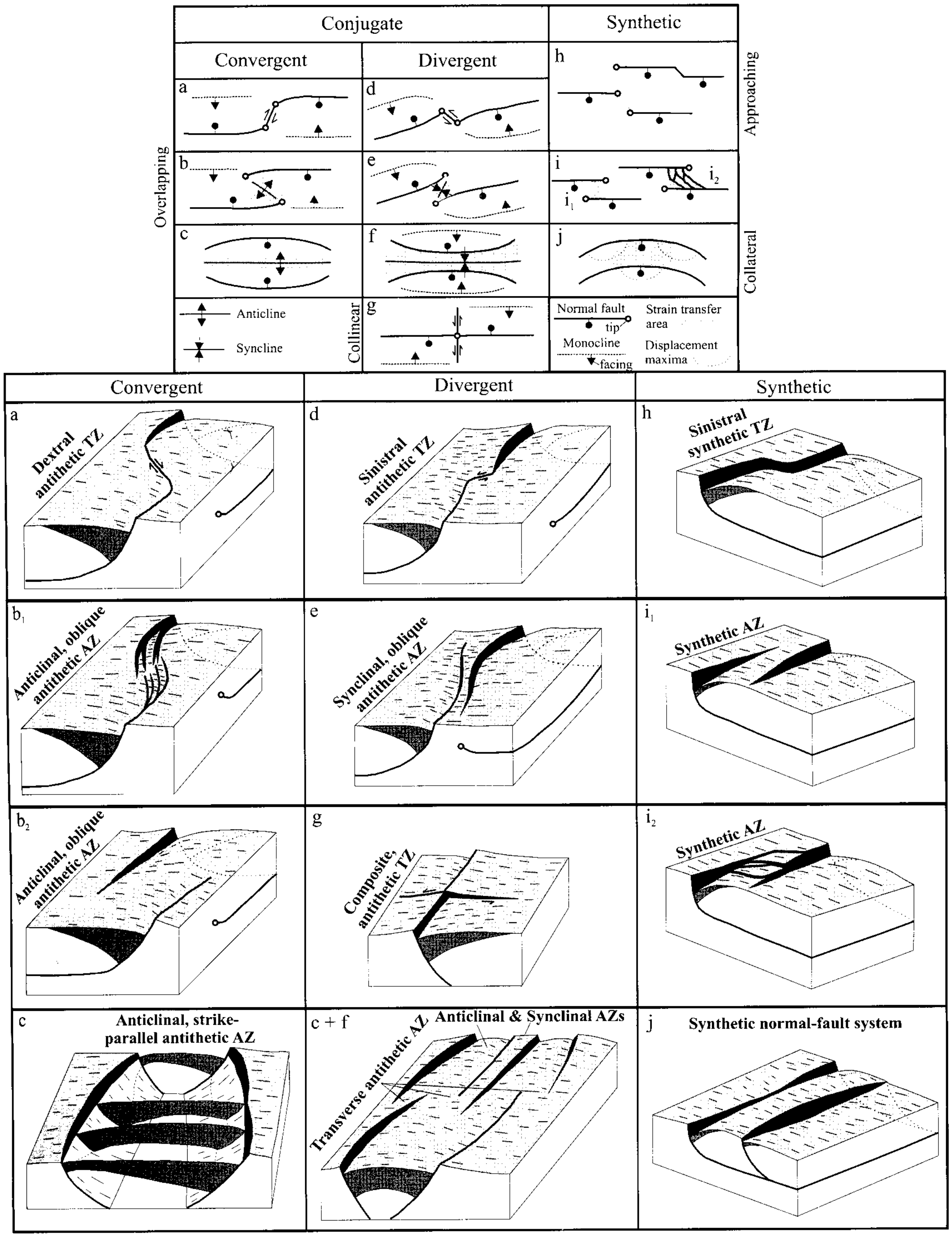

Figure 46 Conceptual models of different geometries of accommodation zones (Faulds et al., 1998)

oblique antithetic AZ (figure 46, b_1) most resembles the SAZ. Figure 47 is a close-up view of this type of AZ. Important characteristics of the geometry of the anticlinal oblique antithetic AZ are scissor-fault type structures that strike obliquely across the

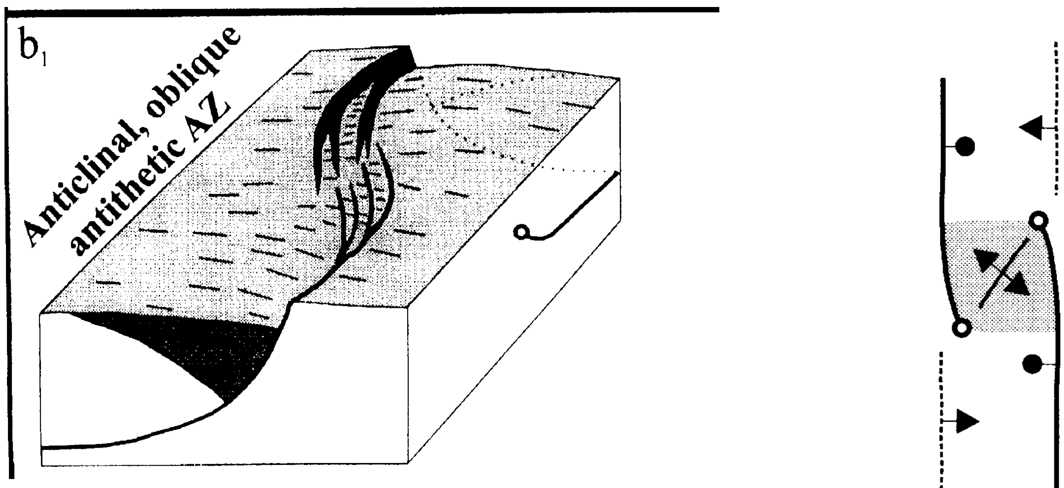

Figure 47 Close-up of conceptual model of an anticlinal oblique antithetic AZ.

basin along the interface between the two opposing tilt domains. Another structure that is observed along this interface is an anticline, whose axis trends approximately perpendicular to the strike of the scissor-faults. Along the axis of this anticline is a zone that separates the two opposing dip domains, similar to the SAZ as defined by Chapin (1989). If this type of geometry exists in the Socorro Basin, the southeast striking Quaternary faults in figure 45 may represent scissor- fault structures that cross the basin. Also, it has been observed that these scissor-type faults can affect on the flow path of a river where the river flows along the structure (Sean Connel, NMBGMR, personal communication, 2003), which may express itself as an observed bend in the river. Appendix V analyzes gravity data and geomorphology in order to identify the geometry of the SAZ. The evidence presented in these appendices supports the presence of buried northwest-southeast trending scissor faults that are associated with the occurrences of high-chloride groundwater.

Other Evidence for Cross-Basin Structures

Other physical evidence that may indirectly indicate that there may structures crossing the basin in this area is the Capitan lineament which crosses the basin at the farthest northern extent where the high-chloride waters are observed and the spring on the west bank of the LFCC, which was discussed above. The Capitan lineament is a prerift structure, along which synrift structures may have propagated. It is unclear what type of flow path is associated with the spring on the west bank of the LFCC, but the spring's presence may indicate that structures are present in the subsurface in this area. If some type of structure does go across the basin in this area, deformation associated with the structures may contribute to a complex hydrologic system, particularly explaining the high spatial variability of groundwater chemistry observed in this area.

Possible Mechanisms of Upwelling of High-chloride Waters

If structures related to the SAZ do play a role in controlling regional groundwater flow paths and the upwelling of high-chloride waters, what mechanisms are forcing high-chloride water to the shallow hydrologic system? If the structures are acting as conduits for high-chloride waters, the SAZ , which is a structural high, could provide such a pathway for movement of these waters to shallow depths, possibly into the shallow aquifer. As the high-chloride waters flow along the fault structures to the south-east due to the natural regional hydraulic gradient within the fractured system, many zones of different permeabilities may be encountered. Therefore, zones of lower permeability may allow the high-chloride waters to penetrate the shallow alluvial aquifer.

Another possible mechanism of forcing these deep sedimentary brines to the shallow system may involve geothermal waters. Buoyant forces may play an important role in mobilizing these high-chloride waters. There are many indicators that geothermal waters might be involved. The Socorro Accommodation Zone has been linked to volcanism for the last 32 m.y. (Chapin, 1989). The Socorro magma body is located just north of the study area and at the most southern occurrence of high-chloride-waters, warm water is produced. Also, high-chloride waters observed in the Mesilla Basin are known geothermal waters (Bothern, 2003). Most high-chloride waters found in the shallow system are not significantly warmer than other water types found in the shallow aquifer. If all of the high-chloride waters are of geothermal origin, then mixing with cold groundwaters may cause the observed lower temperatures; however, there is evidence that suggests that this is not the case. The warm water produced by the well in Bosque Del Apache had a TDS value of ~3300 mg/L while the TDS value for the most concentrated high-chloride water observed (W-83.98-1) was ~13000 mg/L. This suggests that these high-chloride waters are not geothermal waters, but may just be mobilized by geothermal waters. The actual origin of the high-chloride waters is unclear. The chemical signature is indicative of the dissolution of halite, but there are no known halite deposits at depth in this area. However, evaporates are associated with the Popotosa confining bed, suggesting that the high-chloride waters may be old connate waters from the upper Popotosa Formation. Goff et al. (1983) came to a similar conclusion involving high-chloride water observed near the Lucero uplift and was unsure about the origin of the observed high-chloride waters. A better knowledge of the subsurface geology is necessary in order to identify the source of the high-chloride waters.

CONCLUSIONS

High-chloride waters believed to originate as deep sedimentary brines are observed in the shallow hydrologic system in the Socorro Basin and appear to be linked to structures related to the Rio Grande rift as suggested by the occurrence of similar water types observed in adjacent areas along the Rio Grande rift. In this thesis, I have developed a hypothesis that suggests that the occurrence of high-chloride waters in the shallow aquifer in the Socorro Basin as well as the observed high spatial variability of groundwater chemistry are consequences of a complex flow system due to synrift cross-basin structures related to the SAZ. Stable isotope and water-chemistry data for groundwater and surface water samples were used to identify different water types and to evaluate mixing relationships among them. Among the different water types that were identified, the three water types of interest for this study were river water, high-chloride waters and Socorro Springs type waters. The spatial relationship between high-chloride waters and Socorro Spring-river mixed waters suggests that some type of cross-basin structure might control regional flow paths in the Socorro Basin. The location of Socorro Springs (in the vicinity of the Socorro fault zone) and the association of similar high-chloride waters, found in the Mesilla Basin and near the Lucero uplift, with Rio Grande rift faults suggests the flow paths of these two water types are related to Rio Grande rift faults.

Physical evidence of cross-basin structures is mainly limited to known faults on the west edge of the basin that strike to the southeast in the general direction toward the area where the high-chloride and Socorro Springs- type waters were observed. Surficial expressions of these faults are not present in the Rio Grande valley and whether or not these faults do cross the basin is unknown. The SAZ was considered in order to assess whether or not the continuation of these faults across the basin was feasible. A possible geometry of the SAZ was identified as an anticlinal oblique antithetic AZ (figure 47). This AZ geometry is characterized by scissor-type faults that obliquely cross the basin on both sides of the zone separating the two opposing dip domains of tilted fault blocks. An anticline is associated with this geometry, where the axis or hinge of the anticline separates the two dip domains. If the assumed SAZ geometry is valid, then the known faults in the Socorro fault zone may very well cross the basin. The involvement of the SAZ in the regional hydrologic system is reasonable and probably expected due to evidence of water movement along the SAZ. If these structures do cross the basin, the complex system of fractures that probably characterizes the zone where these hypothesized structures are located helps to explain the high variability in groundwater chemistry observed in the Socorro Basin as well as the presence of deep basin brines in the shallow aquifer system.

High-chloride waters flowing along these structures may be forced up into the shallow aquifer due to permeability differences within the fractured rock in the subsurface. In addition, geothermal waters related to the Rio Grande rift may also play an important role in the upwelling of high-chloride waters. However, the high-chloride waters do not appear to be geothermal waters. The origin of these high-chloride waters is still unknown.

Future Work

The results presented in this thesis lead to the following hypothesis: observed spatial variability of groundwater chemistry, including the presence of high-chloride waters is primarily controlled by cross-basin structures associated with the SAZ. The section will suggest future work that can be done to test this hypothesis. The spatial variability of groundwater chemistry and the mixing relationships among the different water types were the primary catalysts for the development of the hypothesis in this thesis. Therefore, it is important to have an adequate sampling coverage so that any spatial trends observed in the groundwater chemistry data are not a result of sampling bias. The groundwater sample locations for this study were limited to mostly monitoring wells within the Rio Grande flood plain. Water chemistry data for groundwater outside the flood plain were from Brandvold (2001). Between the two data sets, the sampling coverage appears to be adequate, but the collection and chemical analysis of more groundwater samples, especially in the area of the hypothesized cross-basin structures would be beneficial. Also, if the high-chloride waters are sedimentary brines, they are probably much older than the other water types observed in the shallow aquifer system. Therefore, the dating of groundwaters with a high-chloride component using tritium, carbon-14, and Chlorine-36 may give additional insight to mixing relationships among the different water types.

Conclusions for this research involving the presence and location of subsurficial structures were based on a very limited amount of physical evidence. Detailed mapping of the basin sediments would contribute a broader understanding of the structures present and the structural evolution of the basin. Also, high resolution gravity and magnetic surveys concentrated in the area of the hypothesized faults along with geophysical modeling could help to test the developed hypothesis.

REFERENCES

Anderholm, S. K. 1983. Hydrogeology of the Socorro and La Jencia Basin, Socorro County, New Mexico. p.303-318. in C.E. Chapin and J.F. Callender (ed.) Socorro Region II New Mexico Geological Society Thirty-Fourth Annual Field Conference October 13-15, 1983. New Mexico Geological Society, New Mexico.

Anderholm, S.K. 1984. Hydrogeology of the Socorro and La Jencia Basins, Socorro County, New Mexico. USGS Water –Resources Investigations Report 84-4342 . USGS, Albuquerque, New Mexico.

Barroll, M.W., and M. Reiter. 1990. Analysis of the Socorro Hydrogeothermal System: Central New Mexico. J. Geophys. Res. 95(B13):21,949-21,963.

Barroll, M.W., and M. Reiter. 1995. Hydrogeothermal Investigation of the Bosque Del Apache, New Mexico. New Mexico Geology. 17(1):1-17.

Beck, W.C. and C.E. Chapin. 1994. Structural and Tectonic Evolution of the Joyita Hills, Central New Mexico: Implications of Basement Control on Rio Grande Rift, in G.R. Keller and S.M. Cather, (ed.) Basins of the Rio Grande Rift:Structure, Stratigraphy, and Tectonic Setting: Boulder, Colorado, Geological Society of America Special Paper 291.

Bothern, L.R. 2003. Geothermal Salt Intrusion into Mesilla Basin Aquifers and the Rio Grande, Dona Ana County, New Mexico, USA. Unpublished Master Thesis. New Mexico State University, Las Cruces.

Brandvold, Lynn. 2001. Arsenic in ground water in the Socorro Basin, New Mexico, New Mexico Geology, 23(1): 2-8.

Burger, H.R. 1992. Exploration Geophysics of the Shallow Subsurface. Prentice Hall, Englewood Cliffs, NJ.

Cather, S.M. 1996. Geologic Maps of Upper Cenozoic Deposits of the Central Socorro Basin. New Mexico Bureau of Geology and Mineral Resources Open-File Report 417.

Cather, S.M., R.M. Chamberlin, C.E. Chapin, and W.C. McIntosh. 1994. Statigraphic Consequences of Episodic Extension in the Lemitar Mountains, Central Rio Grande Rift, in G.R. Keller and S.M. Cather, (ed.) Basins of the Rio Grande Rift:Structure, Stratigraphy, and Tectonic Setting: Boulder, Colorado, Geological Society of America Special Paper 291.

Chamberlin, R.M. 1983. Cenozoic Domino-Style Crustal Extension in the Lemitar Mountains, New Mexico: A Summary. p. 111-118. in C.E. Chapin and J.F. Callender (ed.) Socorro Region II New Mexico Geological Society Thirty-Fourth Annual Field Conference October 13-15, 1983. New Mexico Geological Society, New Mexico.

Chamberlin, R.M. and G.R. Osburn. 1986. Tectonic Framework, Character, and Evolution of Upper Crustal Extensional Domains in the Socorro Area of the Rio Grande Rift, New Mexico. Arizona Geological Society Digest, 16: 464-465

Chapin, C.E. 1989. Volcanism Along the Socorro Accommodation Zone, Rio Grande Rift, New Mexico. p.46-57. In C.E. Chapin and J. Zidek (ed.) Field Excursions to Volcanic Terrains in the Western United States. . Volume I . New Mexico Bureau of Mines and Mineral Resources. Socorro, New Mexico.

Chapin,C.E., R.M. Chamberlin, and J.W. Hawley. 1978. Socorro to Rio Salado. p. 121-128. in J.W. Hawley (ed.) Guidebook to Rio Grande rift in New Mexico and Colorado. New Mexico Bureau of Mines and Mineral Resources Circular 163.

Chapin, C.E. and S.M. Cather. 1994. Tectonic Setting of Axial Basins of the Northern and Central Rio Grande Rift. p. 5-25. in G.R. Keller and S.M. Cather (ed). Basins of the Rio Grande Rift: Structure, Stratigraphi, and Tectonic Setting: Boulder, Colorado, Geological Society of America Special Paper 291.

Craig, H. 1961. Isotopic Variations In Meteroic Waters. Science. 133:1702-2703.

Dansgaard, W. 1964. Stable Isotopes in Precipitation. Tellus. 16(4): 436-468.

Davis, S.N., D.O. Whittemore, and J. Fabryka-Martin. 1998. Uses of Chloride/Bromide Rations in Studies of Potable Water. Groundwater. 36(2):338-350.

Faulds, J.E., and R.J. Varga. 1998. The Role of Accommodation Zones and Transfer Zones in the Regional Segmentation of Extended Terranes. p.1-45. In J.E. Faulds and J.H. Stewart (ed.) Accommodation Zones and Transfer Zones: The Regional Segmentation of the Basin and Range Province. GSA Spec. Paper 323. GSA, Boulder, Colorado.

Goff, F., T. McCormick, J.N. Gardner, P.E. Trujillo, D. Counce, R. Vidale, and R. Charles. 1983. Water Geochemistry of the Lucero Uplift, New Mexico: A Geothermal Investigation of Low-Temperature Mineralized Fluids. LANL Rep. LA-9738-OBES UC-66b. Los Alamos National Lboratories, Los Alamos, New Mexico.

Hem, J.D. 1985. Study and Interpretation of the Chemical Characteristics of Natural Water. U.S. Geological Survey Water-Supply paper 2254. pp.100-102.

International Atomic Energy Agency. 1998a. Standard Operating Procedure For Oxygen Isotope Analysis of Water using CO_2 Equilibration Technique. IAEA Rep. RIALHYI02.02.001.

International Atomic Energy Agency. 1998b. Standard Operating Procedure For D/H Samples Preparation and Measurement. IAEA rep. RIALHYP02.02.001.

Johnson, P.S., W.J. LeFevre, and A. Campbell. 2002. Hydrogeology and Water Resources of the Placitas Area Sandoval County, New Mexico. New Mexico Bureau of Geology and Mineral Resources Open File Report 469.

Mailloux, B.J., M. Person, S. Kelly, N. Dunbar, S. Cather, L. Strayer, and P. Hudleston. 1999. Tectonic controls on the Hydrogeology of the Rio Grande Rift, New Mexico. Water Resour. Res. 35(9):2641-2659.

Mills, S.K. 2003. Quantifying Salinization of the Rio Grande Using Environmental Tracers. Unpublished Master Thesis. New Mexico Institute of Mining and Technology, Socorro.

Newton, B.T., S. Kuhn, P. Johnson, and D.L.Hathaway. 2002. Investigation of Flow and Seepage Conditions on a Critical Reach of the Rio Grande, New Mexico. p. 581-586. in J.F. Kenny (ed.) AWRA 2002 Summer Specialty Conference Proceedings: Groundwater/Surface water Interactions, Keystone, Colorado. 1-3 July 2002. AWRA, Middleburg, Virginia.

Puls, R.W. and M.J. Barcelona. 1996. EPA Ground Water Issue: Low-Flow (Minimal Drawdown) Ground-water Sampling Procedures. USEPA rep. 540/S-95/504. USEPA, Washington, DC.

Rozanski, K., L. Araguas-Araguas, and R. Gonfiantini. 1993. Isotopic Patterns in Modern Global Precipitation. p. 1-36. In P.K. Swart, K.C. Lohmann, J.McKenzie, S. Savin (ed.) Climate Change in Continental Isotopic Records. American Geopphysical Union.

S.S. Papadopulos and Associates. 2003. Technical Memorandum: Exploratory and Shallow Well Drilling , Middle Rio Grande Watershed Study- Phase 1: Unpublished memorandum prepared for the New Mexico Interstate Stream Commission. SSPA, Boulder, Colorado

S.S. Papadopulos and Associates. 2002. Assessment of Flow and Seepage Conditions on the Rio Grande and Adjacent Channels, Isleta to San Marcial, Summer 2001: Unpublished report prepared with Mussetter Engineering, Inc. for the New Mexico Interstate Stream Commission. 24 pp. plus appendices. SSPA, Boulder, Colorado.

S.S. Papadopulos and Associates. 2000. Middle Rio Grande Water Supply Study. Report prepared for the U. S. Army Corps of Engineers Albuquerque district 209and the New Mexico Interstate Stream Commission. 70 pp. plus tables and figures. SSPA, Boulder, Colorado.

Sanford, A.R. Gravity Survey in Central Socorro County, New Mexico. 1968. NM Bureau of Mines and Mineral resources. Circular 91, Socorro, New Mexico.

Western Regional Climate Center. Precipitation and snowfall monthly totals. [Online]. Available at: http://www.wrcc.dri.edu (accessed 06 June 2004) WRRC, Reno, NV.

Wilcox, L.J. 2003. A Telescopic Model of the San Acacia Reach of the Middle Rio Grande, New Mexico. Unpublished Master Thesis. New Mexico Institute of Mining and Technology, Socorro.

APPENDICES

Appendix I The following tables contain location information for groundwater and surface water sampling points. For wells that were sampled well specifications are included.

Table 3 Well specifications for wells that were sampled for this study. Datum for location coordinates is NAD 83.

Well ID	River Mile	Longitude	Latitude	Easting (meters)	Northing (meters)	Measuring Point Elevation (ft)	Ground surface elevatio (feet)	Well material	Well Diameter (inches)	Casing Material	Casing diameter (inches)	Stick Up (inches)	Total Depth (Feet)
W-114.60-2	114.6	-106.90	34.24	325088.23	3790500.20	4661.82	4660.12	pvc	2	steel	4	1.7	24.15
W-114.60-3	114.6	-106.89	34.18	325953.48	3783848.64	4661.04	4660.25	pvc	2	steel	4	0.79	24.35
W-109.49-2	109.49	-106.89	34.18	326096.27	3783847.44	4638.41	4637.58	pvc	2	steel	4	0.83	19.06
W-109.49-3	109.49	-106.89	34.18	325950.72	3783849.02	4638.79	4637.23	pvc	2	steel	4	1.56	20.27
W-109.49-4	109.49	-106.89	34.18	325887.53	3783872.05	4644.4	4643.3	pvc	2	steel	4	1.1	26.6
W-109.49-5	109.49	-106.89	34.18	325931.62	3783813.54	4638.3	4636.94	pvc	4	steel	6	1.36	413
W-Thomas1	102.93	-106.88	34.11	326784.29	3763540.29	4608.909	4607.972	pvc	4			0.9375	5.62
W-99.59-1	99.59	-106.87	34.07	327077.93	3771072.03	4599.2	4598.13	pvc	2	steel	4	1.07	10.84
W-99.59-3	99.59	-106.87	34.07	327080.84	3771079.74	4599.84	4598.38	pvc	4	steel	6.5	1.46	307
W-99.59-4	99.59	-106.87	34.07	327084.74	3771090.77	4598.75	4598.37	pvc	4.25	steel	6	0.38	54.79
W-91.28-1	91.28	-106.84	33.95	329576.02	3757532.36	4555.92	4554.4	pvc	6			1.52	74.45
W-91.28-3	91.28	-106.85	33.95	329097.94	3757885.97	4557.66	4556.64	pvc	2	steel	4	1.02	13.78
W-91.28-3.5	91.28	-106.85	33.95	329008.02	3758026.27	4556.24	4554.56	pvc	2	steel	4	1.68	17.71
W-91.28-4	91.28	-106.85	33.95	328720.38	3758019.26	4555.7	4554.13	pvc	2	steel	4	1.57	21.37
W-Perini1	88.5	-106.87	33.94	327627.69	3763524.88	4549.992	4549.207	pvc	6			0.785	80
W-Sichler1	88.12	-106.85	33.93			4551.856	4549.0359	steel	1.5			2.82	39.18
W-87.62-1	87.62	-106.85	33.92	328904.26	3755093.92	4555.32	4553.93	pvc	2	steel	4	1.39	19.5

Well ID	River Mile	Longitude	Latitude	Easting (meters)	Northing (meters)	Measuring Point Elevation (ft)	Ground surface elevation (feet)	Well material	Well Diameter (inches)	Casing Material	Casing diameter (inches)	Stick Up (inches)	Total Depth (Feet)
W-87.62-2	87.62	-106.85	33.92	328852.45	3755092.63	4548.86	4547.28	pvc	2	steel	4	1.58	13.85
W-87.62-3	87.62	-106.85	33.92	328742.96	3755123.45	4548.23	4546.61	pvc	2	steel	4	1.62	18.41
W-87.62-4	87.62	-106.85	33.92	328685.19	3755151.12	4547.37	4546.5	pvc	2	steel	4	0.87	14.2
W-Cather	86.19							steel	6				100
W-83.98-1	83.98	-106.83	33.87	330343.75	3749067.69	4539.06	4537.94	pvc	2	steel	4	1.12	26.41
W-83.98-3	83.98	-106.85	33.87	328806.90	3749128.53	4534.42	4533.04	pvc	2	steel	4	1.38	18.3
W-83.98-4	83.98	-106.85	33.87	328584.23	3749199.11	4534.26	4532.91	pvc	2	steel	4	1.35	19.41
W-68.72-1	68.72	-106.99	33.68	315368.57	3728479.91	4479.16	4477.53	pvc	2	steel	4	1.63	12.54
W-68.72-2	68.72	-106.99	33.69	315251.70	3728863.80	4474.3	4472.83	pvc	2	steel	4	1.47	19.14
W-68.72-3	68.72	-106.99	33.69	315141.90	3729036.77	4472.74	4470.91	pvc	2	steel	4	1.83	18.66
W-68.72-4	68.72	-107.00	33.69	315099.31	3729088.62	4472.15	4470.45	pvc	2	steel	4	1.7	19.8
W-68.72-5	68.72	-106.99	33.69	315138.27	3729041.27	4471.19	4470.15	pvc	4	steel	6	1.04	122.58
W-68.72-6	68.72	-106.99	33.69	315136.38	3729039.09	4471.56	4470.24	pvc	4	steel	6	1.32	35.02
W-EB-11-19	66.36	-107.00	33.66	314716.66	3725944.23			pvc	2			2.95	10.39
W-EB-11-20	66.36	-107.00	33.66	314653.65	3725996.48			pvc	2			3.19	14.39
W-EB-13	65.6	-106.99	33.65	315335.60	3724700.86			steel	2			0.9	13.42
W-EB-22-18	60.77	-107.04	33.60	310599.33	3719127.50			pvc	2			2.78	8.99

Table 4 Surface water sampling locations

Location ID	Sample type	River Mile	Longitude	Latitude	Easting (meters)	Northing (meters)
DUnit7	Drain					
D-ELMDR	Drain					
D-ESC E-Side	Drain					
D-LLDR1	Drain	94.79	-106.88	33.99	326750.68	3762661.87
D-LLDR2	Drain	93.19	-106.87	33.97	327376.20	3760702.79
D-LLDR3	Drain	92.07	-106.87	33.96	327611.95	3758958.55
D-SRD-91.28	Drain	91.28	-106.85	33.95	328962.70	3758016.89
D-SMC-91.28	Drain	91.28	-106.85	33.95	328936.19	3758017.89
D-SRD-87.62	Drain	87.62	-106.85	33.92	328676.14	3755139.87
L-114.60	LFCC	114.6	-106.90	34.24	325019.99	3790487.40
L-109.49	LFCC	109.49	-106.89	34.18	325992.32	3783830.19
L-99.59	LFCC	99.59	-106.87	34.07	327014.54	3771077.00
L-91.28	LFCC	91.28	-106.85	33.95	329040.71	3758007.88
L-87.62	LFCC	87.62	-106.85	33.92	328767.66	3755099.87
L-83.98	LFCC	83.98	-106.85	33.87	328848.45	3749113.89
L-EB-11	LFCC	66.36				
P-S.Bosque	Pond					
S-LFCC10	Pond	94.67	-106.87	34.00	327174.88	3763723.40
R-114.60	River	114.6	-106.90	34.24	325223.93	3790484.44
R-109.49	River	109.49	-106.88	34.18	326449.63	3783819.61
R-99.59	River	99.59	-106.87	34.07	327247.24	3771052.35
R-RGBA	River	94.67	-106.87	34.00	327308.40	3763755.91
R-91.28	River	91.28	-106.85	33.95	329267.25	3757848.86
R-87.62	River	87.62	-106.85	33.92	328955.69	3755078.36
R-83.98	River	83.98	-106.85	33.87	328997.48	3749220.49
R-68.72	River	68.72	-107.00	33.68	314996.90	3728091.66
R-EB-11	River	66.36				
R-RGCOR	River	59.73	-107.05	33.59	309618.18	3717919.07
P-SocorroSprings	Spring					

Appendix II The following tables contain field chemistry data for groundwater and surface water samples.

Table 5 Groundwater field chemistry data

Locatio ID	DATE	TIME	Electrical Conductivity (mS/cm)	pH	Dissolved Oxygen (mg/l)	Temperature (deg C)	Redox Potential (mV)
W-109.49-2	1/8/2002	11:46	0.66	7.448	0.59	15.2	
W-109.49-3	1/8/2002	13:05	1.509	6.954	0.57	17.2	
W-109.49-4	1/8/2002	14:01	0.876	7.288	0.38	18	
W-109.49-5	1/8/2002	12:53	2.995	7.558	3.45	18.9	
W-114.60-2	1/8/2002	10:22	0.672	7.64	0.65	18.7	
W-114.60-3	1/8/2002	9:10	1.44	6.79	0.68	15.8	
W-99.59-1	1/8/2002	15:14	0.832	7.418	0.53	15.2	
W-99.59-3	1/8/2002	15:02	0.65	7.815	0.75	14.5	
W-99.59-4	1/8/2002	15:51	0.621	7.662	0.59	15.9	
W-83.98-3	1/9/2002	15:01	0.846	7.355	0.75	18.3	
W-83.98-4	1/9/2002	16:46	0.759	7.257	0.69	15.3	
W-87.62-1	1/9/2002	13:54	0.707	7.555	0.77	17.2	
W-87.62-2	1/9/2002	14:28	0.708	7.486	0.61	19	
W-87.62-3	1/9/2002	10:06	1.497	7.779	0.54	14.7	
W-87.62-4	1/9/2002	10:45	2.634	6.922	1.12	15.3	
W-91.28-3	1/9/2002	12:21	0.742	7.332	0.98	20.3	
W-91.28-3.5	1/9/2002	9:16	1.765	7.393	0.54	15.7	
W-91.28-4	1/9/2002	11:40	1.672	6.773	1.04	17.1	
W-68.72-1	1/10/2002	11:11	0.325	7.185	0.63	15.7	
W-68.72-2	1/10/2002	12:16	0.892	7.074	0.83	14.5	
W-68.72-3	1/10/2002	13:24	1.416	6.932	1.96	16.8	
W-68.72-4	1/10/2002	14:25	1.412	7.183	2.04	16.9	
W-68.72-5	1/10/2002	13:22	0.676	7.674	2.42	16.2	
W-68.72-6	1/10/2002	13:44	0.924	7.312	5.02	16.7	
W-83.98-1	1/10/2002	10:02	19.605	6.955	0.91	16.9	
W-EB-11-19	1/10/2002	15:19	0.8	6.783	1.29	8.9	
W-EB-11-20	1/10/2002	15:54	1.271	6.907	1.05	14.6	
W-EB-13	1/10/2002	16:29	1.762	6.672	4.22	11.4	
W-EB-22-18	1/10/2002	17:10	1.882	7.068	0.67	11.1	
W-Found Well	1/10/2002	17:48	1.311	7.204	0.74	11.8	
W-99.59-1	2/15/2002	14:56	0.676	7.67	0.32	11.7	-141
W-99.59-4	2/15/2002	16:46	0.614	7.7	0.72	14.5	-146
W-109.49-2	2/16/2002	11:10	0.639	7.71	0.48	15.7	-81
W-109.49-3	2/16/2002	11:05	1.491	7.13	1.38	20	65
W-109.49-4	2/16/2002	10:14	0.81	7.51	0.44	16.8	87
W-114.60-2	2/16/2002	12:35	0.647	7.89	0.25	17	-144
W-114.60-3	2/16/2002	13:03	1.291	6.92	0.32	16.8	34
W-87.62-2	2/16/2002	16:02	0.663	7.7	0.33	18.9	133
W-87.62-3	2/16/2002	16:39	0.702	8.49	0.38	14.5	-60
W-87.62-4	2/16/2002	16:37	2.6	7.24	0.3	19.2	-64
W-68.72-3	2/17/2002	17:18	1.423	7.04	0.28	16.9	-96

Locatio ID	DATE	TIME	Electrical Conductivity (mS/cm)	pH	Dissolved Oxygen (mg/L)	Temperature (deg C)	Redox Potential (mV)
W-68.72-5	2/17/2002	17:51	0.661	7.75	3.97	17.1	-55
W-68.72-6	2/17/2002	18:09	0.897	7.42	0.5	16.3	-86
W-83.98-1	2/17/2002	13:04	18.82	7.03	0.39	18.8	-38
W-83.98-3	2/17/2002	14:34	0.822	7.41	0.24	16.9	-93
W-83.98-4	2/17/2002	13:55	0.585	7.49	0.33	17	-81
W-91.28-1	2/17/2002	11:17	0.688	7.48	0.2	17.8	-302
W-91.28-3	2/17/2002	10:55	0.725	7.53	0.39	18.1	-41
W-91.28-3.5	2/17/2002	9:49	1.619	7.78	0.41	19.3	121
W-91.28-4	2/17/2002	9:26	1.603	7.03	0.58	16.2	-25
W-68.72-1	2/18/2002	12:22	0.73	7.26	0.31	15.5	-140
W-EB-11-20	2/18/2002	16:23	0.995	7.03	0.62	16.3	-22
W-EB-22-18	2/18/2002	17:58	1.863	6.97	0.41	10.8	-81
W-Thomas1	2/18/2002	9:51	0.95	7.4	0.44	10.2	-121
W-109.49-2	6/11/2002	12:49	0.632	7.49	0.49	16.8	
W-109.49-3	6/11/2002	15:30	1.483	7.03	0.23	18.6	
W-109.49-4	6/11/2002	14:27	0.717	7.28	0.24	20.1	
W-114.60-2	6/11/2002	12:24	0.602	7.74	0.62	17.8	84
W-114.60-3	6/11/2002	10:49	1.362	6.77	5.23	17.7	10
W-99.59-4	6/11/2002	8:39	0.617	7.52	0.53	13.1	-142
W-Thomas1	6/11/2002	15:02	0.948	7.16	0.38	17.3	-179
W-83.98-1	6/12/2002	14:48	18.21	6.98	0.19	20.8	18
W-83.98-3	6/12/2002	15:02	0.803	7.44	0.34	17.1	
W-87.62-2	6/12/2002	11:59	0.597	7.7	0.26	17.4	
W-87.62-3	6/12/2002	11:40	0.991	7.83	0.21	18.3	-135
W-87.62-4	6/12/2002	12:25	0.79	7.32	0.21	21.7	-3
W-91.28-1	6/12/2002	10:06	0.659	7.55	0.12	18.8	
W-91.28-3	6/12/2002	10:05	0.619	7.56	0.36	15.6	142
W-91.28-3.5	6/12/2002	8:38	1.506	7.66	0.29	17.5	
W-91.28-4	6/12/2002	8:00	1.505	6.91	0.47	17.4	-16
W-68.72-1	6/13/2002	10:18	0.809	7.07	1.24	17.9	
W-68.72-3	6/13/2002	9:08	1.384	7.01	0.44	20.2	-135
W-68.72-5	6/13/2002	11:09	0.631	7.64	0.32	22.2	-117
W-68.72-6	6/13/2002	10:12	0.88	7.29	0.36	20.7	-135
W-EB-11-20	6/13/2002	13:31	0.953	7.15	2.88	18.2	
W-EB-22-18	6/13/2002	13:41					
W-Perini1	6/13/2002	15:56	1.163	7.81	0.21	18	-169
W-109.49-2	10/12/2002	16:04	0.58	7.68	0	17.68	-145
W-109.49-3	10/12/2002	16:22	1.25	7.2	0	18.39	-11
W-109.49-4	10/12/2002	15:35	0.938	7.5	0	18.73	-177
W-114.60-2	10/12/2002	13:42	0.69	7.71	0	12.9	-188
W-114.60-3	10/12/2002	14:08	1.1	6.82	0	19.18	-38
W-99.59-4	10/12/2002	12:02	0.716	7.49	0	17.36	-192
W-Thomas1	10/12/2002	18:29	1.14	7.1	0	18.49	-115
W-68.72-1	10/13/2002	9:00	0.916	7.33	0	17.51	-184

Locatio ID	DATE	TIME	Electrical Conductivity (mS/cm)	pH	Dissolved Oxygen (mg/l)	Temperature (deg C)	Redox Potential (mV)
W-68.72-3	10/13/2002	8:45	1.4	7.19	0	17.82	-152
W-68.72-5	10/13/2002	9:30	0.6	7.79	0	16.01	-93
W-68.72-6	10/13/2002	10:25	0.84	7.51	0	15.02	-155
W-83.98-1	10/13/2002	16:57	19	7.25	0	17.18	-106
W-83.98-3	10/13/2002	15:29	0.84	7.53	0	18.62	-153
W-87.62-2	10/13/2002	17:57	0.68	7.85	4.29	12.22	-121
W-87.62-3	10/13/2002	15:33	0.96	7.7	0	17.49	-183
W-87.62-4	10/13/2002	16:53	1.05	7.38	0	19.24	-129
W-Cather	10/13/2002	14:33	0.561	7.94	0.8	20.2	-36
W-EB-11-20	10/13/2002	10:34	0.9	7.39	0	18.28	-201
W-91.28-1	10/14/2002	12:57	0.709	7.59	0	16.31	-311
W-91.28-3	10/14/2002	8:34	0.79	7.76	0	13.25	-25
W-91.28-3.5	10/14/2002	16:55	1.9	7.33	0	18.45	-52
W-91.28-4	10/14/2002	11:48	1.31	7.09	0	19.83	-82
W-Perini1	10/14/2002	14:52	1.3	7.98	0	19.15	-185
W-114.60-2	3/1/2003	11:19	0.448	8	0.68	16.91	-128
W-114.60-3	3/1/2003	10:16	0.867	7.17	1.13	15.94	-40
W-68.72-1	3/1/2003	15:04	1.28	7.35	6.16	14.07	-140
W-68.72-3	3/1/2003	16:49	1.33	7.25	5.25	15.87	-116
W-68.72-4	3/1/2003	16:09	1.36	7.31	5.5	15.87	-110
W-87.62-1	3/1/2003	14:30	0.437	8.06	0.52	10.62	-121
W-87.62-2	3/1/2003	15:06	0.96	7.93	0.82	15.59	-82
W-87.62-3	3/1/2003	15:55	2.47	8.07	0.51	15.35	-191
W-87.62-4	3/1/2003	16:26	0.644	7.66	0.12	12.83	-86
W-EB-11-20	3/1/2003	11:30	0.817	7.45	6.31	17.11	-146
W-87.62-1	3/7/2003	12:40	0.658	7.96	0.3	10.2	
W-87.62-2	3/7/2003	11:47	0.702	7.7	0.2	16.4	
W-87.62-1	3/13/2003	17:04	0.656	7.96	2.2	9	
W-87.62-2	3/13/2003	16:29	0.687	7.69	3.8	16.9	
W-87.62-1	3/21/2003	11:08	0.676	7.98	3.5	8.6	
W-87.62-2	3/21/2003	10:17	0.681	7.74	3.3	16.1	
W-87.62-1	3/29/2003	12:35	0.644	7.5	0.5	8.2	
W-87.62-2	3/29/2003	12:03	0.648	7.74	0.5	15.5	
W-87.62-1	4/5/2003	15:35	0.655	7.94	3.1	8.7	
W-87.62-2	4/5/2003	14:45	0.661	7.73	5.6	16	
W-87.62-1	4/12/2003	15:06	0.656	7.93	0.4	8.9	
W-87.62-2	4/12/2003	14:42	0.661	7.75	0.9	16	
W-87.62-1	4/18/2003	12:44	0.666	7.98	1.3	8.6	
W-87.62-2	4/18/2003	11:57	0.655	7.8	0.5	15	
W-87.62-1	4/26/2003	14:37	0.628	8	1	8.8	
W-87.62-2	4/26/2003	14:00	0.634	7.87	0.3	15.1	
W-87.62-1	5/3/2003	17:33	0.689	7.93	0.9	8.6	
W-87.62-2	5/3/2003	16:46	0.68	7.77	0.4	14.3	
W-87.62-1	5/11/2003	14:57	0.683	7.91	0.4	9	

Locatio ID	DATE	TIME	Electrical Conductivity (mS/cm)	pH	Dissolved Oxygen (mg/l)	Temperature (deg C)	Redox Potential (mV)
W-87.62-2	5/11/2003	14:19	0.681	7.78	0.3	14.2	
W-87.62-1	5/20/2003		0.69	7.96	0.7	9.5	
W-87.62-2	5/20/2003		0.644	7.87	0.6	13.2	
W-87.62-1	5/27/2003		0.668	7.92	0.2	10.4	
W-87.62-2	5/27/2003		0.667	7.81	0	13.7	
W-87.62-1	6/3/2003	17:08	0.661	10.65	0.1	10.4	
W-87.62-2	6/3/2003	16:24	0.646	8.48	0.7	12.9	
W-87.62-1	6/11/2003	10:00	0.694	9.72	0.2	11.3	
W-87.62-2	6/11/2003	9:38	0.653	9.56	0.4	12.1	
ESC-W03A	6/16/2003	10:30	1.69	7.17	0	17.83	-194
W-114.60-2	6/16/2003	9:20	0.591	9.01	0	13.58	-204
W-114.60-3	6/16/2003	8:05	1.3	6.79	0	17.2	-23
W-87.62-1	6/16/2003	8:44	0.694	9.63	0.3	11.7	
W-87.62-2	6/16/2003	8:00	0.656	9.11	0.8	11.7	
W-87.62-3	6/16/2003	10:23	1.405	9.29	1.1	16.2	
W-87.62-4	6/16/2003	11:08	0.972	9.05	0.9	19.2	
W-91.28-3.5	6/16/2003	15:41	1.34	9.31	1.9	17.3	
HWY-W07A	6/17/2003	15:00	0.643	7.63	0	13.14	-151
HWY-W07B	6/17/2003	15:38	0.619	7.69	0	15.69	-217
HWY-W07C	6/17/2003	16:10	0.627	7.67	0	14.45	-231
W-68.72-1	6/17/2003	13:01	1.186	7	2.2	17.5	
W-68.72-3	6/17/2003	14:02	1.271	6.86	2.7	18.2	
W-91.28-3	6/17/2003	16:55	0.762	7.66	0.4	15	

Table 6 Surface water field chemistry data

Location ID	Date	Time	Electrical Conductivity (mS/cm)	PH	Dissolved Oxygen (mg/l)	TEMP(deg C)	Redox Potential (mV)
L-109.49	1/8/2002	13:35	1.008	7.338	5.81	12.7	
L-114.60	1/8/2002	10:08	1.066	6.94	2.9	13.1	
L-99.59	1/8/2002	16:37	0.778	6.531	4.79	14.2	
R-109.49	1/8/2002	12:38	0.649	7.548	7.02	8.1	
R-114.60	1/8/2002	11:30	0.656	8.309	8.9	5.6	
R-99.59	1/8/2002	16:49	0.662	7.222	5.55	8.3	
D-SRD-87.62	1/9/2002	23:07	1.194	7.486	8.96	10.7	
L-83.98	1/9/2002	16:26	0.772	7.892	8.48	14	
L-87.62	1/9/2002	10:20	0.794	7.898	7.42	12.9	
L-91.28	1/9/2002	9:54	0.794	7.752	7	12.7	
R-83.98	1/9/2002	15:58	0.637	7.486	9.87	7.2	
R-87.62	1/9/2002	14:04	0.639	7.609	10.19	7.3	
R-91.28	1/9/2002	12:30	0.639	7.48	10.63	6.8	
L-68.72	1/10/2002	14:19	1.125	8.211	7.87	12.5	
L-EB-11	1/10/2002	18:46	1.123	8.301	7.81	11.3	
R-68.72	1/10/2002	12:56	0.655	7.312	8.79	6.9	
R-EB-11	1/10/2002	15:47	0.66	8.101	8.13	7.1	
R-RGCOR	1/10/2002	17:33	0.65	8.439	8.66	6.9	
L-99.59	2/15/2002	16:28	0.741	8.19	9.65	11.7	174
R-99.59	2/15/2002	16:06	0.642	8.03	11.8	10.6	147
D-SRD-87.62	2/16/2002	15:40	1.276	8.16	9.66	16.8	176
L-109.49	2/16/2002	10:39	0.936	7.95	7.22	11.4	155
L-114.60	2/16/2002	13:38	0.978	7.47	4.25	15.6	187
L-87.62	2/16/2002	17:03	0.772	8.42	9.09	14.4	196
L-87.62	2/16/2002	16:00	0.783	8.34	11.18	14.5	195
R-109.49	2/16/2002	12:02	0.647	8.45	10.48	8	184
R-114.60	2/16/2002	13:03	0.662	8.27	11.55	8	208
R-87.62	2/16/2002	15:24	0.638	8.46	9.99	11	238
L-68.72	2/17/2002	16:39	1.093	8.25	9.12	14.8	250
L-83.98	2/17/2002	15:30	0.765	8.49	10.99	14.6	227
L-91.28	2/17/2002	10:09	0.766	8.05	7.28	12.4	201
R-83.98	2/17/2002	15:34	0.639	8.38	9.52	11.9	256
R-91.28	2/17/2002	11:35	0.635	8.49	10.08	9.5	216
D-ESC E-Side	2/18/2002	10:20	0.597	8.01	0.25	12.2	-106
L-EB-11	2/18/2002	16:54	1.099	8.2	10.01	13.7	229
R-68.72	2/18/2002	13:26	0.646	8.45	10.9	10.4	234
R-EB-11	2/18/2002	15:30	0.646	8.44	10.68	11	254
R-RGCOR	2/18/2002	18:35	0.644	8.41	10.53	10.7	238
D-ESC E-Side	6/11/2002	14:24	0.598	7.96	7.25	24.8	206
L-109.49	6/11/2002	13:51	1.001	7.91	7.13	22.1	201
L-114.60	6/11/2002	11:10	1.141	7.71	7.25	18.3	193
L-99.59	6/11/2002	9:35	0.642	7.97	7.55	15.4	233
R-109.49	6/11/2002	11:35	0.596	7.11	6.98	23.3	

Location ID	Date	Time	Electrical Conductivity (mS/cm)	PH	Dissolved Oxygen (mg/L)	TEMP (deg C)	Redox Potential (mV)
R-114.60	6/11/2002	11:51	0.613	8.43	8.48	22.7	189
R-99.59	6/11/2002	9:19	0.651	8.48	11.03	17.5	194
D-SRD-87.62	6/12/2002	12:42	0.777	7.77	5.19	17.3	213
L-87.62	6/12/2002	11:11	0.855	7.95	6.92	17.4	205
L-91.28	6/12/2002	8:29	0.748	7.49	5.02	15.5	206
R-83.98	6/12/2002	16:20	0.675	8.34	8.74	32.4	
R-87.62	6/12/2002	10:40	0.683	8.31	7.65	21	225
R-91.28	6/12/2002	9:22	0.68	8.28	7.2	18.8	245
L-68.72	6/13/2002	8:15	1.248	7.73	6.97	20.4	155
L-83.98	6/13/2002	15:40	0.831	8.02	8.49	21.2	
L-EB-11	6/13/2002	12:05	1.226	8.08	7.3	25	220
P-S.Bosque	6/13/2002	15:00	0.696	8.46		24.9	
R-68.72	6/13/2002	9:05	1.258	7.56	11.24	20	
R-EB-11	6/13/2002	14:00	1.202	7.89	16.2	30	
R-RGCOR	6/13/2002	12:44	1.249	8.09	8.17	29.9	210
D-ESC E-Side	10/12/2002	17:09	0.57	8.28	9.45	17.65	76
L-109.49	10/12/2002	15:50	0.888	7.93	8.43	17.89	60
L-114.60	10/12/2002	14:30	1.06	7.38	6.39	18.75	22
L-99.59	10/12/2002	12:14	0.64	7.7	5.73	15.88	115
R-109.49	10/12/2002	16:32	0.62	8.49	7.96	19.68	60
R-114.60	10/12/2002	14:12	0.62	8.38	8.49	16.86	109
R-99.59	10/12/2002	11:40	0.64	8.27	9.48	16.1	136
D-SRD-87.62	10/13/2002	17:10	0.959	7.71	8.83	15.7	12
L-68.72	10/13/2002	11:03	0.99	8.36	7.09	13.85	52
L-83.98	10/13/2002	15:44	0.81	8.15	6.71	14.86	51
L-87.62	10/13/2002	16:01	0.956	7.89	8.18	15.69	13
L-EB-11	10/13/2002	11:53	0.84	8.35	10.28	14.31	-15
R-68.72	10/13/2002	9:25	0.744	7.88	10.02	12.24	-41
R-83.98	10/13/2002	14:37	0.65	8.55	9.39	13.82	96
R-87.62	10/13/2002	18:20	0.7	8.63	6.99	13.71	-1
R-EB-11	10/13/2002	11:15	0.757	8.22	10.88	12.58	-65
R-RGCOR	10/13/2002	11:45	0.97	8.6	7.94	12.69	74
D-LLDR4	10/14/2002	13:34	2.2	8.16	11.87	19.82	105
L-91.28	10/14/2002	9:30	0.869	8.06	7.92	14.67	46
R-91.28	10/14/2002	8:58	0.787	8.28	10.89	8.74	59
D-ELMDR	3/1/2003	13:00	1.04	8.34	9.42	10.85	64
DUnit7	3/1/2003	9:10	1.07	7.7	12.44	8.45	192
L-109.49	3/1/2003	12:17	0.592	8.26	10.17	12.97	65
L-114.60	3/1/2003	10:34	0.673	7.86	8.69	13.19	60
L-68.72	3/1/2003	13:50	1.04	8.33	9.68	11.87	102
L-83.98	3/1/2003	17:20	0.509	8.38	10.14	12.92	75
L-87.62	3/1/2003	16:12	0.507	8.16	8.96	12.33	47
L-91.28	3/1/2003	13:43	0.496	8.32	8.99	11.8	70
L-99.59	3/1/2003	13:01	0.483	8.36	9.15	12.13	54
L-EB-11	3/1/2003	12:00	1.05	8.31	9.33	11.29	-9
L-SBB	3/1/2003	13:15	1.03	8.28	9.62	13.28	89
R-109.49	3/1/2003	11:57	0.426	8.57	11.91	8.02	73

Location ID	Date	Time	Electrical Conductivity (mS/cm)	PH	Dissolved Oxygen (mg/L)	TEMP (deg C)	Redox Potential (mV)
R-114.60	3/1/2003	11:34	0.431	8.54	11.63	7.81	51
R-68.72	3/1/2003	14:10	0.616	8.56	10.14	9.76	103
R-83.98	3/1/2003	17:09	0.421	8.44	11.49	10.25	78
R-87.62	3/1/2003	14:39	0.423	8.59	11.61	10.1	39
R-91.28	3/1/2003	13:31	0.423	8.64	11.68	9.83	79
R-99.59	3/1/2003	12:48	0.427	8.5	12.22	9.15	84
R-EB-11	3/1/2003	10:37	0.613	8.61	11.08	8.2	167
R-RGCOR	3/1/2003	9:35	0.606	8.62	11.11	8.15	193
L-87.62	3/7/2003	13:20	0.745	7.99	7.5	12.5	
R-87.62	3/7/2003	13:12	0.655	8.5	9	12.2	
L-87.62	3/13/2003		0.76	8.2	3.6	14.4	
R-87.62	3/13/2003	17:35	0.654	8.62	2.3	17.1	
L-87.62	3/21/2003	11:43	0.827	8.43	7.8	14	
R-87.62	3/21/2003	11:31	0.671	8.35	8.4	12.9	
L-87.62	3/28/2003	10:19	0.809	7.65	8.5	12.4	
R-87.62	3/28/2003	10:12	0.662	8.5	8.8	10.1	
L-87.62	4/5/2003	16:30	0.821	8.58	9.3	16.1	
R-87.62	4/5/2003	15:55	0.75	8.56	8.3	17.3	
L-87.62	4/12/2003	15:41	0.817	8.38	9.7	17.1	
R-87.62	4/12/2003	15:30	0.79	8.4	7.7	21.6	
L-87.62	4/18/2003	13:15	0.83	8.3	9.1	15.4	
R-87.62	4/18/2003	13:07	0.838	8.58	8.9	17	
L-87.62	4/26/2003	15:09	0.796	8.46	8.9	17.2	
R-87.62	4/26/2003	15:01	0.628	8.46	7.6	21.9	
L-87.62	5/3/2003	18:04	0.85	8.28	13.1	16	
R-87.62	5/3/2003	17:53	0.67	8.52	12.2	19.1	
L-87.62	5/11/2003	15:35	0.834	8.37	11.1	16.1	
R-87.62	5/11/2003	15:20	0.747	8.43	10	20.2	
L-87.62	5/20/2003		0.797	8.26	14.4	15	
R-87.62	5/20/2003		0.683	8.45	15.2	18.4	
L-87.62	5/27/2003		0.807	8.51	18.7	19.1	
R-87.62	5/27/2003		0.696	8.74	16.6	28.6	
L-87.62	6/3/2003	17:50	0.809	9.81	6.2	17.2	
R-87.62	6/3/2003	17:40	0.607	10.22	6.9	24.6	
L-87.62	6/11/2003	10:25	0.875	9.42	7.4	15.6	
R-87.62	6/11/2003	10:15	0.782	9.61	7.6	17.5	
D-SRD-91.28	6/16/2003	14:40	0.823	10.06	10.2	18.8	
ESC-SG01	6/16/2003	10:02	0.816	7.11	5.3	17.43	44
L-109.49	6/16/2003	9:42	0.883	7.2	5.85	18.12	64
L-114.60	6/16/2003		1.21	6.77	1.8	15	3
L-87.62	6/16/2003	9:31	0.847	9.66	8.3	15.3	
L-91.28	6/16/2003	14:20	0.775	9.96	12	17.4	
L-99.59	6/16/2003	13:15	0.692	10.14	12.1	21.4	
R-114.60	6/16/2003	8:47	0.71	9.18	7.66	20.38	107
R-87.62	6/16/2003	9:00	0.752	9.86	10.9	16.2	
S-LFCC10	6/16/2003	13:50	0.515	10.29	2.8	16	

Location ID	Date	Time	Electrical Conductivity (mS/cm)	PH	Dissolved Oxygen (mg/L)	TEMP (deg C)	Redox Potential (mV)
D-LLDR3	6/17/2003	13:55	2.25	8.09	11.88	26.32	70
D-SMC-91.28	6/17/2003	14:10	0.789	8.12	14.56	25.17	65
L-68.72	6/17/2003	11:47	1.23	8.07	13.3	24.3	
L-83.98	6/17/2003	14:50	0.807	8.45	14.4	19.9	
R-68.72	6/17/2003	12:00	1.24	8.21	12.5	23.8	
R-91.28	6/17/2003	16:22	0.719	8.41	16.1	20.5	

Appendix III The following tables contain results for chemical lab analyses for groundwater and surface water samples. Concentration are in units of mg/L.

Table 7 Results for laboratory chemical analyses for groundwater samples.

Location ID	Date	Lab Type	TDS	Hardness	HCO_3	pH	B (mg/l)	Br (mg/l)	Ca (mg/l)	Cl (mg/l)	F Mg/l)	Mg (mg/l)	NO_3 (mg/l)	PO_4 (mg/l)	K (mg/l)	Na (mg/l)	SO_4 (mg/l)	Sr (mg/l)
W-99.59-1	2/15/2002	Normal	440	238	250	7.7	0.11	0.17	74	39	0.4	13	<0.1	<0.5	4.4	60	105	1.1
W-99.59-4	2/15/2002	Normal	380	195	210	7.5	0.15	0.19	63	32	0.6	9.2	<0.1	<0.5	4.1	51	94	1.1
W-109.49-2	2/16/2002	Normal	400	205	210	7.46	0.13	0.12	66	38	0.6	9.7	<0.1	<0.5	3.4	54	100	1.2
W-109.49-3	2/16/2002	Field Duplicate	960	585	500	7.43	0.18	0.32	175	100	0.5	36	<0.1	0.67	7.5	105	250	2.9
W-109.49-3	2/16/2002	Normal	960	581	515	7.46	0.18	0.26	175	100	0.5	35	<0.1	0.11	7.3	110	240	3.1
W-109.49-4	2/16/2002	Normal	510	227	260	7.75	0.16	0.15	68	51	0.7	14	<0.1	<0.5	6	88	125	1.7
W-114.60-2	2/16/2002	Normal	410	201	210	7.96	0.11	0.26	64	37	0.7	10	0.13	<0.5	5.3	59	103	1.2
W-114.60-3	2/16/2002	Normal	860	523	520	7.09	0.17	0.33	155	80	1	33	0.2	<0.5	7.7	92	200	2.9
W-87.62-2	2/16/2002	Normal	420	206	215	7.88	0.12	0.24	66	36	0.7	10	<0.1	<0.5	5.9	61	110	1.1
W-87.62-3	2/16/2002	Field Duplicate	440	27	225	8.47	0.15	0.12	8.5	37	0.7	1.4	0.14	0.52	4.6	140	105	0.45
W-87.62-3	2/16/2002	Normal	430	27	225	7.74	0.16	0.19	8.7	36	0.9	1.4	<0.1	<0.5	4.3	140	105	0.44
W-87.62-4	2/16/2002	Normal	1840	751	655	7.47	0.38	0.84	225	230	1.1	46	0.31	<0.5	12	360	600	3.8
W-68.72-3	2/17/2002	Normal	880	527	630	7.31	0.22	0.49	155	93	1	34	0.14	<0.5	6.4	120	135	3.1
W-68.72-5	2/17/2002	Normal	420	174	160	7.85	0.07	0.12	56	38	0.4	8.4	<0.1	<0.5	2.7	66	140	0.71
W-68.72-6	2/17/2002	Normal	600	255	390	7.6	0.16	0.28	79	30	0.5	14	<0.1	<0.5	4.9	110	130	0.93
W-83.98-1	2/17/2002	Normal	14010	2435	1080	7.35	0.63	3.5	530	4000		270	<0.1	<0.5	150	3820	4640	21
W-83.98-3	2/17/2002	Normal	520	268	355	7.59	0.13	0.19	86	52	0.6	13	<0.1	<0.5	4	80	80	1.5
W-83.98-4	2/17/2002	Normal	370	203	240	7.68	0.11	0.11	63	26	0.7	11	<0.1	<0.5	4.2	47	78	0.98
W-91.28-1	2/17/2002	Normal	390	203	275	7.81	0.11	0.15	55	26	0.5	16	<0.1	2.6	9.8	50	57	1.2
W-91.28-3	2/17/2002	Normal	460	246	260	7.68	0.09	0.25	77	38	0.6	13	0.36	<0.5	6	60	110	1.2
W-91.28-3.5	2/17/2002	Normal	1060	132	455	7.92	0.5	0.32	43	89	1.6	6	<0.1	<0.5	6.7	320	330	0.86
W-91.28-4	2/17/2002	Normal	1100	581	700	7.16	0.32	0.44	185	72	1.9	29	<0.1	<0.5	6	170	255	3.1
W-68.72-1	2/18/2002	Normal	430	257	400	7.49	0.11	0.21	78	28	0.7	15	<0.1	<0.5	4	57	30	1.3
W-EB-11-20	2/18/2002	Normal	600	361	475	7.29	0.14	0.21	110	53	0.9	21	0.07	<0.5	4	79	74	2.2

Location ID	Date	Lab Type	TDS	Hardness	HCO_3	pH	B (mg/l)	Br (mg/l)	Ca (mg/l)	Cl (mg/l)	F Mg/l)	Mg (mg/l)	NO_3 (mg/l)	PO_4 (mg/l)	K (mg/l)	Na (mg/l)	SO_4 (mg/l)	Sr (mg/l)
W-EB-22-18	2/18/2002	Normal	1010	697	1070	7.11	0.19	0.59	190	68	0.7	54	<0.1	<0.5	8.1	120	7.9	4.5
W-Thomas1	2/18/2002	Normal	640	360	250	7.61	0.07	0.19	116	56	0.4	17	<0.1	<0.5	4.8	69	225	1.3
W-109.49-2	6/11/2002	Normal	390	220	240	7.6	0.14	0.14	70	38	0.4	11	<0.1	<0.5	4	56	93	0.67
W-109.49-3	6/11/2002	Normal	1000	606	525	7	0.24	0.27	185	115	0.4	35	<0.1	<0.5	7.3	115	275	1.83
W-109.49-4	6/11/2002	Field Duplicate	440	223	235	7.3	0.18	0.18	68	45	0.6	13	<0.1	<0.5	5.9	74	115	0.92
W-109.49-4	6/11/2002	Normal	450	224	242	7.4	0.21	0.14	70	45	0.6	12	<0.1	<0.5	6	78	115	0.81
W-114.60-2	6/11/2002	Normal	380	221	200	7.5	0.1	0.13	72	41	0.4	9.9	<0.1	<0.5	4.3	52	97	0.73
W-114.60-3	6/11/2002	Normal	900	644	640	6.7	0.26	0.18	195	58	0.5	38	3.7	<0.5	7.6	84	195	1.98
W-99.59-4	6/11/2002	Normal	380	221	220	7.5	0.18	0.11	72	35	0.4	10	<0.1	<0.5	4.1	56	95	0.64
W-Thomas1	6/11/2002	Normal	620	363	255	7	0.09	0.15	114	57	0.2	19	<0.1	<0.5	4.7	64	230	0.89
W-83.98-1	6/12/2002	Normal	14250	3142	1070	7.1	0.73	3.8	770	4100	0.3	296	0.53	0.33	146	3900	4500	12
W-83.98-3	6/12/2002	Normal	500	280	335	7.4	0.16	0.17	89	51	0.4	14	0.29	<0.5	3.5	74	105	0.84
W-87.62-2	6/12/2002	Normal	370	206	218	7.6	0.09	0.17	66	37	0.5	10	<0.1	<0.5	4.5	51	95	0.59
W-87.62-3	6/12/2002	Normal	610	76	335	7.9	0.27	0.57	23	65	1.1	4.4	1.06	<0.5	6.8	200	145	0.27
W-87.62-4	6/12/2002	Normal	500	250	245	7.4	0.2	0.24	82	56	0.5	11	<0.1	<0.5	4.8	87	135	0.68
W-91.28-1	6/12/2002	Normal	370	216	315	7.5	0.14	0.21	60	26	0.4	16	<0.1	2.5	9.7	50	52	0.68
W-91.28-3	6/12/2002	Normal	400	233	225	7.4	0.12	0.11	75	40	0.4	11	<0.1	<0.5	4.3	58	98	0.64
W-91.28-3.5	6/12/2002	Normal	950	124	425	7.9	0.5	0.25	40	80	1	5.9	0.15	<0.5	6.6	290	310	0.44
W-91.28-4	6/12/2002	Normal	1060	581	660	6.8	0.35	0.12	185	78	0.3	29	1	<0.5	5.1	175	260	1.66
W-68.72-1	6/13/2002	Field Duplicate	490	332	440	7	0.14	0.22	105	41	0.6	17	<0.1	<0.5	3.9	60	39	0.97
W-68.72-1	6/13/2002	Normal	490	324	445	7.1	0.15	0.22	100	41	0.6	18	<0.1	<0.5	3.9	61	39	0.95
W-68.72-3	6/13/2002	Field Duplicate	850	506	625	7	0.26	0.46	150	92	0.8	32	<0.1	<0.5	6	120	135	1.56
W-68.72-3	6/13/2002	Normal	860	511	630	7	0.26	0.47	150	93	0.8	33	<0.1	<0.5	6	125	140	1.61
W-68.72-5	6/13/2002	Normal	400	184	160	7.7	0.08		60	38	0.3	8.2	<0.1	<0.5	2.8	67	140	0.41
W-68.72-6	6/13/2002	Normal	550	279	400	7.3	0.19		87	28	0.4	15	<0.1	<0.5	5	96	120	0.61
W-EB-11-20	6/13/2002	Normal	580	328	230	7	0.91	0.27	105	98	0.4	16	<0.1	<0.5	4.4	82	155	1.03
W-Perini1	6/13/2002	Field Duplicate	790	244	355	7.9	0.19	0.12	82	95	0.5	9.5	<0.1	<0.5	6.2	185	230	0.6
W-Perini1	6/13/2002	Normal	790	247	350	7.8	0.19	0.19	83	95	0.5	9.6	<0.1	<0.5	6.2	190	230	0.6
W-109.49-2	10/12/2002	Normal	400	211	231	7.4	0.09	0.13	68	35	0.4	10	<0.1	<0.5	4.1	60	85	0.62

Location ID	Date	Lab Type	TDS	Hardness	HCO_3	pH	B (mg/l)	Br (mg/l)	Ca (mg/l)	Cl (mg/l)	F Mg/l)	Mg (mg/l)	NO_3 (mg/l)	PO_4 (mg/l)	K (mg/l)	Na (mg/l)	SO_4 (mg/l)	Sr (mg/l)
W-109.49-3	10/12/2002	Normal	940	535	466	6.8	0.17	0.42	160	95	0.3	33	<0.1	<0.5	8.3	125	255	1.5
W-109.49-4	10/12/2002	Normal	510	241	238	7.2	0.14	0.29	75	56	0.4	13	0.61	<0.5	6.9	84	130	0.92
W-114.60-2	10/12/2002	Normal	450	237	209	7.4	0.14	0.12	75	45	0.3	12	<0.1	<0.5	4.8	65	130	0.76
W-114.60-3	10/12/2002	Normal	820	486	527	6.7	0.17	0.13	140	46	0.4	33	16	<0.5	9.4	105	175	1.6
W-99.59-4	10/12/2002	Normal	410	215	210	7.5	0.09	0.14	68	40	0.3	11	<0.1	<0.5	5.1	60	100	0.57
W-Thomas1	10/12/2002	Normal	860	528	292	6.9	0.1	0.15	170	100	0.1	25	<0.1	<0.5	6	88	295	1.1
W-68.72-1	10/13/2002	Normal	510	310	244	6.8	0.1	0.18	96	76	0.5	17	<0.1	<0.5	4.1	60	110	0.91
W-68.72-3	10/13/2002	Normal	800	456	520	6.9	0.2	0.65	125	90	0.6	35	0.21	<0.5	6.1	120	140	1.5
W-68.72-5	10/13/2002	Normal	430	177	154	7.4	0.06	0.1	55	36	0.2	9.7	<0.1	<0.5	2.6	73	145	0.38
W-68.72-6	10/13/2002	Normal	580	282	390	7.1	0.13	0.28	85	28	0.3	17	0.16	<0.5	5	100	120	0.61
W-83.98-1	10/13/2002	Field Duplicate	13170	2223	1060	6.8	0.77	3.6	445	3800		270	1.9	<0.5	160	3600	4300	14
W-83.98-1	10/13/2002	Normal	13530	2318	1060	6.8	0.79	3.6	450	3800		290	1.6	<0.5	160	3730	4500	14
W-83.98-3	10/13/2002	Normal	560	306	310	7.1	0.14	0.25	96	63	0.4	16	<0.1	<0.5	4.3	81	115	0.91
W-87.62-2	10/13/2002	Normal	440	224	216	7.5	0.16	0.28	70	45	0.3	12	<0.1	<0.5	5.1	65	115	0.61
W-87.62-3	10/13/2002	Normal	760	245	341	7.3	0.22	0.14	70	78	0.4	17	<0.1	<0.5	13	170	200	0.85
W-87.62-4	10/13/2002	Normal	620	303	307	7	0.16	0.23	95	65	0.3	16	<0.1	<0.5	6.2	100	155	0.82
W-Cather	10/13/2002	Normal	330	132	205	7.5	0.09		40	21	0.6	7.7	0.78	<0.5	4.1	62	59	0.49
W-EB-11-20	10/13/2002	Normal	680	287	255	7.1	0.2	0.39	90	91	0.5	15	<0.1	<0.5	6.9	125	200	0.85
W-91.28-1	10/14/2002	Normal	400	210	293	7.2	0.13	0.22	56	25	0.5	17	<0.1	2	9.9	54	54	0.61
W-91.28-3	10/14/2002	Field Duplicate	470	248	249	7.4	0.15		78	40	0.4	13	0.47	<0.5	5.6	70	120	0.61
W-91.28-3	10/14/2002	Normal	480	253	249	7.3	0.14	0.15	80	40	0.4	13	3.3	<0.5	5.4	70	125	0.61
W-91.28-3.5	10/14/2002	Field Duplicate	1220	193	642	7.1	0.26	1	56	95	0.3	13	<0.1	<0.5	8.7	360	310	0.79
W-91.28-3.5	10/14/2002	Normal	1240	232	645	7.1	0.26	0.83	70	95	0.3	14	<0.1	<0.5	8.6	360	310	0.85
W-91.28-4	10/14/2002	Normal	970	507	489	6.7	0.21	0.1	160	85	1.6	26	2	<0.5	5.2	150	265	1.4
W-Perini1	10/14/2002	Normal	760	219	308	7.7	0.13	0.17	72	90	0.6	9.5	<0.1	<0.5	5.9	175	225	0.56
W-114.60-2	3/1/2003	Normal	400	179	193	7.76	0.11	0.12	57	40	0.6	9	<0.1	<0.5	4.9	60	115	0.67
W-114.60-3	3/1/2003	Normal	810	506	535	6.99	0.19	0.17	150	57	0.7	32	0.64	<0.5	7.5	82	185	1.7
W-68.72-1	3/1/2003	Field Duplicate	730	436	410	7.07	0.1	0.21	135	100	0.6	24	<0.1	<0.5	4.2	80	160	1.5
W-68.72-1	3/1/2003	Normal	730	432	409	6.99	0.1	0.2	135	100	0.6	23	<0.1	<0.5	4.2	80	160	1.4

Location ID	Date	Lab Type	TDS	Hardness	HCO_3	pH	B (mg/l)	Br (mg/l)	Ca (mg/l)	Cl (mg/l)	F Mg/l)	Mg (mg/l)	NO_3 (mg/l)	PO_4 (mg/l)	K (mg/l)	Na (mg/l)	SO_4 (mg/l)	Sr (mg/l)
W-68.72-3	3/1/2003	Normal	770	415	520	7.15	0.21	0.33	120	92	0.9	28	0.27	<0.5	5.4	110	130	1.5
W-68.72-4	3/1/2003	Normal	830	373	625	7.28	0.31	0.32	100	55	1.2	30	<0.1	<0.5	5.4	150	135	1.2
W-87.62-1	3/1/2003	Normal	400	200	203	7.49	0.07	0.13	62	40	0.5	11	<0.1	<0.5	4.6	57	110	0.61
W-87.62-2	3/1/2003	Normal	450	208	210	7.51	0.13	0.11	65	39	0.6	11	<0.1	<0.5	5.7	63	130	0.66
W-87.62-3	3/1/2003	Normal	1330	187	318	7.7	0.55	0.28	55	330	0.7	12	<0.1	<0.5	14	380	350	0.85
W-87.62-4	3/1/2003	Normal	590	274	285	7.37	0.15	0.16	85	72	0.5	15	<0.1	<0.5	5	90	160	0.81
W-EB-11-20	3/1/2003	Normal	480	199	285	7.32	0.14	0.16	60	52	0.7	12	<0.1	<0.5	4	85	100	0.74
BRN-E01A	6/16/2003	Normal	490	271	264	7.28	0.07	0.15	87	39	0.4	13	<0.1	<0.5	5.3	60	129	0.84
BRN-E01B	6/16/2003	Normal	430	220	201	7.56	0.14	0.42	70	39	0.4	11	0.11	<0.5	4.4	56	126	0.7
BRN-E01C	6/16/2003	Normal	440	203	247	7.68	0.12	0.14	63	45	0.4	11	<0.1	<0.5	4.7	68	100	0.68
BRN-E06A	6/16/2003	Normal	730	394	288	7.03	0.09	0.17	120	81	0.4	23	0.13	<0.5	7.8	87	240	0.99
ESC-SG01	6/16/2003	Normal	570	272	245	7.7	0.11	0.15	84	64	0.4	15	<0.1	<0.5	5.2	86	163	0.87
ESC-W03A	6/16/2003	Normal	1040	374	310	7.46	0.22	0.23	115	175	0.4	21	<0.1	<0.5	7.3	210	325	1.2
HWY-W07A	6/16/2003	Normal	430	213	223	7.6	0.11	0.13	67	44	0.4	11	<0.1	<0.5	4.6	63	105	0.7
HWY-W07B	6/16/2003	Normal	410	206	210	7.63	0.05	0.13	66	41	0.4	10	<0.1	<0.5	4.8	56	110	0.72
HWY-W07B	6/16/2003	Field Duplicate	410	206	200	7.68	0.05	0.12	66	42	0.4	10	<0.1	<0.5	5	56	112	0.72
HWY-W07C	6/16/2003	Normal	410	205	205	7.69	0.07	0.13	64	41	0.4	11	<0.1	<0.5	5	56	110	0.66
HWY-W07C	6/16/2003	Field Duplicate	410	205	203	7.7	0.08	0.13	64	42	0.4	11	<0.1	<0.5	5	56	110	0.67
W-114.60-2	6/16/2003	Normal	400	200	203	7.74	0.08	0.12	62	42	0.4	11	<0.1	<0.5	4.4	59	104	0.78
W-114.60-3	6/16/2003	Normal	830	515	585	6.82	0.15	0.16	150	49	0.5	34	2.8	<0.5	7.8	90	165	1.7
W-68.72-1	6/16/2003	Normal	720	423	450	7.05	0.09	0.2	130	89	0.5	24	<0.1	<0.5	4.7	86	140	1.4
W-68.72-3	6/16/2003	Normal	790	432	560	6.96	0.12	0.32	122	92	0.7	31	<0.1	<0.5	4.9	112	122	1.5
W-87.62-2	6/16/2003	Normal	410	195	206	7.68	0.07	0.13	60	42	0.5	11	<0.1	<0.5	5	62	102	0.67
W-87.62-3	6/16/2003	Normal	930	188	360	7.69	0.21	0.18	57	136	0.5	11	<0.1	<0.5	11	260	240	0.72
W-87.62-4	6/16/2003	Normal	610	267	307	7.13	0.15	0.15	84	69	0.5	14	<0.1	<0.5	5.4	100	155	0.88
W-91.28-3	6/16/2003	Normal	490	247	240	7.45	0.1	0.12	76	45	0.3	14	<0.1	<0.5	6.7	64	140	0.81
W-91.28-3.5	6/16/2003	Normal	970	199	440	7.56	0.27	0.17	60	83	0.9	12	<0.1	<0.5	8.4	250	305	0.84
W-91.28-3.5	6/16/2003	Field Duplicate	990	197	435	7.47	0.31	0.18	59	83	0.9	12	<0.1	<0.5	8.5	265	305	0.83

Table 8 Results for laboratory chemical analyses for surface water samples.

Location ID	Date	Lab Type	TDS	Hardness	HCO_3	pH	B (mg/l)	Br (mg/l)	Ca (mg/l)	Cl (mg/l)	F Mg/l)	Mg (mg/l)	NO_3 (mg/l)	PO_4 (mg/l)	K (mg/l)	Na (mg/l)	SO_4 (mg/l)	Sr (mg/l)
L-114.60	2/15/2002	Normal	600	314	255	7.52	0.136		96	76	0.6	18	<0.1	<0.5	5.1	86	165	1.9
L-99.59	2/15/2002	Normal	460	225	215	7.81	0.129	0.23	72	51	0.6	11	<0.1	<0.5	4.4	70	125	1.3
R-114.60	2/15/2002	Normal	410	183	205	8.31	0.148	0.19	57	44	0.74	9.8	4.2	<0.5	5.8	69	95	0.91
R-99.59	2/15/2002	Normal	400	186	200	7.89	0.141	0.28	58	41	0.73	9.9	4.2	0.5	5.9	64	94	0.93
D-SRD-87.62	2/16/2002	Normal	780	267	300	7.6	0.239	0.28	84	125	0.93	14	0.1	<0.5	6.6	170	200	1.5
L-109.49	2/16/2002	Normal	600	303	280	7.98	0.147	0.16	95	61	0.48	16	<0.1	<0.5	5.3	93	170	1.8
L-87.62	2/16/2002	Field Duplicate	490	222	230	8.41	0.138	0.14	69	53	0.55	12	<0.1	<0.5	5.2	83	130	1.1
L-87.62	2/16/2002	Normal	490	233	235	8.28	0.139	0.27	75	52	0.53	11	0.28	<0.5	5.3	80	130	1.1
R-109.49	2/16/2002	Normal	410	191	210	8.25	0.15	0.14	60	42	0.58	10	4.1	<0.5	5.8	63	92	0.87
R-87.62	2/16/2002	Normal	410	184	205	8.35	0.136	0.14	58	40	0.49	9.4	3.3	<0.5	6.1	68	93	0.84
L-68.72	2/17/2002	Normal	660	264	260	8.2	0.183	0.24	81	110	0.87	15	0.1	0.5	6.6	130	160	1.6
L-83.98	2/17/2002	Normal	480	227	230	8.4	0.141	0.24	71	53	0.54	12	0.33	<0.5	5.4	78	130	1.1
L-91.28	2/17/2002	Normal	490	232	235	8.09	0.136	0.16	73	51	0.62	12	0.26	<0.5	5.4	76	130	1.1
R-83.98	2/17/2002	Normal	400	184	205	8.32	0.14	0.16	58	41	0.69	9.6	2.9	<0.5	6	65	93	0.79
R-91.28	2/17/2002	Normal	410	186	210	8.31	0.143	0.32	59	42	0.78	9.3	3.5	<0.5	6	63	95	0.76
D-ESC E-Side	2/18/2002	Normal	370	191	200	7.76	0.629	0.1	62	28	0.46	8.7	<0.1	<0.5	3.8	48	96	0.74
L-EB-11	2/18/2002	Normal	680	282	265	8.26	0.183	0.34	90	110	0.84	14	<0.1	<0.5	7.2	130	170	1.4
R-68.72	2/18/2002	Normal	410	187	210	8.36	0.142	0.14	59	41	0.68	9.7	3	0.39	6	60	95	0.76
R-EB-11	2/18/2002	Normal	410	201	210	8.39	0.14	0.13	64	41	0.56	9.9	3.4	0.6	6.3	61	95	0.77
R-RGCOR	2/18/2002	Field Duplicate	400	187	205	8.37	0.143		59	40	0.65	9.7	3.3	<0.5	6	63	94	0.79
R-RGCOR	2/18/2002	Normal	400	182	210	8.33	0.145		57	40	0.59	9.6	3.3	<0.5	6	62	95	0.78
D-ESC E-Side	6/11/2002	Normal	370	225	210	7.7	0.13	0.15	76	30	0.37	8.6	<0.1	<0.5	3.3	50	100	0.53
L-109.49	6/11/2002	Normal	640	353	290	7.8	0.2	0.24	110	77	0.39	19	<0.1	<0.5	5.3	90	190	1.18
L-114.60	6/11/2002	Normal	730	403	295	7.5	0.19	0.23	125	105	0.42	22	0.34	<0.5	5.7	105	220	1.39
L-99.59	6/11/2002	Normal	390	223	215	7.7	0.15	0.1	71	39	0.41	11	0.13	<0.5	4.3	56	105	0.66
R-109.49	6/11/2002	Normal	390	220	218	8	0.15	0.13	70	34	0.48	11		<0.5	5.8	55	100	0.53
R-114.60	6/11/2002	Normal	380	220	215	8.4	0.15		70	34	0.46	11	0.16	<0.5	5.6	56	100	0.59
R-99.59	6/11/2002	Normal	410	229	225	8.5	0.16	0.14	72	37	0.48	12	<0.1	<0.5	5.6	57	110	0.56

Location ID	Date	Lab Type	TDS	Hardness	HCO_3	pH	B (mg/l)	Br (mg/l)	Ca (mg/l)	Cl (mg/l)	F Mg/l)	Mg (mg/l)	NO_3 (mg/l)	PO_4 (mg/l)	K (mg/l)	Na (mg/l)	SO_4 (mg/l)	Sr (mg/l)
D-SRD-87.62	6/12/2002	Normal	490	245	240	7.6	0.19	0.12	80	62	0.46	11	0.13	<0.5	4.9	85	130	0.66
L-83.98	6/12/2002	Normal	510	228	235	8.1	0.19		73	74	0.42	11	<0.1	<0.5	6.3	95	135	0.67
L-87.62	6/12/2002	Normal	530	237	245	8	0.21	0.2	75	77	0.42	12		<0.5	5.9	95	140	0.67
L-91.28	6/12/2002	Normal	470	257	235	7.7	0.18	0.18	83	53	0.46	12	<0.1	<0.5	4.9	72	125	0.64
R-83.98	6/12/2002	Normal	420	222	225	8.7	0.17	0.19	69	43	0.47	12	<0.1	<0.5	6	65	115	0.61
R-87.62	6/12/2002	Normal	440	249	240	8.1	0.18	0.17	80	42	0.46	12	0.1	<0.5	5.2	62	115	0.63
R-91.28	6/12/2002	Normal	440	229	245	8.2	0.17	0.17	72	42	0.5	12	<0.1	<0.5	5.5	68	115	0.63
L-68.72	6/13/2002	Normal	790	324	305	8	0.25	0.24	100	130	0.5	18	0.13	<0.5	8.2	160	220	1.03
L-EB-11	6/13/2002	Normal	780	316	300	8.1	0.25	0.24	97	128	0.5	18	<0.1	<0.5	8	155	220	1.03
P-S.Bosque	6/13/2002	Normal	440	193	283	8.7	0.24	0.23	46	42	0.59	19	<0.1	<0.5	7.4	86	97	
R-68.72	6/13/2002	Normal	770	324	295	8.4	0.26	0.29	100	130	0.5	18	<0.1	<0.5	8	155	215	1.08
R-EB-11	6/13/2002	Normal	750	281	255	8.4	0.26	0.23	86	135	0.51	16	<0.1	<0.5	8.1	160	215	0.98
R-RGCOR	6/13/2002	Normal	820	341	330	8.1	0.27	0.26	105	125	0.51	19	0.1	<0.5	8.3	160	240	1.11
D-ESC E-Side	10/12/2002	Normal	400	221	204	8	0.1		73	35	0.31	9.4	<0.1	<0.5	3.8	52	103	0.47
L-109.49	10/12/2002	Normal	690	328	290	7.6	0.14	0.35	100	76	0.28	19	0.19	<0.5	6.3	115	200	1.1
L-114.60	10/12/2002	Normal	770	407	275	7.4	0.14	0.13	125	110	0.3	23	0.23	<0.5	5	110	235	1.4
L-99.59	10/12/2002	Normal	420	215	208	7.5	0.11	0.17	68	33	0.32	11	<0.1	<0.5	4.7	62	120	0.59
R-109.49	10/12/2002	Normal	420	220	211	8.2	0.12	0.16	70	36	0.41	11	1.9	<0.5	6.5	60	110	0.6
R-114.60	10/12/2002	Normal	420	220	212	8.1	0.12	0.23	70	35	0.41	11	1.4	<0.5	6.5	60	110	0.55
R-99.59	10/12/2002	Normal	470	229	220	8.2	0.13	0.22	72	52	0.39	12	1.2	<0.5	6.6	72	120	0.62
D-SRD-87.62	10/13/2002	Normal	580	257	248	7.7	0.16	0.13	80	65	0.36	14	<0.1	<0.5	7.3	100	160	0.64
L-68.72	10/13/2002	Normal	660	278	260	7.9	0.17	0.14	85	95	0.38	16	0.25	<0.5	6.9	125	180	0.84
L-83.98	10/13/2002	Normal	540	241	229	7.9	0.14	0.12	75	66	0.33	13	0.14	<0.5	6	94	150	0.68
L-87.62	10/13/2002	Field Duplicate	560	248	233	7.7	0.14	0.22	78	65	0.34	13	<0.1	<0.5	6.4	100	160	0.68
L-87.62	10/13/2002	Normal	570	253	234	7.7	0.15	0.27	80	70	0.34	13	0.1	<0.5	6.4	100	160	0.69
L-EB-11	10/13/2002	Normal	660	278	260	8	0.17	0.13	85	91	0.38	16	0.27	<0.5	7.6	125	180	0.85
P-SocorroSprings	10/13/2002	Normal	230	64	162	8.1	0.07		19	12	0.5	4	1.8	<0.5	3.4	55	29	0.32
R-68.72	10/13/2002	Normal	630	274	251	8.1	0.16	0.3	85	82	0.39	15	0.31	<0.5	6.5	115	175	0.81
R-83.98	10/13/2002	Normal	440	234	220	8.2	0.11	0.11	74	40	0.42	12	0.8	<0.5	6.3	63	115	0.65
R-87.62	10/13/2002	Normal	450	237	219	8.2	0.12	0.21	75	40	0.42	12	1.1	<0.5	5.9	62	115	0.63

Location ID	Date	Lab Type	TDS	Hardness	HCO_3	pH	B (mg/l)	Br (mg/l)	Ca (mg/l)	Cl (mg/l)	F Mg/l)	Mg (mg/l)	NO_3 (mg/l)	PO_4 (mg/l)	K (mg/l)	Na (mg/l)	SO_4 (mg/l)	Sr (mg/l)
R-EB-11	10/13/2002	Normal	610	262	252	8	0.17	0.31	80	85	0.4	15	0.46	<0.5	6.7	115	160	0.83
R-RGCOR	10/13/2002	Normal	640	270	254	8.1	0.17	0.36	80	90	0.38	17	<0.1	<0.5	7.2	120	175	0.9
D-LLDR4	10/14/2002	Normal	1390	440	417	7.9	0.28	1.9	130	280	0.97	28	0.78	<0.5	8.3	325	375	1.4
L-91.28	10/14/2002	Normal	550	253	228	7.6	0.11	0.59	80	49	0.49	13	0.23	<0.5	5.6	85	175	0.62
R-91.28	10/14/2002	Normal	460	238	224	8.1	0.12		74	40	0.53	13	0.89	<0.5	5.6	68	125	0.63
D-ELMDR	3/1/2003	Normal	610	245	255	7.9	0.2	0.16	75	85	0.59	14	1.1	<0.5	6.4	105	170	0.85
DUnit7	3/1/2003	Normal	460	203	212	7.99	0.16	0.13	63	46	0.57	11	2.1	<0.5	5.7	71	125	0.62
L-109.49	3/1/2003	Normal	550	259	246	7.92	0.15	0.14	79	58	0.45	15	<0.1	<0.5	4.8	79	162	0.95
L-114.60	3/1/2003	Normal	620	300	244	7.68	0.15	0.16	92	83	0.48	17	0.14	<0.5	4.8	85	190	1.1
L-68.72	3/1/2003	Normal	610	228	239	8.01	0.2	0.17	70	95	0.57	13	0.75	<0.5	6.4	110	165	0.83
L-83.98	3/1/2003	Normal	470	213	215	7.92	0.15	0.13	67	52	0.51	11	0.52	<0.5	5.1	72	135	0.68
L-87.62	3/1/2003	Normal	470	208	210	7.71	0.15	0.13	65	50	0.51	11	0.67	<0.5	5.1	70	135	0.67
L-91.28	3/1/2003	Normal	450	208	210	7.88	0.14	0.13	65	47	0.5	11	0.74	<0.5	5.1	66	130	0.65
L-99.59	3/1/2003	Normal	450	208	205	7.98	0.14	0.13	65	46	0.54	11	0.94	<0.5	5.1	65	125	0.66
L-EB-11	3/1/2003	Normal	620	245	245	8.02	0.2	0.17	75	95	0.57	14	0.79	<0.5	6.1	110	170	0.84
L-SBB	3/1/2003	Normal	600	224	225	7.97	0.2	0.17	70	100	0.55	12	0.34	<0.5	6.1	110	160	0.81
R-109.49	3/1/2003	Normal	390	176	180	8.16	0.15	0.12	55	42	0.6	9.4	4.5	0.69	5.5	55	98	0.5
R-114.60	3/1/2003	Normal	400	179	191	8.14	0.15	0.13	56	42	0.59	9.6	4.6	0.69	5.6	56	100	0.51
R-68.72	3/1/2003	Normal	380	180	179	8.1	0.13	0.12	56	38	0.58	9.7	2.7	<0.5	5.6	53	96	0.53
R-83.98	3/1/2003	Normal	390	177	187	8.1	0.14	0.13	55	43	0.56	9.7	3.3	0.64	5.6	56	100	0.52
R-87.62	3/1/2003	Normal	400	186	186	8.13	0.13	0.12	58	40	0.57	10	3.2	0.68	5.6	57	100	0.54
R-91.28	3/1/2003	Normal	390	179	190	7.8	0.13	0.13	56	40	0.57	9.5	3.1	0.66	5.5	54	100	0.53
R-99.59	3/1/2003	Normal	390	181	185	8.18	0.14	0.13	56	41	0.57	10	3.3	0.61	5.5	55	100	0.53
R-EB-11	3/1/2003	Normal	370	174	180	8.18	0.14	0.11	55	37	0.56	9	2.7	0.54	5.5	50	95	0.51
R-RGCOR	3/1/2003	Normal	370	175	184	8.22	0.14	0.13	55	38	0.6	9.2	3.3	0.63	5.6	51	94	0.51
D-LLDR3	6/16/2003	Normal	1270	369	360	8.04	0.29	0.28	110	280	0.38	23	0.11	<0.5	8.9	290	340	1.6
D-SMC-91.28	6/16/2003	Normal	540	227	245	8.63	0.12	0.14	68	57	0.49	14	<0.1	<0.5	6.2	88	155	0.82
D-SRD-91.28	6/16/2003	Normal	540	213	248	7.9	0.13	0.14	64	57	0.49	13	<0.1	<0.5	5.4	98	148	0.72

Location ID	Date	Lab Type	TDS	Hardness	HCO_3	pH	B (mg/l)	Br (mg/l)	Ca (mg/l)	Cl (mg/l)	F Mg/l)	Mg (mg/l)	NO_3 (mg/l)	PO_4 (mg/l)	K (mg/l)	Na (mg/l)	SO_4 (mg/l)	Sr (mg/l)
L-109.49	6/16/2003	Normal	610	290	266	7.78	0.11	0.14	88	69	0.38	17	<0.1	<0.5	5.4	95	180	1.1
L-114.60	6/16/2003	Normal	740	386	262	7.48	0.098	0.17	120	105	0.39	21	0.53	<0.5	5.5	102	230	1.4
L-68.72	6/16/2003	Normal	760	280	260	8.21	0.15	0.2	84	138	0.49	17	<0.1	<0.5	8	150	205	1.1
L-83.98	6/16/2003	Normal	520	212	223	7.96	0.11	0.13	65	68	0.44	12	<0.1	<0.5	5.4	92	140	0.77
L-87.62	6/16/2003	Normal	550	228	252	7.84	0.13	0.13	70	69	0.42	13	<0.1	<0.5	5.9	97	140	0.79
L-91.28	6/16/2003	Normal	500	212	230	7.64	0.12	0.13	65	56	0.43	12	0.33	<0.5	4.8	86	134	0.71
L-99.59	6/16/2003	Normal	430	214	208	7.74	0.098	0.12	66	42	0.42	12	<0.1	<0.5	4.3	58	119	0.7
R-114.60	6/16/2003	Normal	500	232	240	8.08	0.12	0.15	70	53	0.51	14	1	<0.5	7.1	78	130	0.75
R-68.72	6/16/2003	Normal	800	284	293	8.11	0.15	0.2	84	145	0.47	18		<0.5	8.1	160	215	1.2
R-68.72	6/16/2003	Field Duplicate	790	289	282	8.19	0.15	0.19	86	143	0.47	18	<0.1	<0.5	8.3	155	210	1.1
R-87.62	6/16/2003	Normal	480	222	225	8.06	0.1	0.12	69	49	0.43	12	0.11	<0.5	5.1	76	130	0.72
R-91.28	6/16/2003	Normal	470	218	222	7.92	0.096	0.12	69	48	0.44	11	<0.1	<0.5	5.1	69	132	0.71
S-LFCC10	6/16/2003	Normal	340	166	177	7.75	0.063		53	24	0.35	8.1	<0.1	<0.5	3.7	48	87	0.55

Appendix IV The following tables include Stable isotope data for groundwater and surface water samples.

Table 9 Results for laboratory analyses for stable isotopes of oxygen and hydrogen for groundwater samples

Location ID	Date	Lab Type	δD (per mill)	δ^{18}O (per mill)
W-109.49-4	1/15/2002	Normal	-84	-10.9
W-87.62-2	1/15/2002	Normal	-88	-10.6
W-87.62-3	1/15/2002	Normal	-94	-11.7
W-14.60-2	3/13/2002	Normal	-90	-11.5
W-91.28-1	3/13/2002	Normal	-90	-11.7
W-91.28-3	3/13/2002	Normal	-85	-11.2
W-91.28-3.5	3/13/2002	Normal	-90	-11.7
W-109.49-3	3/14/2002	Normal	-86	-11.4
W-109.49-3	3/14/2002	Field triplicate	-89	-11.0
W-109.49-3	3/14/2002	Field duplicate	-89	-11.1
W-68.72-3	3/14/2002	Normal	-92	-11.3
W-83.98-1	3/14/2002	Normal	-87	-10.6
W-87.62-3	3/14/2002	Normal	-93	-11.7
W-91.28-4	3/14/2002	Normal	-84	-10.7
W-99.59-1	3/14/2002	Normal	-91	-11.5
W-99.59-4	3/14/2002	Normal	-91	-11.1
W-EB-11-20	3/14/2002	Normal	-84	-10.8
W-EB-22-18	3/14/2002	Normal	-79	-10.5
W-Thomas1	3/14/2002	Normal	-91	-12.4
W-109.49-2	3/15/2002	Normal	-87	-11.1
W-114.60-3	3/15/2002	Normal	-91	-11.4
W-68.72-1	3/15/2002	Normal	-88	-11.4
W-68.72-5	3/15/2002	Normal	-90	-12.0
W-68.72-6	3/15/2002	Normal	-93	-11.8
W-83.98-3	3/15/2002	Normal	-87	-11.2
W-83.98-4	3/15/2002	Normal	-85	-11.7
W-109.49-4	7/29/2002	Field Duplicate	-86	-10.5
W-68.72-1	7/29/2002	Normal	-86	-10.6
W-87.62-2	7/29/2002	Normal	-92	-11.5
W-91.28-1	7/29/2002	Normal	-91	-11.4
W-91.28-3.5	7/29/2002	Normal	-91	-11.5
W-109.49-2	7/30/2002	Normal	-86	-10.6
W-109.49-3	7/30/2002	Normal	-84	-10.5
W-114.60-3	7/30/2002	Normal	-84	-10.5
W-68.72-1	7/30/2002	Field Duplicate	-87	-10.5
W-83.98-1	7/30/2002	Normal	-83	-10.1
W-83.98-3	7/30/2002	Normal	-87	-10.7
W-87.62-3	7/30/2002	Normal	-87	-10.5
W-91.28-3	7/30/2002	Normal	-89	-11.2

Location ID	Date	Lab Type	δD (per mill)	$\delta^{18}O$ (per mill)
W-EB-11-20	7/30/2002	Normal	-83	-9.9
W-Thomas1	7/30/2002	Normal	-95	-12.2
W-109.49-4	7/31/2002	Normal	-86	-10
W-114.60-2	7/31/2002	Normal	-90	-11.2
W-68.72-3	7/31/2002	Normal	-87	-10.2
W-68.72-6	7/31/2002	Normal	-81	-11.2
W-68.72-3	8/1/2002	Field Duplicate	-82	-11.1
W-68.72-5	8/1/2002	Normal	-93	-12.1
W-87.62-4	8/1/2002	Normal	-91	-10.8
W-91.28-4	8/1/2002	Normal	-83	-10.2
W-99.59-4	8/1/2002	Normal	-84	-10.5
W-perini1	8/1/2002	Normal	-90	-12.4
W-perini1	8/1/2002	Field Duplicate	-95	-12.3
W-99.59-4	10/12/02	Normal	-87	-11.5
W-114.60-2	10/12/02	Normal	-81	-10.4
W-114.60-3	10/12/02	Normal	-84	-11.1
W-109.49-4	10/12/02	Normal	-82	-11.1
W-109.49-2	10/12/02	Normal	-77	-11.3
W-109.49-3	10/12/02	Normal	-84	-11.0
W-Thomas1	10/12/02	Normal	-91	-12.4
W-68.72-3	10/13/02	Normal	-87	-11.4
W-68.72-1	10/13/02	Normal	-83	-11.5
W-68.72-5	10/13/02	Normal	-89	-12.2
W-68.72-6	10/13/02	Normal	-90	-12.1
W-EB-11-20	10/13/02	Normal	-77	-9.8
W-Cather	10/13/02	Normal	-86	-12.6
W-83.98-3	10/13/02	Normal	-82	-10.9
W-87.62-3	10/13/02	Normal	-83	-11.1
W-87.62-4	10/13/02	Normal	-81	-10.7
W-83.98-1	10/13/02	Normal	-79	-10.8
W-83.98-1	10/13/02	field duplicate	-80	-11.0
W-87.62-2	10/13/02	Normal	-86	-10.8
W-91.28-3	10/14/02	Normal	-80	-10.3
W-91.28-3	10/14/02	field duplicate	-79	-10.5
W-91.28-4	10/14/02	Normal	-82	-10.9
W-91.28-1	10/14/02	Normal	-86	-11.5
W-Perini1	10/14/02	Normal	-90	-12.6
W-91.28-3.5	10/14/02	Normal	-85	-11.2
W-87.62-1	3/1/2003	Normal	-87	-10.6
W-87.62-2	3/1/2003	Normal	-84	-11.1
W-87.62-1	3/7/2003	Normal	-87	-11.0
W-87.62-2	3/7/2003	Normal	-84	-10.8
W-87.62-1	3/13/2003	Normal	-87	-10.9
W-87.62-2	3/13/2003	Normal	-85	-10.6

Location ID	Date	Lab Type	δD (per mill)	$\delta^{18}O$ (per mill)
W-87.62-1	3/21/2003	Normal	-87	-10.9
W-87.62-2	3/21/2003	Normal	-86	-10.9
W-87.62-1	3/28/2003	Normal	-89	-11.2
W-87.62-2	3/28/2003	Normal	-87	-10.7
W-87.62-1	4/5/2003	Normal	-88	-11.3
W-87.62-2	4/5/2003	Normal	-86	-11.0
W-87.62-1	4/12/2003	Normal		-11.4
W-87.62-2	4/12/2003	Normal	-86	-11.5
W-87.62-1	4/18/2003	Normal	-87	-11.2
W-87.62-2	4/18/2003	Normal	-86	-11.2
W-87.62-1	4/26/2003	Normal	-89	-11.4
W-87.62-2	4/26/2003	Normal	-88	-11.5
W-87.62-1	5/3/2003	Normal	-87	-11.6
W-87.62-2	5/3/2003	Normal	-86	-11.4
W-87.62-1	5/11/2003	Normal	-87	-11.6
W-87.62-2	5/11/2003	Normal	-86	-11.3
W-87.62-1	5/20/2003	Normal	-90	-11.3
W-87.62-2	5/20/2003	Normal	-89	-11.8
W-87.62-1	5/27/2003	Normal	-88	-11.6
W-87.62-2	5/27/2003	Normal	-87	-11.2
W-87.62-1	6/3/2003	Normal	-87	
W-87.62-2	6/3/2003	Normal	-88	
W-87.62-1	6/11/2003	Normal	-87	
W-87.62-2	6/11/2003	Normal	-87	
W-87.62-1	6/16/2003	Normal	-89	-10.9
W-87.62-2	6/16/2003	Normal	-90	-11.4

Table 10 Results for laboratory analyses for stable isotopes of oxygen and hydrogen for surface water samples.

Location ID	Date	Lab Type	δD (per mill)	$\delta^{18}O$ (per mill)
L-109.49	10/12/02	Normal	-85	-12.1
L-109.49	8/1/2002	Normal	-88	-11
L-109.49 1/02	3/14/2002	Normal	-90	-11.4
L-114.60	3/14/2002	Normal	-89	-11.3
L-114.60	7/31/2002	Normal	-90	-10.8
L-114.60	10/12/02	Normal	-86	-11.6
L-68.72	3/13/2002	Normal	-84	-10.9
L-68.72	7/31/2002	Normal	-87	-10.2
L-68.72	10/13/02	Normal	-82	-10.9
L-83.98	3/14/2002	Normal	-94	-11.1
L-83.98	7/30/2002	Normal	-87	-10.8
L-83.98	10/13/02	Normal	-80	-10.7
l-87.62	3/15/2002	Normal	-90	-11.5
l-87.62	7/31/2002	Normal	-88	-10.5
L-87.62	10/13/02	Normal		-10.8
L-87.62	10/13/02	field duplicate	-79	-10.9
L-87.62	3/1/2003	Normal	-88	-11.0
L-87.62	3/7/2003	Normal	-87	-11.1
L-87.62	3/13/2003	Normal	-87	-10.8
L-87.62	3/21/2003	Normal	-86	-11.3
L-87.62	3/28/2003	Normal	-88	-11.1
L-87.62	4/5/2003	Normal	-87	-11.5
L-87.62	4/12/2003	Normal	-86	-11.5
L-87.62	4/18/2003	Normal	-86	-11.5
L-87.62	4/26/2003	Normal	-88	-11.6
L-87.62	5/3/2003	Normal	-85	-11.2
L-87.62	5/11/2003	Normal	-85	-11.3
L-87.62	5/20/2003	Normal	-88	-10.8
L-87.62	5/27/2003	Normal	-85	-11.3
L-87.62	6/3/2003	Normal	-85	
L-87.62	6/11/2003	Normal	-85	
L-87.62	6/16/2003	Normal	-87	-10.8
L-87.62 1/02	3/14/2002	Normal	-88	-11.2
L-91.28	3/13/2002	Normal	-87	-11.4
L-91.28	7/30/2002	Normal	-86	-10
L-91.28	10/14/02	Normal	-79	-11.0
L-99.59	3/14/2002	Normal	-86	-11.0
L-99.59	7/30/2002	Normal	-91	-10.8
L-99.59	10/12/02	Normal	-85	-11.3

Location ID	Date	Lab Type	δD (per mill)	$\delta^{18}O$ (per mill)
L-EB-11	3/15/2002	Normal	-87	-11.1
L-EB-11	7/31/2002	Normal	-87	-10
L-EB-11	10/13/02	Normal	-81	-10.5
P-S.Bosque	7/29/2002	Normal	-62	-4.6
P-SocorroSprings	10/13/02	Normal	-69	-10.1
R-109.49	3/15/2002	Normal	-90	-11.9
R-109.49	7/30/2002	Normal	-80	-9.3
R-109.49	10/12/02	Normal	-81	-10.6
R-114.60	3/14/2002	Normal	-96	-11.6
R-114.60	7/30/2002	Normal	-86	-9.1
R-114.60	10/12/02	Normal	-82	-10.6
R-68.72	3/15/2002	Normal	-86	-11.6
R-68.72	7/29/2002	Normal	-83	-9.9
R-68.72	10/13/02	Normal	-81	-10.4
R-83.98	3/14/2002	Normal	-94	-11.7
R-83.98	7/30/2002	Normal	-83	-9.3
R-83.98	10/13/02	Normal	-79	-10.0
R-87.62	3/15/2002	Normal	-92	-11.8
R-87.62	8/1/2002	Normal	-81	-9.7
R-87.62	10/13/02	Normal	-80	-10.2
R-87.62	3/1/2003	Normal	-72	-4.2
R-87.62	3/7/2003	Normal	-88	-11.1
R-87.62	3/13/2003	Normal	-87	-11.1
R-87.62	3/21/2003	Normal	-90	-11.5
R-87.62	3/28/2003	Normal	-90	-10.9
R-87.62	4/5/2003	Normal	-85	-10.7
R-87.62	4/12/2003	Normal	-86	-10.6
R-87.62	4/18/2003	Normal	-76	-7.4
R-87.62	4/26/2003	Normal	-87	-10.9
R-87.62	5/3/2003	Normal	-84	-10.9
R-87.62	5/11/2003	Normal	-83	-10.5
R-87.62	5/20/2003	Normal	-87	-10.7
R-87.62	5/27/2003	Normal	-83	-10.4
R-87.62	6/3/2003	Normal	-84	
R-87.62	6/11/2003	Normal	-83	
R-87.62	6/16/2003	Normal	-88	-10.6
R-91.28	3/13/2002	Normal	-88	-12.0
R-91.28	7/31/2002	Normal	-82	-9.2
R-91.28	10/14/02	Normal	-78	-10.3
R-99.59	3/14/2002	Normal	-87	-11.7
R-99.59	7/29/2002	Normal	-82	-9.6
R-99.59	10/12/02	Normal	-81	-10.9
R-EB-11	3/14/2002	Normal	-87	-11.6
R-EB-11	7/29/2002	Normal	-82	-9.4

Location ID	Date	Lab Type	δD (per mill)	$\delta^{18}O$ (per mill)
R-EB-11	10/13/02	Normal	-85	-10.4
R-N_of_Corral	3/13/2002	Normal	-90	-11.6
R-N_of_Corral	3/15/2002	Field Duplicate	-91	-11.6
R-N_of_Corral	7/30/2002	Normal	-73	-9.7
R-RGCOR	10/13/02	Normal	-80	-10.3
D-ESC E-Side	3/14/2002	Normal	-93	-11.4
D-ESC E-Side	10/12/02	Normal	-84	-11.5
D-LLDR4	10/14/02	Normal	-84	-11.7
D-SRD--87.62	8/1/2002	Normal	-87	-10.9
D-ESC E-Side	7/31/2002	Normal	-90	-10.5
D-SRD-87.62	3/15/2002	Normal	-91	-11.3
D-SRD-87.62	10/13/02	Normal	-81	-10.6

Appendix V The following section analyzes geophysical and geomorphology data in order to assess the probability of the presence of cross-basin structures.

Geophysical Evidence of Cross-Basin structures

Gravity and magnetic data were analyzed in order to assess the structural geometry of the Socorro Basin. Existing gravity data (Sanford, 1968) were used, while magnetic data were collected along selected high-resolution transects . The magnetic data could possibly give insight to the structural framework of the basin, but with the limited data available, data analysis was inconclusive. The magnetic data will be discussed in the next section. This section will discuss the gravity data. Gravity data collected by Sanford (1968) appear to be the best and highest-resolution data of this type for this area. The Bouger gravity map (figure 9) was examined in order to identify the structural geometry discussed above. Figure 48 illustrates the inferred location of an anticline suggested by the gravity data. Gravity lows to the north and south of a relatively flat area around the city of Socorro are observed. The axis of the anticline is inferred be located somewhere on this flat area trending to the northeast. The SAZ as defined by Chapin is located on this flat region, trending in the correct direction (figure 49). High gravity gradients that probably represent rift faults are observed on the west side of the basin to the north of the SAZ and on the east side of the basin to the south of the SAZ. This geometry is consistent with that of the anticlinal oblique antithetic AZ (figure 47). If the SAZ is this type of AZ, then structures crossing the basin south of the SAZ would be the southern part of the scissor-faults associated with this type of AZ.

Figure 48 Inferred location of anticline according to residual Bouger anomaly map (Sanford, 1968). Arrows denote limbs of anticline.

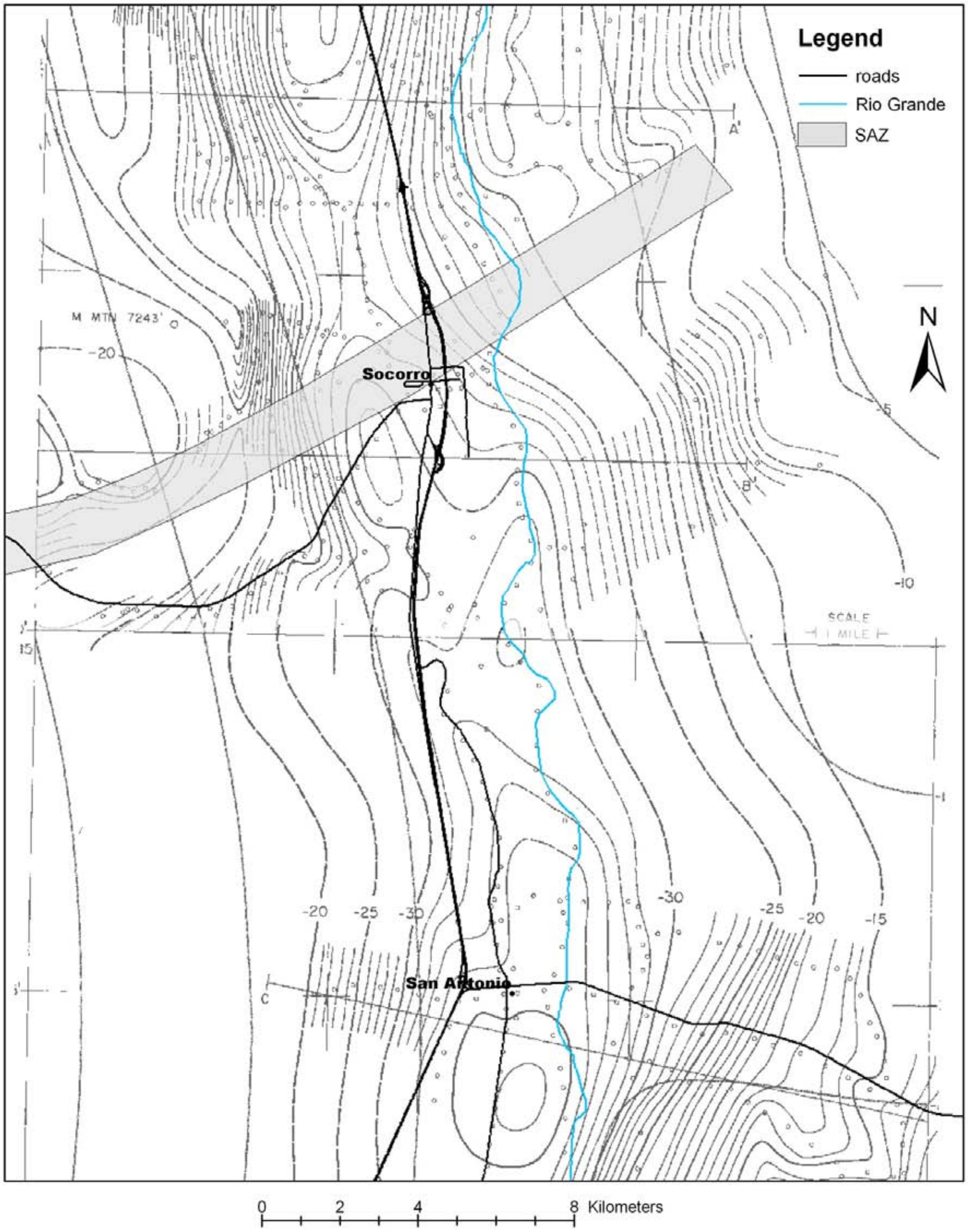

Figure 49 Location of SAZ as defined by Chapin(1984) with respect to gravity data.

Interesting features observed in the gravity data are lineaments defined by gravity troughs (figure 50) that originate with the gravity low to the south and trend towards the northwest. These gravity-defined lineaments line up with the Quaternary faults on the west side of the basin. It is not clear what type of structure these gravity troughs represent. However, on the northwestern boundary of the largest trough, the observed gradient is relatively high, which would be consistent with a fault that crosses the basin obliquely to the southeast. If these lineaments observed in the gravity data are real, they may represent older scissor- type faults along which younger Quaternary faults have propagated.

Projection of Hypothetical Cross-Basin Structures

The locations of these hypothetical cross-basin structures were projected based on the criteria discussed above. Figure 51 shows the location of these projected structures as red dashed lines. The locations of the hypothetical structures that strike across the basin were chosen based on the strike direction of mapped Quaternary faults on the west and east margins of the basin, lineaments observed on the residual Bouger anomaly, and the change in direction of flow path of the Rio Grande. The location of the hypothetical structure that strikes north- south along the eastern edge of the basin was based on data that included mapped Quaternary faults, high gradients observed in the residual Bouger anomaly map, aerial photos and a hill shade model created from the digital elevation model of the study area. Figure 52 shows the hypothetical structures on the hill-shade model. This hypothetical structure can be seen to follow along an apparent shelf. The shelf has been interpreted to be an erosional feature such as a terrace because geological

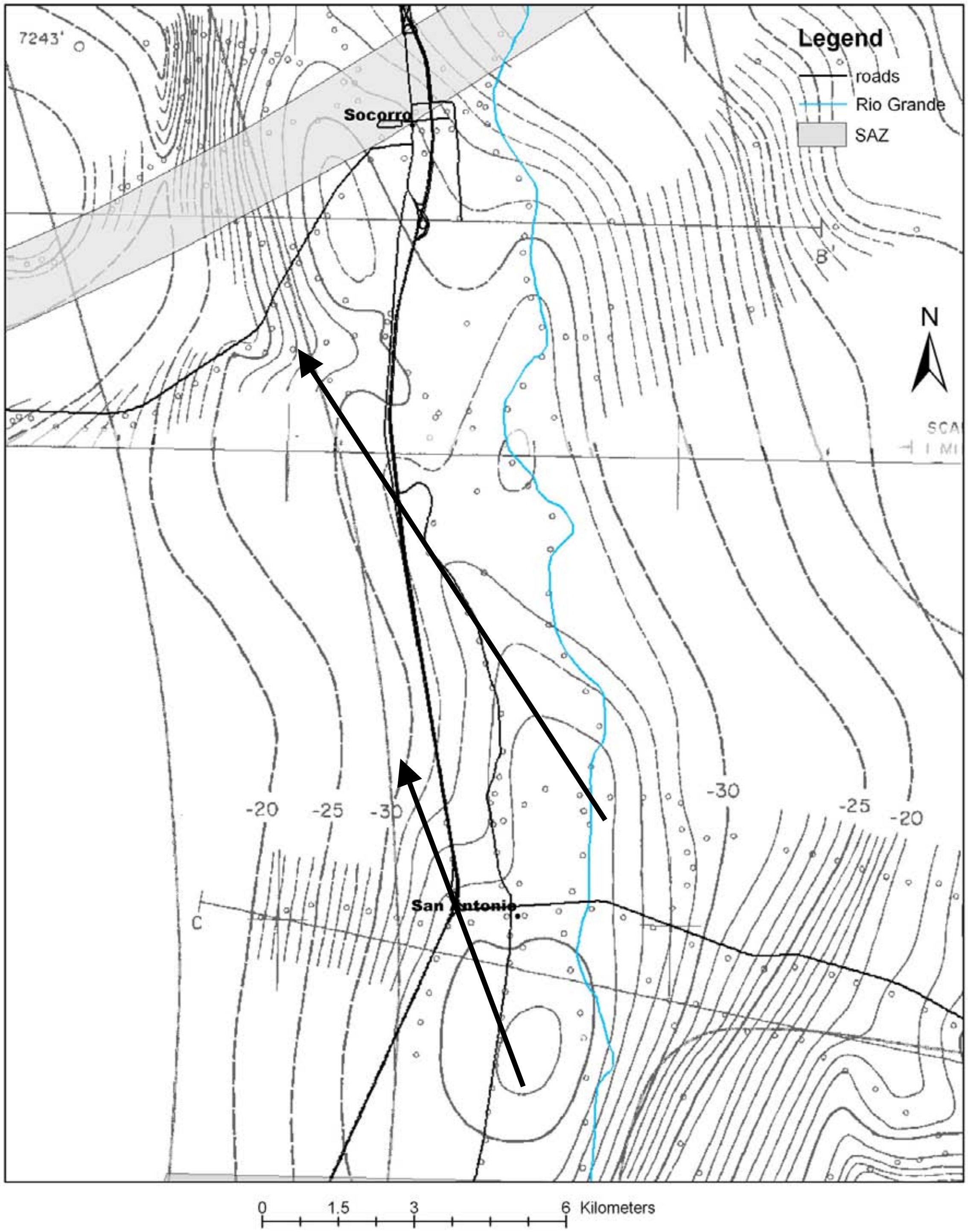

Figure 50 Location of gravity troughs possibly associated with cross-basin scissor faults.

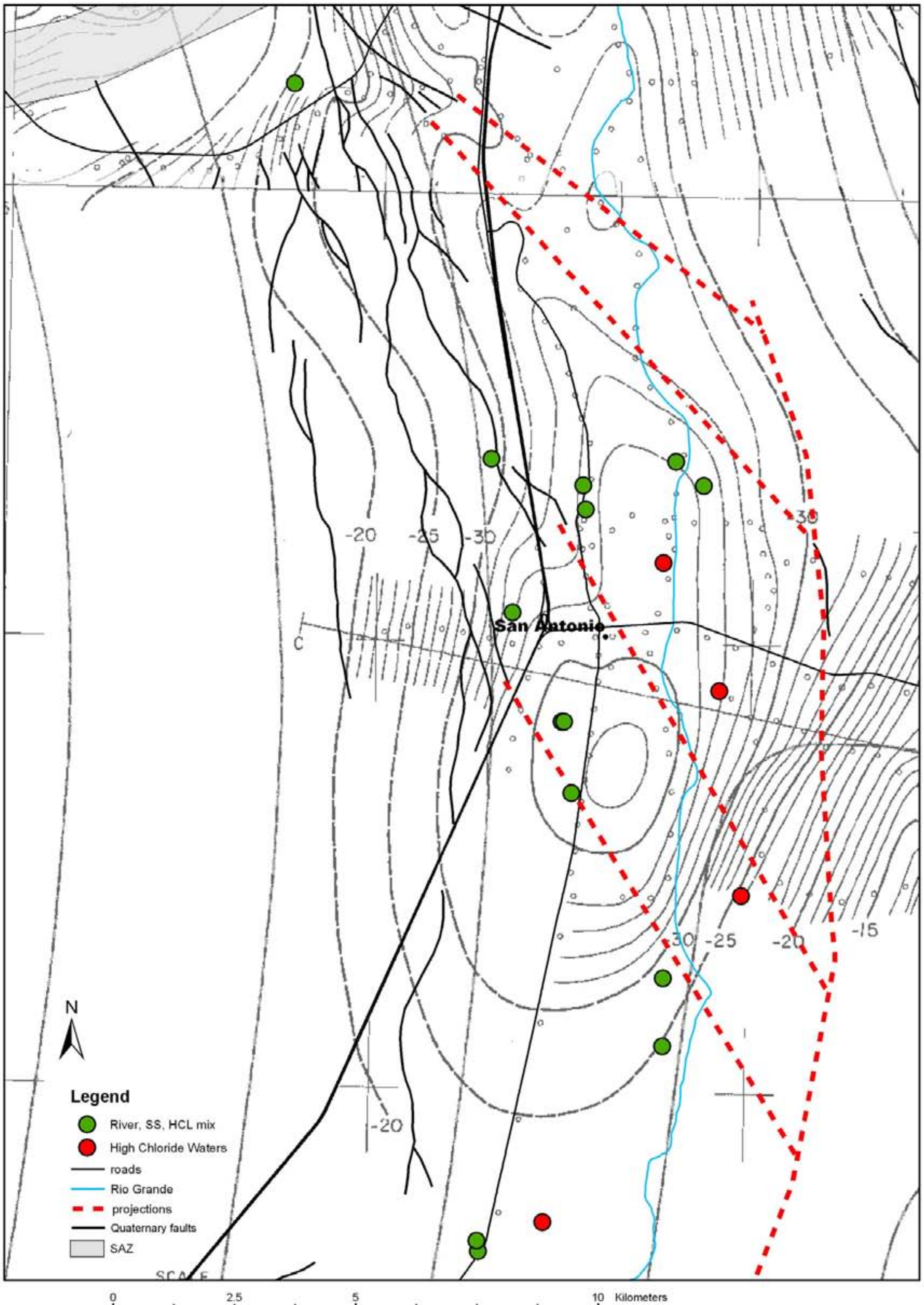

Figure 51 Inferred hypothetical structures associated with the SAZ that may control upwelling of high-chloride waters.

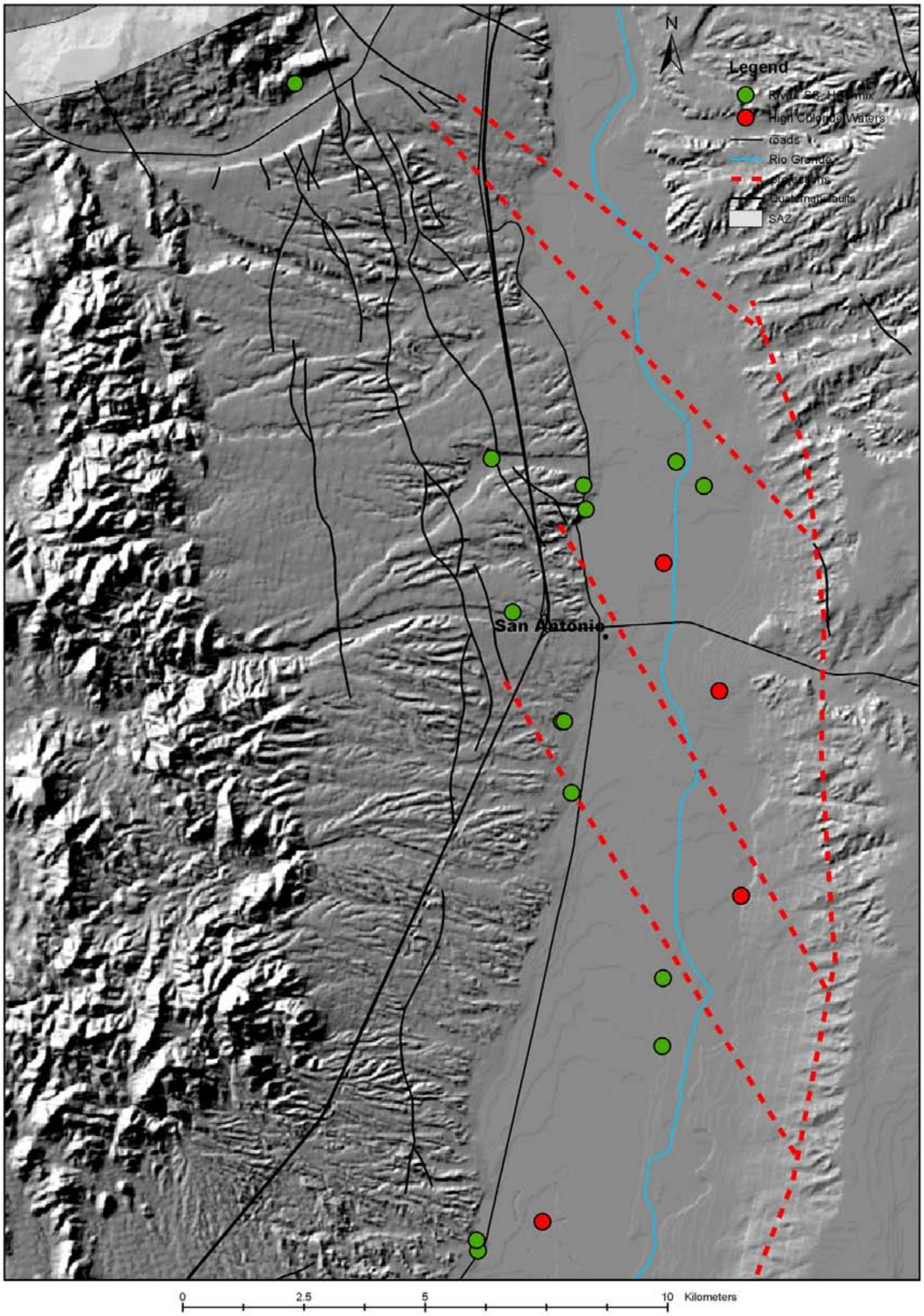

Figure 52 Hypothetical structures on hill shade model. Red dots are high-chloride waters and the green dots represent Socorro Spring-high chloride missed waters.

maps of the area do not show faults along this shelf except for a short fault segment just north of HWY 380. This shelf may be an erosional feature, but it is interesting to note that to the north of the hypothetical structure, the area along the eastern side of the basin is characterized by a gradual erosional slope rather than a shelf-like structure as observed to the south. This change in geomorphology may be due to a structure such as a fault. Figure 53 shows the hypothetical structures on an aerial photo of the study area. The main feature of interest is a lineament at the southern end that lines up with the hypothetical faults. This lineament appears to be a sharp boundary, across which an abrupt change in vegetation occurs. Again, this could be due an underlying structure.

It is important to note that the location of the inferred structures may not be is only hypothetical, but if these structures do exist, the area of interest would probably be broken up with many fractures, which could account for the high variability in water chemistry that is observed.

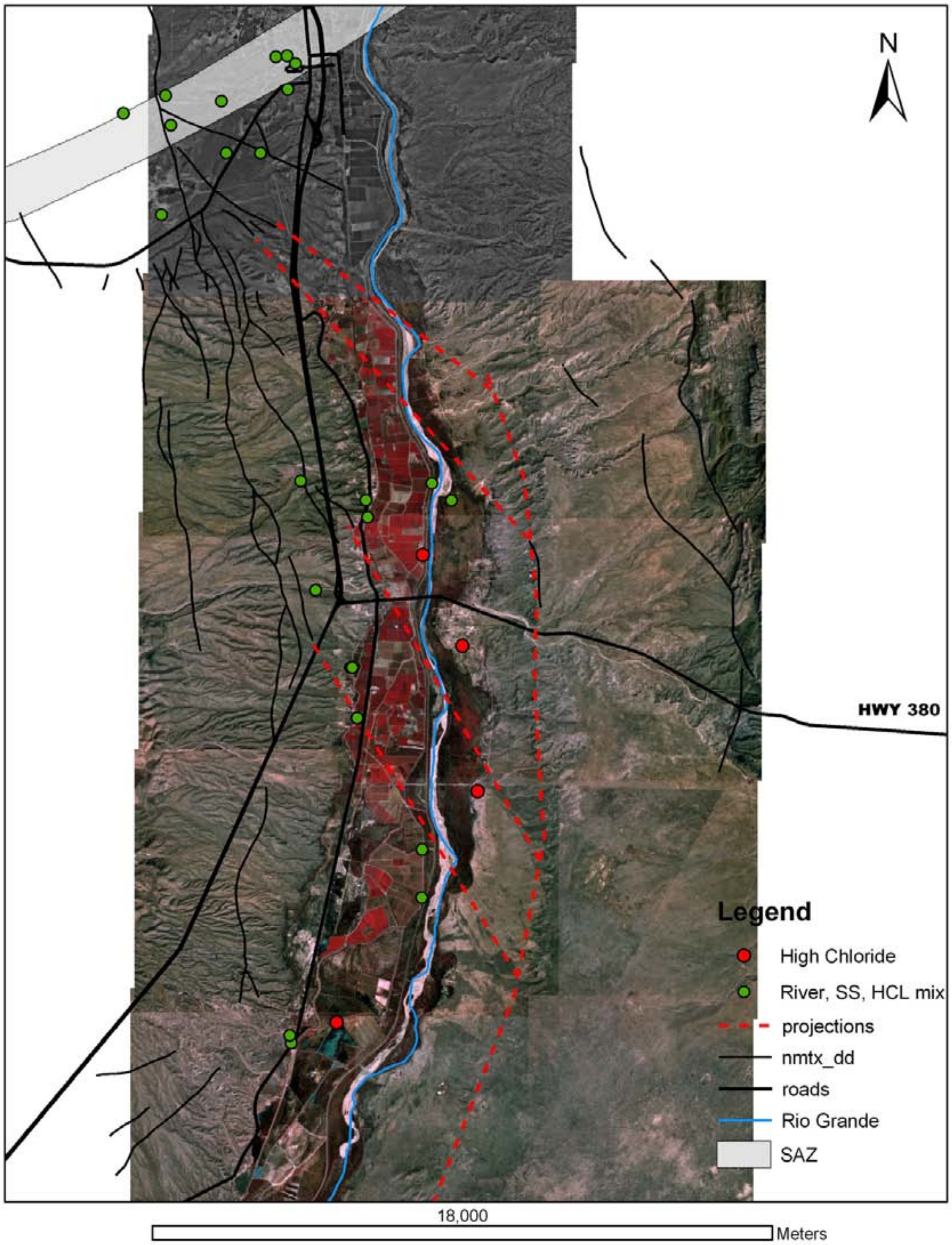

Figure 53 Hypothetical structures on aerial photo.

Appendix VI The following section describes and analyzes magnetic data collected in the study area during the Fall of 2003.

The Magnetic Method

Magnetic data can be useful in studying subsurface structural geology. The magnetic field at a point on the earth's surface is mainly dependent on the earth's magnetic field, but other factors such as geology and buried material with different magnetic properties may produce small variations in the magnetic field at a specific point. For geological studies the principal factor that affects the magnetic field at a specific point is the magnetic susceptibility of the minerals in the rocks or sediments below the point of measurement. Magnetic susceptibility is basically the ability of the material to be affected by an external magnetic field, observed as an induced magnetism of the material. The minerals with the highest susceptibilities include magnetite, ilmenite, and pyrrhotite with magnetite being the most common (Burger, 1992).

The magnetic method can be applied to both deep and shallow structures. Mathematical models of a buried normal faulted semi-infinite sheet with an induced magnetism of a certain strength produces a constant field strength over the foot wall with a decrease in field strength over the hanging wall due to the increased distance between the point of measurement and the faulted sheet. Obviously this type of data could be very useful in locating buried structures such as faults. However, it should be noted that many observed magnetic anomalies can be explained in different ways and do not represent a unique solution. Therefore, in order to come to meaningful and realistic conclusions using magnetic data, knowledge of the subsurface geology is necessary. It is also beneficial to combine the magnetic method with other geophysical exploration techniques.

Methods

An EG&G Geometrics G-856 Memory-Mag proton precession magnetometer was used to survey 5 high resolution transects within the field area. This type of magnetometer measures the total magnetic field strength at a specific point. The distance between measurement points was generally 20-30 paces (~20-30 meters). After a transect was completed, a reading was made at the exact starting point of that transect to check for drift due to diurnal magnetic fluctuations. Figure 54 shows the location of the 5 transects.

Results and Discussion

Figure 54 shows the transects that were surveyed along with a color-coded representation of the data. Figures 55 and 56 shows graphs of magnetic data correlating to the transects shown in figure 54. Transects 1, 2, and 4 were surveyed in areas of mapped faults to indicate whether or not any significant magnetic anomaly associated with these known structures could be observed. Transects 3 and 5 were surveyed in areas of the hypothetical structures discussed above. All hypothetical structures were projected before the collection of the magnetic data.

Transect 1 crosses a known Quaternary fault. Magnetic data for transect 1 indicates a magnetic field strength between 50000 and 49950 nT south of the fault, with a

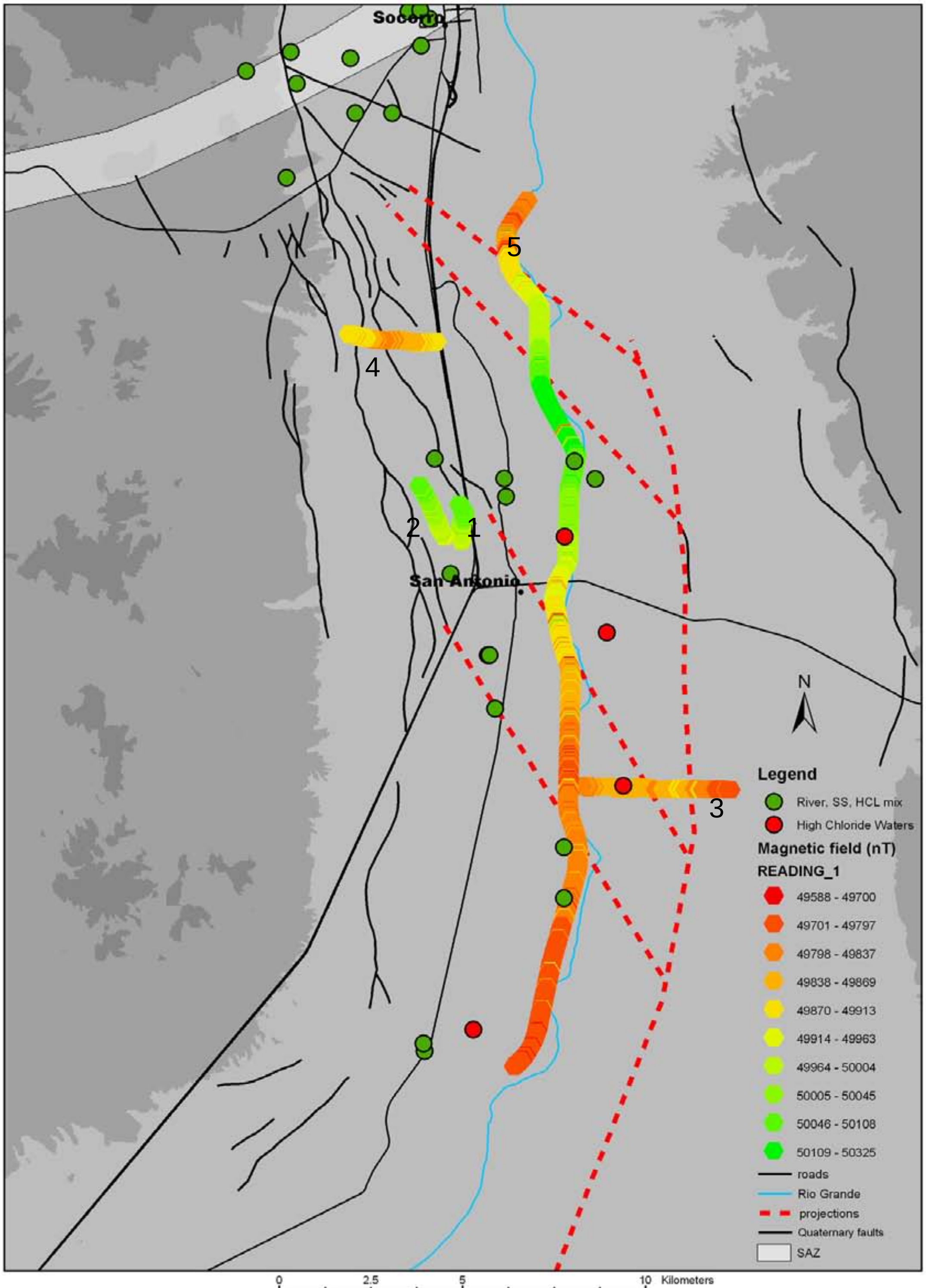

Figure 54 Locations of magnetic transects with respect to projected structures, known faults and groundwater samples. Transect numbers correlate to graphs shown in figure 51. Magnetic data points are color-coded to indicate magnetic field strength.

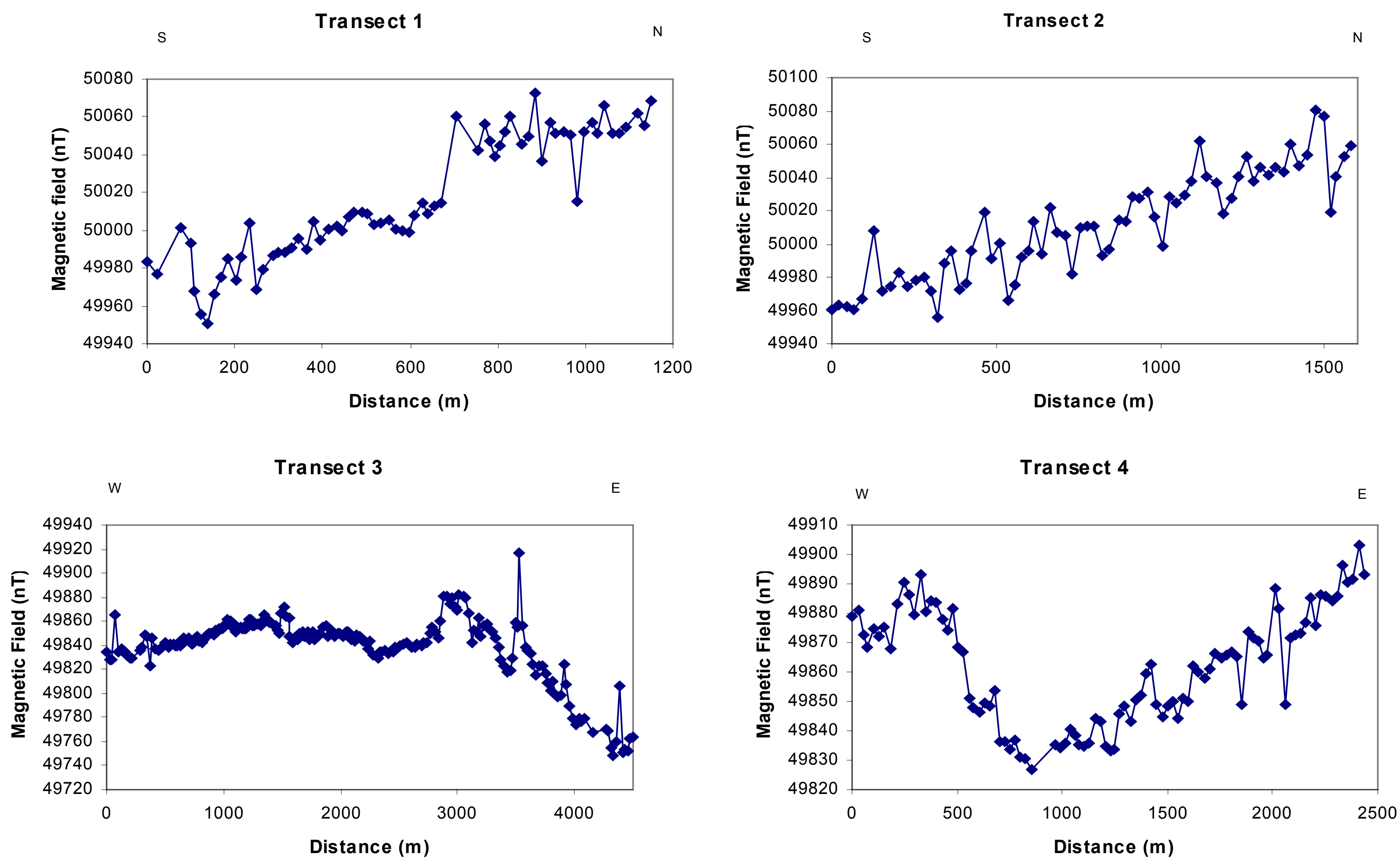

Figure 55 Magnetic data for transects 1-4

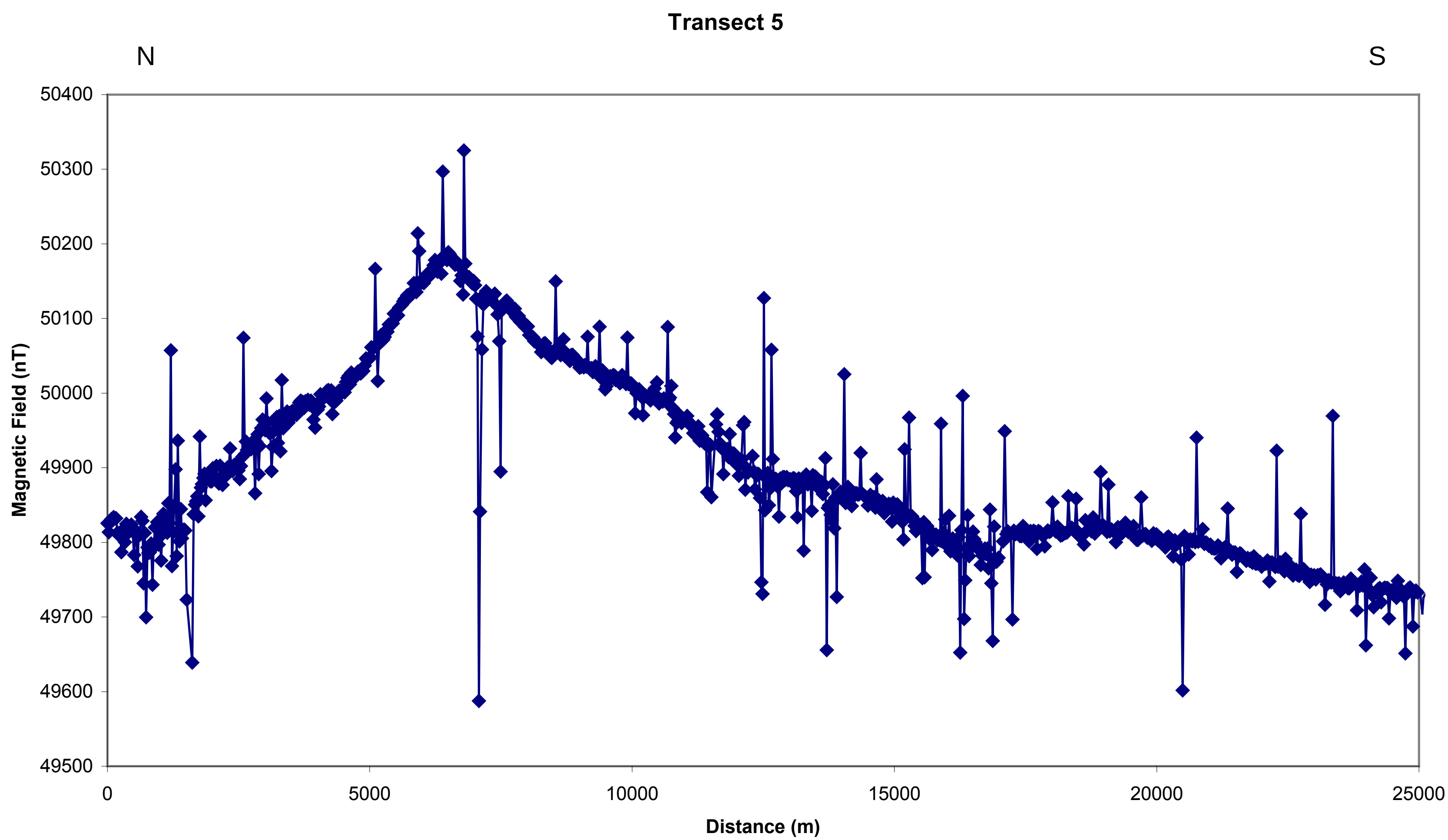

Figure 56 Magnetic data for transect 5.

gradual increase in field strength approaching the fault. In the vicinity of the fault, a sharp increase in magnetic field strength was observed. North of the fault, the field strength ranged between 50040 and 50080 nT. It appears that the presence of the fault was indicated by the magnetic data. However, the data does not necessarily represent a faulted semi-infinite sheet as described above. The hanging wall is located on the northeast side of the fault where we observe a higher magnetic field strength instead of a lower one as expected according to the model described above. The reason for this discrepancy is unknown, but it does suggest that the primary factor affecting the local magnetic field strength is not a semi-infinite magnetic sheet. Instead, the magnetic anomaly may be due to the amount of sediment overlying the bedrock. If the sediment is the primary factor affecting the magnetic field, then thicker deposits of sediment will produce a higher magnetic strength, which would be consistent with the observed data for transect 1. Transect 2 runs parallel to transect 1 but does not appear to cross any known faults. Data shown in figure 55 indicate a gradual increase in magnetic field strength from south to north within the same range as observed in transect 1. However, the sharp increase in magnetic field strength that was observed for transect 1 was not observed for transect 2., which may indicate the absence of a fault. The reason for the observed gradual increase in magnetic field strength is unknown. Transect 4 was surveyed across 2 or possibly 3 known faults. The data (figure 55) shows significant fluctuations in the magnetic field strength, which might represent different thicknesses of sediment in different areas relative to the locations of the faults. However, it is still difficult to come to any concrete conclusions solely based on the magnetic data.

Data for transects 3 (figure 55) and 5 (figure 56) show significant fluctuations in magnetic field strength that do appear to correlate with the location of the projected structures, which may indicate the presence of deep cross-basin structures. However, not enough is known about the geology of the area to come to any concrete conclusions based on this data alone.

Appendix VII The following tables includes magnetic data collected within the study area during the fall 2003.

Table 11 Magnetic data and point locations.

Transect	Point	Longitude	Latitude	UTM Easting (m)	UTM Northing (m)	distance (m)	Accumulated distance (m)	Magnetic Field Strength (nT)
1	1	-106.883689	33.930485	325888	3755852	0.000	0.000	49983.4
1	2	-106.883728	33.930277	325884	3755829	23.345	23.345	49977
1	3	-106.883868	33.930743	325872	3755881	53.367	76.712	50001.6
1	4	-106.883926	33.930932	325867	3755902	21.587	98.299	49993.2
1	5	-106.883938	33.931004	325866	3755910	8.062	106.361	49967.6
1	6	-106.883995	33.931129	325861	3755924	14.866	121.227	49955.6
1	7	-106.884063	33.931263	325855	3755939	16.155	137.383	49951
1	8	-106.884056	33.931417	325856	3755956	17.029	154.412	49966.4
1	9	-106.884048	33.931561	325857	3755972	16.031	170.443	49975.6
1	10	-106.884051	33.931687	325857	3755986	14.000	184.443	49985
1	11	-106.883946	33.931824	325867	3756001	18.028	202.471	49973.4
1	12	-106.883959	33.93195	325866	3756015	14.036	216.507	49986.2
1	13	-106.883952	33.932095	325867	3756031	16.031	232.538	50003.8
1	14	-106.883966	33.932248	325866	3756048	17.029	249.567	49969
1	15	-106.884001	33.932391	325863	3756064	16.279	265.846	49979.6
1	16	-106.883995	33.932572	325864	3756084	20.025	285.871	49986.4
1	17	-106.883997	33.93268	325864	3756096	12.000	297.871	49988
1	18	-106.884	33.932815	325864	3756111	15.000	312.871	49988.2
1	19	-106.88396	33.932969	325868	3756128	17.464	330.335	49990.8
1	20	-106.883942	33.933114	325870	3756144	16.125	346.460	49995.8
1	21	-106.883945	33.933276	325870	3756162	18.000	364.460	49989.6
1	22	-106.883905	33.933421	325874	3756178	16.492	380.952	50005
1	23	-106.883951	33.933546	325870	3756192	14.560	395.513	49994.6
1	24	-106.883911	33.933709	325874	3756210	18.439	413.952	50000.6
1	25	-106.883915	33.933872	325874	3756228	18.000	431.952	50002.6
1	26	-106.883907	33.933998	325875	3756242	14.036	445.987	49999.6
1	27	-106.883921	33.934124	325874	3756256	14.036	460.023	50007.4
1	28	-106.883923	33.934223	325874	3756267	11.000	471.023	50009.2
1	29	-106.883872	33.934395	325879	3756286	19.647	490.670	50009.4
1	30	-106.88381	33.934504	325885	3756298	13.416	504.086	50009
1	31	-106.883726	33.934623	325893	3756311	15.264	519.351	50002.8
1	32	-106.883642	33.934741	325901	3756324	15.264	534.615	50003.6
1	33	-106.883602	33.934886	325905	3756340	16.492	551.107	50005.2
1	34	-106.883562	33.935031	325909	3756356	16.492	567.600	50000.8
1	35	-106.883543	33.935158	325911	3756370	14.142	581.742	50000
1	36	-106.883503	33.935285	325915	3756384	14.560	596.302	49998.6
1	37	-106.883473	33.935402	325918	3756397	13.342	609.644	50007.6
1	38	-106.883389	33.935548	325926	3756413	17.889	627.532	50014.4

Transect	Point	Longitude	Latitude	UTM Easting (m)	UTM Northing (m)	distance (m)	Accumulated distance (m)	Magnetic Field Strength (nT)
1	39	-106.883338	33.935657	325931	3756425	13.000	640.532	50009
1	40	-106.883308	33.935793	325934	3756440	15.297	655.829	50012.6
1	41	-106.883279	33.935919	325937	3756454	14.318	670.147	50014.8
1	42	-106.883079	33.936184	325956	3756483	34.670	704.817	50060
1	43	-106.883454	33.93653	325922	3756522	51.740	756.557	50042
1	44	-106.883392	33.93663	325928	3756533	12.530	769.087	50056
1	45	-106.883329	33.936721	325934	3756543	11.662	780.749	50047.6
1	46	-106.883277	33.936821	325939	3756554	12.083	792.832	50038.8
1	47	-106.883214	33.936912	325945	3756564	11.662	804.494	50044.8
1	48	-106.883151	33.937003	325951	3756574	11.662	816.156	50051.8
1	49	-106.883132	33.937121	325953	3756587	13.153	829.309	50060.4
1	50	-106.882896	33.937206	325975	3756596	23.770	853.078	50046
1	51	-106.883039	33.937312	325962	3756608	17.692	870.770	50049.8
1	52	-106.88301	33.937456	325965	3756624	16.279	887.049	50072.6
1	53	-106.883023	33.937591	325964	3756639	15.033	902.082	50036.2
1	54	-106.883102	33.937726	325957	3756654	16.553	918.635	50057.2
1	55	-106.88318	33.937842	325950	3756667	14.765	933.400	50051.4
1	56	-106.883259	33.937967	325943	3756681	15.652	949.052	50051.8
1	57	-106.883327	33.93811	325937	3756697	17.088	966.140	50050.4
1	58	-106.883416	33.938235	325929	3756711	16.125	982.265	50015.4
1	59	-106.883527	33.93835	325919	3756724	16.401	998.666	50052
1	60	-106.883627	33.938466	325910	3756737	15.811	1014.478	50057
1	61	-106.883726	33.938564	325901	3756748	14.213	1028.690	50051.4
1	62	-106.883837	33.938661	325891	3756759	14.866	1043.556	50065.8
1	63	-106.883937	33.938795	325882	3756774	17.493	1061.049	50051.6
1	64	-106.884026	33.938911	325874	3756787	15.264	1076.314	50051.6
1	65	-106.884137	33.939035	325864	3756801	17.205	1093.518	50054.4
1	66	-106.884346	33.939185	325845	3756818	25.495	1119.013	50062
1	67	-106.884456	33.939292	325835	3756830	15.620	1134.634	50055.6
1	68	-106.884578	33.939398	325824	3756842	16.279	1150.913	50068.8
2	0	-106.888839	33.931497	325414	3755973	0.000	0.000	49960.9
2	1	-106.888972	33.931657	325402	3755991	21.633	21.633	49962.9
2	2	-106.889149	33.931826	325386	3756010	24.839	46.473	49962.2
2	3	-106.889271	33.931959	325375	3756025	18.601	65.074	49960.9
2	4	-106.889513	33.932127	325353	3756044	29.069	94.143	49966.9
2	5	-106.889692	33.932412	325337	3756076	35.777	129.920	50008
2	6	-106.889804	33.9326	325327	3756097	23.259	153.179	49971.3
2	7	-106.88995	33.932823	325314	3756122	28.178	181.357	49974.2
2	8	-106.890062	33.93302	325304	3756144	24.166	205.523	49983
2	9	-106.890164	33.933235	325295	3756168	25.632	231.155	49974.6
2	10	-106.890298	33.933422	325283	3756189	24.187	255.342	49978.4
2	11	-106.890433	33.933618	325271	3756211	25.060	280.402	49979.6
2	12	-106.890512	33.933798	325264	3756231	21.190	301.592	49971.4
2	13	-106.890527	33.933969	325263	3756250	19.026	320.618	49955.4
2	14	-106.890531	33.934176	325263	3756273	23.000	343.618	49988.1
2	15	-106.890546	33.934338	325262	3756291	18.028	361.646	49996.1

Transect	Point	Longitude	Latitude	UTM Easting (m)	UTM Northing (m)	distance (m)	Accumulated distance (m)	Magnetic Field Strength (nT)
2	16	-106.890605	33.934554	325257	3756315	24.515	386.161	49972.5
2	17	-106.890706	33.934723	325248	3756334	21.024	407.185	49976.1
2	19	-106.890742	33.934876	325245	3756351	17.263	424.448	49995.5
2	20	-106.890869	33.935235	325234	3756391	41.485	465.932	50018.9
2	21	-106.891023	33.935368	325220	3756406	20.518	486.451	49990.9
2	22	-106.891114	33.935574	325212	3756429	24.352	510.802	50000.3
2	23	-106.891237	33.935761	325201	3756450	23.707	534.509	49965.6
2	24	-106.891338	33.935931	325192	3756469	21.024	555.533	49975
2	25	-106.891429	33.936119	325184	3756490	22.472	578.005	49991.7
2	26	-106.891583	33.936225	325170	3756502	18.439	596.444	49996
2	27	-106.891684	33.936377	325161	3756519	19.235	615.679	50013.4
2	28	-106.891807	33.936573	325150	3756541	24.597	640.276	49993.6
2	29	-106.891909	33.93677	325141	3756563	23.770	664.046	50021.7
2	30	-106.891999	33.936967	325133	3756585	23.409	687.455	50007.3
2	31	-106.89209	33.937137	325125	3756604	20.616	708.071	50005.2
2	32	-106.892192	33.937334	325116	3756626	23.770	731.840	49982.3
2	33	-106.892293	33.937521	325107	3756647	22.847	754.688	50010.1
2	34	-106.892437	33.937663	325094	3756663	20.616	775.303	50010.9
2	35	-106.89256	33.937851	325083	3756684	23.707	799.010	50011.1
2	36	-106.892629	33.938039	325077	3756705	21.840	820.850	49993.2
2	37	-106.892688	33.938237	325072	3756727	22.561	843.411	49996.9
2	38	-106.892715	33.938498	325070	3756756	29.069	872.480	50014.6
2	39	-106.892741	33.938696	325068	3756778	22.091	894.571	50013.8
2	40	-106.892799	33.938857	325063	3756796	18.682	913.252	50028.4
2	41	-106.892922	33.939045	325052	3756817	23.707	936.959	50027.6
2	42	-106.893012	33.939224	325044	3756837	21.541	958.500	50031.5
2	43	-106.893136	33.93942	325033	3756859	24.597	983.096	50016.4
2	44	-106.893248	33.93959	325023	3756878	21.471	1004.567	49998.8
2	45	-106.893414	33.939759	325008	3756897	24.207	1028.775	50028.8
2	46	-106.893515	33.939919	324999	3756915	20.125	1048.899	50024.7
2	47	-106.89367	33.940106	324985	3756936	25.239	1074.138	50029.6
2	48	-106.89376	33.940267	324977	3756954	19.698	1093.836	50037.4
2	49	-106.893926	33.940445	324962	3756974	25.000	1118.836	50062
2	50	-106.894006	33.940615	324955	3756993	20.248	1139.084	50040.4
2	51	-106.894185	33.940874	324939	3757022	33.121	1172.205	50037.2
2	52	-106.894285	33.941026	324930	3757039	19.235	1191.441	50017.8
2	53	-106.89443	33.941213	324917	3757060	24.698	1216.139	50027.3
2	54	-106.894542	33.941382	324907	3757079	21.471	1237.610	50040.1
2	55	-106.894676	33.941561	324895	3757099	23.324	1260.934	50052.2
2	56	-106.894799	33.941748	324884	3757120	23.707	1284.640	50038.1
2	57	-106.894879	33.941927	324877	3757140	21.190	1305.830	50046
2	58	-106.894949	33.942143	324871	3757164	24.739	1330.568	50041.8
2	59	-106.895017	33.942304	324865	3757182	18.974	1349.542	50046.5
2	60	-106.89513	33.9425	324855	3757204	24.166	1373.708	50043.1
2	61	-106.895284	33.942633	324841	3757219	20.518	1394.226	50059.9
2	62	-106.895429	33.94282	324828	3757240	24.698	1418.925	50047.3

Transect	Point	Longitude	Latitude	UTM Easting (m)	UTM Northing (m)	distance (m)	Accumulated distance (m)	Magnetic Field Strength (nT)
2	63	-106.895595	33.943016	324813	3757262	26.627	1445.552	50053.1
2	64	-106.89572	33.943249	324802	3757288	28.231	1473.783	50080.2
2	65	-106.895886	33.943418	324787	3757307	24.207	1497.990	50077.1
2	66	-106.896061	33.943505	324771	3757317	18.868	1516.858	50019.5
2	67	-106.896171	33.943612	324761	3757329	15.620	1532.479	50040.7
2	68	-106.896359	33.943771	324744	3757347	24.759	1557.238	50052.2
2	69	-106.896481	33.943931	324733	3757365	21.095	1578.333	50059.4
3	158	-106.847173	33.869989	329143	3749082	0.000	0.000	49834.2
3	157	-106.846891	33.869957	329169	3749078	26.306	26.306	49827.7
3	156	-106.846653	33.869943	329191	3749076	22.091	48.397	49827.6
3	155	-106.846468	33.869901	329208	3749071	17.720	66.117	49865.7
3	154	-106.8461	33.86987	329242	3749067	34.234	100.351	49833.9
3	153	-106.845887	33.870008	329262	3749082	25.000	125.351	49837.2
3	152	-106.845573	33.869968	329291	3749077	29.428	154.779	49835.1
3	151	-106.845368	33.869989	329310	3749079	19.105	173.884	49832.4
3	150	-106.84513	33.870002	329332	3749080	22.023	195.907	49829.5
3	149	-106.844891	33.869924	329354	3749071	23.770	219.676	49829.3
3	148	-106.844966	33.869382	329346	3749011	60.531	280.207	49836.2
3	147	-106.844841	33.8696	329358	3749035	26.833	307.040	49838.7
3	146	-106.84466	33.869747	329375	3749051	23.345	330.385	49848.8
3	145	-106.844467	33.869822	329393	3749059	19.698	350.083	49847.3
3	144	-106.844273	33.869843	329411	3749061	18.111	368.194	49823.3
3	143	-106.844034	33.869811	329433	3749057	22.361	390.555	49846.7
3	142	-106.843785	33.86976	329456	3749051	23.770	414.324	49837.7
3	141	-106.843535	33.869728	329479	3749047	23.345	437.670	49835.8
3	140	-106.84334	33.869704	329497	3749044	18.248	455.918	49836.5
3	139	-106.843081	33.869717	329521	3749045	24.021	479.939	49837.8
3	138	-106.842823	33.869784	329545	3749052	25.000	504.939	49841.7
3	137	-106.842586	33.869805	329567	3749054	22.091	527.029	49838.9
3	136	-106.842337	33.869782	329590	3749051	23.195	550.224	49841.2
3	135	-106.842077	33.869777	329614	3749050	24.021	574.245	49840.7
3	134	-106.841991	33.869787	329622	3749051	8.062	582.307	49840.2
3	133	-106.84184	33.869808	329636	3749053	14.142	596.449	49839.7
3	132	-106.841646	33.869819	329654	3749054	18.028	614.477	49841.7
3	131	-106.841473	33.869831	329670	3749055	16.031	630.508	49839.5
3	130	-106.841354	33.869833	329681	3749055	11.000	641.508	49844.4
3	129	-106.841159	33.869818	329699	3749053	18.111	659.619	49846.7
3	128	-106.840986	33.869829	329715	3749054	16.031	675.650	49842.9
3	127	-106.840792	33.869841	329733	3749055	18.028	693.678	49845
3	126	-106.84063	33.869835	329748	3749054	15.033	708.712	49846.2
3	125	-106.840457	33.869828	329764	3749053	16.031	724.743	49841.5
3	124	-106.840295	33.869867	329779	3749057	15.524	740.267	49841.6
3	123	-106.840122	33.869851	329795	3749055	16.125	756.391	49846
3	122	-106.839906	33.869863	329815	3749056	20.025	776.416	49846.9
3	121	-106.839766	33.869875	329828	3749057	13.038	789.455	49843.3
3	120	-106.839551	33.869932	329848	3749063	20.881	810.335	49841.7

Transect	Point	Longitude	Latitude	UTM Easting (m)	UTM Northing (m)	distance (m)	Accumulated distance (m)	Magnetic Field Strength (nT)
3	119	-106.839442	33.869906	329858	3749060	10.440	820.776	49843.5
3	118	-106.839269	33.869873	329874	3749056	16.492	837.268	49845.1
3	117	-106.839095	33.86984	329890	3749052	16.492	853.761	49848.4
3	116	-106.838901	33.869851	329908	3749053	18.028	871.788	49849.7
3	115	-106.838738	33.869827	329923	3749050	15.297	887.085	49849.6
3	114	-106.838598	33.869865	329936	3749054	13.601	900.687	49849.5
3	113	-106.838415	33.869877	329953	3749055	17.029	917.716	49849.1
3	112	-106.838295	33.869851	329964	3749052	11.402	929.118	49852.2
3	111	-106.838145	33.869899	329978	3749057	14.866	943.984	49851.6
3	110	-106.837971	33.869865	329994	3749053	16.492	960.476	49854.2
3	109	-106.837798	33.869841	330010	3749050	16.279	976.755	49853.9
3	108	-106.837636	33.869843	330025	3749050	15.000	991.755	49854.2
3	107	-106.837462	33.869819	330041	3749047	16.279	1008.034	49855.1
3	106	-106.837288	33.869785	330057	3749043	16.492	1024.527	49857.8
3	105	-106.837182	33.869859	330067	3749051	12.806	1037.333	49861.4
3	104	-106.837083	33.869779	330076	3749042	12.728	1050.061	49857.6
3	103	-106.836976	33.869835	330086	3749048	11.662	1061.723	49859.8
3	102	-106.836761	33.869865	330106	3749051	20.224	1081.946	49855.7
3	101	-106.836653	33.869876	330116	3749052	10.050	1091.996	49857.4
3	100	-106.836458	33.869879	330134	3749052	18.000	1109.996	49851.6
3	99	-106.836349	33.869817	330144	3749045	12.207	1122.203	49854.9
3	98	-106.836367	33.869646	330142	3749026	19.105	1141.308	49854.7
3	97	-106.836396	33.86951	330139	3749011	15.297	1156.605	49853.6
3	96	-106.836361	33.869384	330142	3748997	14.318	1170.923	49854
3	95	-106.836243	33.869404	330153	3748999	11.180	1182.103	49854.6
3	94	-106.836123	33.869388	330164	3748997	11.180	1193.283	49853.9
3	93	-106.835993	33.869354	330176	3748993	12.649	1205.932	49858.3
3	92	-106.835863	33.869347	330188	3748992	12.042	1217.974	49861.9
3	91	-106.835754	33.869321	330198	3748989	10.440	1228.414	49860.5
3	90	-106.835657	33.869341	330207	3748991	9.220	1237.634	49861.3
3	89	-106.835485	33.869343	330223	3748991	16.000	1253.634	49856.8
3	88	-106.835365	33.869327	330234	3748989	11.180	1264.814	49856.1
3	87	-106.835137	33.869276	330255	3748983	21.840	1286.655	49858.3
3	86	-106.834953	33.86927	330272	3748982	17.029	1303.684	49857.4
3	85	-106.834791	33.869245	330287	3748979	15.297	1318.981	49855.9
3	84	-106.834607	33.869239	330304	3748978	17.029	1336.010	49860.1
3	83	-106.834456	33.86925	330318	3748979	14.036	1350.046	49866
3	82	-106.834272	33.869244	330335	3748978	17.029	1367.075	49862.3
3	81	-106.834144	33.869345	330347	3748989	16.279	1383.354	49860.7
3	80	-106.834003	33.869329	330360	3748987	13.153	1396.507	49858.7
3	79	-106.833851	33.869277	330374	3748981	15.232	1411.739	49857.7
3	78	-106.833678	33.869289	330390	3748982	16.031	1427.770	49856.9
3	77	-106.833516	33.8693	330405	3748983	15.033	1442.803	49856.4
3	76	-106.833354	33.869276	330420	3748980	15.297	1458.100	49852.9
3	75	-106.833191	33.869251	330435	3748977	15.297	1473.397	49849.4
3	74	-106.833008	33.869299	330452	3748982	17.720	1491.117	49866.2

Transect	Point	Longitude	Latitude	UTM Easting (m)	UTM Northing (m)	distance (m)	Accumulated distance (m)	Magnetic Field Strength (nT)
3	73	-106.83276	33.869303	330475	3748982	23.000	1514.117	49871.6
3	72	-106.832544	33.869333	330495	3748985	20.224	1534.341	49863.9
3	71	-106.832305	33.869291	330517	3748980	22.561	1556.902	49862.8
3	159	-106.832371	33.869308	330511	3748982	6.325	1563.227	49847.1
3	160	-106.832145	33.869357	330532	3748987	21.587	1584.814	49842.1
3	161	-106.831941	33.869414	330551	3748993	19.925	1604.739	49846.3
3	162	-106.831703	33.869445	330573	3748996	22.204	1626.942	49844.9
3	163	-106.831478	33.869511	330594	3749003	22.136	1649.078	49849.7
3	164	-106.83122	33.869587	330618	3749011	25.298	1674.376	49851.7
3	165	-106.830994	33.869618	330639	3749014	21.213	1695.590	49847.9
3	166	-106.830811	33.869674	330656	3749020	18.028	1713.617	49851.6
3	167	-106.830574	33.869714	330678	3749024	22.361	1735.978	49844.2
3	168	-106.830316	33.86979	330702	3749032	25.298	1761.276	49851.8
3	169	-106.830089	33.869775	330723	3749030	21.095	1782.371	49844.8
3	170	-106.829874	33.869814	330743	3749034	20.396	1802.767	49847.3
3	171	-106.829624	33.869791	330766	3749031	23.195	1825.962	49850
3	172	-106.829388	33.869867	330788	3749039	23.409	1849.372	49854.7
3	173	-106.829149	33.869816	330810	3749033	22.804	1872.175	49856.3
3	174	-106.828878	33.869784	330835	3749029	25.318	1897.493	49847.3
3	175	-106.828629	33.869743	330858	3749024	23.537	1921.030	49852
3	176	-106.828369	33.86972	330882	3749021	24.187	1945.217	49846.9
3	177	-106.828056	33.869733	330911	3749022	29.017	1974.234	49850.2
3	178	-106.827796	33.869737	330935	3749022	24.000	1998.234	49849.8
3	179	-106.827537	33.869714	330959	3749019	24.187	2022.421	49846.8
3	180	-106.827298	33.86969	330981	3749016	22.204	2044.625	49850.6
3	181	-106.827038	33.869649	331005	3749011	24.515	2069.140	49851.4
3	182	-106.826799	33.86959	331027	3749004	23.087	2092.227	49845.2
3	183	-106.826528	33.869576	331052	3749002	25.080	2117.307	49843.5
3	184	-106.826322	33.869516	331071	3748995	20.248	2137.555	49848.2
3	185	-106.826061	33.869456	331095	3748988	25.000	2162.555	49847.1
3	186	-106.825811	33.869388	331118	3748980	24.352	2186.907	49844
3	187	-106.825604	33.86931	331137	3748971	21.024	2207.931	49844.1
3	188	-106.825365	33.869286	331159	3748968	22.204	2230.134	49837.7
3	189	-106.825118	33.869326	331182	3748972	23.345	2253.479	49843.3
3	190	-106.824881	33.869357	331204	3748975	22.204	2275.683	49832.1
3	191	-106.824448	33.869345	331244	3748973	40.050	2315.733	49829.1
3	192	-106.824286	33.869356	331259	3748974	15.033	2330.766	49835.1
3	193	-106.824049	33.869396	331281	3748978	22.361	2353.127	49835.1
3	194	-106.8238	33.869391	331304	3748977	23.022	2376.149	49836.2
3	195	-106.823486	33.869359	331333	3748973	29.275	2405.423	49833.7
3	196	-106.823259	33.869362	331354	3748973	21.000	2426.423	49834
3	197	-106.823043	33.869384	331374	3748975	20.100	2446.523	49834.5
3	198	-106.822795	33.869396	331397	3748976	23.022	2469.545	49837.8
3	199	-106.822569	33.869427	331418	3748979	21.213	2490.758	49838.7
3	200	-106.822309	33.869431	331442	3748979	24.000	2514.758	49839.3
3	201	-106.822072	33.869452	331464	3748981	22.091	2536.849	49840.9

Transect	Point	Longitude	Latitude	UTM Easting (m)	UTM Northing (m)	distance (m)	Accumulated distance (m)	Magnetic Field Strength (nT)
3	202	-106.821824	33.869465	331487	3748982	23.022	2559.870	49842.1
3	203	-106.821597	33.869459	331508	3748981	21.024	2580.894	49840.5
3	204	-106.821326	33.869436	331533	3748978	25.179	2606.073	49838.9
3	205	-106.821068	33.869503	331557	3748985	25.000	2631.073	49839
3	206	-106.820828	33.869425	331579	3748976	23.770	2654.843	49841.1
3	207	-106.820461	33.869413	331613	3748974	34.059	2688.902	49839.4
3	208	-106.820211	33.869362	331636	3748968	23.770	2712.672	49842.3
3	209	-106.81994	33.869339	331661	3748965	25.179	2737.851	49842.7
3	210	-106.819681	33.86937	331685	3748968	24.187	2762.038	49850.3
3	211	-106.819466	33.869428	331705	3748974	20.881	2782.918	49854.5
3	212	-106.819217	33.869404	331728	3748971	23.195	2806.113	49850.9
3	213	-106.818917	33.869517	331756	3748983	30.463	2836.576	49846.5
3	214	-106.818724	33.869574	331774	3748989	18.974	2855.550	49860.6
3	215	-106.818411	33.869596	331803	3748991	29.069	2884.619	49881.4
3	216	-106.818141	33.869637	331828	3748995	25.318	2909.937	49880.8
3	217	-106.817882	33.869649	331852	3748996	24.021	2933.958	49874.8
3	218	-106.817634	33.869689	331875	3749000	23.345	2957.303	49880
3	219	-106.81744	33.869701	331893	3749001	18.028	2975.331	49871.3
3	220	-106.817382	33.869539	331898	3748983	18.682	2994.012	49868.7
3	221	-106.817166	33.869516	331918	3748980	20.224	3014.236	49881.8
3	222	-106.816787	33.869494	331953	3748977	35.128	3049.364	49881.2
3	223	-106.81656	33.869498	331974	3748977	21.000	3070.364	49879.6
3	224	-106.816288	33.869402	331999	3748966	27.313	3097.677	49866.6
3	225	-106.816039	33.869406	332022	3748966	23.000	3120.677	49842.1
3	226	-106.815845	33.869418	332040	3748967	18.028	3138.705	49853.1
3	227	-106.815575	33.869422	332065	3748967	25.000	3163.705	49851.5
3	228	-106.815316	33.869444	332089	3748969	24.083	3187.788	49863.2
3	229	-106.815176	33.869473	332102	3748972	13.342	3201.130	49847.6
3	230	-106.814906	33.869495	332127	3748974	25.080	3226.210	49856.8
3	231	-106.814626	33.869526	332153	3748977	26.173	3252.382	49858.2
3	232	-106.814389	33.869584	332175	3748983	22.804	3275.186	49852
3	233	-106.81412	33.869642	332200	3748989	25.710	3300.896	49851.2
3	234	-106.813861	33.869664	332224	3748991	24.083	3324.979	49845.7
3	235	-106.813603	33.869712	332248	3748996	24.515	3349.494	49838.4
3	236	-106.813354	33.869707	332271	3748995	23.022	3372.516	49828.5
3	237	-106.81303	33.869721	332301	3748996	30.017	3402.533	49823.1
3	238	-106.812768	33.869626	332325	3748985	26.401	3428.933	49817.8
3	239	-106.81253	33.869593	332347	3748981	22.361	3451.294	49818.7
3	240	-106.81227	33.869588	332371	3748980	24.021	3475.315	49829.1
3	241	-106.812075	33.869573	332389	3748978	18.111	3493.426	49858.6
3	242	-106.811913	33.869548	332404	3748975	15.297	3508.723	49855.3
3	243	-106.811719	33.869596	332422	3748980	18.682	3527.404	49916.5
3	244	-106.811416	33.869564	332450	3748976	28.284	3555.689	49855.9
3	245	-106.8112	33.869585	332470	3748978	20.100	3575.788	49838.9
3	246	-106.810919	33.869572	332496	3748976	26.077	3601.865	49835.6
3	247	-106.810682	33.869602	332518	3748979	22.204	3624.069	49833

Transect	Point	Longitude	Latitude	UTM Easting (m)	UTM Northing (m)	distance (m)	Accumulated distance (m)	Magnetic Field Strength (nT)
3	248	-106.810444	33.869597	332540	3748978	22.023	3646.091	49823.7
3	249	-106.810152	33.869592	332567	3748977	27.019	3673.110	49814.8
3	250	-106.809882	33.869623	332592	3748980	25.179	3698.289	49823.2
3	251	-106.809578	33.869546	332620	3748971	29.411	3727.700	49823.2
3	252	-106.809329	33.869523	332643	3748968	23.195	3750.895	49816.4
3	253	-106.809092	33.869553	332665	3748971	22.204	3773.099	49809.4
3	254	-106.808875	33.869556	332685	3748971	20.000	3793.099	49802.2
3	255	-106.808639	33.869605	332707	3748976	22.561	3815.660	49810.1
3	256	-106.808413	33.869662	332728	3748982	21.840	3837.500	49799.1
3	257	-106.808186	33.869648	332749	3748980	21.095	3858.595	49797.7
3	258	-106.807946	33.869552	332771	3748969	24.597	3883.192	49798.9
3	259	-106.807696	33.86952	332794	3748965	23.345	3906.537	49823.9
3	260	-106.807405	33.869551	332821	3748968	27.166	3933.703	49808
3	261	-106.807115	33.869618	332848	3748975	27.893	3961.596	49789.4
3	262	-106.806856	33.86964	332872	3748977	24.083	3985.679	49779.2
3	263	-106.806522	33.86969	332903	3748982	31.401	4017.080	49774.3
3	264	-106.806296	33.869766	332924	3748990	22.472	4039.552	49779.4
3	265	-106.806047	33.869733	332947	3748986	23.345	4062.897	49777.1
3	266	-106.805852	33.869691	332965	3748981	18.682	4081.579	49779
3	267	-106.806608	33.869698	332895	3748983	70.029	4151.607	49767.7
3	268	-106.805364	33.869644	333010	3748975	115.278	4266.885	49770.7
3	269	-106.805146	33.869557	333030	3748965	22.361	4289.246	49769.4
3	270	-106.804897	33.869543	333053	3748963	23.087	4312.333	49754.7
3	271	-106.804682	33.8696	333073	3748969	20.881	4333.213	49748.3
3	272	-106.804456	33.869639	333094	3748973	21.378	4354.591	49759.5
3	273	-106.804164	33.869617	333121	3748970	27.166	4381.757	49806.6
3	274	-106.803871	33.869585	333148	3748966	27.295	4409.052	49750.9
3	275	-106.803634	33.869615	333170	3748969	22.204	4431.255	49753.8
3	276	-106.803428	33.869609	333189	3748968	19.026	4450.281	49752.3
3	277	-106.803158	33.869604	333214	3748967	25.020	4475.301	49762.1
3	278	-106.802877	33.869626	333240	3748969	26.077	4501.378	49764.3
4	93	-106.918046	33.981263	322817	3761542	0.000	0.000	49878.9
4	92	-106.917723	33.9812704	322847	3761542	29.861	29.861	49881.2
4	91	-106.917504	33.9811878	322867	3761532	22.204	52.065	49872.8
4	90	-106.917277	33.9811373	322888	3761526	21.674	73.739	49868.3
4	89	-106.916934	33.9810853	322920	3761520	32.234	105.973	49874.8
4	88	-106.916677	33.9810562	322943	3761516	24.032	130.005	49872.1
4	87	-106.916404	33.9810186	322968	3761512	25.547	155.552	49875.5
4	86	-106.916092	33.9809237	322997	3761500	30.683	186.234	49868
4	85	-106.915812	33.9807872	323023	3761485	29.929	216.164	49882.9
4	84	-106.915528	33.980696	323049	3761474	28.193	244.356	49890.3
4	83	-106.915207	33.9806836	323078	3761472	29.643	273.999	49886.2
4	82	-106.914959	33.9806794	323101	3761471	22.927	296.926	49879.6
4	81	-106.914676	33.9805645	323127	3761458	29.070	325.996	49893.4
4	80	-106.914401	33.9805728	323153	3761459	25.454	351.450	49880.5
4	79	-106.914128	33.9805333	323178	3761454	25.643	377.093	49884.1

Transect	Point	Longitude	Latitude	UTM Easting (m)	UTM Northing (m)	distance (m)	Accumulated distance (m)	Magnetic Field Strength (nT)
4	78	-106.913872	33.980494	323201	3761449	24.054	401.147	49883.8
4	77	-106.913576	33.9804645	323229	3761445	27.559	428.706	49878
4	76	-106.913329	33.9803713	323251	3761434	25.031	453.736	49874.1
4	75	-106.91307	33.9803112	323275	3761427	24.852	478.588	49881.7
4	74	-106.912801	33.9802661	323300	3761422	25.335	503.924	49868.3
4	73	-106.91253	33.9801876	323325	3761413	26.510	530.434	49866.7
4	72	-106.912261	33.9801609	323349	3761409	25.074	555.508	49850.9
4	71	-106.912026	33.9802199	323371	3761415	22.655	578.163	49847.7
4	70	-106.911742	33.9802244	323397	3761415	26.230	604.393	49846.5
4	69	-106.911485	33.9802164	323421	3761414	23.767	628.160	49849.4
4	68	-106.911218	33.9801869	323446	3761410	24.850	653.010	49848.2
4	67	-106.910981	33.9801383	323468	3761405	22.607	675.617	49853.7
4	66	-106.910699	33.9800922	323494	3761399	26.567	702.184	49836.5
4	65	-106.910427	33.9800294	323519	3761392	26.036	728.220	49836.1
4	64	-106.910191	33.9799874	323540	3761386	22.372	750.592	49833.9
4	63	-106.909943	33.9799263	323563	3761379	23.900	774.492	49837
4	62	-106.909675	33.9799346	323588	3761380	24.774	799.266	49831.3
4	61	-106.909401	33.9799306	323613	3761379	25.296	824.563	49830.5
4	60	-106.90911	33.9799469	323640	3761380	26.921	851.484	49827.1
4	59	-106.907908	33.9797931	323751	3761361	112.438	963.922	49835.3
4	58	-106.907647	33.9798058	323775	3761362	24.149	988.071	49834.4
4	57	-106.907404	33.9798424	323798	3761366	22.783	1010.853	49835.7
4	56	-106.907146	33.9798766	323821	3761369	24.155	1035.008	49840.7
4	55	-106.906878	33.9798527	323846	3761366	24.936	1059.944	49838.5
4	54	-106.906641	33.9798773	323868	3761368	22.042	1081.987	49835.5
4	53	-106.906381	33.9798791	323892	3761368	24.061	1106.048	49834.5
4	52	-106.906124	33.9799144	323916	3761371	24.042	1130.090	49835.8
4	51	-106.905862	33.9799554	323940	3761375	24.665	1154.754	49844.3
4	50	-106.905595	33.9799866	323965	3761378	24.891	1179.646	49843.1
4	49	-106.905351	33.979992	323987	3761379	22.501	1202.147	49834.5
4	48	-106.905071	33.9800285	324013	3761382	26.254	1228.400	49833.3
4	47	-106.90486	33.9800538	324033	3761385	19.624	1248.024	49833.7
4	46	-106.904608	33.9800854	324056	3761388	23.551	1271.575	49845.8
4	45	-106.904347	33.9801171	324080	3761391	24.384	1295.959	49848.6
4	44	-106.904069	33.9800828	324106	3761387	25.995	1321.954	49843.1
4	43	-106.903792	33.9800845	324132	3761386	25.652	1347.605	49850.6
4	42	-106.903541	33.9800755	324155	3761385	23.154	1370.760	49852
4	41	-106.903254	33.9800737	324181	3761384	26.539	1397.299	49859.4
4	40	-106.902987	33.9800347	324206	3761379	25.060	1422.359	49862.7
4	39	-106.902703	33.9799693	324232	3761372	27.163	1449.522	49849.1
4	38	-106.902444	33.9799368	324256	3761368	24.262	1473.784	49844.9
4	37	-106.90218	33.9798811	324280	3761361	25.150	1498.934	49848.6
4	36	-106.901914	33.9798709	324305	3761359	24.601	1523.535	49850.2
4	35	-106.901656	33.9798246	324329	3761354	24.445	1547.980	49844
4	34	-106.901386	33.9797978	324353	3761350	25.076	1573.056	49850.9
4	33	-106.9011	33.9797388	324380	3761343	27.204	1600.260	49849.9

Transect	Point	Longitude	Latitude	UTM Easting (m)	UTM Northing (m)	distance (m)	Accumulated distance (m)	Magnetic Field Strength (nT)
4	32	-106.900867	33.9796668	324401	3761335	22.999	1623.259	49862.1
4	31	-106.900598	33.9796588	324426	3761334	24.836	1648.095	49860.1
4	30	-106.900286	33.9796548	324455	3761333	28.886	1676.981	49858.1
4	29	-106.900013	33.979668	324480	3761334	25.229	1702.210	49861.2
4	28	-106.899739	33.9796369	324505	3761330	25.602	1727.812	49866.5
4	27	-106.899437	33.9796163	324533	3761327	28.010	1755.823	49864.8
4	26	-106.899186	33.9795813	324556	3761323	23.451	1779.274	49866
4	25	-106.898922	33.9795531	324581	3761319	24.650	1803.924	49867
4	24	-106.898643	33.9795348	324606	3761316	25.802	1829.726	49865.3
4	23	-106.898358	33.9794865	324633	3761311	26.902	1856.628	49848.9
4	22	-106.89806	33.9794678	324660	3761308	27.661	1884.288	49873.6
4	21	-106.897832	33.9794285	324681	3761303	21.513	1905.802	49871.8
4	20	-106.897541	33.9793492	324708	3761294	28.248	1934.049	49870.4
4	19	-106.897309	33.9793259	324729	3761291	21.587	1955.636	49864.7
4	18	-106.897088	33.9793693	324750	3761295	20.952	1976.588	49865.9
4	17	-106.896736	33.9794647	324782	3761305	34.202	2010.789	49888.4
4	16	-106.896501	33.9794837	324804	3761307	21.826	2032.615	49881.6
4	15	-106.896234	33.979503	324829	3761309	24.787	2057.402	49848.8
4	14	-106.895958	33.9795371	324854	3761312	25.793	2083.196	49871.7
4	13	-106.895702	33.9795371	324878	3761312	23.674	2106.870	49872.4
4	12	-106.895415	33.9795441	324905	3761312	26.522	2133.391	49873.2
4	11	-106.895164	33.9795754	324928	3761315	23.448	2156.839	49876.8
4	10	-106.894901	33.979593	324952	3761317	24.416	2181.255	49885.2
4	9	-106.894622	33.9795993	324978	3761317	25.761	2207.016	49875.7
4	8	-106.89436	33.9795844	325002	3761315	24.260	2231.277	49886.5
4	7	-106.894096	33.9796221	325027	3761318	24.791	2256.067	49886
4	6	-106.893831	33.9796521	325051	3761321	24.659	2280.726	49884
4	5	-106.893559	33.9796592	325076	3761322	25.162	2305.888	49886
4	4	-106.893288	33.9796463	325101	3761320	25.121	2331.009	49896.3
4	3	-106.892997	33.9795942	325128	3761313	27.448	2358.457	49890.5
4	2	-106.892748	33.9796544	325151	3761320	23.981	2382.439	49891.5
4	1	-106.89245	33.9796968	325179	3761324	27.938	2410.376	49903
4	0	-106.892232	33.9797735	325199	3761332	21.895	2432.272	49893.3
5	0	-106.866035	34.0153144	327691	3765229	0.000	0.000	49825.5
5	1	-106.866255	34.015138	327671	3765210	28.182	28.182	49813.7
5	2	-106.866388	34.0149658	327658	3765191	22.687	50.869	49827.2
5	3	-106.866513	34.0148054	327646	3765173	21.226	72.095	49831
5	4	-106.866682	34.0146219	327630	3765153	25.659	97.755	49829.2
5	5	-106.866824	34.014472	327617	3765137	21.144	118.899	49833.7
5	6	-106.866953	34.014303	327604	3765118	22.205	141.103	49832.4
5	7	-106.867097	34.014109	327591	3765097	25.330	166.434	49832.4
5	8	-106.867224	34.0139217	327579	3765077	23.863	190.297	49812.8
5	9	-106.867369	34.0137373	327565	3765056	24.402	214.699	49809.5
5	10	-106.86754	34.0135456	327549	3765035	26.494	241.193	49813.6
5	11	-106.867676	34.0133554	327536	3765014	24.604	265.797	49786.9
5	12	-106.867829	34.0132004	327521	3764998	22.244	288.041	49810.8

Transect	Point	Longitude	Latitude	UTM Easting (m)	UTM Northing (m)	distance (m)	Accumulated distance (m)	Magnetic Field Strength (nT)
5	13	-106.867944	34.0130382	327510	3764980	20.883	308.923	49813.2
5	14	-106.868108	34.0128449	327495	3764959	26.271	335.195	49800.3
5	15	-106.868268	34.0126563	327480	3764938	25.592	360.786	49825
5	16	-106.868354	34.0124265	327471	3764913	26.690	387.476	49812.3
5	17	-106.868512	34.0122981	327456	3764899	20.432	407.908	49816.2
5	18	-106.868681	34.0121307	327440	3764880	24.247	432.155	49820.1
5	19	-106.86884	34.0119458	327425	3764860	25.226	457.381	49823.9
5	20	-106.86895	34.0117741	327415	3764841	21.566	478.948	49815
5	21	-106.86912	34.0115703	327399	3764819	27.536	506.484	49783.1
5	22	-106.869261	34.011404	327385	3764801	22.609	529.093	49815.8
5	23	-106.869388	34.0112447	327373	3764783	21.201	550.293	49810.6
5	24	-106.869536	34.0110525	327359	3764762	25.336	575.629	49767.7
5	25	-106.869652	34.0109031	327348	3764746	19.695	595.324	49812.3
5	26	-106.869767	34.0107377	327337	3764728	21.199	616.523	49810.1
5	27	-106.869914	34.0105692	327323	3764709	23.110	639.633	49834.2
5	28	-106.87008	34.0103803	327308	3764689	25.993	665.626	49829
5	29	-106.870214	34.0102223	327295	3764671	21.426	687.052	49745.3
5	30	-106.870364	34.0100476	327281	3764652	23.804	710.856	49812.4
5	31	-106.870499	34.0098611	327268	3764632	24.179	735.035	49699.5
5	32	-106.870664	34.0096629	327252	3764610	26.766	761.801	49793
5	33	-106.870775	34.009519	327242	3764594	18.932	780.733	49785.9
5	34	-106.870905	34.0093362	327229	3764574	23.580	804.313	49786.6
5	35	-106.871062	34.0091055	327214	3764549	29.425	833.737	49798.3
5	36	-106.871201	34.0089255	327201	3764529	23.750	857.487	49743.4
5	37	-106.871313	34.008737	327190	3764508	23.325	880.812	49793.9
5	38	-106.871407	34.0085444	327181	3764487	23.059	903.870	49820
5	39	-106.871494	34.0083453	327173	3764465	23.497	927.367	49796.5
5	40	-106.871608	34.0081605	327162	3764445	23.009	950.376	49827.1
5	41	-106.871701	34.0079676	327153	3764424	23.099	973.475	49796.9
5	42	-106.871777	34.0077693	327146	3764402	23.082	996.557	49816.1
5	43	-106.871849	34.007559	327139	3764379	24.253	1020.810	49775.7
5	44	-106.871897	34.0073576	327134	3764356	22.753	1043.564	49810.7
5	45	-106.871953	34.0071544	327128	3764334	23.152	1066.716	49838.1
5	46	-106.872015	34.006964	327122	3764313	21.860	1088.576	49827
5	47	-106.872049	34.0067493	327118	3764289	24.036	1112.612	49835.4
5	48	-106.872086	34.0065321	327115	3764265	24.314	1136.926	49812.8
5	49	-106.87212	34.0063225	327111	3764242	23.456	1160.382	49852.5
5	50	-106.872135	34.0061185	327109	3764219	22.676	1183.058	49825.4
5	51	-106.872155	34.0058912	327107	3764194	25.286	1208.343	50057.3
5	52	-106.872154	34.0056978	327107	3764173	21.452	1229.795	49768.3
5	53	-106.872142	34.0054941	327107	3764150	22.623	1252.418	49813.6
5	54	-106.872128	34.005314	327108	3764130	20.008	1272.427	49849.3
5	55	-106.872114	34.0050897	327109	3764105	24.915	1297.341	49897.7
5	56	-106.872087	34.0048902	327111	3764083	22.280	1319.621	49781.5
5	57	-106.872067	34.0046776	327113	3764060	23.641	1343.263	49936.2
5	58	-106.872029	34.0044333	327116	3764032	27.333	1370.596	49801.4

Transect	Point	Longitude	Latitude	UTM Easting (m)	UTM Northing (m)	distance (m)	Accumulated distance (m)	Magnetic Field Strength (nT)
5	59	-106.872002	34.0041772	327118	3764004	28.515	1399.111	49844.6
5	60	-106.871975	34.0039776	327120	3763982	22.266	1421.378	49805.4
5	61	-106.87193	34.0038181	327124	3763964	18.180	1439.558	49816.8
5	62	-106.871882	34.0036283	327128	3763943	21.520	1461.078	49816.9
5	63	-106.871835	34.0034092	327131	3763918	24.685	1485.763	49815.8
5	64	-106.87179	34.0031959	327135	3763895	24.018	1509.781	49723.1
5	65	-106.87167	34.0022219	327144	3763787	108.604	1618.385	49639
5	66	-106.871582	34.0020179	327152	3763764	24.018	1642.402	49837.5
5	67	-106.871508	34.0018011	327158	3763740	25.003	1667.405	49850.5
5	68	-106.871437	34.0015977	327165	3763717	23.517	1690.923	49855.1
5	69	-106.871405	34.0014019	327167	3763695	21.919	1712.841	49861.6
5	70	-106.871364	34.0012044	327171	3763673	22.227	1735.068	49834.8
5	71	-106.871332	34.0009982	327173	3763650	23.057	1758.125	49941.9
5	72	-106.871292	34.0007992	327176	3763628	22.376	1780.502	49873.2
5	73	-106.871271	34.0005929	327178	3763605	22.957	1803.459	49878.2
5	74	-106.8712	34.0003948	327184	3763583	22.961	1826.420	49886.3
5	75	-106.871154	34.0001972	327188	3763561	22.304	1848.724	49892
5	76	-106.871124	34.0000188	327190	3763541	20.001	1868.725	49856.5
5	77	-106.871103	33.9997919	327192	3763516	25.234	1893.959	49887.9
5	78	-106.871043	33.9995715	327197	3763492	25.054	1919.013	49884.5
5	79	-106.87098	33.9993751	327202	3763470	22.553	1941.567	49886.6
5	80	-106.870924	33.999182	327207	3763448	22.037	1963.604	49881.8
5	81	-106.870866	33.9989645	327212	3763424	24.719	1988.322	49882
5	82	-106.87082	33.9987753	327216	3763403	21.406	2009.729	49899.3
5	83	-106.870731	33.9985701	327224	3763380	24.185	2033.914	49889.4
5	84	-106.870649	33.9983703	327231	3763358	23.427	2057.341	49883.9
5	85	-106.870577	33.9981827	327237	3763337	21.854	2079.195	49902.4
5	86	-106.870478	33.9980021	327246	3763317	22.006	2101.201	49883.4
5	87	-106.870408	33.9978007	327252	3763294	23.254	2124.454	49878.8
5	88	-106.870304	33.9975992	327261	3763272	24.355	2148.809	49902.6
5	89	-106.870224	33.9974266	327268	3763252	20.495	2169.305	49886.5
5	90	-106.870096	33.9972159	327280	3763229	26.187	2195.491	49877
5	91	-106.86997	33.9970463	327291	3763210	22.144	2217.635	49890.3
5	92	-106.86983	33.9968486	327303	3763188	25.437	2243.073	49891.1
5	93	-106.869685	33.9966644	327316	3763167	24.445	2267.518	49890.2
5	94	-106.869545	33.9965087	327329	3763149	21.572	2289.090	49900.6
5	95	-106.869405	33.9963308	327342	3763129	23.594	2312.684	49899.7
5	96	-106.869258	33.9961738	327355	3763112	22.078	2334.762	49925.7
5	97	-106.869096	33.9959996	327370	3763092	24.436	2359.198	49901.1
5	98	-106.868938	33.9958258	327384	3763073	24.157	2383.355	49895.5
5	99	-106.868763	33.9956514	327400	3763053	25.225	2408.580	49903
5	100	-106.868609	33.9955153	327414	3763038	20.761	2429.341	49904.2
5	101	-106.868451	33.9953633	327428	3763021	22.269	2451.611	49904.2
5	102	-106.868264	33.9952054	327445	3763003	24.636	2476.246	49903.3
5	103	-106.868123	33.9950572	327457	3762986	20.987	2497.233	49896.5
5	104	-106.867949	33.9949087	327473	3762969	22.999	2520.232	49884.7

Transect	Point	Longitude	Latitude	UTM Easting (m)	UTM Northing (m)	distance (m)	Accumulated distance (m)	Magnetic Field Strength (nT)
5	105	-106.867758	33.9947466	327491	3762951	25.189	2545.422	49902.5
5	106	-106.86758	33.9946017	327507	3762935	22.982	2568.404	49914.7
5	107	-106.867387	33.9944323	327524	3762915	25.912	2594.316	50074.2
5	108	-106.86722	33.9942902	327539	3762899	22.036	2616.352	49918.3
5	109	-106.867071	33.9941548	327553	3762884	20.429	2636.781	49935
5	110	-106.866893	33.9939773	327569	3762864	25.603	2662.384	49924
5	111	-106.866754	33.9938478	327582	3762850	19.318	2681.702	49924.3
5	112	-106.866594	33.993725	327596	3762836	20.094	2701.796	49930
5	113	-106.866443	33.9935666	327610	3762818	22.417	2724.213	49925.2
5	114	-106.866316	33.9934587	327621	3762806	16.737	2740.950	49925
5	115	-106.866109	33.9933092	327640	3762789	25.352	2766.302	49934.7
5	116	-106.865926	33.9931604	327657	3762772	23.625	2789.927	49936.3
5	117	-106.865776	33.9930034	327670	3762754	22.265	2812.192	49865.8
5	118	-106.865616	33.9928511	327685	3762737	22.395	2834.587	49934.9
5	119	-106.865432	33.9926838	327701	3762718	25.225	2859.812	49944.7
5	120	-106.865279	33.9925316	327715	3762701	22.015	2881.827	49891.5
5	121	-106.865083	33.9923796	327733	3762684	24.709	2906.536	49929.3
5	122	-106.864911	33.9922002	327748	3762664	25.472	2932.008	49953
5	123	-106.864725	33.9920533	327765	3762647	23.661	2955.669	49964.4
5	124	-106.864537	33.9918781	327782	3762627	26.065	2981.734	49957.3
5	125	-106.864351	33.9917308	327799	3762611	23.724	3005.458	49950.4
5	126	-106.864174	33.9915732	327815	3762593	23.919	3029.377	49992.9
5	127	-106.863987	33.9914168	327832	3762575	24.541	3053.918	49960.9
5	128	-106.863804	33.9912515	327849	3762557	24.934	3078.851	49947.1
5	129	-106.863615	33.9910751	327866	3762537	26.223	3105.074	49946.1
5	130	-106.863456	33.9909198	327880	3762519	22.611	3127.685	49895.5
5	131	-106.863277	33.9907537	327896	3762501	24.782	3152.466	49928
5	132	-106.863108	33.9905905	327912	3762482	23.864	3176.330	49949.4
5	133	-106.862918	33.9904082	327929	3762462	26.817	3203.148	49961.2
5	134	-106.86275	33.9902481	327944	3762444	23.556	3226.704	49967.8
5	135	-106.862603	33.9900783	327957	3762425	23.216	3249.920	49933.2
5	136	-106.862444	33.9898984	327972	3762404	24.797	3274.716	49969.2
5	137	-106.862296	33.9897164	327985	3762384	24.400	3299.116	49921.9
5	138	-106.862175	33.9895317	327996	3762363	23.316	3322.432	50017.4
5	139	-106.862072	33.9893168	328005	3762339	25.665	3348.097	49953
5	140	-106.862284	33.9891575	327985	3762322	26.382	3374.479	49970.5
5	141	-106.862179	33.9889371	327994	3762297	26.279	3400.758	49966.2
5	142	-106.862112	33.9887313	328000	3762274	23.647	3424.405	49975.2
5	143	-106.862038	33.9885237	328006	3762251	24.040	3448.445	49960.6
5	144	-106.861983	33.9882823	328011	3762224	27.249	3475.695	49973.3
5	145	-106.861946	33.9880652	328014	3762200	24.321	3500.015	49971.1
5	146	-106.861917	33.9878384	328016	3762175	25.289	3525.304	49975.9
5	147	-106.861899	33.9875996	328017	3762149	26.545	3551.849	49970.3
5	148	-106.861887	33.987385	328018	3762125	23.830	3575.679	49973.6
5	149	-106.861884	33.9871354	328018	3762097	27.691	3603.370	49970.9
5	150	-106.861862	33.98688	328019	3762069	28.398	3631.768	49981

Transect	Point	Longitude	Latitude	UTM Easting (m)	UTM Northing (m)	distance (m)	Accumulated distance (m)	Magnetic Field Strength (nT)
5	151	-106.861825	33.9866598	328022	3762044	24.666	3656.434	49987.2
5	152	-106.861865	33.9864206	328018	3762018	26.794	3683.228	49989.7
5	153	-106.861847	33.9861041	328019	3761983	35.136	3718.364	49988.3
5	154	-106.861844	33.9858277	328019	3761952	30.662	3749.026	49980.3
5	155	-106.861846	33.9856216	328018	3761929	22.857	3771.883	49989
5	156	-106.861825	33.9853983	328020	3761904	24.842	3796.725	49986.8
5	157	-106.861836	33.985178	328018	3761880	24.454	3821.178	49990.8
5	158	-106.861821	33.9849182	328019	3761851	28.854	3850.032	49984.6
5	159	-106.861856	33.9846327	328015	3761819	31.825	3881.857	49989.8
5	160	-106.861836	33.984419	328017	3761796	23.778	3905.636	49985
5	161	-106.86187	33.9842218	328013	3761774	22.078	3927.713	49964.6
5	162	-106.861858	33.9839531	328014	3761744	29.825	3957.538	49953.8
5	163	-106.861825	33.9837546	328016	3761722	22.229	3979.767	49976.4
5	164	-106.861809	33.9835101	328017	3761695	27.159	4006.926	49978
5	165	-106.861788	33.9832836	328019	3761670	25.195	4032.121	49982.1
5	166	-106.86176	33.9830571	328021	3761645	25.254	4057.375	49998.3
5	167	-106.861818	33.9828189	328015	3761618	26.953	4084.327	49991.6
5	168	-106.861802	33.9826229	328016	3761596	21.800	4106.127	49992.6
5	169	-106.861805	33.9823514	328015	3761566	30.113	4136.240	49995.7
5	170	-106.861758	33.9821062	328019	3761539	27.539	4163.779	49996.3
5	171	-106.861757	33.9818812	328019	3761514	24.952	4188.730	50003.1
5	172	-106.861823	33.9816853	328013	3761493	22.579	4211.309	50004.1
5	173	-106.861843	33.9814606	328010	3761468	25.002	4236.311	49995.5
5	174	-106.861841	33.9812009	328010	3761439	28.802	4265.112	50003.7
5	175	-106.861759	33.9810122	328017	3761418	22.247	4287.359	49971.8
5	176	-106.861742	33.980774	328018	3761391	26.472	4313.832	49986.9
5	177	-106.861735	33.9805815	328018	3761370	21.362	4335.194	49995.7
5	178	-106.861735	33.9803183	328018	3761341	29.195	4364.389	49990
5	179	-106.86173	33.980112	328018	3761318	22.880	4387.269	50000.7
5	180	-106.86174	33.9798615	328017	3761290	27.807	4415.076	50003.2
5	181	-106.861745	33.9796491	328016	3761267	23.557	4438.633	49997.9
5	182	-106.86171	33.9794099	328018	3761240	26.716	4465.349	50001.8
5	183	-106.861742	33.9791593	328015	3761212	27.956	4493.305	50006.6
5	184	-106.861725	33.9789154	328016	3761185	27.104	4520.409	50001
5	185	-106.861735	33.9786824	328015	3761159	25.860	4546.269	50014.7
5	186	-106.861711	33.9784556	328016	3761134	25.264	4571.533	50020.3
5	187	-106.861685	33.9782165	328018	3761108	26.615	4598.148	50023.4
5	188	-106.861709	33.9779961	328016	3761083	24.549	4622.697	50011.9
5	189	-106.861688	33.9777669	328017	3761058	25.490	4648.187	50027.6
5	190	-106.861644	33.9775474	328021	3761033	24.689	4672.875	50020.9
5	191	-106.861659	33.9773037	328019	3761006	27.065	4699.940	50019.9
5	192	-106.861659	33.9770708	328018	3760981	25.836	4725.776	50022.6
5	193	-106.861641	33.9768688	328020	3760958	22.470	4748.246	50023.4
5	194	-106.861648	33.97664	328018	3760933	25.397	4773.643	50028.8
5	195	-106.861638	33.9764017	328019	3760906	26.443	4800.087	50028.8
5	196	-106.861617	33.9761629	328020	3760880	26.564	4826.651	50026.5

Transect	Point	Longitude	Latitude	UTM Easting (m)	UTM Northing (m)	distance (m)	Accumulated distance (m)	Magnetic Field Strength (nT)
5	197	-106.861605	33.9759298	328021	3760854	25.866	4852.517	50028.8
5	198	-106.861593	33.9757235	328022	3760831	22.913	4875.430	50029.6
5	199	-106.861587	33.9754827	328022	3760804	26.720	4902.150	50036.9
5	200	-106.861562	33.9752505	328024	3760778	25.853	4928.003	50046.6
5	201	-106.861598	33.975008	328020	3760752	27.098	4955.100	50044.3
5	202	-106.861591	33.974784	328020	3760727	24.861	4979.961	50045.2
5	203	-106.861576	33.9745536	328021	3760701	25.587	5005.548	50048.4
5	204	-106.861567	33.9743331	328021	3760677	24.473	5030.021	50061.2
5	205	-106.86156	33.9741504	328022	3760656	20.272	5050.293	50060.4
5	206	-106.861616	33.9738579	328016	3760624	32.845	5083.138	50061.5
5	207	-106.861575	33.9736631	328019	3760602	21.934	5105.072	50166.6
5	208	-106.861545	33.973457	328022	3760580	23.031	5128.103	50062.8
5	209	-106.861557	33.9732273	328020	3760554	25.512	5153.615	50016.4
5	210	-106.861571	33.9730013	328018	3760529	25.088	5178.703	50066.1
5	211	-106.861565	33.9727136	328018	3760497	31.910	5210.613	50077.5
5	212	-106.861552	33.9725014	328019	3760474	23.572	5234.185	50073.1
5	213	-106.861526	33.9722961	328021	3760451	22.898	5257.082	50071.6
5	214	-106.861538	33.9720505	328019	3760424	27.268	5284.350	50075
5	215	-106.861497	33.9718344	328023	3760400	24.261	5308.611	50083.9
5	216	-106.861509	33.9715817	328021	3760372	28.056	5336.667	50082.2
5	217	-106.861485	33.9713559	328023	3760346	25.132	5361.799	50091.8
5	218	-106.861456	33.9711483	328025	3760323	23.191	5384.991	50091.8
5	219	-106.86143	33.9709075	328027	3760297	26.809	5411.800	50093.1
5	220	-106.861379	33.970692	328031	3760273	24.362	5436.161	50093.6
5	221	-106.861333	33.9704695	328035	3760248	25.027	5461.188	50106.3
5	222	-106.861275	33.9702394	328040	3760222	26.084	5487.273	50107
5	223	-106.861212	33.9700098	328045	3760197	26.140	5513.413	50105.5
5	224	-106.861145	33.9697736	328051	3760170	26.908	5540.321	50104.2
5	225	-106.861089	33.9695808	328056	3760149	22.004	5562.325	50114.6
5	226	-106.86099	33.9693708	328065	3760125	25.039	5587.364	50116.7
5	227	-106.860914	33.969176	328071	3760104	22.701	5610.065	50118.4
5	228	-106.8608	33.9689514	328081	3760079	27.047	5637.112	50123
5	229	-106.860676	33.9687248	328092	3760053	27.629	5664.740	50126.1
5	230	-106.860586	33.9685169	328100	3760030	24.518	5689.258	50127.1
5	231	-106.860485	33.9683147	328109	3760008	24.280	5713.538	50130.9
5	232	-106.860383	33.9681136	328118	3759985	24.239	5737.777	50128
5	233	-106.860269	33.9678893	328128	3759960	27.013	5764.790	50130.7
5	234	-106.860153	33.9676937	328139	3759938	24.204	5788.995	50134.6
5	235	-106.860055	33.9674562	328147	3759912	27.833	5816.828	50133.8
5	236	-106.859955	33.9672661	328156	3759890	23.036	5839.864	50147.3
5	237	-106.859843	33.9670719	328166	3759869	23.895	5863.758	50146.6
5	238	-106.859744	33.9668586	328175	3759845	25.373	5889.131	50135.6
5	239	-106.859624	33.9666613	328185	3759823	24.545	5913.676	50214.2
5	240	-106.859501	33.9664565	328196	3759800	25.376	5939.052	50190.3
5	241	-106.859413	33.9662506	328204	3759777	24.255	5963.306	50149.5
5	242	-106.859286	33.9660473	328215	3759754	25.415	5988.722	50148

Transect	Point	Longitude	Latitude	UTM Easting (m)	UTM Northing (m)	distance (m)	Accumulated distance (m)	Magnetic Field Strength (nT)
5	243	-106.859179	33.9658939	328225	3759737	19.688	6008.410	50152.2
5	244	-106.85909	33.9656955	328233	3759715	23.474	6031.883	50147.4
5	245	-106.858995	33.965455	328241	3759688	28.097	6059.980	50152.2
5	246	-106.858874	33.9652132	328252	3759661	29.058	6089.038	50158.6
5	247	-106.858757	33.9650218	328262	3759639	23.820	6112.858	50161
5	248	-106.858637	33.9648259	328273	3759618	24.397	6137.255	50156.7
5	249	-106.858513	33.9646344	328284	3759596	24.143	6161.397	50161.7
5	250	-106.858396	33.9644124	328294	3759571	26.867	6188.264	50165.6
5	251	-106.858258	33.9642009	328307	3759548	26.711	6214.976	50171.1
5	252	-106.858103	33.9639862	328321	3759524	27.792	6242.767	50178.4
5	253	-106.857979	33.9638027	328332	3759503	23.341	6266.109	50173.4
5	254	-106.857845	33.9636165	328344	3759482	24.108	6290.216	50162.6
5	255	-106.857736	33.9634385	328353	3759462	22.156	6312.372	50172.7
5	256	-106.85758	33.9632228	328367	3759438	27.941	6340.313	50175.2
5	257	-106.857415	33.9630334	328382	3759417	25.943	6366.256	50160.1
5	258	-106.857279	33.9628242	328394	3759393	26.425	6392.682	50296.8
5	259	-106.857139	33.9626059	328407	3759369	27.437	6420.119	50184.4
5	260	-106.857001	33.9623925	328419	3759345	26.866	6446.985	50182.1
5	261	-106.856864	33.9622144	328431	3759325	23.473	6470.458	50178.4
5	262	-106.856715	33.9619987	328445	3759301	27.612	6498.069	50188.6
5	263	-106.856568	33.9618047	328458	3759279	25.437	6523.506	50186.3
5	264	-106.856435	33.9616084	328470	3759257	24.994	6548.500	50181.4
5	265	-106.856289	33.9614084	328483	3759235	26.009	6574.509	50177
5	266	-106.856172	33.961212	328493	3759213	24.316	6598.825	50178.5
5	267	-106.856035	33.9610261	328506	3759192	24.182	6623.008	50172.2
5	268	-106.855896	33.9608255	328518	3759169	25.703	6648.711	50176.6
5	269	-106.855766	33.9606352	328530	3759148	24.271	6672.982	50174.5
5	270	-106.85563	33.9604424	328542	3759126	24.796	6697.778	50170.1
5	271	-106.85548	33.9602321	328555	3759103	27.171	6724.950	50150.3
5	272	-106.855343	33.9600406	328568	3759081	24.720	6749.670	50157.7
5	273	-106.855207	33.9598228	328580	3759057	27.231	6776.901	50132
5	274	-106.855103	33.9597006	328589	3759043	16.589	6793.489	50325.2
5	275	-106.854951	33.9594857	328603	3759019	27.665	6821.154	50173.5
5	276	-106.854829	33.9593107	328614	3759000	22.465	6843.619	50157.6
5	277	-106.854692	33.9591258	328626	3758979	24.064	6867.683	50155.6
5	278	-106.854536	33.958935	328640	3758957	25.636	6893.319	50155.1
5	279	-106.85436	33.9586557	328656	3758926	34.972	6928.291	50150.1
5	280	-106.854221	33.9584553	328668	3758904	25.704	6953.995	50147.2
5	281	-106.854074	33.958261	328681	3758882	25.466	6979.461	50150.5
5	282	-106.853941	33.9580573	328693	3758859	25.723	7005.184	50144.3
5	283	-106.853811	33.9578724	328705	3758838	23.779	7028.964	50126.4
5	284	-106.853677	33.9576755	328717	3758816	25.070	7054.034	50075.9
5	285	-106.853532	33.9574676	328730	3758793	26.696	7080.730	49587.7
5	286	-106.8534	33.957293	328742	3758773	22.881	7103.611	49841.3
5	287	-106.853184	33.957009	328761	3758742	37.281	7140.892	50058.3
5	288	-106.853051	33.9568127	328773	3758720	25.008	7165.900	50118.6

Transect	Point	Longitude	Latitude	UTM Easting (m)	UTM Northing (m)	distance (m)	Accumulated distance (m)	Magnetic Field Strength (nT)
5	289	-106.852896	33.9565867	328787	3758694	28.889	7194.790	50133.2
5	290	-106.852767	33.9563925	328798	3758672	24.626	7219.416	50136.7
5	291	-106.852632	33.9561909	328810	3758650	25.580	7244.996	50131.7
5	292	-106.852268	33.955648	328843	3758589	69.016	7314.012	50125.9
5	293	-106.852012	33.9552858	328866	3758549	46.609	7360.621	50131.5
5	294	-106.851885	33.9551226	328877	3758530	21.553	7382.174	50133.3
5	295	-106.851742	33.9549009	328890	3758505	27.908	7410.082	50117.9
5	296	-106.851615	33.9546965	328901	3758482	25.536	7435.618	50105.3
5	297	-106.851428	33.9544717	328918	3758457	30.370	7465.988	50069.6
5	298	-106.851294	33.9542696	328930	3758435	25.591	7491.579	49894.8
5	299	-106.851168	33.9540742	328942	3758413	24.621	7516.200	50110.8
5	300	-106.851078	33.9539053	328950	3758394	20.470	7536.670	50118.5
5	301	-106.850917	33.9537072	328964	3758372	26.530	7563.201	50120.2
5	302	-106.850804	33.9535363	328974	3758352	21.664	7584.865	50122.4
5	303	-106.850691	33.9533192	328984	3758328	26.248	7611.113	50123.9
5	304	-106.850625	33.953141	328990	3758308	20.685	7631.798	50120.9
5	305	-106.850536	33.9529146	328998	3758283	26.434	7658.232	50113.3
5	306	-106.850441	33.9526879	329006	3758258	26.620	7684.852	50111.2
5	307	-106.850357	33.952454	329013	3758232	27.093	7711.945	50113.6
5	308	-106.850352	33.9522629	329013	3758211	21.200	7733.146	50107.8
5	309	-106.850293	33.9520014	329018	3758181	29.515	7762.660	50113.2
5	310	-106.850298	33.9517922	329017	3758158	23.199	7785.859	50102.3
5	311	-106.850282	33.9515497	329018	3758131	26.940	7812.799	50100
5	312	-106.850333	33.9513243	329013	3758106	25.459	7838.257	50103.5
5	313	-106.850382	33.9510891	329008	3758080	26.476	7864.734	50095.7
5	314	-106.850412	33.9509084	329005	3758060	20.232	7884.966	50094.9
5	315	-106.850453	33.9507531	329001	3758043	17.629	7902.594	50096.6
5	316	-106.850472	33.9505499	328999	3758021	22.608	7925.203	50095.4
5	317	-106.850536	33.9503027	328992	3757993	28.034	7953.237	50089.1
5	318	-106.850597	33.9500528	328986	3757966	28.282	7981.519	50089.9
5	319	-106.850663	33.9497855	328980	3757936	30.274	8011.793	50089.3
5	320	-106.85072	33.9495289	328974	3757908	28.949	8040.742	50077.6
5	321	-106.850777	33.9493028	328968	3757883	25.627	8066.368	50077.5
5	322	-106.85084	33.9491187	328962	3757863	21.227	8087.595	50075.9
5	323	-106.850856	33.9488917	328960	3757837	25.222	8112.817	50074.8
5	324	-106.850897	33.9486685	328956	3757813	25.040	8137.857	50069.6
5	325	-106.850962	33.9485184	328950	3757796	17.713	8155.570	50070.5
5	326	-106.851017	33.9482523	328944	3757767	29.948	8185.518	50068.8
5	327	-106.851057	33.9480093	328940	3757740	27.208	8212.726	50065.1
5	328	-106.851107	33.9477672	328935	3757713	27.253	8239.979	50063.8
5	329	-106.851173	33.9475378	328928	3757688	26.148	8266.128	50055
5	330	-106.85123	33.9473162	328922	3757663	25.151	8291.279	50063.2
5	331	-106.851264	33.9471049	328919	3757640	23.643	8314.922	50066.4
5	332	-106.851298	33.9468721	328915	3757614	26.015	8340.937	50067
5	333	-106.851385	33.9466393	328907	3757589	27.047	8367.984	50061.8
5	334	-106.851396	33.9464204	328905	3757564	24.291	8392.275	50055.8

Transect	Point	Longitude	Latitude	UTM Easting (m)	UTM Northing (m)	distance (m)	Accumulated distance (m)	Magnetic Field Strength (nT)
5	335	-106.851442	33.9462081	328901	3757541	23.928	8416.203	50057.1
5	336	-106.851492	33.9459713	328895	3757515	26.668	8442.871	50048.8
5	337	-106.851555	33.9457462	328889	3757490	25.646	8468.517	50047.1
5	338	-106.851603	33.9455326	328884	3757466	24.099	8492.616	50052.7
5	339	-106.851646	33.9453032	328880	3757441	25.754	8518.370	50050.8
5	340	-106.851696	33.9450978	328875	3757418	23.264	8541.634	50149.6
5	341	-106.85178	33.944871	328867	3757393	26.311	8567.944	50055.9
5	342	-106.851853	33.9446677	328859	3757371	23.533	8591.477	50062.5
5	343	-106.851869	33.9444693	328858	3757349	22.059	8613.535	50057
5	344	-106.851909	33.9442463	328853	3757324	25.002	8638.537	50050.9
5	345	-106.851942	33.9440194	328850	3757299	25.357	8663.894	50059.2
5	346	-106.851983	33.9437889	328846	3757273	25.853	8689.748	50072.2
5	347	-106.852039	33.9435544	328840	3757248	26.506	8716.254	50050
5	348	-106.852067	33.9433322	328837	3757223	24.778	8741.032	50053
5	349	-106.852084	33.9431024	328835	3757198	25.544	8766.576	50048.3
5	350	-106.852107	33.9428763	328832	3757173	25.159	8791.735	50050.3
5	351	-106.852111	33.9426577	328832	3757148	24.254	8815.989	50043
5	352	-106.852112	33.9424339	328831	3757123	24.815	8840.805	50051.1
5	353	-106.852106	33.942206	328831	3757098	25.290	8866.095	50051.3
5	354	-106.852113	33.9419753	328830	3757073	25.597	8891.692	50044.7
5	355	-106.852097	33.9417166	328831	3757044	28.736	8920.428	50043.2
5	356	-106.852097	33.9414866	328831	3757018	25.503	8945.931	50042.6
5	357	-106.852127	33.9412401	328827	3756991	27.484	8973.415	50043
5	358	-106.852129	33.9410046	328827	3756965	26.120	8999.535	50034.3
5	359	-106.852121	33.9407728	328827	3756939	25.721	9025.256	50034.8
5	360	-106.852133	33.9405448	328825	3756914	25.308	9050.564	50037.2
5	361	-106.852125	33.9403073	328826	3756888	26.352	9076.916	50034.5
5	362	-106.852125	33.9400913	328825	3756864	23.964	9100.880	50037.4
5	363	-106.85212	33.939853	328825	3756837	26.440	9127.320	50035.6
5	364	-106.852131	33.9396443	328824	3756814	23.164	9150.484	50075.7
5	365	-106.852121	33.9394183	328824	3756789	25.085	9175.569	50033.7
5	366	-106.852114	33.9391848	328824	3756763	25.901	9201.469	50032.9
5	367	-106.852138	33.9389356	328822	3756736	27.736	9229.205	50033.3
5	368	-106.852127	33.93871	328822	3756711	25.036	9254.241	50028.2
5	369	-106.852137	33.9384913	328821	3756686	24.277	9278.518	50031.9
5	370	-106.852131	33.9382607	328821	3756661	25.580	9304.098	50036
5	371	-106.852138	33.9380432	328820	3756637	24.134	9328.232	50027
5	372	-106.852103	33.9377955	328823	3756609	27.677	9355.909	50024.8
5	373	-106.852143	33.9375777	328818	3756585	24.435	9380.344	50089
5	374	-106.852138	33.9373397	328818	3756559	26.390	9406.734	50020.3
5	375	-106.852138	33.9371138	328818	3756534	25.055	9431.788	50030.5
5	376	-106.852137	33.9368926	328818	3756509	24.552	9456.340	50028.2
5	377	-106.852129	33.9366057	328818	3756477	31.821	9488.161	50005.3
5	378	-106.852141	33.9363792	328816	3756452	25.152	9513.312	50009.2
5	379	-106.852145	33.9361441	328815	3756426	26.084	9539.396	50019.4
5	380	-106.852141	33.9359373	328815	3756403	22.940	9562.336	50020.9

Transect	Point	Longitude	Latitude	UTM Easting (m)	UTM Northing (m)	distance (m)	Accumulated distance (m)	Magnetic Field Strength (nT)
5	381	-106.852158	33.9357128	328813	3756378	24.946	9587.282	50022.7
5	382	-106.852155	33.9354769	328813	3756352	26.160	9613.443	50020.6
5	383	-106.852154	33.9352552	328813	3756327	24.603	9638.045	50024.3
5	384	-106.852157	33.9350072	328812	3756300	27.502	9665.547	50023.2
5	385	-106.852167	33.9347815	328811	3756275	25.045	9690.592	50017.4
5	386	-106.85215	33.9345561	328812	3756250	25.055	9715.647	50019.9
5	387	-106.85216	33.9343353	328810	3756225	24.499	9740.146	50018.7
5	388	-106.852176	33.9341015	328808	3756200	25.985	9766.131	50013.2
5	389	-106.852156	33.9338773	328810	3756175	24.942	9791.073	50015
5	390	-106.852162	33.933721	328809	3756157	17.334	9808.406	50024.1
5	391	-106.852172	33.9334836	328808	3756131	26.349	9834.755	50021.4
5	392	-106.85217	33.9332621	328807	3756106	24.571	9859.326	50014.5
5	393	-106.852173	33.9330353	328807	3756081	25.159	9884.486	50012.2
5	394	-106.852194	33.932788	328804	3756054	27.492	9911.978	50074.6
5	395	-106.852189	33.932584	328804	3756031	22.640	9934.618	50012.1
5	396	-106.852185	33.9323542	328804	3756006	25.490	9960.108	50012.2
5	397	-106.852186	33.9321138	328804	3755979	26.665	9986.773	50013
5	398	-106.852174	33.9318975	328804	3755955	24.010	10010.783	50007.9
5	399	-106.852173	33.9316871	328804	3755932	23.342	10034.126	50006.5
5	400	-106.85219	33.9314617	328802	3755907	25.056	10059.181	49973.2
5	401	-106.852192	33.9312403	328801	3755882	24.546	10083.728	50000.1
5	402	-106.8522	33.9309921	328800	3755855	27.541	10111.268	50003.7
5	403	-106.852188	33.9307826	328801	3755831	23.270	10134.538	50005
5	404	-106.852195	33.9305366	328800	3755804	27.281	10161.820	50002.3
5	405	-106.85219	33.9303379	328800	3755782	22.050	10183.870	49995
5	406	-106.852167	33.9301129	328801	3755757	25.042	10208.912	49970.6
5	407	-106.85214	33.9298906	328803	3755732	24.790	10233.702	49995.1
5	408	-106.852198	33.9296466	328797	3755706	27.600	10261.302	49996.6
5	409	-106.852184	33.9294379	328798	3755682	23.177	10284.479	49995.2
5	410	-106.852184	33.9292323	328798	3755660	22.814	10307.293	49995.8
5	411	-106.852184	33.9290121	328798	3755635	24.413	10331.706	49997.7
5	412	-106.852214	33.9288383	328794	3755616	19.485	10351.190	49990.2
5	413	-106.852223	33.9285814	328793	3755587	28.503	10379.694	49993.3
5	414	-106.852216	33.928341	328793	3755561	26.670	10406.364	49996.9
5	415	-106.852215	33.9281361	328793	3755538	22.732	10429.096	50006.3
5	416	-106.852195	33.927931	328794	3755515	22.813	10451.909	49997.3
5	417	-106.852169	33.9277579	328796	3755496	19.364	10471.273	50014.4
5	418	-106.852197	33.9275329	328793	3755471	25.087	10496.361	49994.2
5	419	-106.852189	33.927376	328794	3755454	17.417	10513.777	49986.2
5	420	-106.852162	33.9271767	328796	3755432	22.246	10536.023	49991.1
5	421	-106.852189	33.9269666	328793	3755408	23.430	10559.453	49990.7
5	422	-106.85219	33.9267535	328792	3755385	23.646	10583.099	49988.9
5	423	-106.852173	33.9265632	328794	3755364	21.155	10604.255	49993
5	424	-106.852193	33.9263521	328791	3755340	23.492	10627.747	49989.8
5	425	-106.852206	33.9261408	328790	3755317	23.463	10651.210	49988.1
5	426	-106.852215	33.9259092	328788	3755291	25.704	10676.914	50088.5

Transect	Point	Longitude	Latitude	UTM Easting (m)	UTM Northing (m)	distance (m)	Accumulated distance (m)	Magnetic Field Strength (nT)
5	427	-106.852261	33.9257005	328784	3755268	23.536	10700.450	49991.5
5	428	-106.852281	33.9254999	328782	3755246	22.328	10722.777	49994.1
5	429	-106.852331	33.9252964	328776	3755223	23.052	10745.830	50009.6
5	430	-106.852427	33.9250793	328767	3755199	25.662	10771.492	49980.7
5	431	-106.852478	33.92489	328762	3755179	21.523	10793.015	49977.9
5	247	-106.85255	33.9248704	328755	3755176	7.016	10800.031	49971.9
5	246	-106.852631	33.9246689	328747	3755154	23.566	10823.598	49940.7
5	245	-106.852748	33.9244609	328736	3755131	25.474	10849.072	49960
5	244	-106.852867	33.9242718	328725	3755111	23.687	10872.759	49962.2
5	243	-106.852983	33.9240869	328714	3755090	23.155	10895.914	49971.1
5	242	-106.853112	33.9238803	328701	3755068	25.805	10921.718	49967.6
5	241	-106.853242	33.9237095	328689	3755049	22.438	10944.156	49959.9
5	240	-106.853374	33.9235761	328677	3755034	19.217	10963.373	49964.8
5	239	-106.853479	33.9232829	328666	3755002	33.929	10997.302	49965
5	238	-106.853625	33.9230377	328652	3754975	30.374	11027.676	49965.4
5	237	-106.853754	33.9228606	328640	3754956	22.964	11050.640	49969.3
5	236	-106.853862	33.9226892	328630	3754937	21.482	11072.122	49961.8
5	235	-106.853994	33.9224814	328617	3754914	26.072	11098.195	49960.6
5	234	-106.854115	33.9223084	328606	3754895	22.208	11120.402	49959
5	233	-106.854214	33.9221133	328596	3754873	23.507	11143.910	49954.3
5	232	-106.85433	33.9219112	328585	3754851	24.847	11168.757	49946.3
5	231	-106.85445	33.9217367	328573	3754832	22.331	11191.088	49953
5	230	-106.854583	33.9215358	328561	3754810	25.420	11216.508	49944
5	229	-106.854709	33.9213442	328549	3754789	24.238	11240.745	49944.3
5	228	-106.854821	33.9211506	328538	3754768	23.864	11264.609	49955.5
5	227	-106.854935	33.9209521	328527	3754746	24.391	11289.000	49936.3
5	226	-106.855031	33.9207592	328518	3754725	23.162	11312.161	49945.2
5	225	-106.855108	33.920567	328510	3754704	22.479	11334.640	49943.4
5	224	-106.855179	33.9203047	328503	3754675	29.842	11364.482	49936.4
5	223	-106.85526	33.9201179	328495	3754654	22.030	11386.512	49932.5
5	222	-106.855316	33.9199091	328490	3754631	23.723	11410.235	49935.3
5	221	-106.855367	33.9196961	328485	3754607	24.081	11434.316	49867.3
5	220	-106.855258	33.9194197	328494	3754577	32.275	11466.591	49928
5	219	-106.855381	33.9192142	328482	3754554	25.519	11492.110	49930.5
5	218	-106.855348	33.9190374	328485	3754534	19.846	11511.956	49860.6
5	217	-106.855552	33.9182606	328465	3754448	88.183	11600.138	49958.1
5	216	-106.855624	33.9180414	328457	3754424	25.230	11625.368	49971.6
5	215	-106.855683	33.9178277	328452	3754401	24.305	11649.673	49948
5	214	-106.855716	33.9176265	328448	3754378	22.533	11672.206	49932.9
5	213	-106.855751	33.9174222	328445	3754356	22.887	11695.093	49930.7
5	212	-106.85577	33.9172205	328442	3754334	22.433	11717.526	49925.4
5	211	-106.855805	33.917001	328439	3754309	24.565	11742.091	49891.4
5	210	-106.855848	33.9167782	328434	3754285	25.037	11767.128	49924.9
5	209	-106.855868	33.9165592	328432	3754260	24.355	11791.483	49921.1
5	208	-106.855888	33.9163468	328430	3754237	23.629	11815.112	49925
5	207	-106.855896	33.9161205	328429	3754212	25.106	11840.219	49914.1

Transect	Point	Longitude	Latitude	UTM Easting (m)	UTM Northing (m)	distance (m)	Accumulated distance (m)	Magnetic Field Strength (nT)
5	206	-106.855881	33.9159078	328429	3754188	23.640	11863.858	49945.3
5	205	-106.855875	33.9156859	328430	3754164	24.610	11888.468	49913.8
5	204	-106.855875	33.9154566	328429	3754138	25.436	11913.904	49919.2
5	203	-106.85582	33.91523	328434	3754113	25.651	11939.555	49918.9
5	202	-106.855821	33.9149979	328433	3754087	25.757	11965.311	49908.8
5	201	-106.855754	33.9147805	328439	3754063	24.877	11990.188	49905.1
5	200	-106.855718	33.9145742	328442	3754040	23.126	12013.314	49907.6
5	199	-106.855671	33.9143703	328446	3754017	23.040	12036.354	49889.2
5	198	-106.855619	33.9141411	328450	3753992	25.865	12062.219	49904.9
5	197	-106.855567	33.9139304	328454	3753968	23.848	12086.067	49910.9
5	196	-106.855507	33.9136714	328460	3753939	29.274	12115.341	49957.1
5	195	-106.855449	33.913484	328465	3753919	21.473	12136.813	49961.3
5	194	-106.85539	33.9132748	328470	3753895	23.826	12160.640	49870.6
5	193	-106.855328	33.913052	328475	3753870	25.378	12186.018	49899.5
5	192	-106.855265	33.9128236	328480	3753845	25.981	12211.998	49893.7
5	191	-106.855091	33.912069	328495	3753761	85.226	12297.225	49915.9
5	190	-106.855027	33.9118574	328500	3753738	24.196	12321.421	49894.7
5	189	-106.855001	33.9116389	328502	3753713	24.363	12345.784	49871.2
5	188	-106.854943	33.9113996	328507	3753687	27.083	12372.867	49889.7
5	187	-106.854894	33.9112112	328511	3753666	21.363	12394.230	49891.8
5	186	-106.854841	33.9109988	328516	3753642	24.090	12418.320	49891.3
5	185	-106.854791	33.9107965	328520	3753619	22.888	12441.208	49859.5
5	184	-106.854742	33.9105912	328524	3753597	23.233	12464.440	49746.6
5	183	-106.8547	33.910373	328528	3753572	24.508	12488.949	49730.8
5	182	-106.854651	33.9101675	328532	3753549	23.227	12512.175	50127.4
5	181	-106.854595	33.9099479	328536	3753525	24.903	12537.079	49843
5	180	-106.854542	33.9097183	328541	3753499	25.944	12563.023	49885.6
5	179	-106.854496	33.9095045	328545	3753476	24.070	12587.093	49893
5	178	-106.854432	33.9092943	328550	3753452	24.073	12611.167	49849.7
5	177	-106.854388	33.9090817	328554	3753429	23.928	12635.095	49872.4
5	176	-106.854346	33.9088917	328557	3753408	21.418	12656.513	50057.9
5	175	-106.854294	33.9086735	328562	3753383	24.687	12681.200	49911.6
5	174	-106.854237	33.9084674	328567	3753360	23.459	12704.659	49879.3
5	173	-106.854183	33.9082544	328571	3753337	24.143	12728.802	49885.3
5	172	-106.854128	33.9080416	328576	3753313	24.150	12752.952	49884.4
5	171	-106.85407	33.9078216	328581	3753288	24.979	12777.931	49874.4
5	170	-106.854023	33.9076146	328585	3753265	23.363	12801.294	49834.6
5	169	-106.853978	33.907412	328588	3753243	22.860	12824.154	49885.7
5	168	-106.85392	33.9071896	328593	3753218	25.242	12849.396	49883.4
5	167	-106.853865	33.9069788	328598	3753195	23.930	12873.326	49887.3
5	166	-106.853806	33.9067524	328603	3753169	25.695	12899.021	49887.3
5	165	-106.853745	33.9065444	328608	3753146	23.754	12922.775	49883.8
5	164	-106.853686	33.9063215	328613	3753121	25.309	12948.084	49887.3
5	163	-106.85363	33.9060895	328618	3753096	26.244	12974.328	49883.4
5	162	-106.853565	33.9058695	328623	3753071	25.131	12999.458	49884.5
5	161	-106.853508	33.9056684	328628	3753049	22.916	13022.374	49884.6

Transect	Point	Longitude	Latitude	UTM Easting (m)	UTM Northing (m)	distance (m)	Accumulated distance (m)	Magnetic Field Strength (nT)
5	160	-106.853429	33.9054617	328635	3753026	24.073	13046.447	49880.2
5	159	-106.853346	33.90525	328642	3753002	24.702	13071.149	49886
5	158	-106.853167	33.9050676	328659	3752981	26.161	13097.310	49885.7
5	157	-106.853207	33.9048034	328654	3752952	29.550	13126.860	49868.5
5	156	-106.85311	33.9045953	328663	3752929	24.770	13151.630	49833.8
5	155	-106.853028	33.9043812	328670	3752905	24.922	13176.551	49885.4
5	154	-106.852949	33.9041857	328677	3752883	22.891	13199.442	49884.5
5	153	-106.852867	33.9039847	328684	3752861	23.548	13222.990	49881.1
5	152	-106.852787	33.9037617	328691	3752836	25.829	13248.820	49881
5	151	-106.852712	33.9035509	328698	3752813	24.374	13273.194	49789.1
5	150	-106.852634	33.9033537	328705	3752791	23.027	13296.221	49878.7
5	149	-106.852556	33.9031491	328711	3752768	23.809	13320.030	49890.6
5	148	-106.852366	33.9029524	328729	3752746	28.022	13348.052	49877.7
5	147	-106.852402	33.9027228	328725	3752720	25.674	13373.726	49884.7
5	146	-106.852333	33.9025146	328731	3752697	23.953	13397.679	49880.5
5	145	-106.852231	33.9022953	328740	3752672	26.078	13423.757	49842.5
5	144	-106.852161	33.9021113	328746	3752652	21.399	13445.155	49889.9
5	143	-106.852066	33.9019093	328754	3752629	24.084	13469.239	49882.1
5	142	-106.852011	33.90171	328759	3752607	22.670	13491.909	49888
5	141	-106.851933	33.9015109	328766	3752585	23.252	13515.161	49877.5
5	140	-106.851869	33.9012953	328771	3752561	24.636	13539.797	49874.1
5	139	-106.851796	33.9010833	328778	3752537	24.455	13564.253	49872.3
5	138	-106.851711	33.9008752	328785	3752514	24.377	13588.629	49872.6
5	137	-106.851628	33.9006693	328792	3752491	24.096	13612.725	49881.1
5	136	-106.851528	33.9004824	328801	3752470	22.720	13635.445	49864.7
5	135	-106.851472	33.9002684	328806	3752446	24.285	13659.730	49875.6
5	134	-106.851384	33.9000546	328813	3752423	25.056	13684.787	49912.7
5	133	-106.851285	33.8998385	328822	3752398	25.678	13710.465	49655.8
5	132	-106.851236	33.8996421	328826	3752377	22.241	13732.706	49845.9
5	131	-106.85114	33.8994477	328835	3752355	23.315	13756.020	49849.6
5	130	-106.851069	33.8992077	328841	3752328	27.420	13783.441	49836.8
5	129	-106.851013	33.8990064	328846	3752306	22.931	13806.372	49829.6
5	128	-106.850967	33.898812	328850	3752284	21.966	13828.338	49877.9
5	127	-106.850918	33.8985858	328854	3752259	25.500	13853.838	49818.8
5	126	-106.850887	33.8983951	328856	3752238	21.347	13875.185	49860
5	125	-106.850846	33.8981355	328859	3752209	29.046	13904.230	49726.7
5	124	-106.850811	33.8979581	328862	3752189	19.936	13924.167	49858.7
5	123	-106.850787	33.8977326	328864	3752164	25.111	13949.278	49862.2
5	122	-106.850766	33.8974948	328866	3752138	26.440	13975.718	49867.6
5	121	-106.850764	33.8972668	328865	3752112	25.302	14001.020	49860.5
5	120	-106.850739	33.8970892	328867	3752093	19.840	14020.860	49861.3
5	119	-106.850728	33.8968696	328868	3752068	24.367	14045.227	50025.4
5	118	-106.850736	33.8966527	328867	3752044	24.070	14069.298	49852.7
5	117	-106.850734	33.8964257	328866	3752019	25.181	14094.478	49868.8
5	116	-106.850722	33.896233	328867	3751998	21.392	14115.871	49874.3
5	115	-106.850732	33.8959975	328866	3751972	26.149	14142.020	49866.2

Transect	Point	Longitude	Latitude	UTM Easting (m)	UTM Northing (m)	distance (m)	Accumulated distance (m)	Magnetic Field Strength (nT)
5	114	-106.850738	33.8957738	328865	3751947	24.821	14166.840	49864.3
5	113	-106.850729	33.8955923	328865	3751927	20.136	14186.977	49848.5
5	112	-106.850722	33.8953658	328865	3751901	25.141	14212.117	49860.8
5	111	-106.850738	33.8951496	328863	3751878	24.031	14236.148	49864.2
5	110	-106.850728	33.8949514	328864	3751856	22.007	14258.156	49865.9
5	109	-106.850736	33.8947369	328863	3751832	23.798	14281.954	49865.7
5	108	-106.85074	33.8945263	328862	3751808	23.355	14305.309	49864
5	107	-106.850738	33.8943143	328862	3751785	23.511	14328.820	49864.8
5	106	-106.850748	33.8940723	328860	3751758	26.854	14355.674	49919.8
5	105	-106.850756	33.8938873	328859	3751738	20.540	14376.214	49865.7
5	104	-106.850747	33.8936759	328860	3751714	23.463	14399.676	49863.8
5	103	-106.850755	33.8934744	328859	3751692	22.359	14422.035	49862.7
5	102	-106.850747	33.8932589	328859	3751668	23.913	14445.948	49861.5
5	101	-106.85074	33.8930575	328859	3751646	22.351	14468.299	49859.9
5	100	-106.850743	33.8928323	328858	3751621	24.971	14493.270	49849.3
5	99	-106.850745	33.8926219	328858	3751597	23.339	14516.609	49860.3
5	98	-106.850734	33.8923867	328858	3751571	26.106	14542.715	49863.7
5	97	-106.850721	33.8921666	328859	3751547	24.444	14567.159	49859.8
5	96	-106.850737	33.8919821	328857	3751526	20.523	14587.681	49860.7
5	95	-106.850708	33.8917871	328860	3751505	21.783	14609.465	49860.7
5	94	-106.850718	33.8915245	328858	3751476	29.134	14638.599	49846.4
5	93	-106.850737	33.8913504	328856	3751456	19.395	14657.994	49884.5
5	92	-106.850717	33.8910984	328857	3751428	28.003	14685.997	49855.2
5	91	-106.850732	33.8909399	328856	3751411	17.645	14703.642	49856.5
5	90	-106.850731	33.890727	328855	3751387	23.603	14727.244	49852.9
5	89	-106.850746	33.8905022	328853	3751362	24.976	14752.221	49852.2
5	88	-106.850745	33.8902894	328853	3751339	23.602	14775.823	49855.2
5	87	-106.850756	33.8899961	328852	3751306	32.549	14808.372	49839
5	86	-106.850751	33.889836	328852	3751288	17.771	14826.142	49852
5	85	-106.850734	33.8892238	328852	3751220	67.911	14894.053	49851.5
5	84	-106.850744	33.8889589	328851	3751191	29.398	14923.451	49850.5
5	83	-106.850758	33.8888476	328849	3751179	12.418	14935.869	49848.3
5	82	-106.850733	33.8886438	328851	3751156	22.723	14958.592	49827.7
5	81	-106.850727	33.8884484	328851	3751134	21.681	14980.273	49853.3
5	80	-106.850751	33.8881993	328848	3751107	27.721	15007.994	49846.2
5	79	-106.850757	33.8879977	328847	3751084	22.367	15030.361	49849.8
5	78	-106.850742	33.8877494	328848	3751057	27.583	15057.944	49851
5	77	-106.850738	33.8875444	328848	3751034	22.740	15080.684	49844.3
5	76	-106.850754	33.8873165	328846	3751009	25.306	15105.991	49834
5	75	-106.850748	33.8871218	328847	3750987	21.611	15127.601	49836.3
5	74	-106.850737	33.8869145	328847	3750964	23.008	15150.609	49827.5
5	73	-106.850745	33.8866988	328846	3750940	23.949	15174.558	49803.8
5	72	-106.850752	33.8864987	328845	3750918	22.195	15196.753	49924.5
5	71	-106.850754	33.8862923	328844	3750895	22.897	15219.650	49839.5
5	70	-106.850744	33.8859961	328845	3750862	32.862	15252.512	49835.3
5	69	-106.850744	33.885728	328844	3750833	29.735	15282.248	49967.3

Transect	Point	Longitude	Latitude	UTM Easting (m)	UTM Northing (m)	distance (m)	Accumulated distance (m)	Magnetic Field Strength (nT)
5	68	-106.850755	33.8854425	328843	3750801	31.679	15313.927	49835.7
5	67	-106.850697	33.8852522	328848	3750780	21.794	15335.721	49835
5	66	-106.850718	33.8850976	328845	3750763	17.258	15352.979	49831.8
5	65	-106.850734	33.8850043	328844	3750752	10.454	15363.433	49829.2
5	64	-106.850736	33.884796	328843	3750729	23.106	15386.539	49822.1
5	63	-106.85073	33.8845838	328843	3750706	23.540	15410.080	49815.3
5	62	-106.850719	33.8843607	328844	3750681	24.778	15434.858	49824.4
5	61	-106.850696	33.8841446	328845	3750657	24.059	15458.917	49824.6
5	60	-106.850722	33.8839067	328842	3750631	26.494	15485.411	49823.5
5	59	-106.850725	33.8836883	328842	3750607	24.218	15509.629	49818.9
5	58	-106.850703	33.883456	328843	3750581	25.845	15535.474	49752.1
5	57	-106.85073	33.8832506	328840	3750558	22.921	15558.395	49827
5	56	-106.850741	33.8830709	328839	3750538	19.952	15578.347	49753.2
5	55	-106.850737	33.8828844	328839	3750517	20.700	15599.047	49821.1
5	54	-106.850744	33.8826761	328838	3750494	23.116	15622.164	49821.7
5	53	-106.85074	33.8824394	328838	3750468	26.240	15648.404	49817.8
5	52	-106.850744	33.8822905	328837	3750452	16.524	15664.928	49812.8
5	51	-106.850755	33.8820786	328836	3750428	23.524	15688.452	49803.1
5	50	-106.850754	33.881803	328835	3750398	30.573	15719.025	49789.8
5	49	-106.850756	33.8815791	328835	3750373	24.830	15743.855	49806.3
5	48	-106.850748	33.8813511	328835	3750347	25.302	15769.157	49809.8
5	47	-106.850761	33.8811395	328833	3750324	23.497	15792.655	49810.2
5	46	-106.850766	33.880889	328832	3750296	27.787	15820.441	49802.8
5	45	-106.850751	33.8806612	328833	3750271	25.309	15845.750	49807.9
5	44	-106.850697	33.8804232	328838	3750244	26.864	15872.615	49802.6
5	43	-106.850754	33.8802886	328832	3750230	15.831	15888.446	49958.8
5	42	-106.850743	33.8800905	328833	3750208	21.990	15910.436	49801.4
5	41	-106.850745	33.8798656	328832	3750183	24.948	15935.383	49812.1
5	40	-106.850742	33.8795736	328832	3750150	32.391	15967.775	49830.7
5	39	-106.850776	33.8793581	328828	3750126	24.116	15991.891	49807.1
5	38	-106.850774	33.8791326	328828	3750101	25.011	16016.902	49794.8
5	37	-106.850747	33.8788817	328830	3750074	27.942	16044.844	49835.6
5	36	-106.85076	33.8786516	328828	3750048	25.548	16070.391	49788.1
5	35	-106.850763	33.8785262	328828	3750034	13.908	16084.299	49799.7
5	34	-106.85078	33.8782855	328826	3750007	26.739	16111.038	49805.1
5	33	-106.850766	33.8780709	328827	3749984	23.845	16134.883	49800.7
5	32	-106.85077	33.8779162	328826	3749967	17.156	16152.039	49797
5	31	-106.850746	33.8776789	328828	3749940	26.417	16178.456	49784.1
5	30	-106.850751	33.8774316	328827	3749913	27.437	16205.893	49782.4
5	29	-106.85075	33.8772123	328826	3749888	24.322	16230.215	49807.1
5	28	-106.850755	33.8769891	328826	3749864	24.755	16254.971	49652.3
5	27	-106.850757	33.8767789	328825	3749840	23.317	16278.288	49816.4
5	26	-106.850766	33.8765492	328824	3749815	25.484	16303.772	49996.1
5	25	-106.850765	33.8763434	328823	3749792	22.823	16326.594	49697.4
5	24	-106.850768	33.8761177	328823	3749767	25.040	16351.634	49749.2
5	23	-106.850782	33.8758866	328821	3749741	25.672	16377.307	49792.2

Transect	Point	Longitude	Latitude	UTM Easting (m)	UTM Northing (m)	distance (m)	Accumulated distance (m)	Magnetic Field Strength (nT)
5	22	-106.850784	33.8756925	328820	3749720	21.526	16398.833	49836.1
5	21	-106.850785	33.875454	328820	3749693	26.447	16425.280	49781.5
5	20	-106.85079	33.8752433	328819	3749670	23.376	16448.656	49791.7
5	19	-106.850774	33.8749929	328820	3749642	27.818	16476.474	49799.2
5	18	-106.850776	33.8747879	328819	3749620	22.737	16499.211	49814.4
5	17	-106.850775	33.874577	328819	3749596	23.383	16522.594	49804.2
5	16	-106.850771	33.8743814	328819	3749575	21.700	16544.294	49800.3
5	15	-106.850779	33.8741164	328818	3749545	29.407	16573.702	49795.6
5	14	-106.850772	33.8738793	328818	3749519	26.300	16600.002	49790.9
5	13	-106.850769	33.8736679	328818	3749495	23.460	16623.462	49792.9
5	12	-106.850776	33.8734323	328817	3749469	26.127	16649.589	49769.7
5	11	-106.850793	33.8732152	328815	3749445	24.145	16673.734	49782.5
5	10	-106.850791	33.8729885	328814	3749420	25.141	16698.874	49786.7
5	9	-106.850786	33.8727344	328814	3749392	28.190	16727.065	49791.7
5	8	-106.850791	33.8725243	328813	3749369	23.298	16750.363	49784.4
5	7	-106.850796	33.8723201	328812	3749346	22.658	16773.021	49791.8
5	6	-106.850807	33.8721139	328811	3749323	22.885	16795.905	49765.3
5	5	-106.850807	33.8718649	328811	3749296	27.624	16823.530	49843.8
5	4	-106.850801	33.8716334	328811	3749270	25.680	16849.210	49745.2
5	3	-106.850804	33.8714171	328810	3749246	24.002	16873.212	49668.1
5	2	-106.850813	33.8711727	328809	3749219	27.110	16900.322	49821.1
5	1	-106.850822	33.8709636	328807	3749196	23.204	16923.526	49776.6
5	0	-106.850823	33.8707298	328807	3749170	25.937	16949.463	49774.3
5	278	-106.850816	33.870402	328807	3749133	36.360	16985.823	49779.4
5	277	-106.850681	33.8696262	328818	3749047	86.948	17072.772	49801.2
5	276	-106.8508	33.8693639	328806	3749018	31.102	17103.874	49948.7
5	275	-106.850802	33.8690965	328805	3748989	29.650	17133.524	49811.2
5	274	-106.850809	33.8688475	328804	3748961	27.633	17161.157	49814.6
5	273	-106.850811	33.8685764	328804	3748931	30.068	17191.225	49812.3
5	272	-106.850812	33.8682981	328803	3748900	30.866	17222.091	49811
5	271	-106.850817	33.8680238	328802	3748870	30.426	17252.518	49696.8
5	270	-106.850819	33.8677776	328801	3748842	27.309	17279.826	49815.5
5	269	-106.850823	33.8675134	328800	3748813	29.304	17309.131	49811
5	268	-106.850822	33.867236	328800	3748782	30.773	17339.904	49813.1
5	267	-106.850822	33.8669933	328799	3748755	26.916	17366.820	49813.3
5	266	-106.850836	33.8667303	328798	3748726	29.195	17396.015	49808.4
5	265	-106.850827	33.8664762	328798	3748698	28.202	17424.216	49808.3
5	264	-106.850824	33.866218	328798	3748669	28.631	17452.847	49821.7
5	263	-106.85083	33.8659564	328797	3748640	29.020	17481.868	49814.2
5	262	-106.850822	33.8656888	328797	3748611	29.690	17511.558	49814.2
5	261	-106.850812	33.8654268	328797	3748582	29.084	17540.642	49808.7
5	260	-106.850783	33.8651697	328799	3748553	28.628	17569.270	49801.3
5	259	-106.850757	33.8649105	328801	3748524	28.855	17598.125	49815.3
5	258	-106.850735	33.8646534	328803	3748496	28.590	17626.716	49809.3
5	257	-106.850704	33.8643932	328805	3748467	28.991	17655.706	49815.6
5	256	-106.850662	33.8641124	328808	3748436	31.385	17687.091	49813.9

Transect	Point	Longitude	Latitude	UTM Easting (m)	UTM Northing (m)	distance (m)	Accumulated distance (m)	Magnetic Field Strength (nT)
5	255	-106.850618	33.863856	328812	3748407	28.730	17715.821	49791.4
5	254	-106.850568	33.8635978	328816	3748378	29.004	17744.825	49815.2
5	253	-106.850518	33.863338	328820	3748349	29.198	17774.023	49814.1
5	252	-106.850444	33.8630676	328827	3748319	30.754	17804.777	49810.6
5	251	-106.850362	33.8627884	328834	3748288	31.893	17836.671	49808.3
5	250	-106.850292	33.8625199	328840	3748258	30.467	17867.137	49794.8
5	249	-106.850214	33.8622484	328846	3748228	30.967	17898.104	49814.1
5	248	-106.850133	33.8620081	328853	3748201	27.685	17925.789	49816
5	247	-106.850034	33.8617241	328862	3748170	32.809	17958.598	49814
5	246	-106.849957	33.8615009	328869	3748145	25.749	17984.347	49815.2
5	245	-106.849867	33.8612436	328876	3748116	29.745	18014.091	49853.5
5	244	-106.849745	33.8609739	328887	3748086	31.965	18046.056	49819.5
5	243	-106.849643	33.8607305	328896	3748059	28.590	18074.647	49814.9
5	242	-106.849519	33.8604427	328907	3748027	33.913	18108.559	49821.1
5	241	-106.849414	33.8602017	328916	3748000	28.472	18137.031	49815.5
5	240	-106.849297	33.8599361	328926	3747970	31.356	18168.387	49809.3
5	239	-106.849175	33.8596811	328937	3747942	30.483	18198.869	49810
5	238	-106.849068	33.8594278	328947	3747913	29.786	18228.655	49811.6
5	237	-106.848954	33.8591813	328957	3747886	29.292	18257.947	49812.4
5	236	-106.84885	33.8589239	328966	3747857	30.124	18288.071	49813.3
5	235	-106.84873	33.8586758	328976	3747829	29.668	18317.739	49861.8
5	234	-106.84863	33.8584153	328985	3747800	30.349	18348.088	49817.9
5	233	-106.848522	33.858147	328995	3747770	31.392	18379.480	49819.5
5	232	-106.848432	33.857893	329002	3747742	29.369	18408.849	49816.6
5	231	-106.848348	33.8576392	329010	3747714	29.207	18438.056	49818.5
5	230	-106.848265	33.8573886	329017	3747686	28.843	18466.899	49858.2
5	229	-106.84819	33.8571294	329023	3747657	29.567	18496.466	49812.7
5	228	-106.848121	33.856863	329029	3747627	30.239	18526.705	49808.1
5	227	-106.848067	33.8566166	329034	3747600	27.785	18554.490	49810
5	226	-106.848012	33.8563704	329038	3747573	27.777	18582.267	49809
5	225	-106.847959	33.8561149	329043	3747544	28.757	18611.024	49797.1
5	224	-106.847908	33.8558654	329047	3747516	28.059	18639.083	49829.8
5	223	-106.847856	33.8555963	329051	3747487	30.237	18669.320	49815.1
5	222	-106.847809	33.8553413	329055	3747458	28.605	18697.925	49817.6
5	221	-106.847806	33.8550538	329055	3747426	31.901	18729.826	49818.5
5	220	-106.847784	33.8548079	329056	3747399	27.346	18757.172	49814.7
5	219	-106.847767	33.8545445	329057	3747370	29.258	18786.430	49833.3
5	218	-106.847753	33.8542616	329058	3747338	31.398	18817.829	49811.9
5	217	-106.847739	33.8540235	329059	3747312	26.433	18844.262	49822.4
5	216	-106.847723	33.8537428	329060	3747281	31.174	18875.437	49821.2
5	215	-106.847718	33.8534864	329060	3747252	28.440	18903.877	49819.6
5	214	-106.847713	33.853219	329060	3747223	29.670	18933.547	49894
5	213	-106.84772	33.8529228	329058	3747190	32.855	18966.402	49823.9
5	212	-106.847703	33.8526731	329059	3747162	27.741	18994.143	49818.7
5	211	-106.847677	33.8524049	329061	3747132	29.841	19023.984	49819.7
5	210	-106.84768	33.8521456	329061	3747104	28.760	19052.744	49814.1

Transect	Point	Longitude	Latitude	UTM Easting (m)	UTM Northing (m)	distance (m)	Accumulated distance (m)	Magnetic Field Strength (nT)
5	209	-106.847669	33.851891	329061	3747075	28.253	19080.997	49877.5
5	208	-106.847671	33.8516453	329060	3747048	27.257	19108.254	49814.7
5	207	-106.84766	33.8513837	329061	3747019	29.033	19137.288	49817.4
5	206	-106.847658	33.8511246	329061	3746990	28.732	19166.019	49815.5
5	205	-106.847659	33.8508579	329060	3746961	29.587	19195.606	49814.4
5	204	-106.847657	33.8506066	329060	3746933	27.872	19223.478	49800.1
5	203	-106.847675	33.8502941	329057	3746898	34.691	19258.169	49820.4
5	202	-106.847683	33.8500441	329056	3746871	27.747	19285.917	49813.9
5	201	-106.847697	33.8497692	329054	3746840	30.509	19316.425	49811.8
5	200	-106.847733	33.8495083	329050	3746811	29.138	19345.563	49812.6
5	199	-106.84777	33.8492573	329046	3746783	28.041	19373.604	49821.7
5	198	-106.84781	33.8489955	329042	3746754	29.279	19402.883	49826.2
5	197	-106.847852	33.8487337	329038	3746725	29.291	19432.174	49817
5	196	-106.847908	33.8484667	329032	3746696	30.063	19462.237	49813.5
5	195	-106.847963	33.8481998	329027	3746666	30.029	19492.266	49813.7
5	194	-106.848032	33.8478709	329019	3746630	37.035	19529.302	49813.3
5	193	-106.848086	33.8476336	329014	3746604	26.799	19556.100	49821.8
5	192	-106.848176	33.8473595	329005	3746574	31.518	19587.618	49808.2
5	191	-106.848227	33.8471274	329000	3746548	26.170	19613.788	49803.7
5	190	-106.848313	33.846867	328991	3746519	29.968	19643.756	49803.2
5	189	-106.848389	33.846624	328984	3746492	27.846	19671.602	49809.6
5	188	-106.84848	33.8463312	328975	3746460	33.552	19705.155	49860.4
5	187	-106.848559	33.8460616	328967	3746430	30.777	19735.932	49809.1
5	186	-106.848623	33.8458311	328961	3746405	26.233	19762.165	49810.6
5	185	-106.848711	33.8455781	328952	3746377	29.232	19791.397	49811.1
5	184	-106.848804	33.8452977	328943	3746346	32.272	19823.669	49806.2
5	183	-106.848874	33.8450841	328936	3746322	24.569	19848.238	49806.8
5	182	-106.848952	33.8448039	328928	3746292	31.884	19880.122	49805.4
5	181	-106.849034	33.8445675	328920	3746265	27.306	19907.428	49802.2
5	180	-106.849107	33.8443127	328913	3746237	29.061	19936.489	49812
5	179	-106.849205	33.8440592	328903	3746209	29.527	19966.016	49805.4
5	178	-106.849282	33.8438021	328896	3746181	29.388	19995.404	49810.5
5	177	-106.849357	33.8435681	328888	3746155	26.875	20022.278	49802.8
5	176	-106.849417	33.8433156	328882	3746127	28.551	20050.829	49803.7
5	175	-106.849502	33.843091	328874	3746102	26.117	20076.946	49805.6
5	174	-106.849562	33.842825	328868	3746073	30.042	20106.988	49800.2
5	173	-106.849664	33.8425804	328858	3746046	28.711	20135.699	49800
5	172	-106.849739	33.8423327	328851	3746019	28.321	20164.020	49793
5	171	-106.849822	33.8420425	328842	3745987	33.110	20197.130	49806.4
5	170	-106.849895	33.8417934	328835	3745959	28.435	20225.565	49807.8
5	169	-106.849976	33.8415324	328827	3745930	29.910	20255.475	49805.2
5	168	-106.850057	33.8412602	328819	3745900	31.105	20286.580	49798.7
5	167	-106.850132	33.841018	328811	3745874	27.742	20314.322	49781.3
5	166	-106.850221	33.840749	328803	3745844	30.949	20345.271	49802.7
5	165	-106.850288	33.8405032	328796	3745817	27.957	20373.228	49797
5	164	-106.850372	33.8402411	328788	3745788	30.104	20403.332	49798.7

Transect	Point	Longitude	Latitude	UTM Easting (m)	UTM Northing (m)	distance (m)	Accumulated distance (m)	Magnetic Field Strength (nT)
5	163	-106.85047	33.8399471	328778	3745755	33.825	20437.157	49801.6
5	162	-106.850554	33.8396907	328770	3745727	29.499	20466.657	49776.9
5	161	-106.850632	33.8394409	328762	3745700	28.627	20495.283	49601.6
5	160	-106.850728	33.8391763	328753	3745670	30.675	20525.958	49808.6
5	159	-106.8508	33.8389288	328745	3745643	28.240	20554.198	49805.4
5	158	-106.850871	33.8386817	328738	3745616	28.176	20582.374	49798.4
5	157	-106.85095	33.8384075	328731	3745586	31.299	20613.673	49784
5	156	-106.851025	33.8381486	328723	3745557	29.527	20643.200	49804.1
5	155	-106.851118	33.8378871	328714	3745528	30.257	20673.458	49801.4
5	154	-106.851196	33.8376392	328706	3745501	28.426	20701.883	49804.1
5	153	-106.851277	33.8373839	328698	3745473	29.299	20731.182	49800.2
5	152	-106.851357	33.8371283	328690	3745444	29.285	20760.467	49940.4
5	151	-106.851412	33.8368665	328685	3745415	29.471	20789.938	49801
5	150	-106.851495	33.8366214	328677	3745388	28.265	20818.202	49802.5
5	149	-106.851572	33.8363719	328669	3745361	28.569	20846.772	49803.6
5	148	-106.851637	33.8361168	328662	3745333	28.943	20875.715	49817.7
5	147	-106.85176	33.8358413	328650	3745302	32.603	20908.318	49798
5	146	-106.851857	33.8355529	328641	3745270	33.207	20941.525	49799.9
5	145	-106.851912	33.8353173	328635	3745244	26.640	20968.165	49798.3
5	144	-106.852007	33.8350886	328626	3745219	26.833	20994.997	49795.3
5	143	-106.852073	33.8348363	328619	3745191	28.638	21023.635	49796.8
5	142	-106.85214	33.834596	328613	3745165	27.375	21051.010	49792.5
5	141	-106.852203	33.8343172	328606	3745134	31.466	21082.476	49792
5	140	-106.852315	33.8340672	328596	3745106	29.598	21112.074	49791.8
5	139	-106.852392	33.833807	328588	3745078	29.728	21141.802	49792.7
5	138	-106.852468	33.833561	328580	3745051	28.162	21169.963	49795.9
5	137	-106.852548	33.833302	328572	3745022	29.679	21199.642	49793.9
5	136	-106.852624	33.8330627	328565	3744996	27.445	21227.087	49778.5
5	135	-106.852709	33.8327841	328557	3744965	31.875	21258.962	49790.6
5	134	-106.852791	33.8325392	328548	3744938	28.226	21287.188	49792.6
5	133	-106.852878	33.8322322	328540	3744904	34.991	21322.179	49794.6
5	132	-106.852968	33.8319713	328531	3744875	30.092	21352.272	49845.4
5	131	-106.853046	33.8317201	328523	3744847	28.780	21381.052	49787.7
5	130	-106.85313	33.8314719	328515	3744820	28.621	21409.673	49786.3
5	129	-106.85321	33.8311996	328507	3744790	31.086	21440.759	49783.6
5	128	-106.853279	33.8309683	328500	3744764	26.445	21467.204	49786.5
5	127	-106.853355	33.8307139	328493	3744736	29.082	21496.286	49786.3
5	126	-106.853445	33.8304298	328484	3744705	32.597	21528.883	49760.4
5	125	-106.853528	33.8301638	328475	3744676	30.486	21559.369	49781.4
5	124	-106.853607	33.8299098	328468	3744648	29.087	21588.456	49785.4
5	123	-106.853682	33.8296707	328460	3744621	27.435	21615.891	49784.3
5	122	-106.853768	33.8294372	328452	3744595	27.095	21642.986	49781.3
5	121	-106.853858	33.8291139	328443	3744560	36.817	21679.803	49777.9
5	120	-106.853936	33.8288621	328435	3744532	28.825	21708.628	49775.4
5	119	-106.854017	33.8286122	328427	3744504	28.724	21737.352	49778.9
5	118	-106.85411	33.828331	328418	3744473	32.341	21769.693	49775.4

Transect	Point	Longitude	Latitude	UTM Easting (m)	UTM Northing (m)	distance (m)	Accumulated distance (m)	Magnetic Field Strength (nT)
5	117	-106.854168	33.8280984	328412	3744448	26.364	21796.057	49778.4
5	116	-106.854249	33.8278455	328404	3744420	29.037	21825.094	49772.6
5	115	-106.854327	33.8276004	328396	3744393	28.111	21853.205	49781.1
5	114	-106.854397	33.827338	328389	3744364	29.832	21883.037	49771.5
5	113	-106.854496	33.8270979	328380	3744337	28.144	21911.181	49771.7
5	112	-106.854584	33.8268555	328371	3744311	28.104	21939.285	49772.3
5	111	-106.85466	33.8266042	328364	3744283	28.736	21968.021	49773.7
5	110	-106.854739	33.8263324	328356	3744253	31.025	21999.046	49767.3
5	109	-106.854803	33.8260866	328349	3744226	27.895	22026.941	49770.1
5	108	-106.854844	33.8257738	328345	3744191	34.892	22061.833	49771.6
5	107	-106.854933	33.8255761	328336	3744169	23.431	22085.264	49771.5
5	106	-106.854962	33.8253242	328333	3744141	28.065	22113.329	49775.8
5	105	-106.855034	33.8250351	328326	3744109	32.749	22146.079	49747.9
5	104	-106.855095	33.8247645	328320	3744080	30.532	22176.610	49772.7
5	103	-106.855144	33.8245388	328315	3744055	25.450	22202.060	49773.2
5	102	-106.855204	33.8242977	328309	3744028	27.310	22229.370	49769.4
5	101	-106.855266	33.8240424	328302	3744000	28.896	22258.266	49767
5	100	-106.855325	33.8237968	328296	3743973	27.773	22286.039	49922.7
5	99	-106.855381	33.82354	328291	3743944	28.972	22315.011	49767.6
5	98	-106.855461	33.8232135	328283	3743908	36.951	22351.962	49773.5
5	97	-106.855509	33.8229901	328278	3743883	25.175	22377.138	49766
5	96	-106.855544	33.8227832	328274	3743861	23.170	22400.307	49770.3
5	95	-106.855631	33.8224616	328266	3743825	36.553	22436.860	49761.1
5	94	-106.855674	33.8222764	328261	3743805	20.944	22457.804	49777.9
5	93	-106.85573	33.8220216	328255	3743776	28.713	22486.518	49768.4
5	92	-106.855786	33.8217836	328250	3743750	26.919	22513.437	49765.3
5	91	-106.855844	33.82156	328244	3743725	25.370	22538.806	49769.2
5	90	-106.855918	33.8212785	328237	3743694	31.949	22570.756	49763.3
5	89	-106.855964	33.8210187	328232	3743666	29.136	22599.892	49755.6
5	88	-106.856022	33.8207437	328226	3743635	30.986	22630.879	49761.4
5	87	-106.856072	33.8205192	328221	3743610	25.315	22656.193	49763.3
5	86	-106.856137	33.8202582	328214	3743582	29.554	22685.747	49756.3
5	85	-106.856193	33.8200055	328208	3743554	28.520	22714.267	49755.1
5	84	-106.856259	33.8197337	328202	3743524	30.754	22745.021	49838.3
5	83	-106.856301	33.8195112	328198	3743499	24.990	22770.012	49760.3
5	82	-106.856363	33.8192595	328191	3743471	28.488	22798.500	49764.1
5	81	-106.856424	33.8189799	328185	3743440	31.516	22830.016	49760.4
5	80	-106.856487	33.8187053	328179	3743410	31.024	22861.039	49757.9
5	79	-106.856544	33.8184686	328173	3743384	26.766	22887.806	49751.3
5	78	-106.856593	33.8182227	328168	3743357	27.651	22915.457	49746.8
5	77	-106.856665	33.8179595	328161	3743327	29.951	22945.408	49756.7
5	76	-106.856706	33.817685	328156	3743297	30.681	22976.089	49751.2
5	75	-106.856762	33.8174345	328151	3743269	28.257	23004.346	49756.1
5	74	-106.856828	33.8171719	328144	3743240	29.756	23034.102	49750.5
5	73	-106.856897	33.8168842	328137	3743209	32.551	23066.652	49755.9
5	72	-106.856949	33.8166168	328132	3743179	30.040	23096.692	49755.9

Transect	Point	Longitude	Latitude	UTM Easting (m)	UTM Northing (m)	distance (m)	Accumulated distance (m)	Magnetic Field Strength (nT)
5	71	-106.856998	33.8163967	328127	3743155	24.840	23121.533	49756.9
5	70	-106.857051	33.8161489	328121	3743127	27.900	23149.433	49753.3
5	69	-106.85712	33.815873	328114	3743097	31.268	23180.700	49750.9
5	68	-106.857177	33.8156268	328109	3743070	27.807	23208.508	49716.6
5	67	-106.857262	33.8152901	328100	3743032	38.170	23246.678	49743.7
5	66	-106.857304	33.8150545	328096	3743006	26.427	23273.105	49749.3
5	65	-106.857359	33.8148112	328090	3742980	27.439	23300.544	49748.8
5	64	-106.857414	33.8145968	328085	3742956	24.331	23324.874	49746.1
5	63	-106.857456	33.8143135	328080	3742924	31.654	23356.529	49969.2
5	62	-106.857534	33.8140816	328073	3742899	26.747	23383.275	49745.1
5	61	-106.857598	33.8138077	328066	3742869	30.941	23414.217	49745.3
5	60	-106.857653	33.8135521	328061	3742840	28.796	23443.013	49744.3
5	59	-106.857712	33.8132695	328054	3742809	31.807	23474.819	49745
5	58	-106.857773	33.813032	328048	3742783	26.956	23501.775	49734.7
5	57	-106.857833	33.8127664	328042	3742754	29.981	23531.756	49744
5	56	-106.857881	33.8125029	328037	3742724	29.562	23561.318	49746.1
5	55	-106.857943	33.8122547	328031	3742697	28.112	23589.431	49744.5
5	54	-106.857996	33.8120292	328026	3742672	25.492	23614.923	49743.3
5	53	-106.858062	33.8118021	328019	3742647	25.909	23640.832	49738.6
5	52	-106.858141	33.8115366	328011	3742618	30.343	23671.175	49738.5
5	51	-106.858182	33.8112573	328007	3742587	31.217	23702.392	49751.5
5	50	-106.858233	33.8109913	328002	3742557	29.868	23732.260	49745.2
5	49	-106.858281	33.8107457	327997	3742530	27.604	23759.864	49746.2
5	48	-106.858361	33.810478	327989	3742501	30.598	23790.462	49744.2
5	47	-106.858414	33.8102388	327983	3742474	26.992	23817.454	49708.8
5	46	-106.858472	33.8099855	327978	3742446	28.591	23846.044	49742.8
5	45	-106.858523	33.8097457	327972	3742420	27.023	23873.067	49741.7
5	44	-106.858591	33.8094735	327965	3742390	30.827	23903.894	49747.2
5	43	-106.858649	33.809225	327960	3742362	28.078	23931.973	49742.1
5	42	-106.85873	33.8089592	327952	3742333	30.429	23962.401	49763.8
5	41	-106.858777	33.8087146	327947	3742306	27.475	23989.876	49662.2
5	40	-106.85886	33.8084406	327939	3742276	31.339	24021.216	49738.6
5	39	-106.858942	33.808204	327930	3742249	27.313	24048.528	49736.7
5	38	-106.859021	33.8079484	327923	3742221	29.283	24077.812	49752.7
5	37	-106.859115	33.807688	327913	3742193	30.151	24107.963	49729.2
5	36	-106.859218	33.8074476	327903	3742166	28.347	24136.309	49713.1
5	35	-106.859287	33.8072243	327897	3742141	25.569	24161.878	49732.2
5	34	-106.859417	33.806942	327884	3742110	33.540	24195.419	49732.7
5	33	-106.859498	33.8067009	327876	3742084	27.774	24223.193	49737.3
5	32	-106.859606	33.8064338	327865	3742054	31.267	24254.459	49738.6
5	31	-106.859721	33.8062173	327854	3742030	26.267	24280.726	49719.7
5	30	-106.859848	33.8059556	327842	3742002	31.317	24312.043	49737.4
5	29	-106.859977	33.8057238	327830	3741976	28.333	24340.376	49739
5	28	-106.860121	33.8054849	327816	3741950	29.684	24370.059	49738.9
5	27	-106.860254	33.8052449	327803	3741924	29.326	24399.385	49738.7
5	26	-106.86039	33.8050069	327790	3741897	29.261	24428.647	49698.2

Transect	Point	Longitude	Latitude	UTM Easting (m)	UTM Northing (m)	distance (m)	Accumulated distance (m)	Magnetic Field Strength (nT)
5	25	-106.860535	33.8047718	327776	3741872	29.318	24457.965	49732.9
5	24	-106.860688	33.8045339	327761	3741845	29.948	24487.913	49735.9
5	23	-106.860824	33.8043025	327748	3741820	28.606	24516.519	49736.2
5	22	-106.860972	33.804095	327734	3741797	26.737	24543.255	49735.8
5	21	-106.861129	33.8038657	327719	3741772	29.318	24572.573	49725.6
5	20	-106.861269	33.8036664	327706	3741750	25.643	24598.217	49748.3
5	19	-106.861431	33.8034428	327691	3741726	28.942	24627.159	49736.6
5	18	-106.861588	33.8032072	327675	3741700	29.931	24657.089	49736.4
5	17	-106.86176	33.8030229	327659	3741680	25.924	24683.013	49733
5	16	-106.861968	33.8028138	327640	3741657	30.116	24713.130	49726.9
5	15	-106.862153	33.8026156	327622	3741635	27.866	24740.996	49651.1
5	14	-106.862326	33.8024387	327606	3741616	25.376	24766.372	49734.8
5	13	-106.862529	33.8022202	327586	3741592	30.655	24797.027	49738
5	12	-106.862743	33.8019885	327566	3741567	32.454	24829.482	49739.7
5	11	-106.862957	33.8017914	327546	3741545	29.501	24858.982	49735.9
5	10	-106.863121	33.8016152	327530	3741526	24.736	24883.719	49687.2
5	9	-106.863328	33.8014399	327511	3741507	27.275	24910.993	49732.3
5	8	-106.863569	33.8012415	327488	3741485	31.364	24942.357	49735.4
5	7	-106.863815	33.8010421	327465	3741463	31.730	24974.087	49732.7
5	6	-106.86404	33.8008497	327444	3741442	29.855	25003.942	49734.7
5	5	-106.864231	33.8006974	327426	3741426	24.466	25028.408	49730.7
5	4	-106.864509	33.8004717	327400	3741401	35.868	25064.276	49704.9
5	3	-106.864655	33.8003645	327386	3741390	18.060	25082.336	49725.6
5	2	-106.8649	33.8001968	327363	3741371	29.308	25111.644	49729.6
5	1	-106.865132	33.8000494	327341	3741356	26.963	25138.607	49730.8
5	0	-106.865369	33.7999332	327319	3741343	25.481	25164.088	49727.9